National Library of Canada
Acquisitions and Bibliographic Services Branch
395 Wellington Street
Ottawa, Ontario
K1A 0N4

Bibliothèque nationale du Canada
Direction des acquisitions et des services bibliographiques
395, rue Wellington
Ottawa (Ontario)
K1A 0N4

Your file Votre référence

Our file Notre référence

NOTICE

The quality of this microform is heavily dependent upon the quality of the original thesis submitted for microfilming. Every effort has been made to ensure the highest quality of reproduction possible.

If pages are missing, contact the university which granted the degree.

Some pages may have indistinct print especially if the original pages were typed with a poor typewriter ribbon or if the university sent us an inferior photocopy.

Reproduction in full or in part of this microform is governed by the Canadian Copyright Act, R.S.C. 1970, c. C-30, and subsequent amendments.

AVIS

La qualité de cette microforme dépend grandement de la qualité de la thèse soumise au microfilmage. Nous avons tout fait pour assurer une qualité supérieure de reproduction.

S'il manque des pages, veuillez communiquer avec l'université qui a conféré le grade.

La qualité d'impression de certaines pages peut laisser à désirer, surtout si les pages originales ont été dactylographiées à l'aide d'un ruban usé ou si l'université nous a fait parvenir une photocopie de qualité inférieure.

La reproduction, même partielle, de cette microforme est soumise à la Loi canadienne sur le droit d'auteur, SRC 1970, c. C-30, et ses amendements subséquents.

Canada

Detection of Specific DNA Sequences by Electrochemical Impedance Measurements Using Si/SiO_2 Substrates

Caroline Joan Wilson

A Thesis

in

The Department

of

Chemistry and Biochemistry

Presented in Partial Fulfillment of the Requirements
for the Degree of Master of Science at
Concordia University
Montreal, Quebec, Canada

August, 1994

ISBN 0-315-97688-8

Canada

ABSTRACT

Detection of Specific DNA Sequences by Electrochemical Impedance Measurements Using Si/SiO_2 Substrates

Caroline Joan Wilson

Electrochemical impedance measurements were made on modified silicon/silicon dioxide electrodes. Single stranded deoxyribonucleic acid was covalently immobilized through 3-aminopropyltriethoxysilane onto a silicon/silicon dioxide electrode. With the single stranded DNA modified sensor it is possible to recognize batch and *in situ* hybridizations with the in-phase and out-of-phase impedance measurements. With the impedance system, we are able to determine when no hybridization takes place as no flatband potential shifts are observed. The kinetics taking place at the surface of the modified sensor are observed with *in situ* hybridizations. With the results obtained throughout this research, we can state that the shifts of the flatband potential observed are due to the modifications taking place at the surface of the silicon sensor. The silicon/silicon dioxide sensor is sensitive, selective and reasonably reproducible.

ACKNOWLEDGMENT

I would like to express my deep appreciation to Dr. Marcus F. Lawrence who generously provided me with his continued enthusiastic guidance, encouragement and advice throughout the course of this work.

Thanks are also due to Dr. Ann English and Dr. Susan Mikkelsen for serving on my research committee.

I would also like to acknowledge Dr. J.R. Martin from Ecole Centrale de Lyon, France, for his valuable information with the setup of the electrochemical impedance system.

Also, my thanks go to the Chemistry and Biochemistry Department and all its members for their help and enthusiastic support.

Finally, I dedicate this thesis to my family who have supported and encouraged me throughout this work.

TABLE OF CONTENTS

LIST OF FIGURES

LIST OF TABLES

TABLE OF SYMBOLS

ϵ_o	permittivity of free space
ϵ	relative permittivity of the semiconductor
N_D	dopant density
A	area of working electrode
q	electron charge
V	applied dc potential
$\tilde{V}$	total ac potential
V_p	in-phase potential
V_q	out-of-phase potential
V_{fb}	flatband potential
k	Boltzmann constant
T	temperature
G	conductance
C	capacitance
$\tilde{Z}$	total impedance
Z_p	in-phase impedance
Z_q	out-of-phase impedance
R	resistance
I	total dc current
$\tilde{I}$	total ac current
I_p	in-phase current
I_q	out-of-phase current
Q_{sc}	semiconductor charge
ψ_s	surface potential

π	pi
ω	$(2\pi f)$ ac frequency
$t_{\frac{1}{2}}$	half time for probe hybridization
N	probe complexity
L	probe strand length
c	probe concentration in solution
K	first order rate constant for formation of one hybrid molecule
K_n	nucleation constant

CHAPTER 1

INTRODUCTION

1.1 Overview

In the last two decades, the development of immunoassays particularly in clinical and pharmaceutical[1], forensic[2,3], environmental[4] and bioprocess[5] analysis has been based on their high sensitivity and specificity, allowing simple and rapid detection of a broad spectrum of analytes even in a complex sample matrix[6]. Today, devices that can continuously and specifically detect the biological molecules involved are needed in biotechnology and medical monitoring. Currently, a wide variety of assay formats are being used, such as the application of radioimmunoassay (RIA), enzyme immunoassay (EIA), and fluorescence immunoassay (FIA)[7].

Besides their daily use in molecular biology laboratories, there is a general interest in, and great potential for, the application of nucleic acid probes in the specific, rapid diagnosis of human, animal and plant pathogens[8,9], in the detection of specific genes in animal and plant breeding[10], and in the diagnosis of human genetic disorders[11]. In addition, there is an increasing requirement to replace radioisotopes with nonradioactive labels for the detection of nucleic acid probes[12].

Rapid advances in semiconductor technology had led to devices having a very high functionality and complexity. Not only is silicon a good material for the fabrication of

microelectronic circuits, but it is also a favorable material that could be used as a sensor. The sensing of chemical properties by silicon devices may be achieved by the deposition of additional chemically active materials[13].

The main goal of this thesis is to design a silicon-based semiconducting sensor capable of the selective detection of particular deoxyribonucleic acid (DNA) sequences. An overview of the basic concepts and materials used in this study comprises the remaining sections of this chapter. Some of these concepts will be treated in more detail in subsequent chapters.

1.2 Chemically Sensitive Electronic Devices

Interest in chemically sensitive electronic devices has increased greatly in the past decade[14]. The focus of research has been on devices based on the field effect principle, which makes it possible to determine the potential difference across an insulator/liquid interface by measuring the surface potential of a silicon substrate[15]. Because such a device is a field effect transistor in which the gate metal is replaced by a reference/electrolyte/solid interface combination as seen in Figure 1.1, these devices are called ion-sensitive field effect transistors (ISFET's)[16,17]. It has been demonstrated, for example, that devices based on the SiO_2/electrolyte interface are sensitive to variations in pH[18].

The transistor structure is only important, however, to the extent that it is a suitable device for measuring the flatband potentials of electrolyte/insulator/semiconductor (EIS) structures.

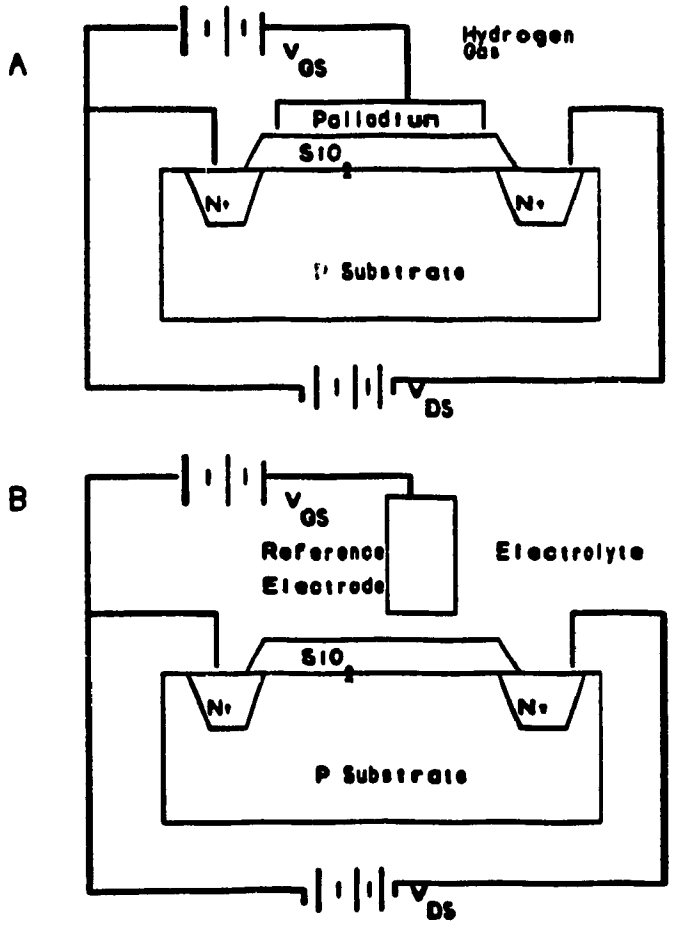

Figure 1.1
Examples of Field Effect Transducers. (a) A hydrogen gas sensor. (b) An ISFET for sensing ionic activity. Where N^+ corresponds to the source and drain, V_{DS} is the voltage applied between the source and drain and V_{GS} is the gate voltage.[14]

The early work demonstrating the usefulness of the field effect principle in making chemically sensitive electronic devices, was oriented mainly to the experimental aspects, namely fabrication technology, testing and measurement electronics[19]. Much effort has also gone into the development of membrane coverings for the insulator, to obtain sensors for ions other than H^+. This has resulted in the development of potassium, calcium[20], and sodium[21,22] sensitive devices, and also an immobilized enzyme penicillin sensor[23]. Another trend in this direction is the use of polymeric insulator membranes[20,24]. In general these devices were developed with biomedical applications in mind, although some applications in analytical chemistry where response time is important have also been mentioned[25].

1.3 Electrochemistry and Chemical Sensing at Semiconductor Electrodes

Electrochemistry is the relationship between electrical properties and chemical reactions, this involves the measurement of some electrical property under conditions which, directly or indirectly, permit an association between the magnitude of the signal measured and the concentration of some particular species. The electrical properties most commonly measured are voltage, current, or resistance, or a combination of these.

In the electrochemical cell, there exists a series of electrical potential changes between the semiconductor

working electrode and the counter electrode. These potential changes are confined to regions near the corresponding interfaces and, therefore, to the semiconductor/electrolyte interface.

The working electrode's Fermi level (E_F) is an important variable in semiconductor electrochemistry because it can be controlled by an externally applied potential. Thermodynamically, the Fermi level is the electrochemical potential of electrons in the solid. An equivalent definition arises from the distribution of electrons among energy levels in a solid: the Fermi level is the energy at which the probability of occupation by an electron is exactly ½.

Semiconductors are characterized by two energy bands which may or may not be occupied by electrons. The highest occupied energy band is called the valence band and the lowest empty energy band the conduction band. These two energy bands are separated by an energy difference called the bandgap. In intrinsic (ideal) semiconductors, where there are no defects or doping states giving rise to energy levels within the bandgap, the Fermi level resides in the middle of the bandgap. In actual semiconductor lattices, however, impurities or structural imperfections create energy levels or states in the bandgap region, shifting the Fermi level either towards the bottom of the conduction band (n-type) or towards the top of the valence band (p-type), as shown in Figure 1.2. Surface states also possess electronic states,

spatially located at the surface of the semiconductor, and they have the following properties: they can trap or emit charge carriers and their energy level may be located in the bandgap or in either band (valence or conduction). However, only the energy levels located in the bandgap or slightly above or below the band edges will be able to charge or discharge in the presence of an applied potential. This exchange gives rise to a capacitive contribution and will in turn modify the behavior of the EIS structure.

When a semiconductor electrode in contact with an electrolyte solution containing a redox-active species reaches equilibrium, the Fermi level of the semiconductor is equal to the potential of the solution. Under either

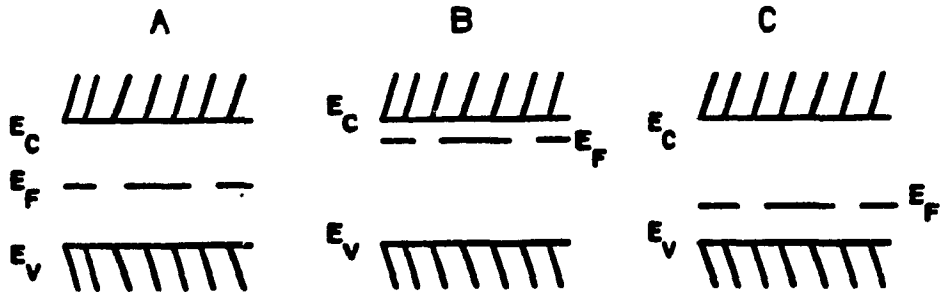

Figure 1.2
The Band Structure in (a) an intrinsic (b) an n-type and (c) a p-type semiconductor. Where E_C, E_V, and E_F correspond to the energy of the conductance band, valence band and Fermi level of a semiconductor, respectively.

equilibrium or nonequilibium (externally applied dc potential) conditions, band bending may exist in the semiconductor at the semiconductor/electrolyte interface. Regardless of the band bending situation, the relative position of E_F (semiconductor) to both E_c and E_v remains unchanged in the bulk of the semiconductor. This is illustrated in Figure 1.3.

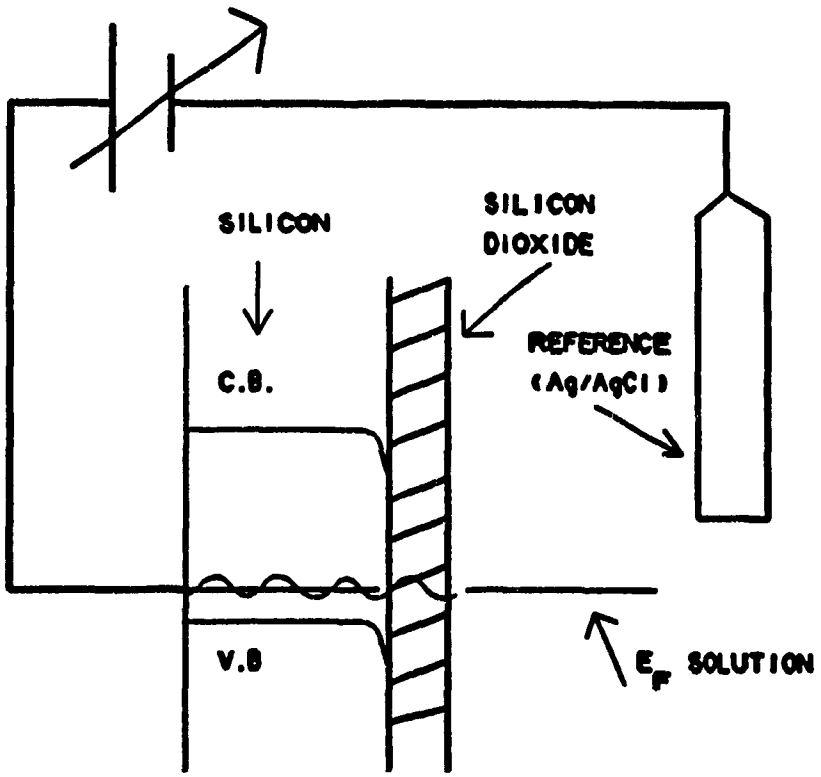

Figure 1.3
Band Structure of a p-type Semiconductor at Equilibrium with the Electrolyte.

The degree of band bending in the semiconductor is directly dependent on the potential applied to the semiconductor working electrode. As shown in Figure 1.3, band bending within the semiconductor creates a space charge region, in which the electrical potential varies from a surface to a bulk value. The space charge region is occupied by fixed charges due to ionized doping sites near the surface of the semiconductor. The potential varies smoothly across the width of the space charge layer.

For any given semiconductor and electrolyte, there exists a unique applied potential for which the potential drop between the surface and the bulk of the electrode is zero; that is, there is no space charge layer. This potential is called the flatband potential, V_{fb}, since the band edges are not bent.

1.4 Sensor Technology

Biosensors today represent a very interesting category of sensors. Many research groups throughout the world are working to improve them and are trying to find ways of commercializing this technology. Biosensors are not a recent development: their principle was first demonstrated in 1962 by Clark and Lyons which showed that by combining glucose oxidase with a Clark pO_2 electrode, it was possible to measure glucose by detecting the drop in oxygen when glucose was converted to gluconic acid and hydrogen peroxide[25]. ISE sensors for the detection of urea, creatinine, glucose and

penicillin have also been developed commercially over the last ten years[27].

A biosensor is composed of two main elements: a biological recognition element, in close contact with the second element, the transducer. The recognition element can be an enzyme, antibody or receptor. The transducer is the electronic device specific for the physicochemical changes occurring inside the biological element, its role is to transduce the recognition event into an electrical signal.

Three main techniques have been proposed to sensitize an ordinary ISFET gate to species other than protons[12,24,28-30]. They are deposition of a sensitive membrane surface, ion implantation, and chemical grafting of suitable molecules.

Ion implantation and the deposition of membranes have several disadvantages. The poor adherence of a physically adsorbed membrane to the dielectric can lead to seepage of water under the membrane, eventually causing a short circuit between the insulator and water. Penetration of small molecules like CO_2 can also disturb the electrical response of the ISFET because of their acid-base equilibria which can influence the ionization of the superficial hydroxide of the silicon dioxide layer. Finally, there can be leaching of ionophores from the membrane, which eventually becomes insensitive[31,32].

The other way of functionalizing a gate is to covalently modify the surface with silane molecules bearing a terminal

group which exhibits the desired chemical reactivity or affinity[33-35]. This is examined in more detail in Chapter 3. The technique used for the modification of the silicon electrode described in this thesis is covalent modification, or chemical grafting, with 3-aminopropyltriethoxysilane (APTS)[36].

1.4.1 Detection of DNA Sequences Using Nonisotopic Methods

The structure of DNA is shown in Figure 1.4. According to the Watson and Crick model, the DNA molecule consists of two polynucleotide chains. Each strand is made up of a nucleotide chain in which deoxyribose and phosphate groups alternate. Nucleic acid hybridization tests for the

Table 1.1
Applications of Nucleic Acid Hybridization Assays

APPLICATIONS	Reference
Forensics	2
Blood Stains	40, 41
Inherited Disorders	11
Cystic Fibrosis	42, 43
Phenylketonuria	44, 45
Sickle Cell Anemia	46
Paternity Testing	47
Plant Breeding	10

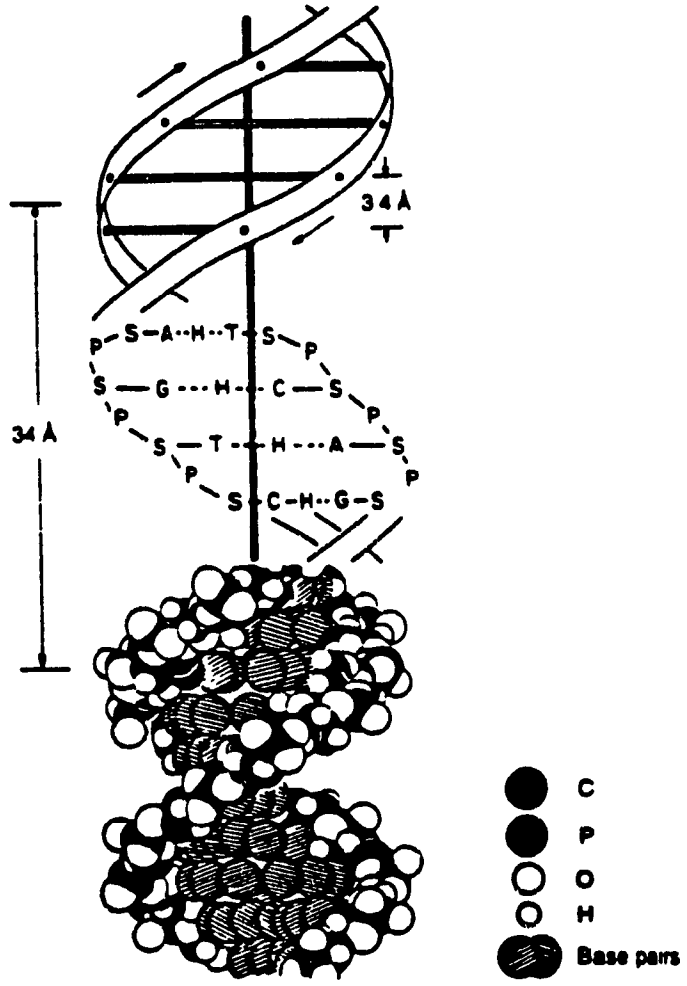

Figure 1.4
The double helical structure of DNA as determined by Watson and Crick. (Reproduced from Reference 48.)

detection of specific DNA and RNA sequences are used in research[37] and have important applications in medicine[38] and forensics[2,39]. Some examples of these applications are listed in Table 1.1.

There is an increasing interest world wide in the detection of nucleic acid sequences by nonradioactive means, by using probes or sensors. A DNA probe consists of a labelled DNA sequence which can detect the complementary strand, whereas the DNA sensor is the combination of a solid-state transducer and a single stranded DNA sequence which can detect the complementary strand. Millan and Mikkelsen have recently developed a sensor based on chemical modification of glassy carbon electrodes with single stranded DNA, allowing observation of hybridization with complementary strands through cyclic voltammetry of a redox-active complex that associates with double stranded DNA[49]. In the research laboratory, the use of ^{32}P for detection is the method of choice and is likely to remain so for the forseeable future[50a], in spite of the half life of only 14 days for ^{32}P. On the other hand, in the diagnostic laboratory the use of nonradioactive labels has many potential advantages. Perhaps the major one is that nonradioactive labels such as enzymes, fluorophores or biotin[50b] are stable for at least 6 months, thus leading to a substantial reduction in cost by avoiding the need to prepare them every 2 or 3 weeks. In addition, there is no radiation exposure from routine daily use and there are no storage and disposal problems.

In this thesis we propose modification of the Si/SiO_2/APTS electrode by reaction with a particular N-bromosuccinimide treated sequence of DNA[51] to covalently immobilize single stranded DNA. Once the electrode is modified with single stranded DNA is successful, it can be used to determine the presence or absence of its complementary strand by impedance measurements following hybridization. This has been the main focus of this work.

CHAPTER 2

EXPERIMENTAL METHODS

2.1 Materials

2.1.1 Chemicals

The source and purity of all the chemicals are specified in Table 2.1. All chemicals were used as received. Whenever applicable, the source of materials obtained from other

Table 2.1
List of Chemicals, Their Source and Purity

Chemicals	Source	Purity
Methanol	J.T. Baker	99.99%
Acetone	Anachemia	99.99%
Sulfuric Acid	Mallinckrodt	99.99%
Sodium Bicarbonate	Sigma	Reagent grade
N-bromosuccinimide	Sigma	Not specified
Potassium Dichromate	Fisher	Reagent grade
tris-[hydroxymethyl]aminomethane hydrochloride	Sigma	99%-99.5%
tris-[hydroxymethyl]aminomethane	Sigma	99.9%
3-aminopropyltriethoxysilane	Sigma	Not specified
Sodium Chloride	Fisher	Reagent grade

companies and their purity, are specified. Water used in preparing solutions was distilled and deionized.

2.1.2 Silicon/Silicon Dioxide Semiconductor Electrodes (Substrates)

The electrodes were 1 x 1 cm^2 taken from a diced Si/SiO_2 wafer (0.3 mm thick) purchased from C.S.E.M. (Neuchâtel, Switzerland). The Si doping density was about 10^{-21} m^{-3} (Al doped) and the surface crystal orientation was <100>. A gold film deposited under vacuum on the back of the Si/SiO_2 substrate provided an ohmic contact. The active area of the substrate, where the chemical grafting was performed, corresponds to a circular area of 0.070 cm^2 in the center of the wafer. The thickness of the thermal SiO_2 in this central area was close to 100 Å, compared to 1000 Å over the rest of the substrate (Figure 2.1). All experiments were carried out in the dark to avoid perturbing the semiconductor behavior.

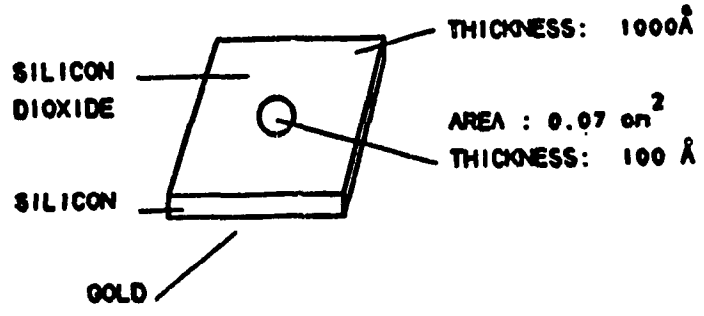

Figure 2.1
Diagram of a Silicon/Silicon Dioxide Electrode

2.1.3 Preparation of the Electrolyte

All the impedance results obtained during this investigation were acquired by using a 10mM aqueous solution of (tris[hydroxymethyl]aminomethane hydrochloride) at a pH adjusted to 7.10 with (tris[hydroxymethyl]amino-methane) and with a 50mM NaCl concentration. For convenience, this buffered electrolyte is referred to as Tris HCl.

2.1.4 Preparation of Synthetic Deoxyribonucleic Acid Solutions

The synthetic single stranded deoxyribonucleic acids, polydeoxyadenylic acid (Poly(dA)), polythymidylic acid (Poly(dT)), oligothymidilic acid ($Oligo(dT)_{20}$), polydeoxycytidylic acid (Poly(dC)), (all from Sigma), and oligoadenylic acid ($Oligo(dA)_{18}$) (from the Oligonucleotide Synthesis Laboratory, Department of Biochemistry, Queen's University) were used as received and dissolved in 1M aqueous $NaHCO_3$, pH 8, to obtain 1 mg/ml concentrations. Samples were stored in vials at -10°C.

2.1.5 Preparation of Calf Thymus Deoxyribonucleic Acid Solutions

A 1 mg/ml solution of calf thymus deoxyribonucleic acid (Type 1, Sigma, used as received), was prepared by dissolving it in 1M aqueous $NaHCO_3$. The samples were stored in 500 μl vials at -10°C. Single stranded deoxyribonucleic acid was obtained by heating the double stranded DNA solution for 15 minutes at 90°C and then cooling it rapidly in an ice bath.

2.1.6 Preparation of the Concentrated Sulfochromic Acid

The concentrated sulfochromic acid was prepared by adding 190 ml of concentrated sulfuric acid to 10 ml of a saturated aqueous solution of potassium dichromate. This solution was used at room temperature (22°C) and was prepared on the day it was used.

2.1.7 Preparation of Modified Electrodes

2.1.7.1 Cleaning of the Substrate

Substrate cleaning is very important because the reaction mechanism that follows is based on the generation of OH groups on the surface and the ensuing reaction with silane (APTS) in solution (described in the fol'owing sections).

$$\underset{\text{substrate}}{\text{Si-OH}} + \underset{\text{solution}}{\text{Si(R)}_n} \longrightarrow \underset{\text{sublayer}}{\text{Si-O-Si(R)}_{n-1}}$$

The cleaning procedure consisted of immersing the substrates in boiling methanol (64°C) for 10 minutes, rinsing with deionized water, immersing the substrates in boiling acetone (56°C) for 10 minutes, followed by air-drying at room temperature (22°C).

2.1.7.2 Hydroxylation of the Silica Layer

The hydroxylation of the silica surface was performed with concentrated sulfochromic acid. The substrate was immersed in sulfochromic acid for 3 minutes and then rinsed thoroughly with deionized water.

2.1.7.3 Electrode Modification with APTS

The hydroxylated Si/SiO_2 electrode surface was coated with 2.5 μl of a 5% aqueous 3-aminopropyltriethoxysilane solution (APTS) and air-dried at room temperature (22°C) for one hour. Excess APTS was removed by rinsing the modified electrode with Tris HCl buffer (electrolyte) for 20 minutes.

2.1.7.4 Single Stranded Deoxyribonucleic Acid Coupling

The APTS modified electrode was reacted with single stranded DNA (oligo$(dT)_{20}$, poly(dT) or calf thymus DNA), using the N-bromosuccinimide method[51] (Figure 2.2). The N-bromosuccinimide - DNA solutions were prepared by adding 20 μl of an aqueous solution of 0.01 M N-bromosuccinimide to 1 ml of 1 mg/ml single stranded DNA in 1M aqueous $NaHCO_3$, and left to react for 15 minutes at 0°C. To the APTS derivatized electrode, 2.5 μl of the bromosuccinimide-DNA solution were

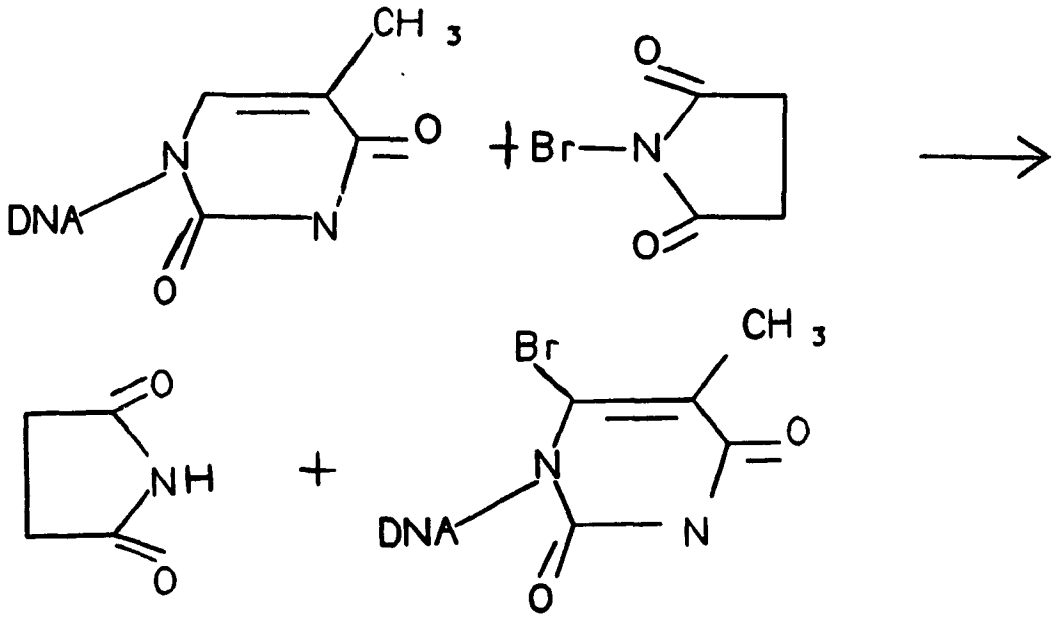

Figure 2.2 Bromination of oligothymidylic acid.

added and the electrode was air-dried at room temperature (22°C) overnight. The modified electrode was then rinsed with Tris HCl buffer. The modified electrodes were equilibrated for 30 minutes in 20 mls of Tris HCl buffer, to ensure that excess DNA was removed from the electrode surface. The gold contact on the electrode was then rinsed with deionized water, and dried with N_2.

2.1.7.5 Hybridization of Immobilized Single Stranded DNA

Immobilized single stranded DNA was hybridized either in a separate step (the batch method) or by *in situ* hybridization with solutions of the complementary polymer or oligomer.

The batch method used either oligo$(dA)_{18}$ or poly(dA) having a concentration of 1 mg/ml in 1M aqueous $NaHCO_3$. To the modified substrate, 3 μl of the single stranded DNA were added. The substrate was left to dry at room temperature for 20 minutes (oligo$(dA)_{18}$) or 40 minutes (poly(dA)). The electrode was never allowed to dry corpletely during hybridization, and deionized water was added as required. After hybridization, the electrode was thoroughly rinsed with Tris HCl solution and equilibrated for 15 minutes to ensure that excess polymer or oligomer was removed from the surface of the electrode.

For *in situ* hybridization, the single stranded DNA solution was added directly to 12 ml of electrolyte before

placing it in the electrochemical cell. Concentrations of single stranded DNA ranged from 0.16 ng/ml to 1.6 ng/ml.

2.1.7.6 Denaturation of Immobilized DNA

Hybridized DNA was denatured by immersing the electrode in boiling deionized water for 20 minutes (oligo$(dA)_{18}$), or 40 minutes (poly(dA)). When not in use, the electrodes were stored in Tris HCl buffer.

2.2 Electrochemical Methods

2.2.1 Electrochemical Cell

The electrochemical cell used in this study was a classical three electrode configuration designed to minimize ohmic drop between the working electrode and the counter electrode. The area of the working electrode was 0.070 cm^2. The counter electrode was a 0.50 cm^2 platinum foil and a saturated Ag/AgCl (Bioanalytical Systems) was used as a reference electrode. The design of the electrochemical cell is shown in Figure 2.3. The volume of Tris HCl used in the electrochemical cell was 12 ml.

2.2.2 Cyclic Voltammetry

DC Potentials were applied to the working electrode with a Scanning Potentiostat (EG & G Princeton Applied Research, Model 362). The current-voltage response was recorded on an XY recorder (Philips, Model PM 8143). The cell shown in

Figure 2.3 was used for these measurements, which were also performed in the dark.

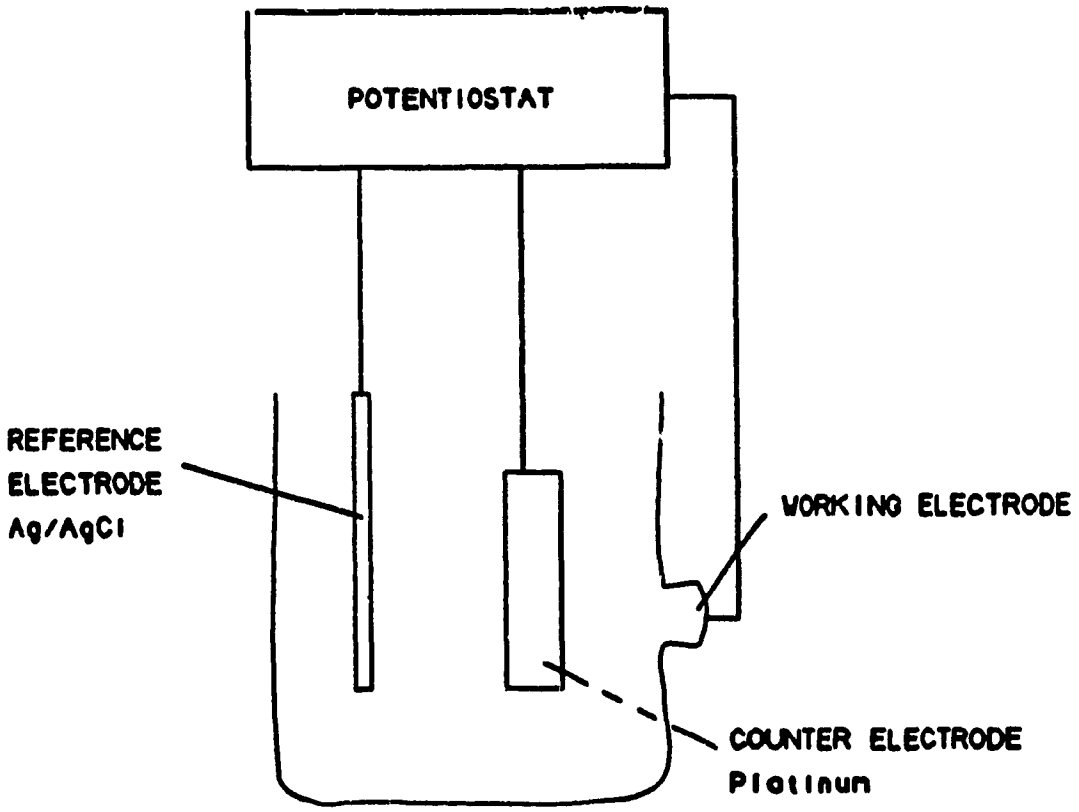

Figure 2.3
Electrochemical Cell used for Impedance Measurements

2.2.3 AC Impedance Technique

The ac impedance technique is a powerful method for investigating the electrical behavior of interfaces. The approach consists of measuring the capacitance of the semiconductor-electrolyte interface as a function, of the dc potential applied to the working electrode. Throughout the experiment, a small sinusoidal component of fixed amplitude and frequency is added to the applied dc potential. The measured responses are the magnitude of the ac component of the current at the same frequency, and its phase angle with respect to the applied ac potential. The magnitudes of the ac current at phase angles of 0 degrees (in-phase) and 90 degrees (out-of-phase), relate respectively to the resistive part and the capacitive part of the simplified equivalent circuit usually taken to represent the semiconductor-electrolyte interface. The interface capacitance (C) is known to be related to the applied dc potential (V) through the Mott-Schottky equation[52]:

$$\frac{1}{C^2} = \frac{2}{\epsilon \epsilon^{\circ} q N_D A} \left(V - V_{fb} - \frac{kT}{q}\right) \qquad (1)$$

where ϵ° and ϵ are the permittivity of free space and the relative permittivity of the semiconductor, N_D is the dopant density, A is the area of the working electrode, q is the electronic charge, V is the applied potential, V_{fb} is the flatband potential, k is the Boltzmann constant and T is the absolute temperature. Thus a plot of C^{-2} versus V is a

straight line with an intercept at the flatband potential (V_{fb}), a value which effectively depends on the electrical charge distribution at the semiconductor-electrolyte interface under study. The changes that can occur at the SiO_2 surface due to adsorption or chemical bonding will be reflected by variations in its flatband potential and therefore provide information as to the relative energy levels of states present at the interface.

The impedance measurements were performed using the potentiostatic three electrode technique. The experimental setup is given in Figure 2.4. A three electrode GPIB Potentiostat/Galvanostat (Model HA-501G, Hokuto Denko Limited) monitors the dc potential applied to the working electrode with respect to the Ag/AgCl electrode (Figure 2.3). A sine modulated voltage with an amplitude of 10 mV rms and in the frequency range of 10 kHz - 30 kHz, delivered by an SR530 lock-in amplifier (Stanford Research Systems) was applied to the working electrode through the potentiostat. We have developed a program (see Appendix I) which monitors the voltage, V, applied to the working electrode and reads the current, I, which are measured alternately after having been filtered by a Dual Hi-Low Filter (Wavetek Rockland, Model 442) to obtain the ac components. These two parameters are measured in-phase and out-of-phase with SR510 and SR530 lock-in amplifiers. The lock-in amplifiers compare the ac current signals with a reference signal at the same frequency as the one that has been applied to the cell. Measurements

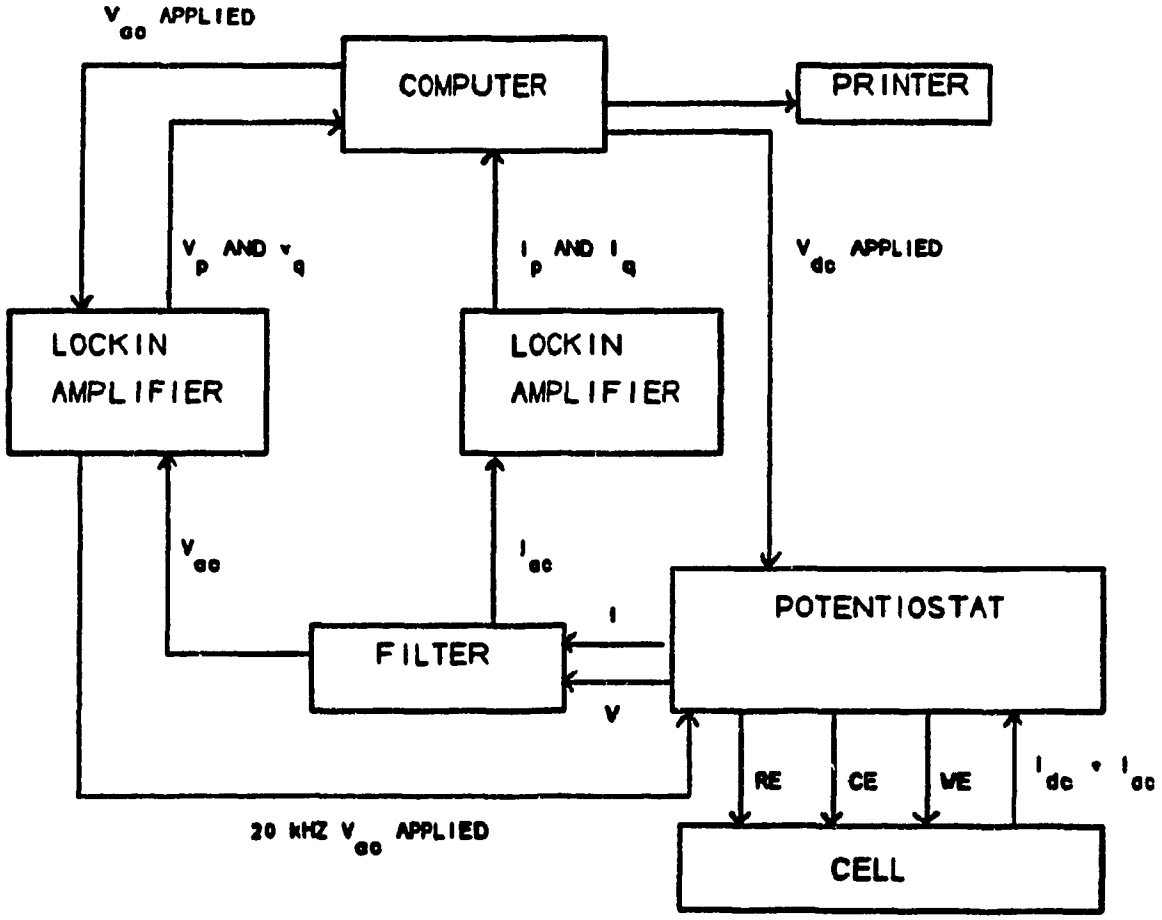

Figure 2.4
Block diagram of the experimental setup; WE, working electrode; CE, counter electrode; RE, reference electrode.

are transmitted through an IEEE 488 interface (National Instruments) and stored in a 386 DX 33 MHz personal computer, which calculates the impedance from Ohm's Law:

$$\tilde{V} = \tilde{Z}\,\tilde{I} = (Z_p + iZ_q)\,\tilde{I} \qquad (2)$$

with

$$\tilde{V} = V_p + iV_q \qquad (3)$$

and

$$\tilde{I} = I_p + iI_q \qquad (4)$$

For each continuous polarization value, and for a given modulation frequency, in-phase (Z_p) and out-of-phase (Z_q) impedances can be expressed as (using equations 2, 3, and 4):

$$Z_p = \frac{V_pI_p + V_qI_q}{I_p^2 + I_q^2} \qquad (5)$$

$$Z_q = \frac{V_qI_p - V_pI_q}{I_p^2 + I_q^2} \qquad (6)$$

Experimental measurement time depends on the number of recorded experimental points. Generally each curve presented in this thesis was obtained in about 20 minutes.

Treating the entire heterostructure (electrolyte/dielectric/semiconductor) as an ideal blocked interface made of several capacitors in series, one can relate the out-of-phase impedance, Z_q, to the total capacitance, C, using the following equation

$$Z_q = \frac{1}{C\omega} \tag{7}$$

where ω is the ac signal frequency $(2\pi f)$. Therefore, the out-of-phase impedance of the device is inversely related to the capacitance of the heterostructure and consequently to the thickness of the dielectric[52]. The thickness of the dielectric layer, d, can be obtained with the expression

$$C = \frac{\epsilon_0 \epsilon A}{d} \tag{8}$$

where ϵ_0 is the permittivity of free space, ϵ is the dielectric constant of the dielectric material, and A is the surface area.

CHAPTER 3

RESULTS AND DISCUSSION: PART I
CHARACTERIZATION OF SEMICONDUCTOR ELECTRODES

3.1 Overview

With the development of transistors, signal generation and processing with automated systems is readily accomplished. Research in biochemical sensors is now focussed on perfecting as a sensing layer, a material or a structure showing good molecular or ionic recognition properties associated with a good stability. Many organic and biochemical compounds are highly specific in their recognition of unknown species, but their fixation to or incorporation with a transducer must allow retention of selectivity, reversibility and sensitivity of the soluble recognition agent. In this thesis, materials and preparation techniques meeting such requirements are presented. The purpose of this chapter is to demonstrate impedance changes at the SiO_2-solution interface following hydroxylation, modification with 3-aminopropyltriethoxysilane, and covalent binding of single stranded DNA.

3.2 Determination of the Semiconductor Impedance

An impedance measurement system was made operational by writing a program (Appendix I) to interface a personal computer 386 DX with two lock-in amplifiers and a potentiostat. Using this program, a low-amplitude ac signal

(10 mV rms) was superimposed on the dc signal applied to the electrochemical cell.

Figure 3.1 shows the behavior of a p-type Si/SiO_2 semiconductor substrate. Three polarization ranges can be distinguished in the out-of-phase impedance (Z_q) versus V curve corresponding to inversion (V < -0.4V vs Ag/AgCl), depletion (-0.4V vs Ag/AgCl < V < +0.2V vs Ag/AgCl) and accumulation (V > +0.2V vs Ag/AgCl) of majority charge carriers (holes) in the silicon valence band. Band

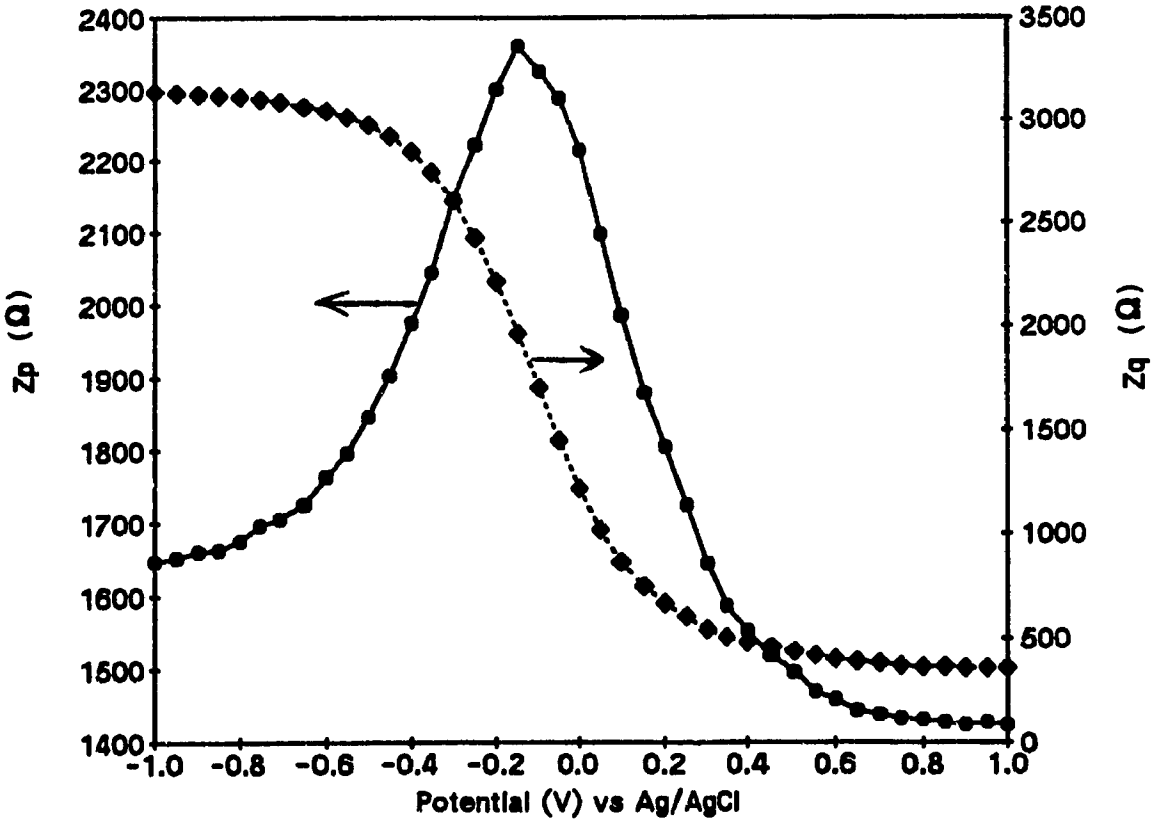

Figure 3.1 In-phase (Z_p) and out-of-phase (Z_q) impedances measured on a hydroxylated Si/SiO_2 electrode in Tris HCl at a frequency of 20 kHz.

(A) Accumulation

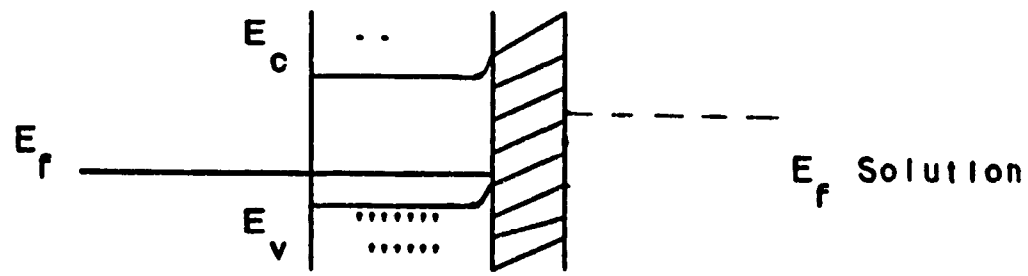

(B) Depletion

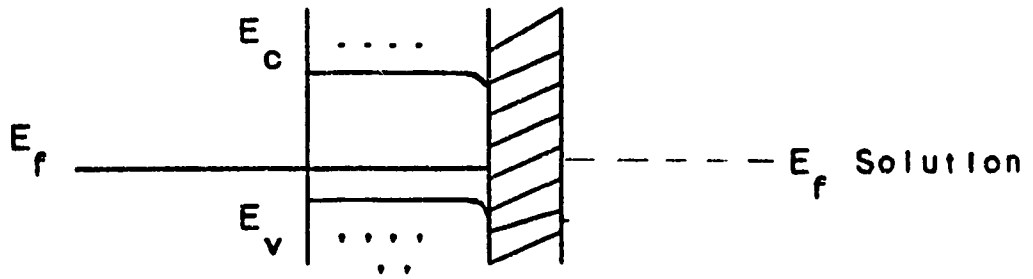

(C) Inversion

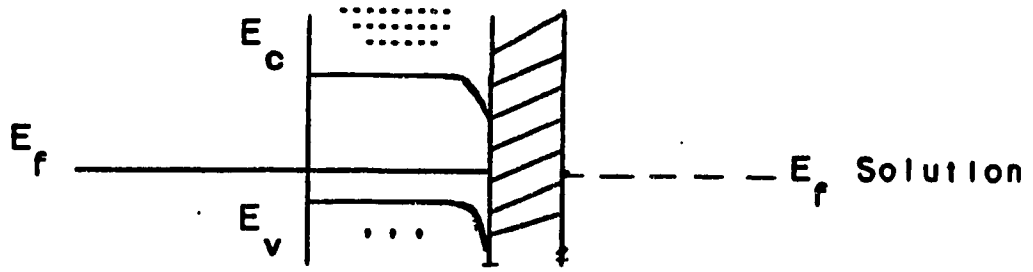

Figure 3.2 Bandgap bending of a p-type silicon substrate showing the three distinct regimes of majority charge carrier density within the valence band of the silicon. They correspond to (a) Accumulation (b) Depletion and (c) Inversion regions. Electron energy increases upwards.

bending at the Si/SiO_2/electrolyte interface corresponding to each of these ranges are illustrated in Figure 3.2. The peak in the Z_p versus V curve (Figure 3.1) is related to the presence of surface states in the bandgap. The position and amplitude of this peak characterize the energy level and the density of these surface states, respectively, and depend on the quality of the oxide layer which can differ from one electrode to another.

With a low amplitude ac signal (10 mV rms) the variation of the semiconductor charge (Q_{SC}) and the surface potential (Ψ_s) lead to a measure of the differential capacitance of the Si/SiO_2 interface, (C_{SC}):[53]

$$C_{SC} = -\frac{d Q_{SC}}{d \Psi_s} \qquad (9)$$

As we have mentioned, according to the dc bias voltage and frequency used, we can distinguish several ranges of operation.

3.2.1 Accumulation Range

In this range, the semiconductor capacitance is determined by the majority charge carriers. Therefore $C_{SC} >> C_i$, where C_i corresponds to the capacitance of the insulator, and the equivalent circuit can be reduced to the case shown in Figure 3.4.A.

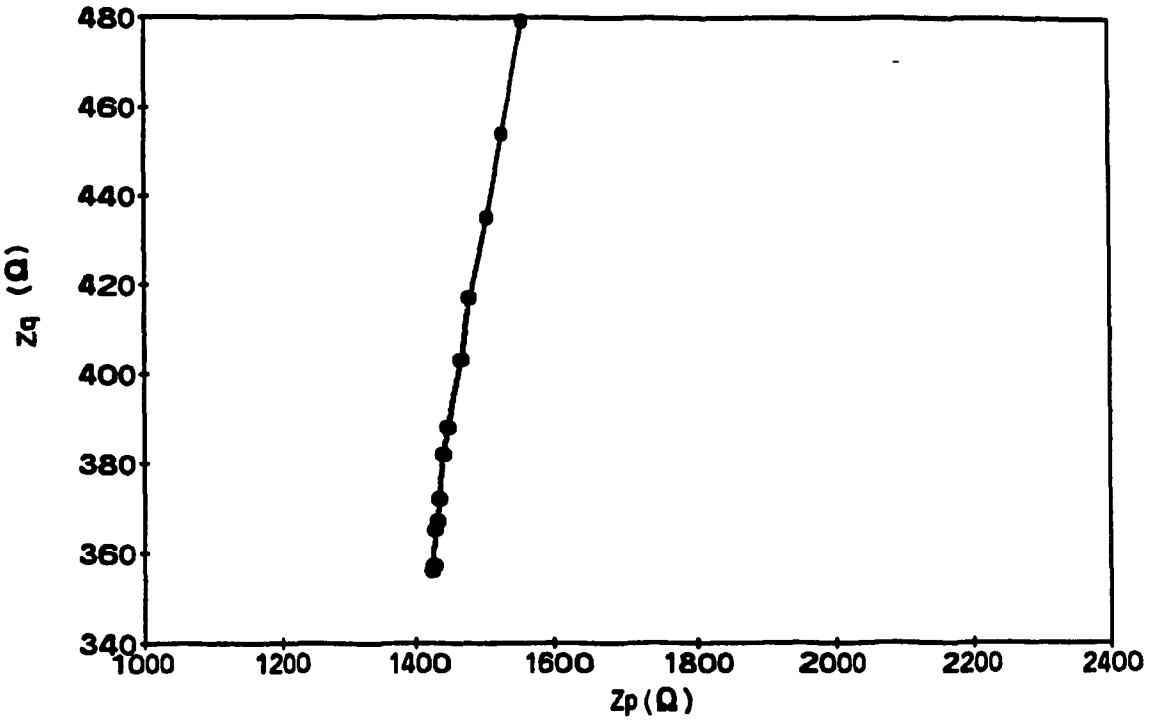

Figure 3.3 Nyquist Representation of the Impedance in the Accumulation Range of a Si/SiO_2 Electrode.

In the Nyquist representation[54], we obtain a vertical line denoting a purely capacitative system (Figure 3.3).

$$Z = R_s - \frac{j}{C_i \omega} \tag{10}$$

3.2.2 Depletion Range

In the intermediate potential range, the semiconductor impedance is a result of one capacitance and one conductance. The capacitance is due to the semiconductor depletion layer (C_{SDL}) and surface states (C_{ss}), and the conductance is associated only with the surface states (G_{ss}). The equivalent circuit is shown in Figure 3.4.B.

A. Accumulation

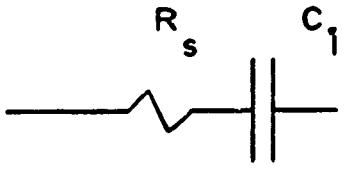

B. Depletion

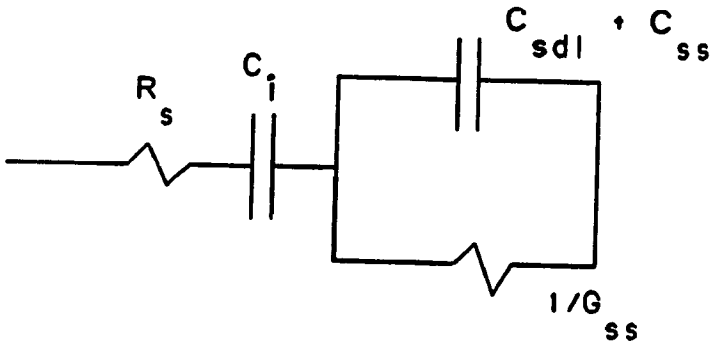

C. Inversion

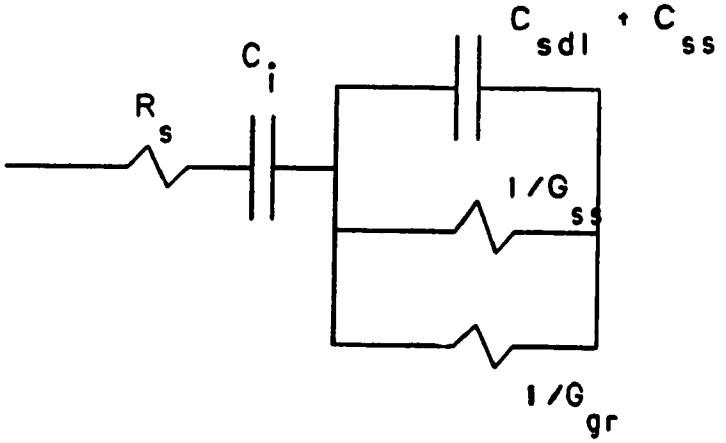

Figure 3.4 Equivalent circuits for the semiconductor/oxide (insulator)/electrolyte in the (A) accumulation, (B) depletion, and (C) inversion range. R_s denotes the series resistance, C_i, C_{sdl}, and C_{ss} being respectively the capacitances of the insulator, semiconductor depletion layer, and surface states, and G_{ss} and G_{gr} the conductances of the surface states and the minority charge carriers respectively[33].

3.2.3 Inversion Range

In this range the semiconductor capacitance has added components due to minority charge carriers in the semiconductor depletion layer (C_{sdl}). In addition to the conductance associated with the surface states, G_{ss}, the conductance associated with the generation - recombination process of the minority charge carriers, G_{gr}, must also be considered. The equivalent circuit in this case is given in Figure 3.4.C.

3.3 Determination of the Semiconductor Oxide Layer Thickness

At a high ac frequency the electrolyte/oxide/semiconductor (EOS) structure can be represented by a resistance in parallel with the capacitance of the dielectric. Under these conditions, the in-phase impedance value represents the resistance of the electrolyte and the oxide layer, whereas the out-of-phase (quadrature) impedance corresponds to the capacitance of the dielectric alone. The out-of-phase impedance is given by equation 7.

The oxide layer thickness of a semiconductor can be determined by measuring the capacitance in the accumulation region (Figure 3.5) and using equation 8. Using a SiO_2 dielectric constant of $\epsilon = 3.81$, $\epsilon^o = 8.84 \times 10^{-14}$ F/cm, A = 0.070 cm^{-2} and a capacitance at +1 V versus Ag/AgCl of 2.22×10^{-8} F, the experimental thickness of the oxide layer for the substrate corresponding to Figure 3.5 is 106 Å. An average value of 102 ± 20 Å was obtained from

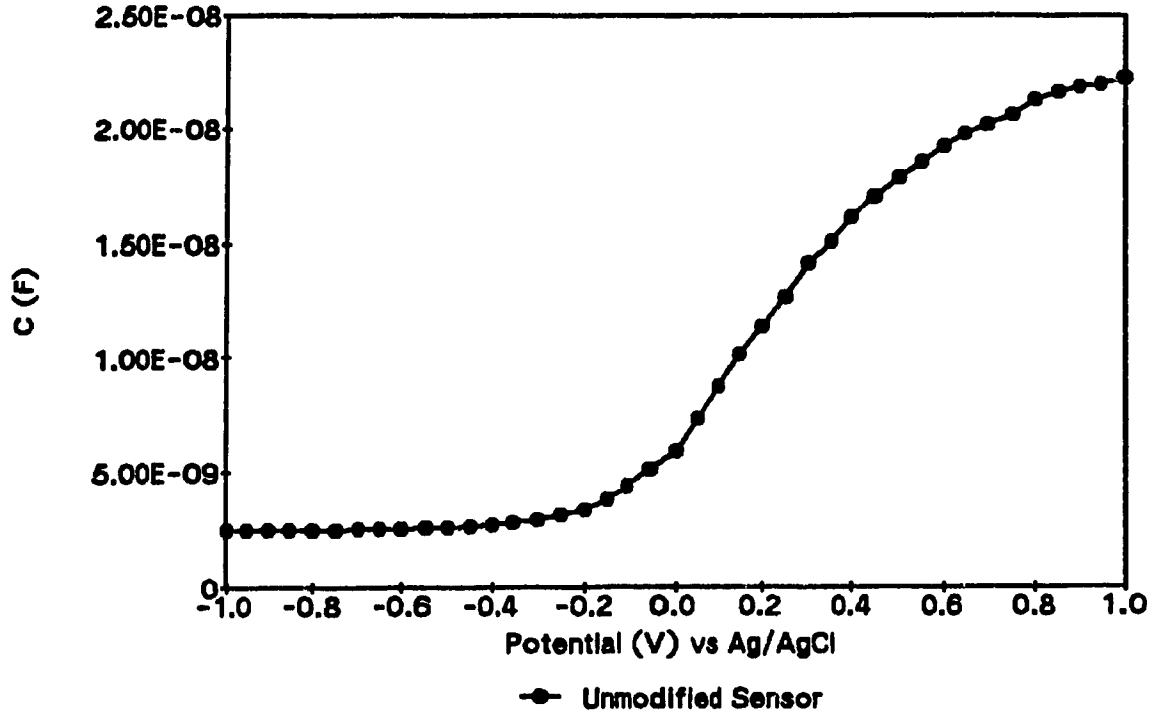

Figure 3.5 Capacitance vs dc potential. Plot for an unmodified electrode in Tris HCl and frequency of 20 kHz.

10 separate measurements (different substrates), in agreement with the thickness specified by C.S.E.M. (Neuchâtel, Switzerland).

3.4 Determination of the Semiconductor Flatband Potential and Doping Density

The flatband potential characterizes the energetic position of the bands in a semiconductor relative to the redox energy level of the electrolyte. It can be changed by the formation of dipolar structures at the interface due to interaction with components of the electrolyte. The flatband

potential is significantly altered by the specific adsorption of ions from the electrolyte, in addition to the formation of ionic groups on the surface of the semiconductor due to reactions with the electrolyte. The production of a depletion layer within the semiconductor leads to the appearance of a space charge capacitance as given by the Mott-Schottky equation (equation 1). A plot of $1/C^2_{sdl}$ vs V has a slope related to the dopant density, N_D, and an X-intercept corresponding to V_{fb}. Modifications taking place on the surface of the oxide layer will cause a shift in the flatband potential. The flatband potential can be obtained from a Mott-Schottky Plot, as shown in Figure 3.6, by extrapolating the depletion range to the X-axis[55]. The flatband potential obtained for a typical unmodified silicon substrate is +0.05 versus Ag/AgCl. The doping density, N_D, is obtained from the slope of the depletion range of this graph and from equation 1, where the Si dielectric constant $\epsilon = 11.7$[56], and $\epsilon^o = 8.84 \times 10^{-14}$ F/cm. For this particular substrate (Figure 3.6), $N_D = 2 \times 10^{21}$ m^{-3}. The doping densities are observed to vary for substrates originating from different wafers and even for substrates originating from the same wafer. Measurements made on three different substrates taken from a single wafer gave an average N_D of 6×10^{21} $m^{-3} \pm 3 \times 10^{21}$ m^{-3}, in agreement with the doping density of about 10^{21} m^{-3} specified by C.S.E.M. (Neuchâtel, Switzerland).

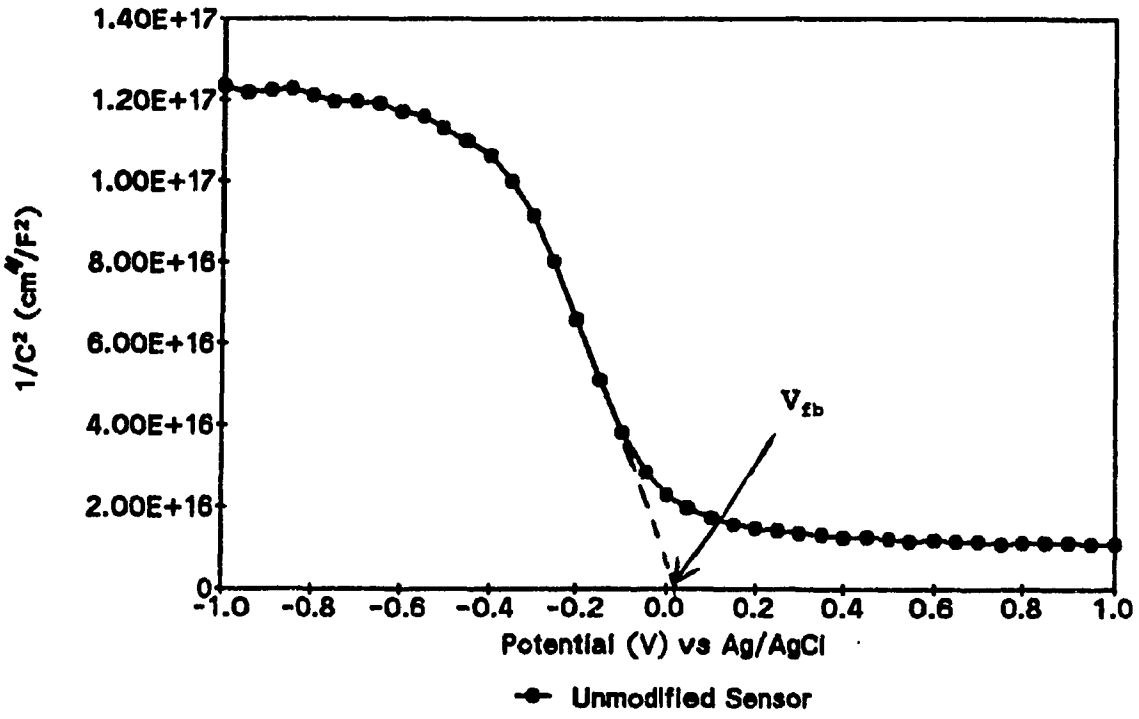

Figure 3.6 Mott-Schottky Plot of an unmodified electrode for the determination of flatband potential and doping density.

3.5 Determination of the Optimum AC Signal Frequency

Figures 3.7(A, B), show the dependence of impedance on frequency, measured using a single substrate. The in-phase curve (Z_p vs V) shows that at frequencies higher than 20 kHz, negative Z_p values are obtained because the potentiostat is not fast enough and causes a dephasing of the signal. At frequencies lower than 20 kHz, the position and amplitude of the peak which characterizes the energy level and the density of the surface states respectively is not well-defined.

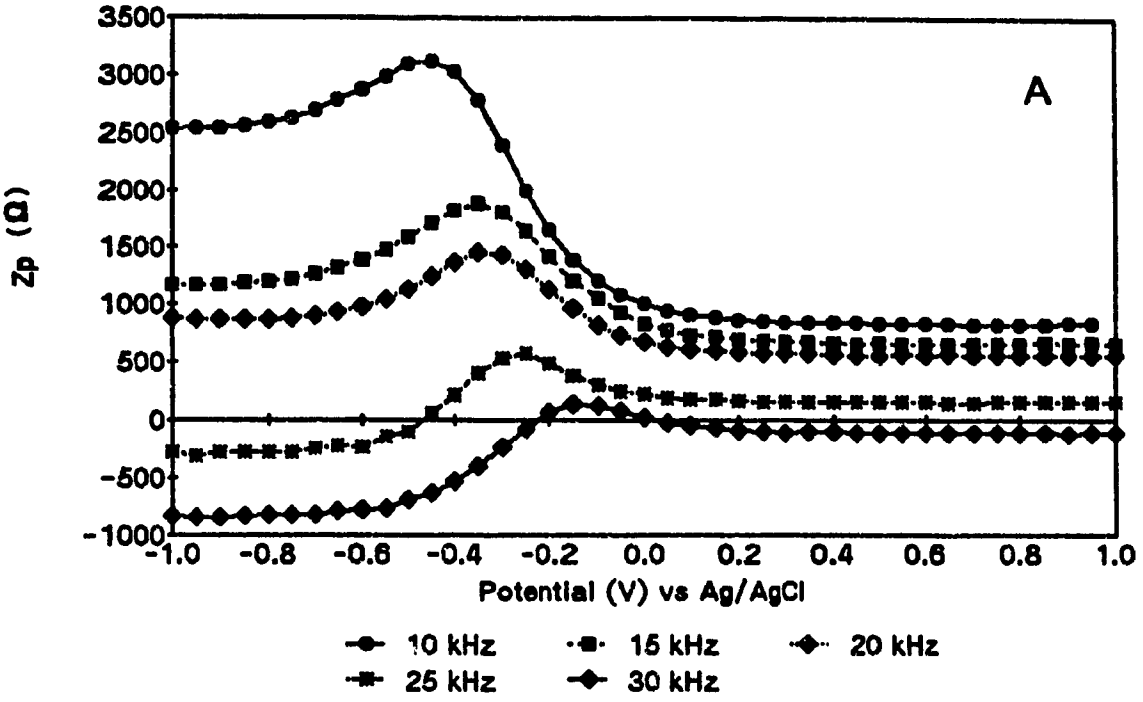

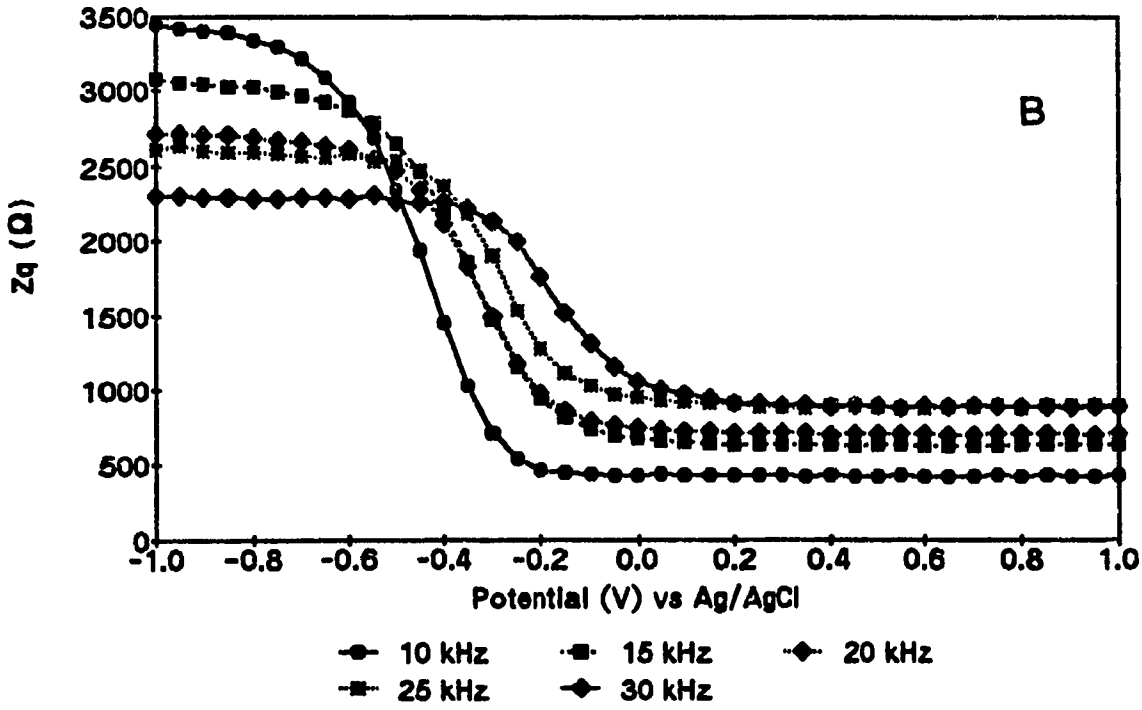

Figure 3.7 Frequency Dependence of (A) In-Phase and (B) Out-of-Phase Impedance of an Unmodified Silicon Electrode in Tris HCl, pH 7.10.

The out-of-phase (Z_q vs V) curves, show that at either very high or very low frequencies, the curve is shifted from the original position in the accumulation range, which represents the flatband position in the semiconductor as well as the thickness of the oxide layer (which is known to be about 100 Å). Thus we have chosen 20 kHz as the optimal frequency for our measurements using this system.

3.6 Equilibration of the Semiconductor

Figures 3.8 (A, B) correspond to three consecutive experiments performed with the same unmodified electrode. As can be seen, the second and third readings of in-phase and out-of-phase impedance curves are similar and the system has stabilized; thus we can assume that equilibrium has been reached after 20 minutes (time for the first run) in contact with the electrolyte. This behavior has been observed with all unmodified and modified electrodes. A cyclic voltammogram of a clean Si/SiO_2 electrode in contact with Tris HCl buffer, taken between -1.4 V and +1.0 V versus Ag/AgCl, at a scan rate of 2 mV/s, showed no evidence of redox chemistry occurring at the surface of the working electrode (Figure 3.9). The change in V_{fb} during the first 20 minutes could therefore be attributed to an adsorption effect at the SiO_2(unmodified or modified)/electrolyte interface. All further data were obtained during the second set of readings, corresponding to the stabilized condition.

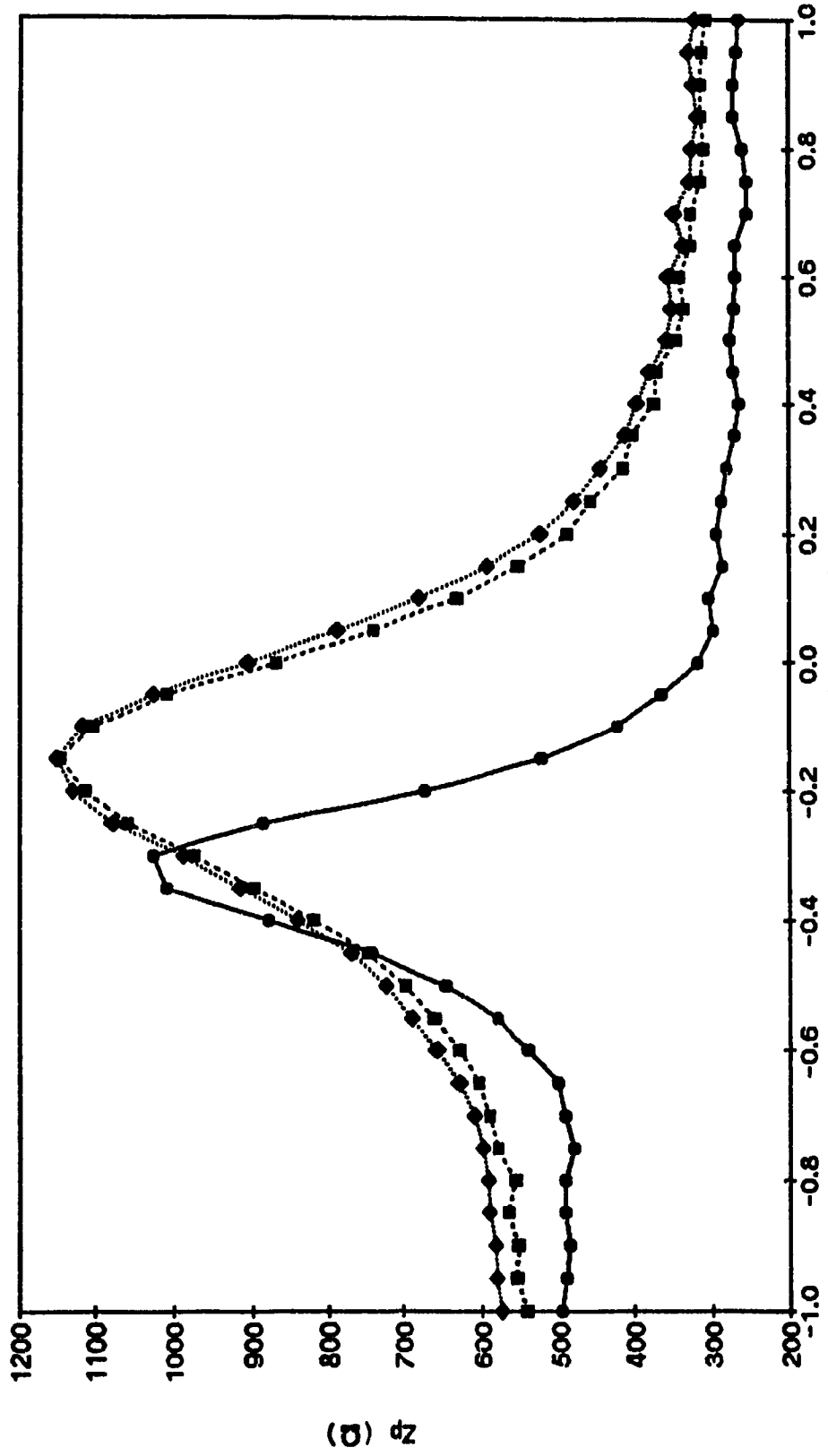

Figure 3.8A In-phase impedance measurements of an unmodified silicon electrode, read three consecutive times.

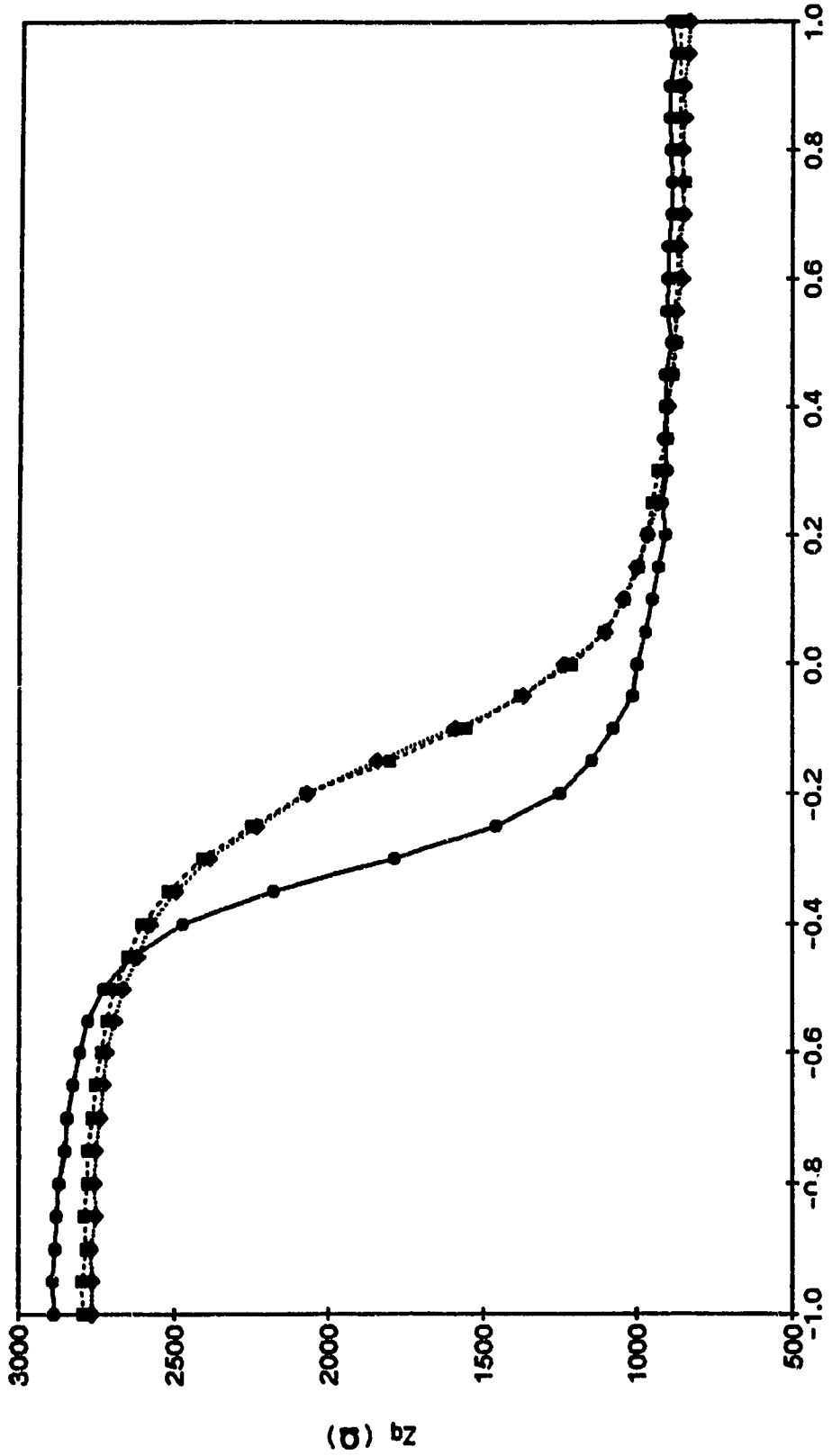

Figure 3.8B Out-of-phase impedance measurements of an unmodified silicon electrode, read three consecutive times.

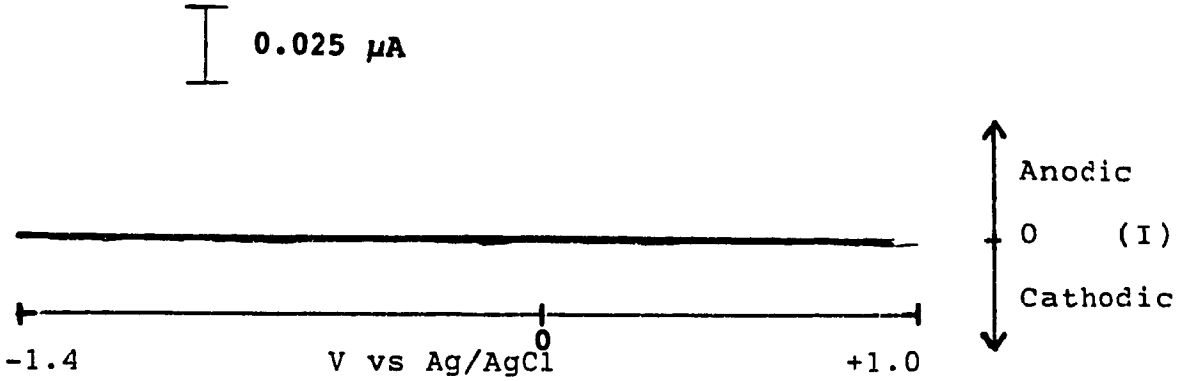

Figure 3.9
Cyclic voltammogram of a clean silicon electrode in contact with Tris HCl buffer. Scan rate was 2 mV/s starting at an initial potential of -1.4 V vs Ag/AgCl (40 minutes for full cycle). The current scale is 0.025 μA/cm.

3.7 Dependence on Electrolyte Concentration

The impedance of the system is the opposition offered by the electrochemical circuit to the flow of an alternating current between the working electrode (at a fixed dc potential) and the counter electrode. Thus the impedance of the system is expected to depend on the concentration of the electrolyte in the electrochemical cell.

In Figure 3.10A, the buffer concentration dependence is shown for the impedance of a Si/SiO_2 electrode. As we increase the Tris HCl salt concentration, the conductivity of the system increases and therefore impedance of the system decreases. Slight shifts are also observed in the corresponding out-of-phase (Z_q) impedance versus potential curves (Figure 3.10B).

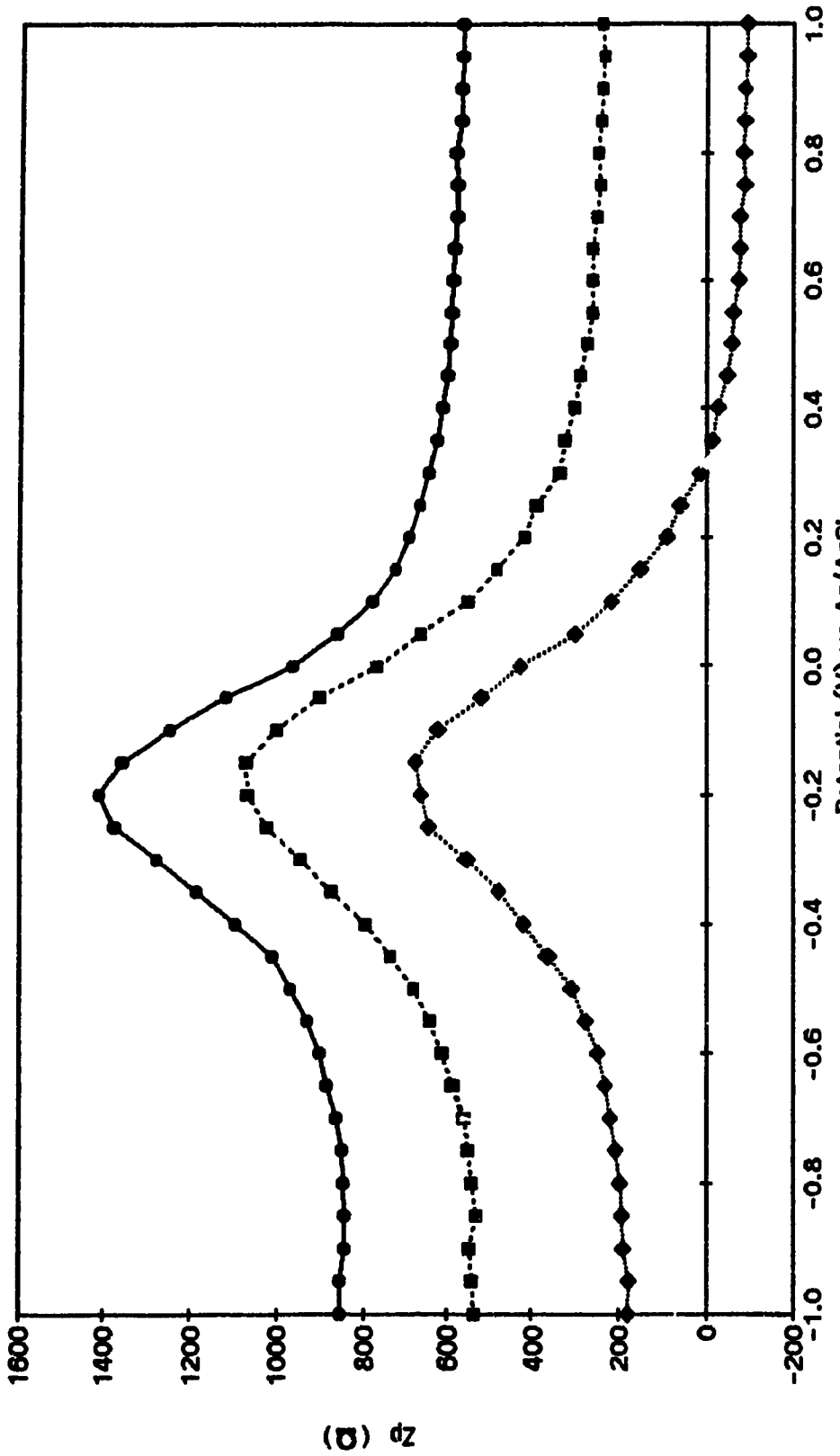

Figure 3.10A In-phase impedance measurements of a silicon electrode for the determination of Tris HCl salt concentration dependence. (NaCl concentration kept constant at 50 mM).

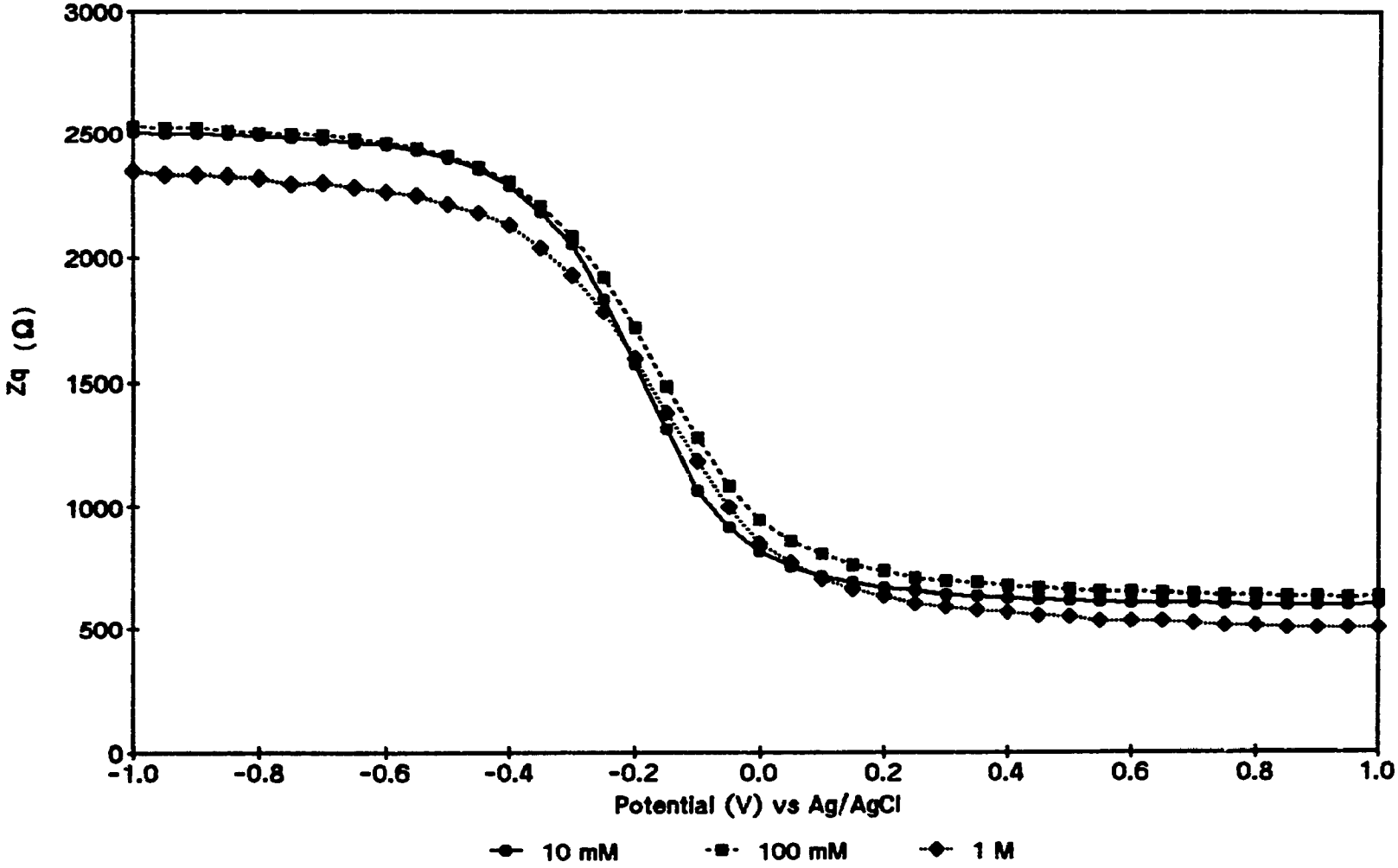

Figure 3.10B Out-of-phase impedance measurements on a silicon electrode for the determination of Tris HCl salt concentration dependence. (NaCl concentration kept constant at 50 mM).

The dependence of impedance on NaCl concentration is shown in Figure 3.11A. As expected, similar effects as those observed upon increasing the buffer ion concentration are observed upon increasing the NaCl concentration. Significant shifts in the flatband potential are observed upon changing the NaCl concentration (Figure 3.11B), with the curve at 50 mM NaCl giving an N_D value close to the specified value of about 10^{21} m^{-3}. It was observed that if the Tris HCl salt concentration was lowered by a factor of two and the NaCl kept at a concentration of 50 mM, high impedance values of about 100,000 ohms were obtained. The in-phase impedance peak was poorly defined and the out-of-phase impedance curve was shifted towards a more negative potential. If the concentration of NaCl was reduced by a factor of two and the Tris HCl kept at a concentration of 10 mM, the in-phase impedance values increased by about 7,000 ohms and the response in the Z_p versus V becomes less well defined. In all further experiments, we have used a concentration of 10 mM Tris salt and 50 mM NaCl.

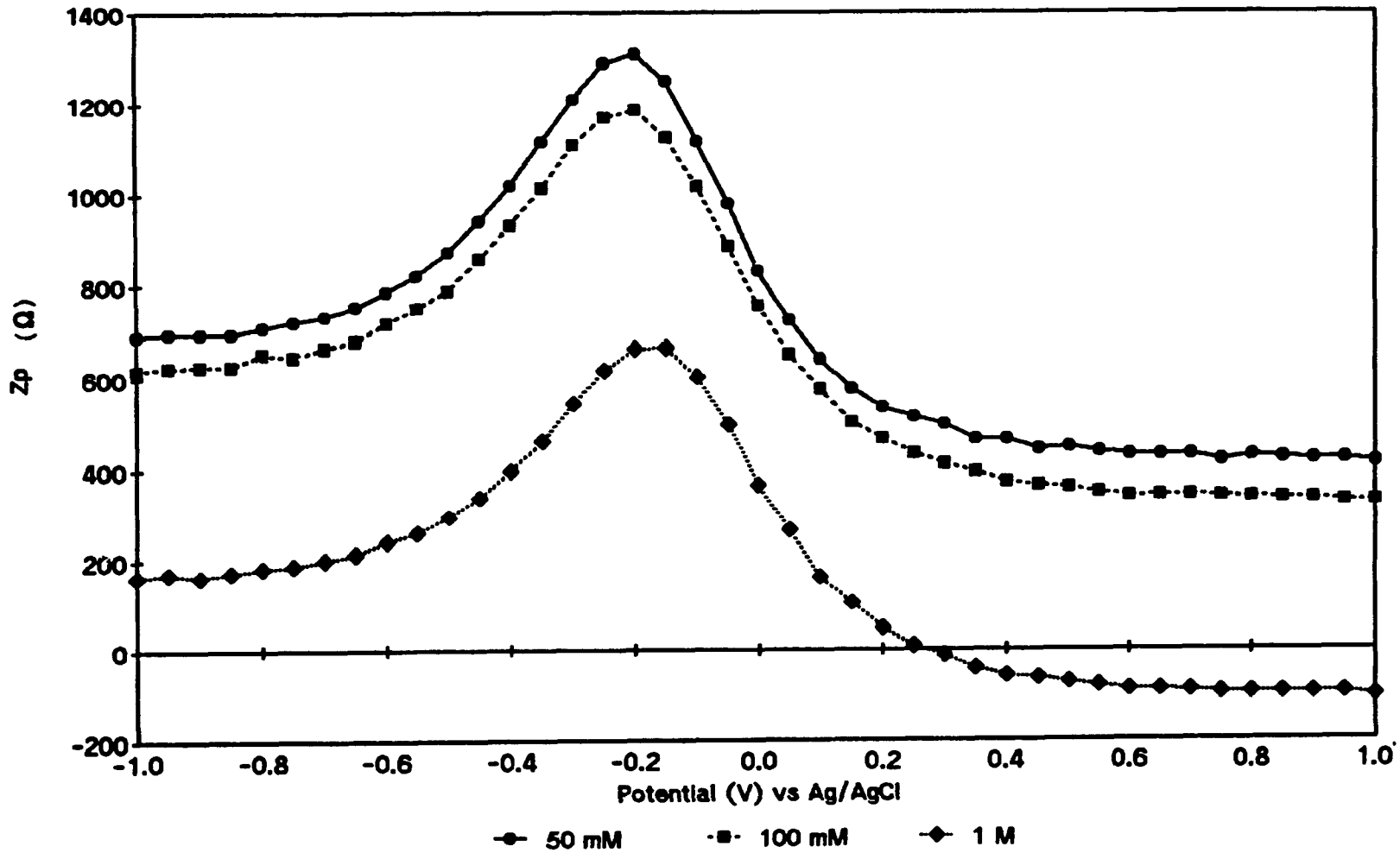

Figure 3.11A In-phase impedance measurements on a silicon electrode for the determination of the NaCl concentration dependence. (Tris HCl salt concentration kept constant at 10 mM).

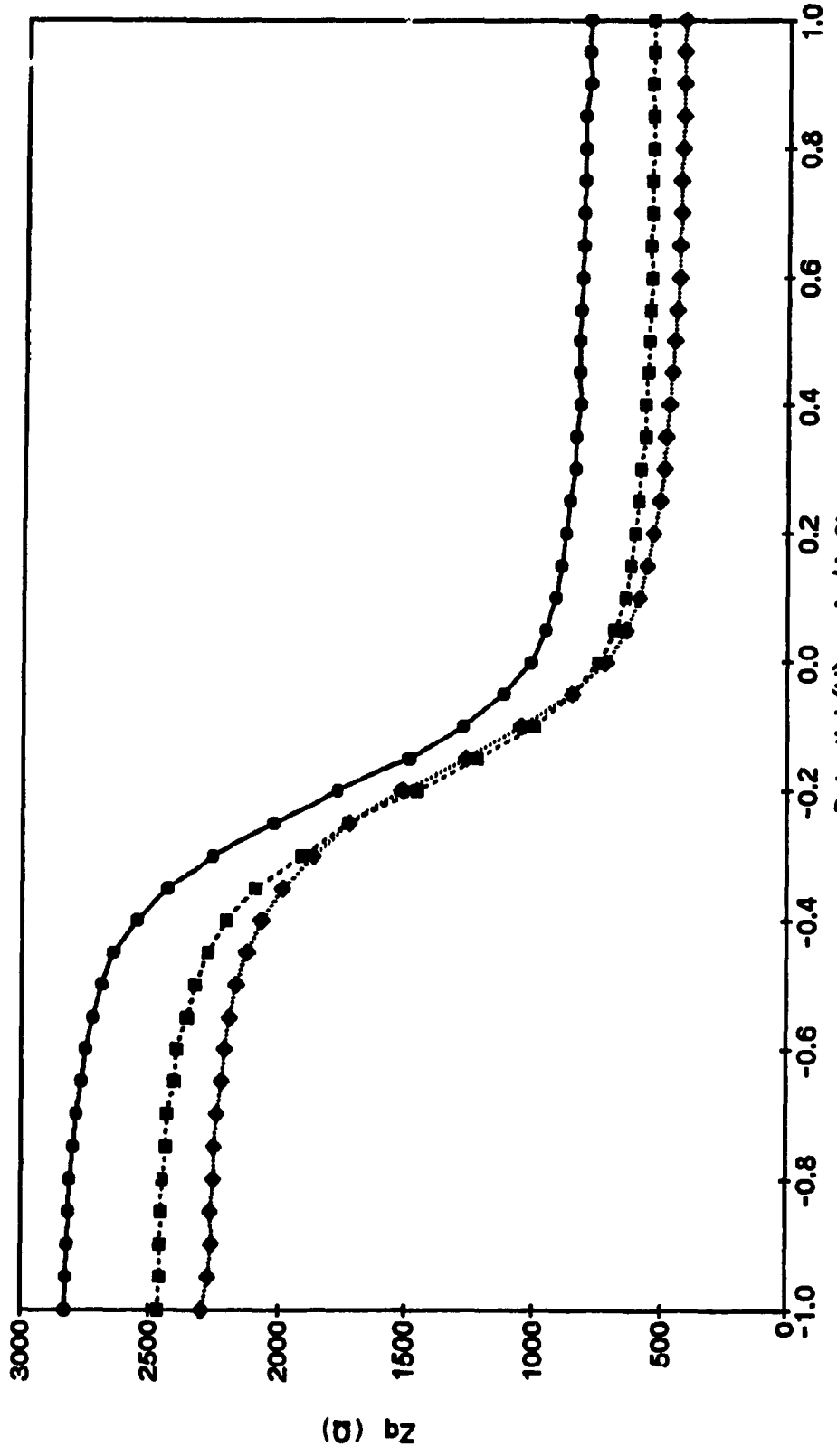

Figure 3.11B Out-of-phase impedance measurements on a silicon electrode for the determination of the NaCl concentration dependence. (Tris HCl salt concentration kept constant at 10 mM).

3.8 Hydroxylation of the Silicon Dioxide Surface

Treatment of the SiO_2 surface of the electrode with sulfochromic acid allows a surface of silanol groups to be generated by hydrolysis of siloxane bonds[34], as shown in Figure 3.12. The silanol surface is essential for binding 3-aminopropyltriethoxysilane to the surface of the SiO_2 substrate.

As shown in Figures 3.13(A, B), hydrolysis of surface siloxanes tends to decrease the measured impedance. There is an average change of -113 ± 75 ohms for Z_p maximum but there is no shift along the potential axis. The average changes for Z_p and Z_q vs V in the depletion range due to hydroxylation of the silicon dioxide surface are given in Table 3.1. A decrease is observed for both the in-phase and out-of-phase impedance and there is a small shift in V_{fb} of 30 ± 15 mV. The small changes observed in Z_p

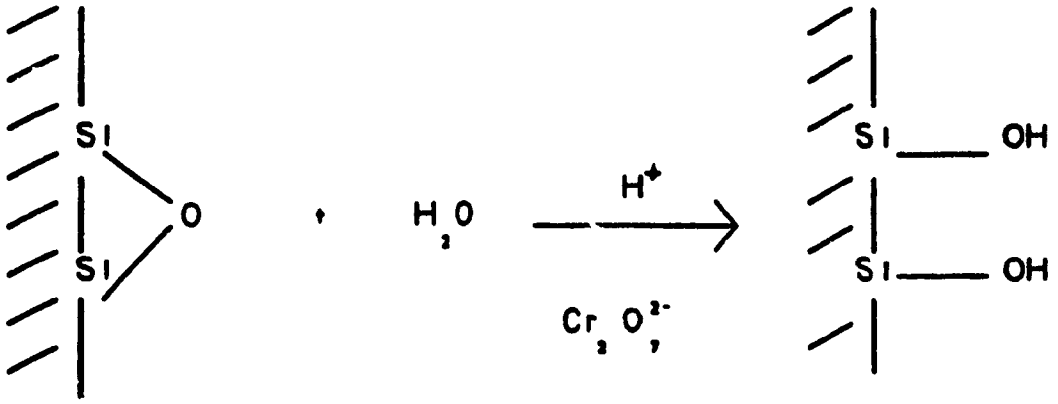

Figure 3.12 Hydroxylation of Silicon Dioxide Surface

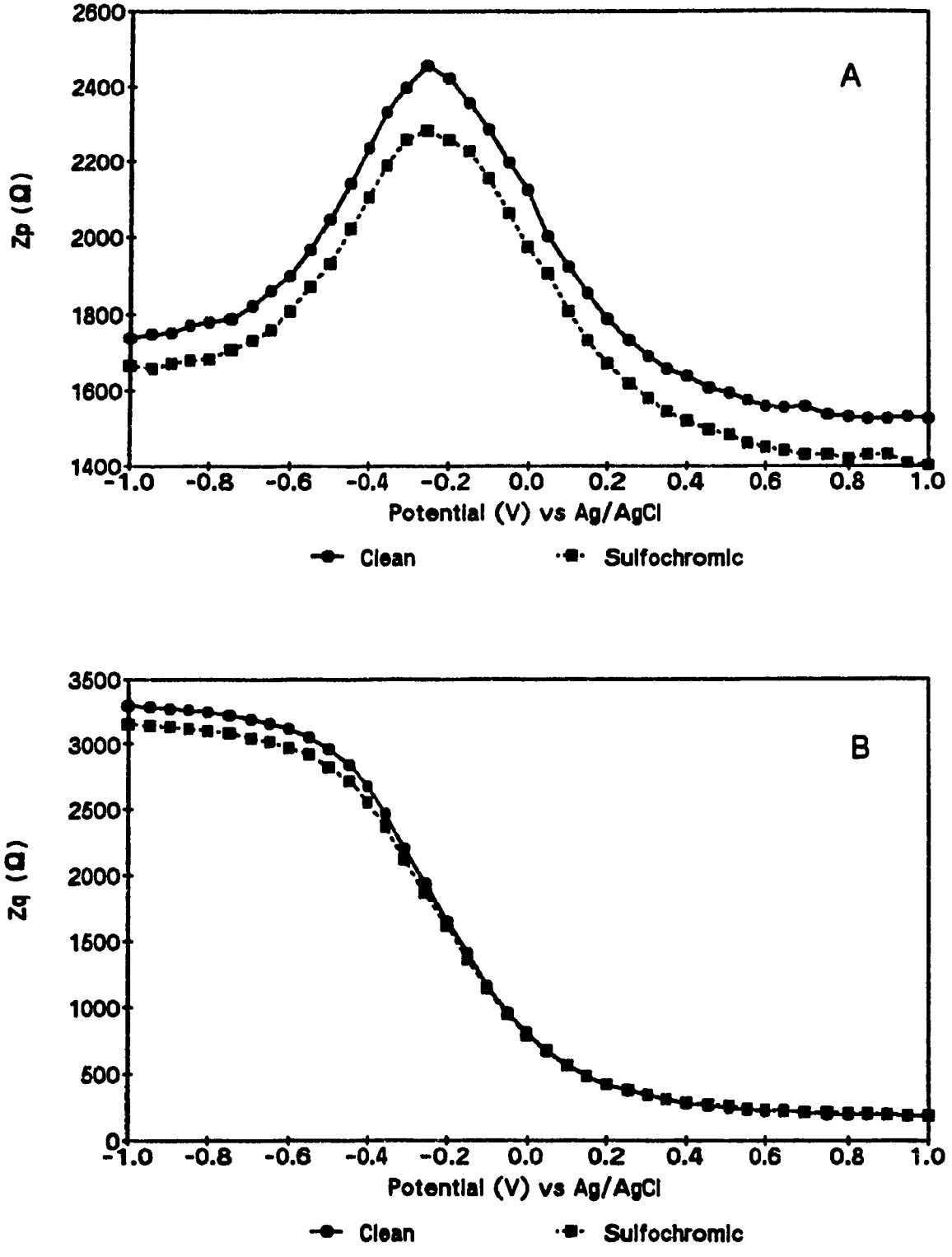

Figure 3.13 (A) In-phase and (B) Out-of-phase Impedance Measurements of an electrode following treatment with sulfochromic acid.

Table 3.1
Average Changes in Z_p and Z_q after Sulfochromic Treatment (average for 10 measurements made with 10 different electrodes).

Average Change of the peak maximum, in Z_p vs V curves	
$\triangle Z_p$ (ohms)	- 113 ± 75
$\triangle V$ (mV)	5 ± 1
Average Change of Z_q* and V_{fb}, in Z_q vs V curves	
$\triangle Z_q$ (ohms)	- 170 ± 82
$\triangle V_{fb}$ (mV)	- 30 ± 15

* The $\triangle Z_q$ value given in Table 3.1 (as in all subsequent tables reporting $\triangle Z_q$ values) is the value taken at -0.25 V vs Ag/AgCl, which is located in the middle of the depletion region and is the potential at which the maximum variation is observed in most cases.

could be due to changes in conductivity at the back contact (removal of grease possibly present due to handling) following cleaning with the sulfochromic acid solution. In fact all vertical shifts observed for the Z_p versus V curves could be due to changes in the quality of the electrical contacts made with the electrochemical cell; these include contact with the gold film of the working electrode, the counter electrode and the reference electrode.

3.9 Electrode Modification with Single Stranded DNA

Once we have hydroxylated the SiO_2 surface, it can then be modified with 3-aminopropyltriethoxysilane (APTS):

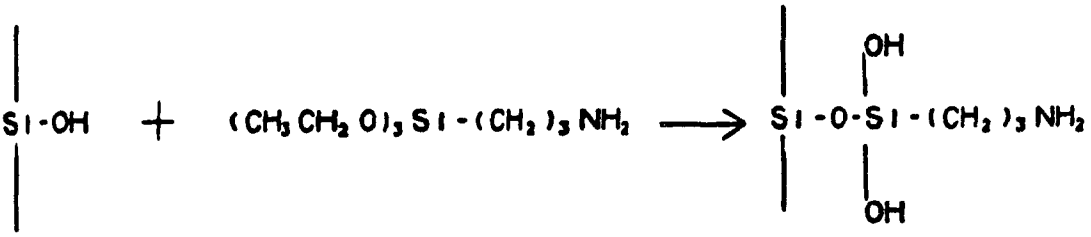

Figure 3.14 Modification of the silanol surface with APTS

This reagent was chosen for its reactivity with silanol groups in aqueous solution. Based on the work of Caravajal *et al* who have characterized APTS - modified silicas by silicon-29 and carbon-13 nuclear magnetic resonance[36], APTS shows many possible bonding schemes at the surface of SiO_2,

depending on the conditions under which it is attached (Figure 3.15). Under our conditions (5% aqueous APTS (v/v) and dried at room temperature) we expect bonding schemes A, B, C and D to prevail at the surface of our substrate. It should be noted that since the solution used for the subsequent covalent bonding of the DNA sequence to APTS is at a pH of about 8 (1 mg/ml of single stranded DNA in 1 M aqueous $NaHCO_3$ solution and 20 μl of 0.01M N-bromosuccinimide solution), the terminal NH_2 group is free for further modification as the pKa of the terminal NH_2 is 9.01[57], thus little protonation is taking place.

It has been observed that the APTS modification causes changes in the in-phase and out-phase impedance values as shown in Table 3.2. The peak of the Z_p vs V curve has a vertical shift of 72 ± 66 ohms and there is an horizontal shift of -50 ± 5 mV. The change observed for the Z_q is of -432 ± 268 mV and the average flatband potential change after the APTS modification is of -52 ± 10 mV.

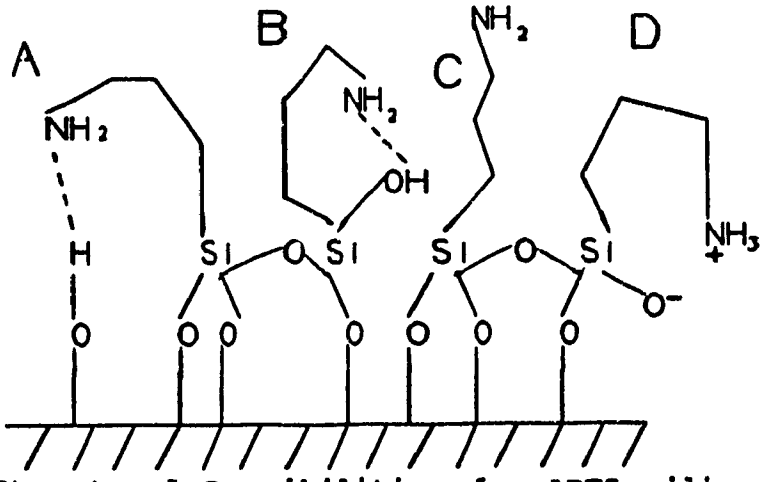

Figure 3.15 Structural Possibilities for APTS silicon dioxide surface[36].

Table 3.2
Average Changes in Z_p and Z_q after APTS Modification (average for 10 measurements made with 10 different electrodes).

Average Change of the peak maximum, in Z_p vs V curves	
$\triangle Z_p$ (ohms)	- 72 ± 66
$\triangle V$ (mV)	- 50 ± 5
Average Change of Z_q and V_{fb}, in Z_q vs V curves	
$\triangle Z_q$ (ohms)	- 432 ± 268
$\triangle V_{fb}$ (mV)	- 52 ± 10

Single stranded calf thymus DNA was reacted with N-bromosuccinimide resulting in the bromination of a fraction of the thymine bases. The bromine is then displaced by the primary amino group in the APTS-derivatized Si/SiO_2 electrode, (as shown in Figure 3.16).

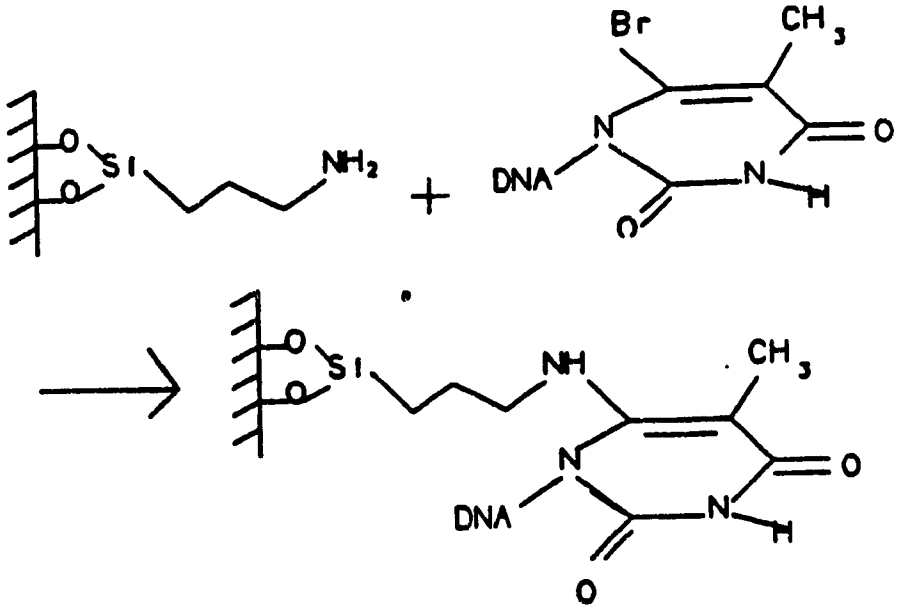

Figure 3.16 Displacement of the bromine by the primary amino

Figures 3.17(A, B) show that there are changes in the in-phase and out-of-phase impedance curves after each modification step. The impedance curves keep their general shape after each step, but they are shifted along the potential axis in the negative direction. These shifts indicate displacement of the flatband potential caused by the new charge distribution at the interface as a result of surface modifications.

Table 3.3 shows the average changes for Z_p and Z_q in the depletion region due to the single stranded calf thymus DNA modification. In the depletion region, the in-phase impedance curve, shows an average of horizontal shift of

Table 3.3
Average Changes in Z_p and Z_q after covalent modification with single stranded calf thymus DNA (average for 10 measurements made with 10 different electrodes).

Average Change of the peak maximum, in Z_p vs V curves	
$\triangle Z_p$ (ohms)	128 ± 102
$\triangle V$ (mV)	- 62 ± 19
Average Change of Z_q and V_{fb}, in Z_q vs V curves	
$\triangle Z_q$ (ohms)	- 495 ± 429
$\triangle V_{fb}$ (mV)	- 78 ± 43

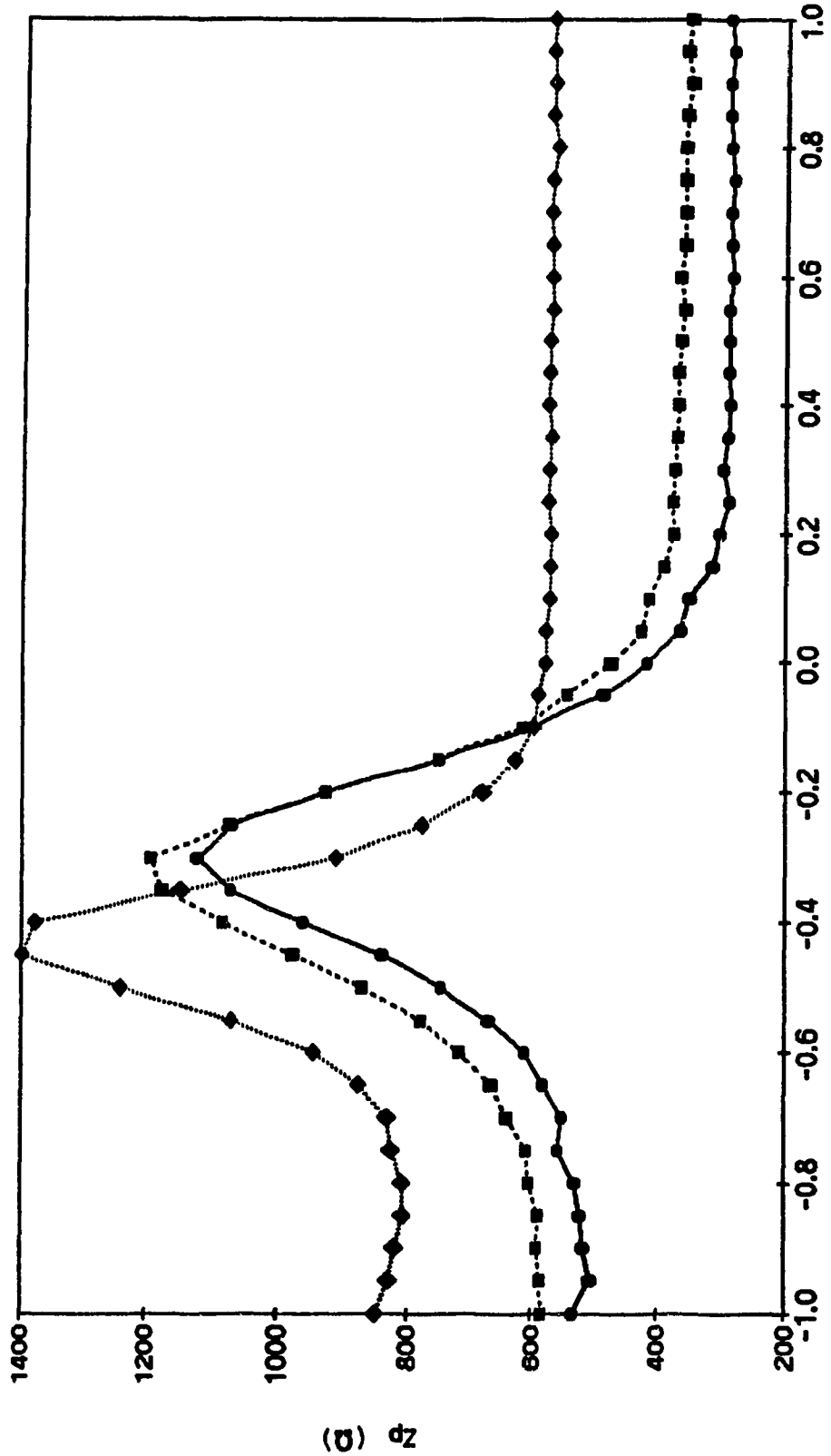

Figure 3.17A In-phase impedance measurements of a single stranded calf thymus DNA modified electrode.

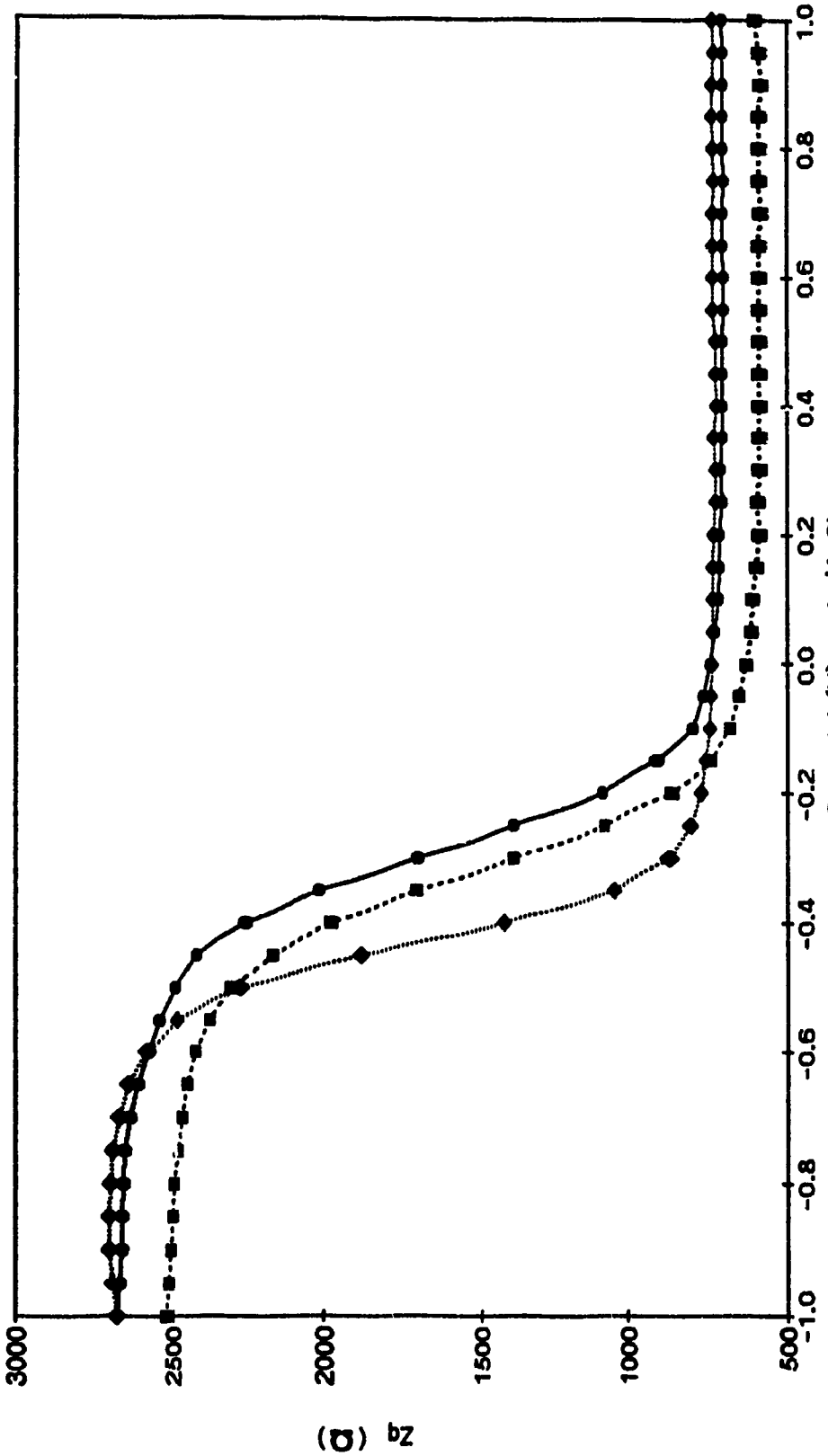

Figure 3.17B Out-of-phase impedance measurements of a single stranded calf thymus DNA modified electrode.

+128 ± 102 ohms and the average variation for the $Z_p$max is of -62 ± 19 mV. The out-of-phase impedance decreases upon modification and there is an average shift of -78 ± 43 mV for the flatband potential.

One of the main goals of this research was to prepare a sequence-selective DNA sensor based on impedance measurements. Single stranded calf thymus deoxyribonucleic acid (an average length of 15 million bases)[58], was replaced by oligothymidylic acid (oligo$(dT)_{20}$), a synthetic oligomer of 18-20 bases. A comparison was made with polythymidylic acid with an average length of 4,000 bases[58], poly (dT). As shown in Figures 3.18(A, B), for oligo$(dT)_{20}$ modification, and Figures II.1(A, B), for poly(dT) modification, similar results were obtained to those obtained with single stranded calf thymus DNA. Figures 3.17B, 3.18B and II.1B, show that upon modification with single stranded DNA, there is an average decrease of 800 to 1200 ohms in the depletion range.

Table 3.4 presents the average changes observed for Z_p and Z_q in the depletion range following the modifications with thymidylic acid oligomer and polymer. The modification with oligo$(dT)_{20}$ causes the maximum Z_p value to increase by 176 ± 103 ohms and to shift by -55 ± 9 mV along the potential axis. For the poly(dT) modification, the maximum Z_p value varies by +76 ± 66 ohms and the potential shift is of -60 ± 16 mV. The average change in flatband potential is of -48 ± 13 mV and -90 ± 58 mV for the oligo$(dT)_{20}$ and poly(dT) modifications, respectively.

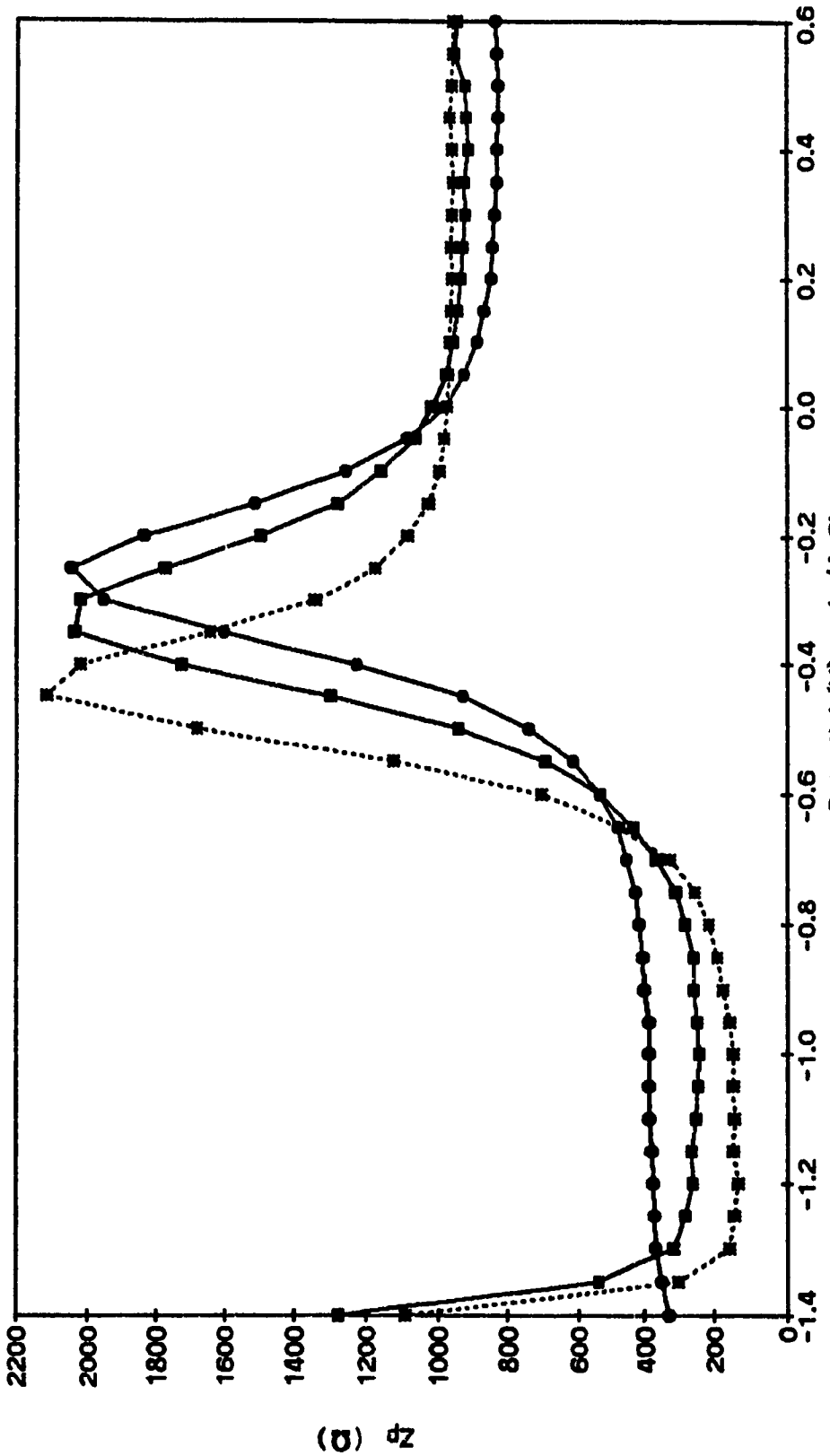

Figure 3.18A Comparison of in-phase impedance measurements of a sulfochromic treated, APTS modified and oligo$(dT)_{20}$ modified electrode.

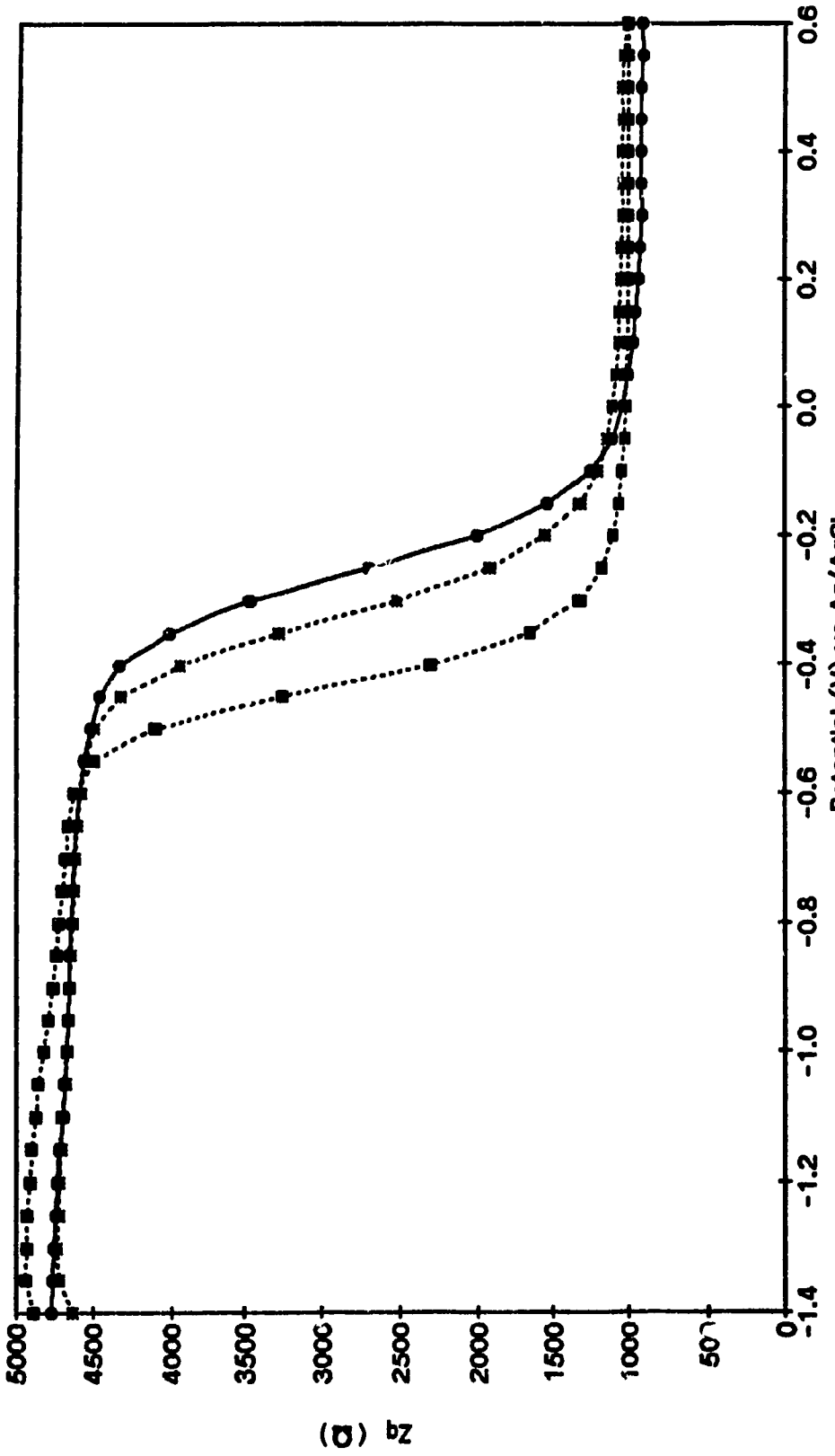

Figure 3.18B Comparison of out-of-phase impedance measurements of a sulfochromic treated, APTS modified, and oligo$(dT)_{20}$ modified electrode.

Table 3.4
Average Changes in Z_p and Z_q after Oligo$(dT)_{20}$ and Poly(dT) Modifications (average for 10 measurements made with 10 different electrodes for each type of modification).

Average Change of the peak maximum, in Z_p vs V curves		
	APTS-Oligo$(dT)_{20}$	APTS-Poly(dT)
$\triangle Z_p$ (ohms)	176 ± 103	76 ± 66
$\triangle V$ (mV)	- 55 ± 9	- 60 ± 16
Average Change of Z_q and V_{fb}, in Z_q vs V curves		
	APTS-Oligo$(dT)_{20}$	APTS-Poly(dT)
$\triangle Z_q$ (ohms)	- 602 ± 510	- 387 ± 290
$\triangle V_{fb}$ (mV)	- 48 ± 13	- 90 ± 153

3.10 Stability of Modified Electrodes

Since one of the objectives of this research was to create a stable as well as sensitive electrode, we first considered the stability of the device after reaction with APTS. Because APTS is covalently bound to the surface, a stable signal is expected. Figures II.2(A, B) of Appendix II show that the in-phase (Z_p) and out-of-phase (Z_q) impedance versus potential curves, following APTS modification, do not shift along the potential axis after exposure of the electrode to boiling deionized water for 30 minutes, but the maximum Z_p value is reduced by approximately 300 ohms. This reduction in impedance could be

attributed to the removal of excess APTS from the silanol surface, or to a change in the quality of the electrical contact.

The stability of the single stranded DNA modified electrodes was examined using the same procedure as used for the APTS layer, but in four consecutive steps. A small decrease in impedance (about 300 ohms) can be seen in the Z_p versus V curve (Figure II.3A) after the second exposure of the electrode to boiling deionized water. No change in curvature was observed between the second and fourth exposures of the electrode to boiling deionized water. In the Z_q versus V curve (Figure II.3B) the flatband potential remains unchanged after 4 boiling treatments; however, a decrease in impedance of about 250 ohms is observed in the inversion region following the first boiling treatment only. Again the decrease in impedance mentioned above could be a consequence of a slight loss of single stranded DNA from the sensing surface or a change in the quality of the electrical contact. Figures II.4(A, B) correspond to the curves obtained with a poly(dT) modified electrode, and show similar results to those of the oligo$(dT)_{20}$ modified electrode (Figures II.3(A, B)).

The storage stability of DNA-modified electrodes in the electrolyte (buffer) is shown in Figures 3.19(A, B) for oligo$(dT)_{20}$ (Figures II.5(A, B) for poly(dT)). The results show that oligo$(dT)_{20}$ and poly(dT) modified electrodes are

stable to at least 6 hours of storage at 22°C. This stability allows studies of *in situ* hybridization with a complementary strand.

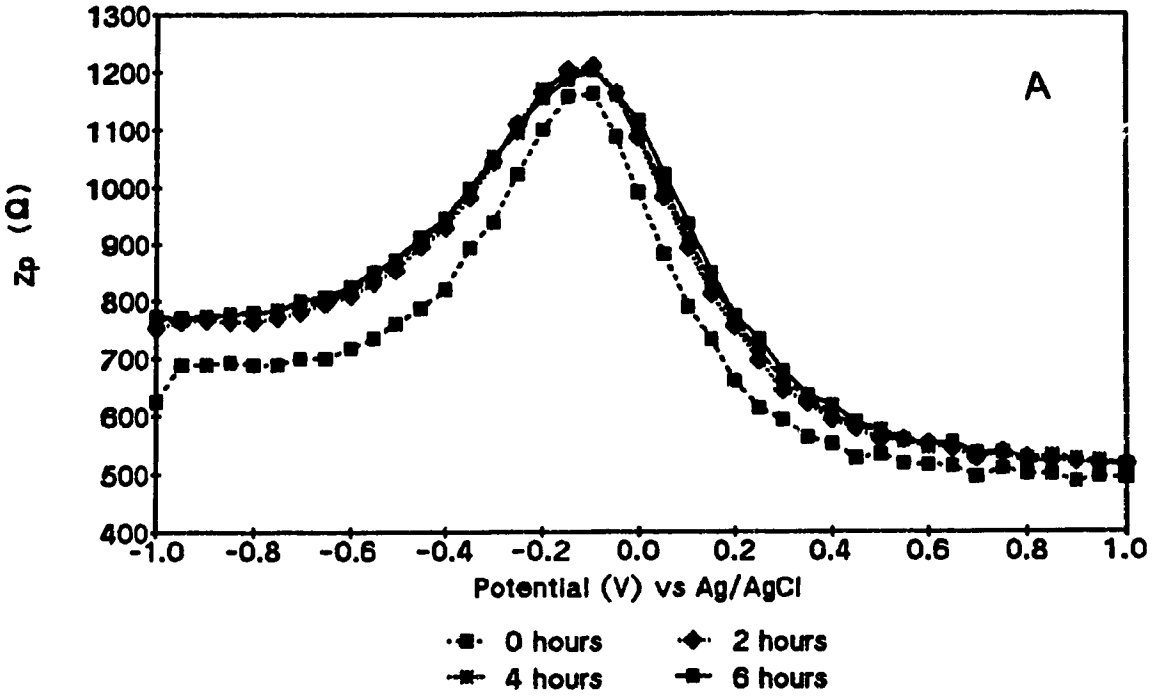

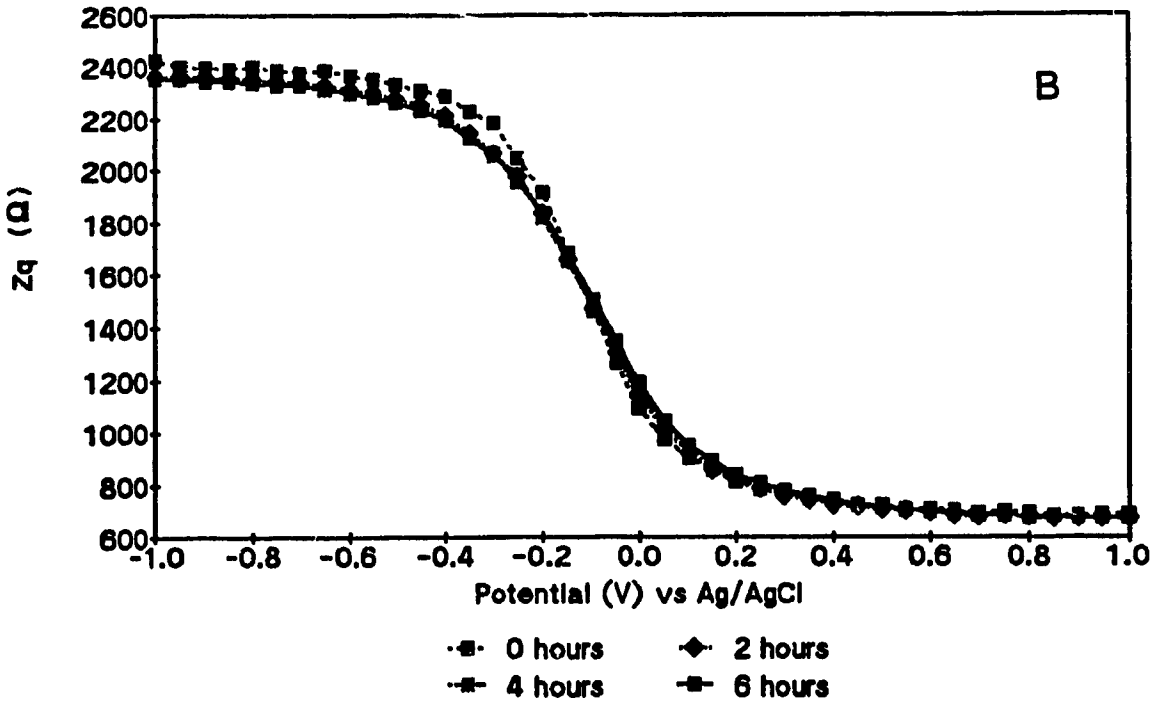

Figure 3.19 (A) In-phase and (B) Out-of-phase impedance measurements to study storage stability of an oligo$(dT)_{20}$ modified electrode in Tris HCl.

CHAPTER 4

RESULTS AND DISCUSSION: PART II
SELECTIVITY, SENSITIVITY AND REVERSIBILITY OF DNA MODIFIED SILICON ELECTRODES

4.1 Overview

Today, a variety of DNA probes are available in research and development laboratories, such as double stranded DNA, synthetic oligonucleotides and single stranded cRNA[59]. In all cases, the extent of hybridization between the nucleic acid sequences and probes is proportional to their degree of homology. Strict conditions of hybridization are set so as to ensure a high degree of specificity for the target sequence.

DNA probes may be used with a wide range of methods, each exploiting the strategy of molecular hybridization in a slightly different way[59]. Three commonly used methods that employ DNA probes for the detection of target sequences are filter hybridization, southern blotting, and sandwich hybridization. In filter-based assays, the sample DNA is immobilized onto a filter and the labelled DNA probe is in solution. The southern blotting method involves the transfer of an entire electrophoretic separation to a nitrocellulose membrane, which is then exposed to the labelled DNA probe. The sandwich hybridization technique employs an activated solid support having an immobilized capture probe and a labelled detection probe. All of these methods require labelled DNA probes[50b].

A direct detection of the hybridization by impedance measurements on Si/SiO_2 substrates modified with single stranded DNA is presented. We will show in this chapter that when such DNA electrodes are placed in contact with a specific single stranded oligomer or polymer, the hybridization that takes place with the immobilized strand induces a variation of the heterostructure impedance: any variation of the surface potential causes a shift of the out-of-phase impedance versus voltage curve in the depletion range (a change in V_{fb}). The capacitance, which is related to the thickness of the layer of immobilized biomolecules, can be obtained directly from the impedance measurements in the accumulation range. With the impedance technique used in this research it is possible to monitor both batch and *in situ* hybridizations. It should be noted that with the impedance technique, no labeling of the DNA is needed.

4.2 Batch Hybridization

Batch hybridization is the simplest of both techniques as it involves the placement of denatured (single strand) DNA on the hydroxylated silicon electrode surface as previously mentioned. The hybridization takes place by directly applying the complementary strand to the modified single stranded electrode.

As it was mentioned in Chapter 3, the silicon electrode has been modified with two different synthetic thymidylic acid strands, one 18-20 bases long (oligo$(dT)_{20}$) and the

other 4,000 bases long (poly(dT)). We will show that hybridization of both types of strands with a complementary strand, adenylic acid, generates a significant signal. The type of bonds between thymidylic acid and adenylic acid are shown in Figure 4.1.

4.2.1 Hybridization with Poly(dA)

Figure 4.2(A, B) corresponding to an electrode modified with poly(dT) (Figure II.6 for oligo$(dT)_{20}$), shows the results obtained upon direct application of the same quantity of poly(dA). In the in-phase impedance versus

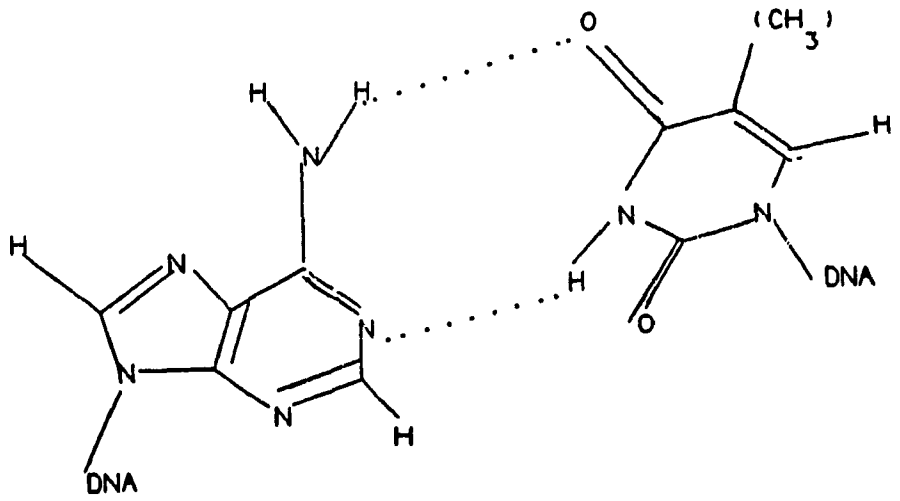

Figure 4.1 Complementary base pairing (A=T) of Adenine and Thymine, illustrating the hydrogen bonds.

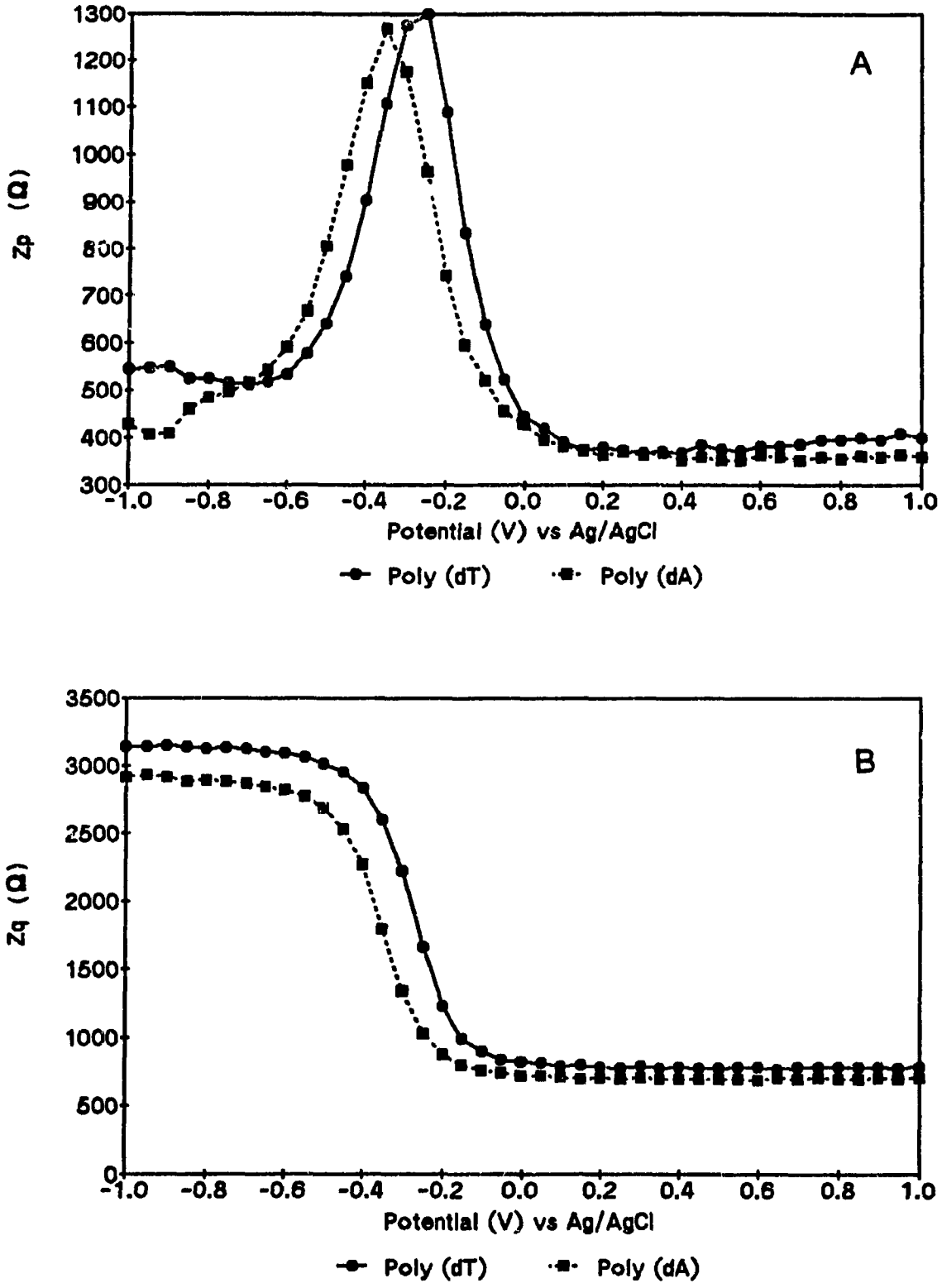

Figure 4.2 (A) In-phase and (B) Out-of-phase impedance measurements of a poly(dT) - poly(dA) modified electrode.

potential curve, a shift of the peak towards a more negative potential is observed upon hybridization. The shift due to poly(dT)-poly(dA) hybridization (Figure 4.2) is more pronounced than that corresponding to the oligo$(dT)_{20}$-poly(dA) hybridization (Figure II.6(A, B)). These differences can be explained if we take into account the length of the thymidylic acid strand involved in each of the two cases. The poly(dT) electrode provides a much greater number of bases over which hybridization takes place with the poly(dA).

In the out-of-phase impedance versus potential graphs, in both cases, the impedance in the depletion range decreases upon hybridization (capacitance increases), and this change is more pronounced for the poly(dT) modified electrode than for the oligo$(dT)_{20}$ modified electrode. A decrease in out-of-phase impedance is also in agreement with the greater variation of surface charges expected in the case of poly(dT) modified electrode in comparison to that of the oligo$(dT)_{20}$ electrode, due to the negative charges in the phosphates of the single stranded DNA[60].

4.2.2 Hybridization with Oligo$(dA)_{18}$

If the electrcdes modified with single stranded DNA are hybridized with oligo$(dA)_{18}$, Figures II.7(A, B) and II.8(A, B) are obtained, corresponding to oligo$(dT)_{20}$ and poly(dT) modified electrodes respectively. Except for a decrease of about 200 ohms (Z_p and Z_q) in the inversion region (Figure

II.7) for the oligo$(dT)_{20}$ - oligo$(dA)_{18}$ system, results similar to those found upon hybridization with the longer adenylic acid strand, poly(dA), are obtained. In the in-phase impedance versus potential curves (Figures II.7A and II.8A), there is a shift towards a more negative potential upon application of the oligo$(dA)_{18}$ to the poly(dT) or oligo$(dT)_{20}$ modified electrodes. Again, the shift observed for the out-of-phase curve is slightly more prominent with the poly(dT) modified electrode, but still, neither of these changes are as pronounced as those observed in the case of poly(dT)-poly(dA) (Figure 4.2B). In the depletion region of Figure 4.2B, at the dc potential of -0.25 V, there is a difference of 750 ohms between the out-of-phase impedance value for the single stranded and the double stranded electrode. But for poly(dT)-oligo$(dA)_{18}$ (Figure II.8B), in the middle of the depletion range, which is also at -0.25 V dc potential, the difference in out-of-phase impedance is only of 400 ohms. The impedance decrease could be due to an increase in the dielectric constant upon formation of the double stranded DNA or to a decrease in the thickness of the surface layer upon hybridization.

4.2.3 Capacitance of Heterostructures for Batch Hybridization

The plot of capacitance versus potential can be related to the dielectric layer thickness of the electrode as previously mentioned. Figure 4.3 shows the typical variation

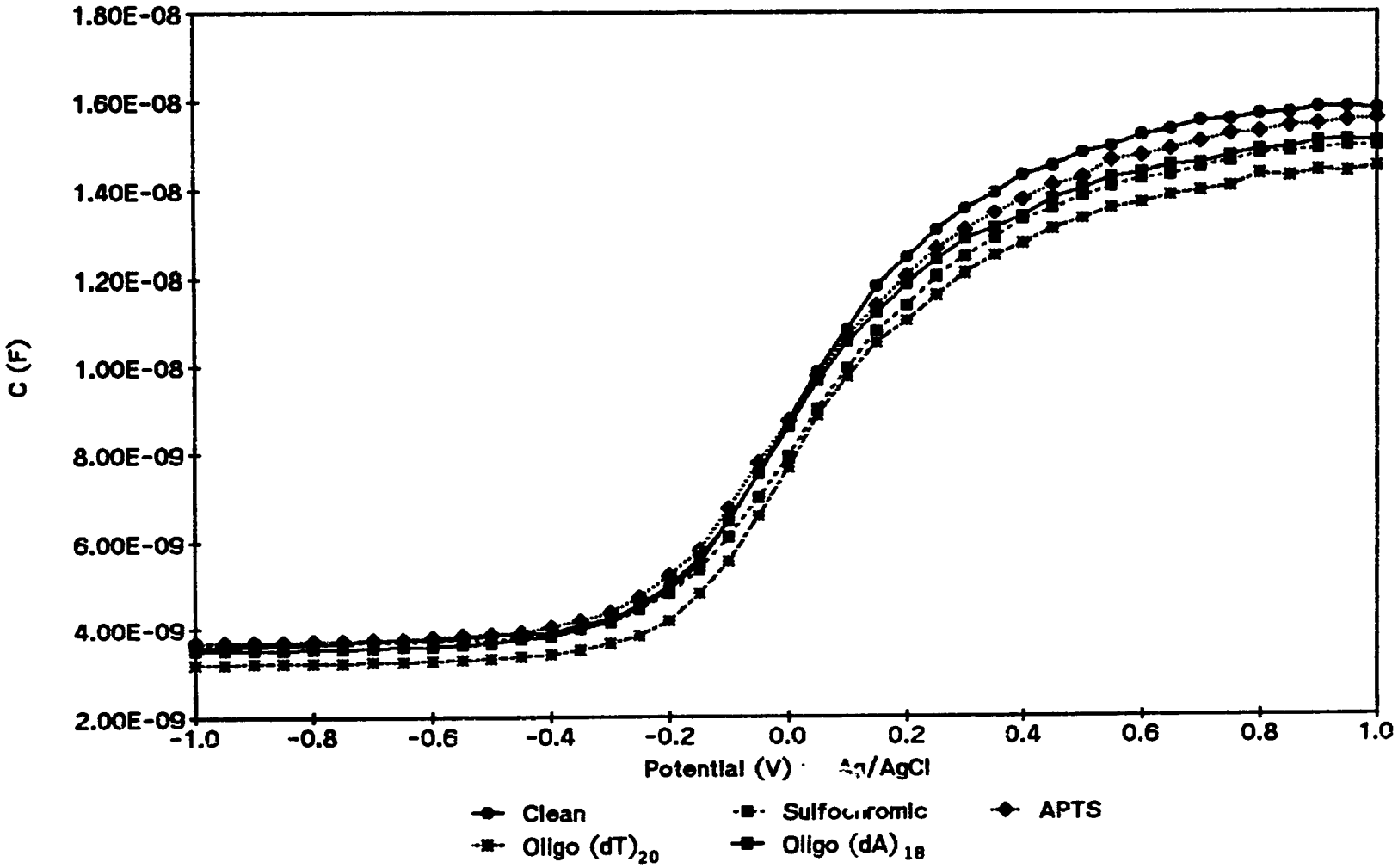

Figure 4.3 Capacitance measurements of an oligo$(dT)_{20}$ modified electrode hybridized with oligo$(dA)_{18}$.

of the capacitance upon modification of the electrode surface. The capacitance was calculated from Z_q versus V curves given in Appendix II (Figure II.9) using equation 7. This plot corresponds to an oligo$(dT)_{20}$ modified electrode batch hybridized with oligo$(dA)_{18}$. Similar graphs for oligo$(dT)_{20}$ - poly(dA), poly(dT) - poly(dA), and poly(dT) - oligo$(dA)_{18}$, are found in Appendix II, (Figures II.10(A, B), II.11(A, B), and II.12(A, B)).

If one attempts to interpret the capacitance results strictly in terms of variations of the overlayer thickness, discrepancies appear as demonstrated by the values given in Table 4.1. It is observed in Figure 4.3 that except for the APTS modification and the hybridization step, there is a capacitance decrease after each modification. The discrepancy is particularly clear with respect to the APTS modification where one expects a decrease in capacitance corresponding to an increase in the thickness of the overlayer. Clearly these results tend to indicate that another variable, namely the dielectric constant of the grafted compounds, need to be taken into account. An increase in dielectric constant at the heterostructure interface can also lead to an increase in capacitance and further study is required to clarify this point. Although the situation with respect to the APTS modification is not clear at this time, there are indications in the literature that point to a substantial increase in dielectric constant which occurs upon hybridization.

Table 4.1
Average change in layer thickness following each step of substrate modification of the substrate.

Modification	Change in Thickness (Å)
Unmodified	---
Hydroxylated*	+ 10.3 ± 5
APTS*	- 7.1 ± 2
$Oligo(dT)^{*}_{20}$	+ 13.0 ± 3
$Oligo(dT)_{20}$ - $Oligo(dA)^{\#}_{18}$	- 6.7 ± 6
$Oligo(dT)_{20}$ - $Poly(dA)^{\#}$	- 11.9 ± 4
Poly(dT)*	+ 11.9 ± 8
Poly(dT) - $Oligo(dA)^{\#}_{18}$	- 6.2 ± 5
Poly(dT) - $Poly(dA)^{\#}$	- 14.4 ± 3

* For these modifications the averages are for 5 different sample preparations.

For the hybridization steps the averages are for 2 different preparations.

Double helical deoxyribonucleic acid has a highly ordered internal structure with a remarkable regularity. On the other hand, single stranded DNA is a random coil polymer with no internal regularity[60]. It is quite reasonable to assume that double stranded DNA has a large permanent dipole moment because of the repeating polar structural units with the polarity in one direction[61,62]. Takashima *et al* found the high frequency dielectric constants of single and double stranded calf thymus DNA to be 20 and 1500 dielectric units respectively[63]. Takashima carried out the dielectric measurements with DNA samples fragmented by sonic oscillations. It may also be possible that a slight decrease in layer thickness may be contributing to the lower impedance values observed upon hybridization.

4.2.4 Reversibility and Reproducibility of Batch Hybridization at Modified Electrodes

One of the objectives of this research is to produce a reusable electrode capable of detecting the complementary strand several times before complete remodification of the electrode is needed. By denaturing the hybridized oligomer or polymer modified electrode, it is possible to reuse it several times. In this work six successive hybridizations have been observed using the same modified electrode, which was achieved using the oligo$(dT)_{20}$ - poly(dA) combination. Results were also obtained for three successive hybridizations using the poly(dT) - oligo $(dA)_{18}$ combination,

and these graphs can be found in Appendix II, Figures II.13(A, B) and II.14(A, B).

Figures 4.4(A, B) correspond to a poly(dT) modified electrode (Figures II.15(A,B) for oligo$(dT)_{20}$). For clarity, the Figures for only the first two successive hybridizations are shown. It is observed that in both cases the peak for the in-phase impedance of the denatured electrode decreases in comparison to that of the original electrode. Whereas in the plot of the out-of-phase impedance versus potential, the impedance in the depletion region increases slightly after denaturing the electrode. Upon rehybridization the in-phase impedance peak is very similar to that obtained on the first hybridization, the impedance increases and it is shifted back towards a more negative potential due to the change of surface state charge at the modified semiconductor electrode/electrolyte interface. In the out-of-phase curves we can observe an impedance decrease in the depletion region upon rehybridization similar to that obtained after the first hybridization.

Tables 4.2 and 4.3, for poly(dT)-poly(dA) and oligo$(dT)_{20}$-poly(dA) respectively, show the results corresponding to the average changes for Z_p and Z_q in the depletion range, observed with hybridized and denatured modified electrodes. It is shown that the average changes in the depletion range for hybridization, denaturing and rehybridization steps for the poly(dT)-poly(dA) combination (Table 4.2) are more significant than those observed for the

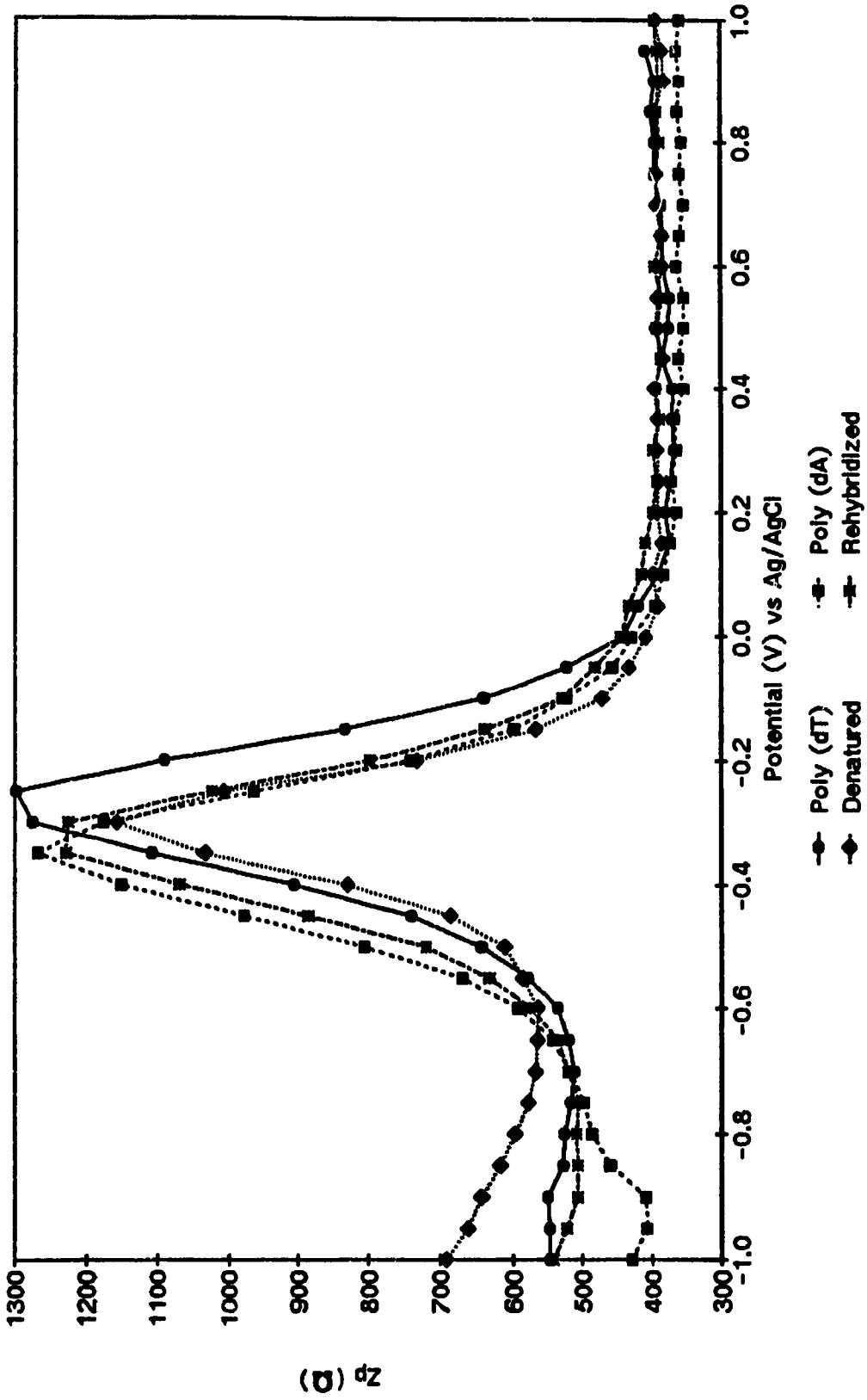

Figure 4.4A In-phase impedance measurements of a poly(dT) modified electrode hybridized twice with poly(dA).

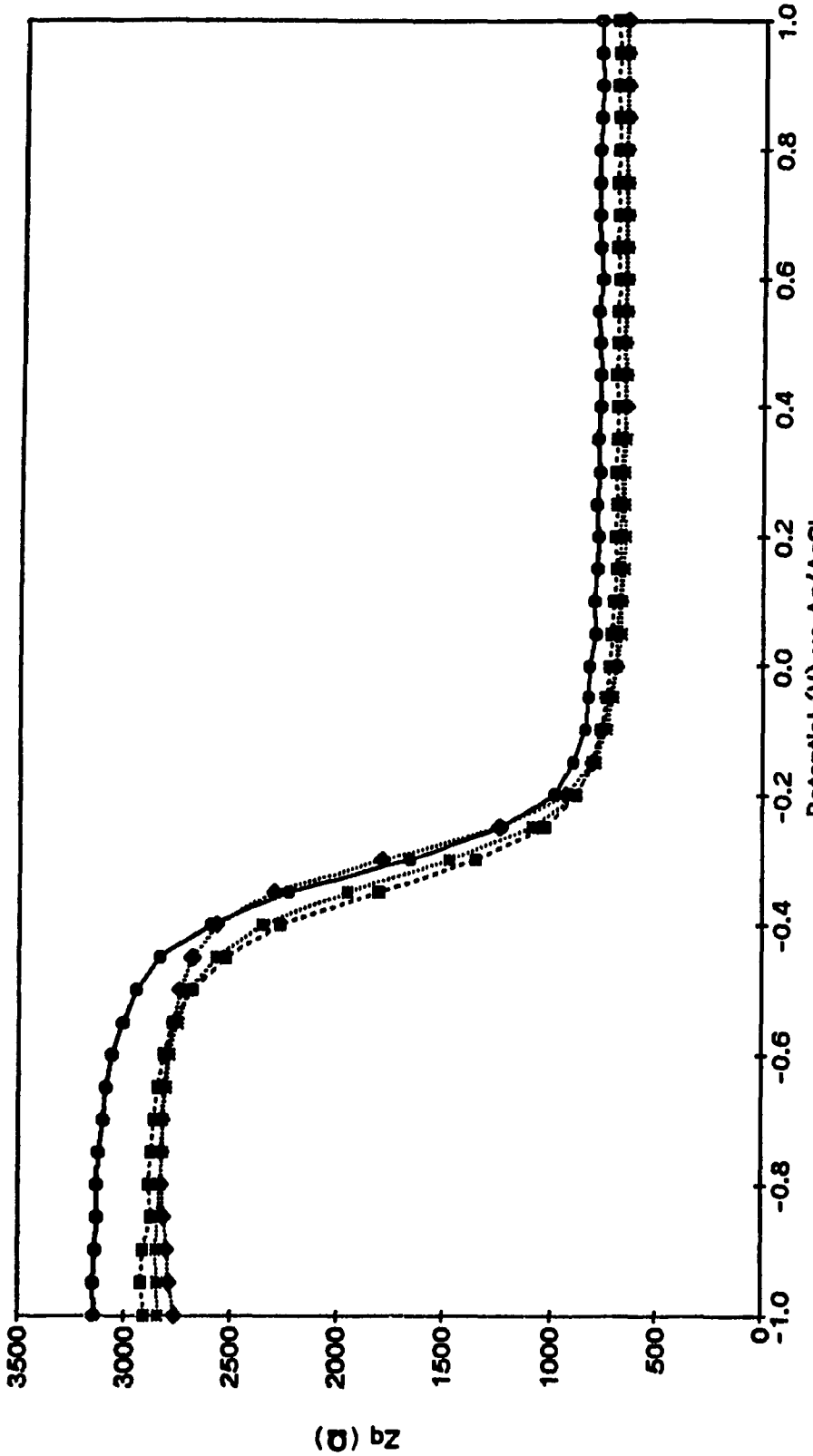

Figure 4.4B Out-of-phase impedance measurements of a poly(dT) modified electrode hybridized twice with poly(dA).

Table 4.2
Average Changes for Z_p and Z_q in the Depletion Range for a Poly(dT) Modified Electrode, Hybridized with Poly(dA) (average for measurements made with 5 different electrodes).

Average Change of the peak maximum, in Z_p vs V curves			
	First Hybridization	First Denaturing	Second Hybridization
$\triangle Z_p$(ohms)	69 ± 35	91 ± 13	37 ± 17
$\triangle V$ (mV)	- 51 ± 5	48 ± 3	- 52 ± 7
Average Change of Z_q and V_{fb}, in Z_q vs V curves			
	First Hybridization	First Denaturing	Second Hybridization
$\triangle Z_q$ (ohms)	- 346 ± 110	577 ± 383	- 583 ± 257
$\triangle V_{fb}$ (mV)	- 45 ± 24	50 ± 30	- 56 ± 26

Table 4.3
Average Changes for Z_p and Z_q in the Depletion Range for an Oligo$(dT)_{20}$ Modified Electrode, Hybridized with Poly(dA) (average for measurements made with 5 different electrodes).

Average Change of the peak maximum, in Z_p vs V curves			
	First Hybridization	First Denaturing	Second Hybridization
$\triangle Z_p$(ohms)	64 ± 30	294 ± 130	148 ± 88
$\triangle$V (mV)	- 46 ± 6	51 ± 3	- 48 ± 5
Average Change of Z_q and V_{fb}, in Z_q vs V curves			
	First Hybridization	First Denaturing	Second Hybridization
$\triangle Z_q$ (ohms)	- 154 ± 58	324 ± 90	- 169 ± 71
$\triangle V_{fb}$ (mV)	- 30 ± 8	40 ± 12	- 30 ± 8

oligo$(dT)_{20}$-poly(dA) combination (Table 4.3). For poly(dT) modified electrodes, the position of the maximum Z_p is shifted along the potential axis by -51 ± 5 mV upon hybridization and by +48 ± 3 mV upon denaturing, similar results are observed for oligo$(dT)_{20}$ modified electrodes. The average shifts of flatband potential and of Z_q in the depletion range ($\triangle Z_q$), are consistently larger for the poly(dT) modified electrode than for the oligo$(dT)_{20}$ modified electrode.

Similar results to those obtained when hybridization took place with poly(dA) were found upon hybridization with oligo$(dA)_{18}$ (Figures II.16(A, B) and II.17(A, B)). Tables 4.4 and 4.5, show the average changes for Z_p and Z_q in the depletion range for the oligo$(dT)_{20}$-oligo$(dA)_{18}$ and poly(dT)-oligo$(dA)_{18}$ combinations, respectively.

Table 4.4
Average Changes for Z_p and Z_q for an Oligo$(dT)_{20}$ Modified Electrode, Hybridized with Oligo$(dA)_{18}$ (average for measurements made with 5 different electrodes).

Average Change of the peak maximum, in Z_p vs V curves			
	First Hybridization	First Denaturing	Second Hybridization
$\triangle Z_p$ (ohms)	43 ± 26	39 ± 29	35 ± 16
$\triangle V$ (mV)	- 44 ± 8	57 ± 12	- 50 ± 12
Average Change of Z_q and V_{fb}, in Z_q vs V curves			
	First Hybridization	First Denaturing	Second Hybridization
$\triangle Z_q$ (ohms)	- 235 ± 109	166 ± 64	- 202 ± 115
$\triangle V_{fb}$ (mV)	- 40 ± 14	44 ± 15	- 40 ± 14

Table 4.5
Average Changes for Z_p and Z_q for a Poly(dT) Modified Electrode, Hybridized with $Oligo(dA)_{18}$ (average for measurements made with 5 different electrodes).

Average Change of the peak maximum, in Z_p vs V curves			
	First Hybridization	First Denaturing	Second Hybridization
$\triangle Z_p$ (ohms)	62 ± 43	21 ± 8	12 ± 6
$\triangle V$ (mV)	- 52 ± 4	50 ± 3	- 47 ± 5
Average Change of Z_q and V_{fb}, in Z_q vs V curves			
	First Hybridization	First Denaturing	Second Hybridization
$\triangle Z_q$ (ohms)	- 264 ± 99	268 ± 102	- 138 ± 73
$\triangle V_{fb}$ (mV)	- 42 ± 11	58 ± 25	- 42 ± 11

4.2.5 Selectivity and Interference Effects During Batch Hybridization

4.2.5.1 Selectivity

To ensure that the changes seen in the in-phase and out-of-phase impedance curves upon hybridization were actually due to hybridization taking place at the modified electrode surface, several control electrodes have been tested.

Figures II.18(A,B) correspond to an oligo$(dT)_{20}$ modified electrode upon direct application of single stranded calf thymus DNA at room temperature (22 °C). In the in-phase impedance versus potential curve we are able to see the change in the position of the peak in relation to the applied dc bias. Upon hybridization, the in-phase impedance peak is shifted towards a more negative potential as was observed upon hybridization with a synthetic strand. After denaturing the electrode, the curve shifts back, close to the original position. Upon rehybridization, the results approach the in-phase and out-of-phase curves obtained upon the first hybridization of the electrode. These results were compared to those obtained with a poly(dT) modified electrode, (Figure II.19(A, B)). The results obtained upon rehybridization of this electrode with single stranded calf thymus DNA, however, were not reproducible.

This may indicate that the oligo$(dT)_{20}$ and poly(dT) modified electrodes can to some extent hybridize with single stranded calf thymus DNA, but that this hybridization depends upon the probability of getting a sequence of adenosine residues in the calf thymus DNA, long enough to cause a

change in impedance at the modified electrode/electrolyte interface. This probability could well reflect geometric restrictions involved which can prevent random base pairing.

Another control electrode was prepared to verify that the changes observed in the in-phase and out-of-phase impedance curves are due to thymidylic acid - adenylic acid pairing. Figures 4.5(A, B) correspond to the effect observed upon direct application of poly(dC) on an oligo$(dT)_{20}$ modified electrode (Figures II.20(A,B) for poly(dT)). The cytidylic acid polymer has little effect on the surface of these modified electrodes as there is only a very slight change in the Z_q impedance curves in the depletion range between the single stranded modified electrode and the "would be" double stranded modified electrode, thus no hybridization takes place as expected.

A blank hybridization was also done to verify that the results obtained upon application of adenylic acid solution to the thymidylic acid modified electrode are due only to the hybridization. These results can be observed in Figures II.21(A, B). To an oligo$(dT)_{20}$ modified electrode, 4.0 μL of 1M aqueous $NaHCO_3$ solution were applied and only a very slight change in the impedance curves was observed, particularly with respect to V_{fb}, in comparison to the changes observed with the hybridization of the same electrode with oligo$(dA)_{18}$. Although the sodium bicarbonate does cause slight changes in the impedance values over the dc range

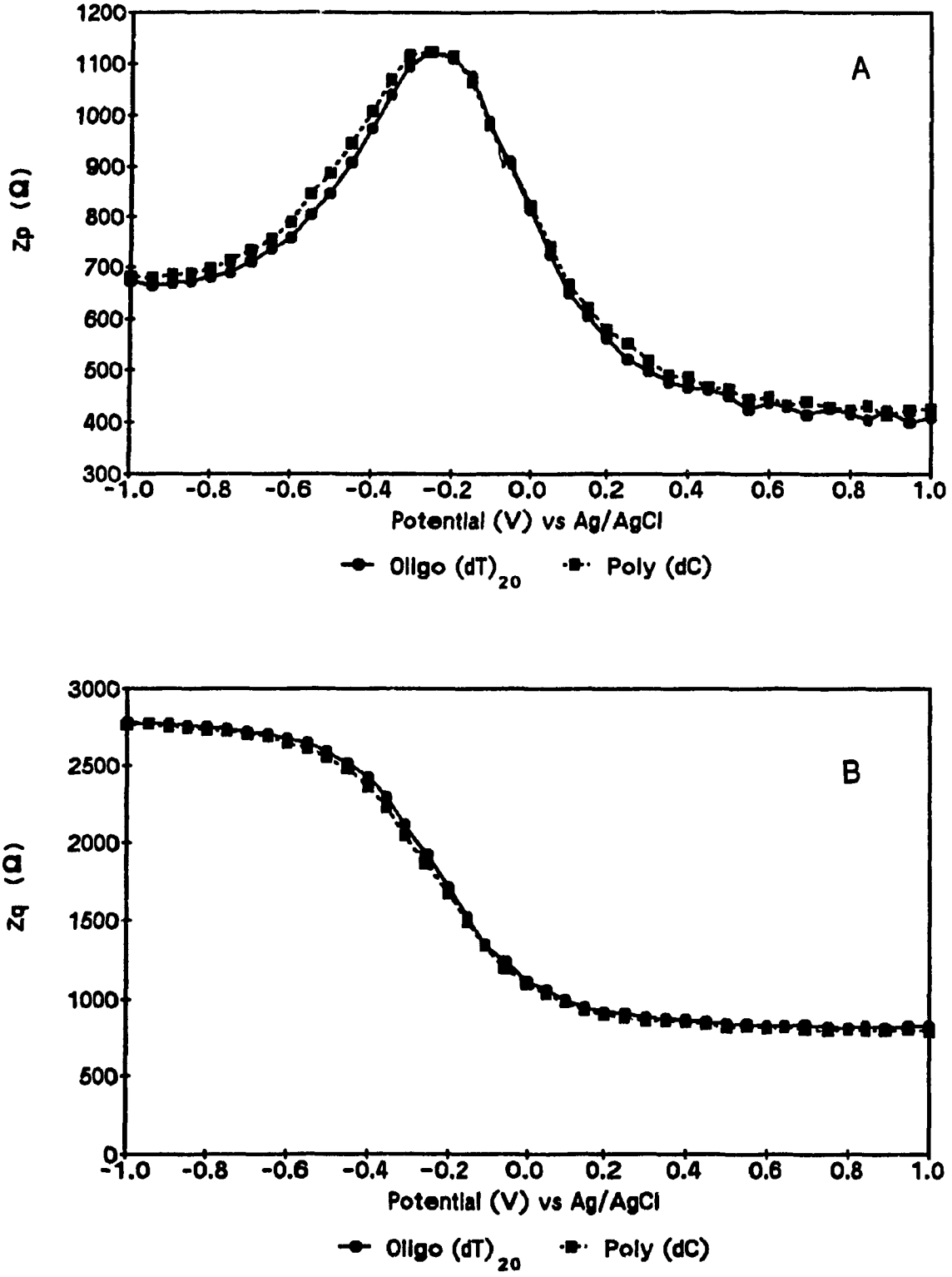

Figure 4.5 (A) In-phase and (B) Out-of-phase impedance measurements of an oligo$(dT)_{20}$ modified electrode hybridized with poly(dC).

covered, the changes in V_{fb} observed in the out-of-phase impedance curves are therefore attributed to thymine-adenine base pairing.

4.2.5.2 Interference Effects

As a first step in identifying possible interference effects when detecting a specific oligonucleotide, solutions of oligo$(dA)_{18}$ with single stranded calf thymus DNA, and poly(dA) with single stranded calf thymus DNA, with a 1:1 ratio, were prepared. These solutions were directly applied to the modified electrodes. Figures II.22(A, B) and Figures II.23(A, B) show the results of a batch hybridization with oligo$(dA)_{18}$ and single stranded (calf thymus) DNA onto oligo$(dT)_{20}$ and poly(dT) modified silicon electrodes respectively. Similar results were observed when the hybridization of the modified electrodes was obtained with application of poly(dA) with single stranded calf thymus DNA solution (Figures II.24(A, B) and Figures II.25(A, B)). In general, in the out-of-phase impedance versus potential graphs, there is a decrease in impedance in the depletion range after complementary hybridization corresponding to a shift of V_{fb} towards more negative potentials, thus giving similar results to those obtained with the pure oligomer and polymer. This could be interpreted as indicating an absence of interference on the part of the single stranded (calf thymus) DNA with the complementary strand, but the results

shown in Figures II.18 and II.19 for batch hybridization of the single stranded (calf thymus) DNA onto oligo$(dT)_{20}$ and poly(dT) at room temperature have shown that single stranded (calf thymus) DNA can hybridize with these oligonucleotides, and it may well be contributing in the observed shifts of V_{fb} presented in Figures II.22, II.23, II.24 and II.25.

4.3 *In Situ* Hybridization

The sensitivity of *in situ* hybridization is limited by several variables, including preservation of nucleic acid fixation, accessibility of molecular probe to the nucleic acids during hybridization, and the sensitivity of the detection systems. We will show that the impedance measurements are not significantly affected by the above variables.

4.3.1 *In Situ* Hybridization with Oligo$(dA)_{18}$

The purpose of *in situ* hybridization in this research is mainly to study the kinetics taking place at the modified electrode surface. Figures 4.6(A, B) for oligo$(dT)_{20}$ modified electrode (Figures II.26(A,B) for poly(dT)), show the variation of in-phase and out-of-phase impedance with time upon addition of 20 μl of 1 mg/ml of oligo$(dA)_{18}$ to 12 ml of Tris HCl electrolyte. In both cases, the in-phase impedance tends to increase with time, whereas in the out-of-

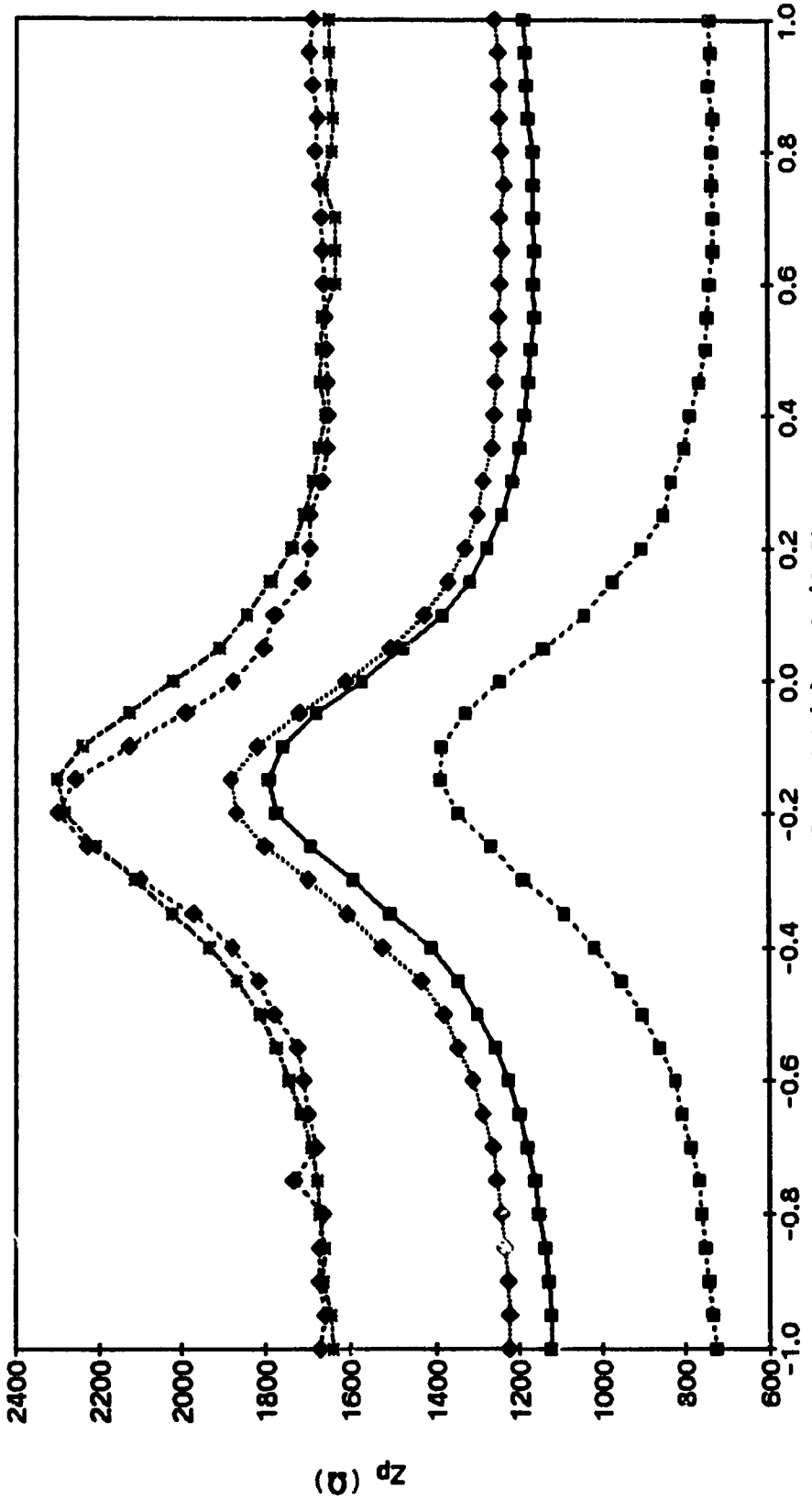

Figure 4.6A In-phase impedance measurements of an oligo(dT)$_{20}$ modified electrode, *in situ* hybridized with oligo(dA)$_{18}$.

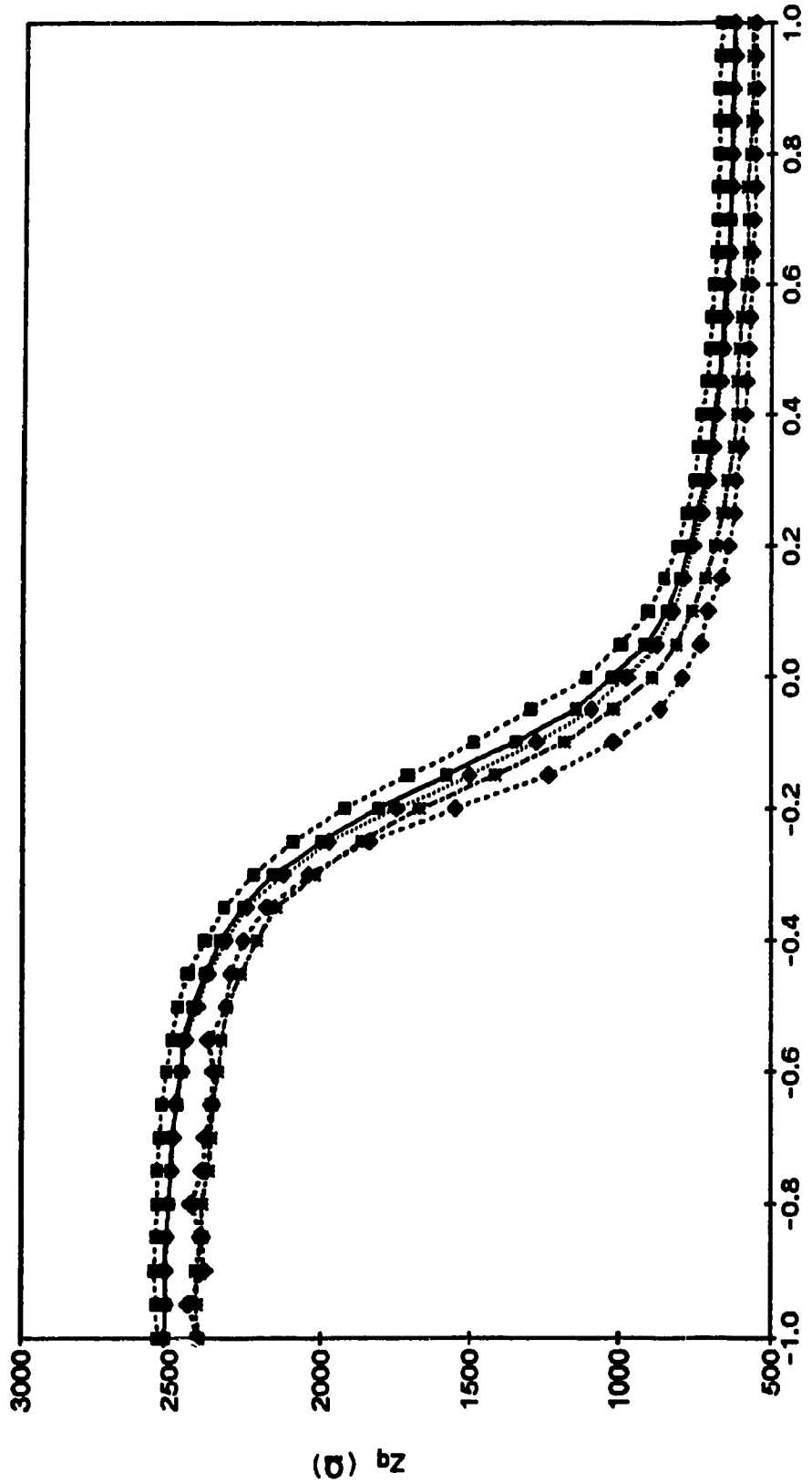

Figure 4.6B Out-of-phase impedance measurements of an oligo(dT)$_{20}$ modified electrode, *in situ* hybridized with oligo(dA)$_{18}$.

phase curves the impedance generally decreases. Although the overall decrease of the in-phase impedance measured over the entire dc range is a different behavior to that observed in the batch hybridization studies, the variations of V_{fb} with time in the out-of-phase impedance plots are in good agreement, in terms of both direction and magnitude of the shifts.

Table 4.6 corresponds to the average changes for Z_p and Z_q in the depletion region observed for *in situ* hybridization with oligo$(dA)_{18}$ on thymidylic acid modified electrodes. It can be seen that the average changes in the depletion range for the poly(dT) modified electrodes are higher than those for the oligo$(dT)_{20}$, whereas the average flatband potential shift of the electrodes after 6 hours of exposure to the electrolyte and complementary strand is similar in both cases (-42 ± 9 mV and -44 ± 15 mV for poly(dT) and oligo$(dT)_{20}$, respectively). After 6 hours, the average change of the maximum Z_p value along the potential axis is of -51 ± 6 mV for the poly(dT) modified electrodes, similar results were obtained for oligo$(dT)_{20}$ modified electrodes. The average value for the maximum Z_p is 535 ± 273 ohms for oligo$(dT)_{20}$ modified electrodes and 148 ± 23 ohms for poly(dT) modified electrodes.

Table 4.6
Average Changes for Z_p and Z_q for Poly(dT) and Oligo(dT)$_{20}$ Modified Electrodes, *In Situ* Hybridized with Oligo(dA)$_{18}$ after 6 Hours (average for measurements made with 5 different electrodes for each type of modification).

Average Change of the peak maximum, in Z_p vs V curves		
	Oligo(dT)$_{20}$	Poly(dT)
$\triangle Z_p$ (ohms)	535 ± 273	148 ± 23
$\triangle V$ (mV)	- 47 ± 4	- 51 ± 6
Average Change of Z_q and V_{fb}, in Z_q vs V curves (6 h)		
	Oligo(dT)$_{20}$	Poly(dT)
$\triangle Z_q$ (ohms)	- 77 ± 33	- 268 ± 112
$\triangle V_{fb}$ (mV)	- 44 ± 15	- 42 ± 9

4.3.2 *In Situ* Hybridization with Poly(dA)

The hybridization with poly(dA) of an oligo$(dT)_{20}$ and a poly(dT) modified electrode were compared. As shown in Figures II.27(A, B), an overall increase in the in-phase impedance versus potential curves, following the incorporation of 20 μl of 1 mg/ml of poly(dA) to 12 ml of Tris HCl electrolyte, can be observed. In the out-of-phase impedance versus potential curve, a decrease in impedance (increase in capacitance) with time is observed over the entire dc potential range. These results are similar to those obtained upon hybridization of oligo$(dA)_{18}$ with an olido$(dT)_{20}$ modified electrode (Figure 4.6A).

The *in situ* hybridization of a poly(dT) modified electrode, with poly(dA) shows a behavior slightly different from those illustrated in Figures 4.6A, II.26A, and II.27A. The increase in in-phase impedance with time (Figure II.28A) is clearly not as pronounced as in the oligo$(dT)_{20}$ - poly(dA) system, but the shift of V_{fb} towards more negative values (Figure II.28B) is similar.

The average changes for Z_p and Z_q in the depletion region, upon *in situ* hybridization of poly(dA) with the thymidylic acid modified electrodes observed after 6 hours, are shown in Table 4.7. The averages for $\triangle Z_q$, $\triangle V$ and $\triangle V_{fb}$ are similar for both types of modification. The average change in $Z_p$max for the oligo$(dT)_{20}$, 322 ± 281 ohms, however, is more significant than the average change for the poly(dT), 31 ± 18 ohms.

4.3.3 Interference Effects During *In Situ* Hybridization

In situ hybridization of 20 μl of 1:1 mixtures of single stranded calf thymus DNA and oligo$(dA)_{18}$ or poly(dA) with both types of modified single stranded DNA electrodes (oligo$(dT)_{20}$, poly(dT)) were compared. Similar hybridization results to those obtained with pure synthetic single strands only, were observed. Figures II.29(A, B) correspond to the in-phase and out-of-phase impedance measurements of a poly(dT) modified electrode, *in situ* hybridized with a mixture of poly(dA) and single stranded calf thymus DNA (Figures II.30(A, B), for a poly(dT) modified electrode, *in situ* hybridized with a mixture of oligo$(dA)_{18}$ and single stranded calf thymus DNA). The corresponding graphs for a oligo$(dT)_{20}$ modified electrode can be found in Appendix II (Figures II.31(A, B) and II.32(A, B)). The shifts observed here could be attributed to the hybridization of the complementary strand since attempts at *in situ* hybridization using 20 μl of single stranded DNA only, (double the concentration used in the above described mixtures), at the same temperature (22°C), were unsuccessful since no shifts of V_{fb} were observed (Figures II.33(A, B)).

Table 4.7
Average Changes for Z_p and Z_q for Poly(dT) and Oligo$(dT)_{20}$ Modified Electrodes, *In Situ* Hybridized with Poly(dA) after 6 Hours (average for measurements made with 5 different electrodes).

Average Change of the peak maximum, in Z_p vs V curves		
	Oligo$(dT)_{20}$	Poly(dT)
$\triangle Z_p$ (ohms)	344 ± 281	31 ± 18
$\triangle V$ (mV)	- 46 ± 8	- 52 ± 5
Average Change of Z_q and V_{fb}, in Z_q vs V curves (6 h)		
	Oligo$(dT)_{20}$	Poly(dT)
$\triangle Z_q$ (ohms)	- 129 ± 20	- 196 ± 6
$\triangle V_{fb}$ (mV)	- 40 ± 12	- 42 ± 11

Tables 4.8 and 4.9 correspond to the average changes for Z_p and Z_q in the depletion region due to the *in situ* hybridization with poly(dA) or oligo$(dA)_{18}$, respectively, in presence of single stranded calf thymus DNA. The average $\triangle Z_p$, $\triangle V$, $\triangle Z_q$, and $\triangle V_{fb}$ values, determined from measurements taken at time 0 and at 6 hours of exposure, resemble those obtained for oligo$(dT)_{20}$ hybridized with oligo$(dA)_{18}$ or poly(dA) and poly(dT)-oligo$(dA)_{18}$.

Table 4.8
Average changes for Z_p and Z_q for poly(dT) and oligo(dT)$_{20}$ modified electrodes, *in situ* hybridized with poly(dA) in presence of single stranded calf thymus DNA after 6 hours (average for measurements made with 5 different electrodes).

Average Change of the peak maximum, in Z_p vs V curves		
	Oligo(dT)$_{20}$	Poly(dT)
$\triangle Z_p$ (ohms)	457 ± 300	10 ± 1
$\triangle V$ (mV)	- 51 ± 7	- 45 ± 9
Average Change of Z_q and V_{fb}, in Z_q vs V curves (6 h)		
	Oligo(dT)$_{20}$	Poly(dT)
$\triangle Z_q$ (ohms)	- 142 ± 37	- 301 ± 10
$\triangle V_{fb}$ (mV)	- 40 ± 12	- 42 ± 14

Table 4.9
Average changes for Z_p and Z_q for poly(dT) and oligo$(dT)_{20}$ modified electrodes, *in situ* hybridized with oligo$(dA)_{18}$ in presence of single stranded calf thymus DNA after 6 hours (average for measurements made with 5 different electrodes).

Average Change of the peak maximum, in Z_p vs V curves		
	Oligo$(dT)_{20}$	Poly(dT)
$\triangle Z_p$ (ohms)	27 ± 16	173 ± 59
$\triangle V$ (mV)	- 42 ± 7	- 48 ± 8
Average Change of Z_q and V_{fb}, in Z_q vs V curves (6 h)		
	Oligo$(dT)_{20}$	Poly(dT)
$\triangle Z_q$ (ohms)	- 264 ± 99	- 217 ± 98
$\triangle V_{fb}$ (mV)	- 42 ± 11	- 44 ± 15

In Chapter 3, we have already demonstrated the stability of the modified single stranded electrode in the electrolyte, and as mentioned, no changes are seen in the impedance curves when the electrode has been in contact with the Tris HCl solution for six hours. Another control electrode was tested to check if the sodium bicarbonate solution interferes with the results obtained during *in situ* hybridization. Results similar to those obtained with the stability tests were observed. These results show that, under the conditions we have used, the single stranded modified sensors studied are selective and have a good sensitivity.

4.3.4 *In situ* Hybridization Time Dependence

As demonstrated previously, an abrupt decrease of values for out-of-phase impedance was observed in the depletion range upon the first couple of hours after the addition of the complementary strand. Figure 4.7 illustrates the change in out-of-phase impedance with time, taken at a fixed potential in the depletion range (-0.250 V) for a poly(dT) modified electrode, *in situ* hybridized with oligo$(dA)_{18}$ (values taken from Figure II.26). These values are compared to those obtained for a blank hybridization (20 µl of 1 M aqueous $NaHCO_3$ in 12 ml Tris HCl buffer). It can be observed that the change in Z_q is much sharper within the first three hours of exposure. The out-of-phase impedance value usually reaches an equilibrium point after about 5 to 8 hours of exposure to solution. Similar results were obtained for

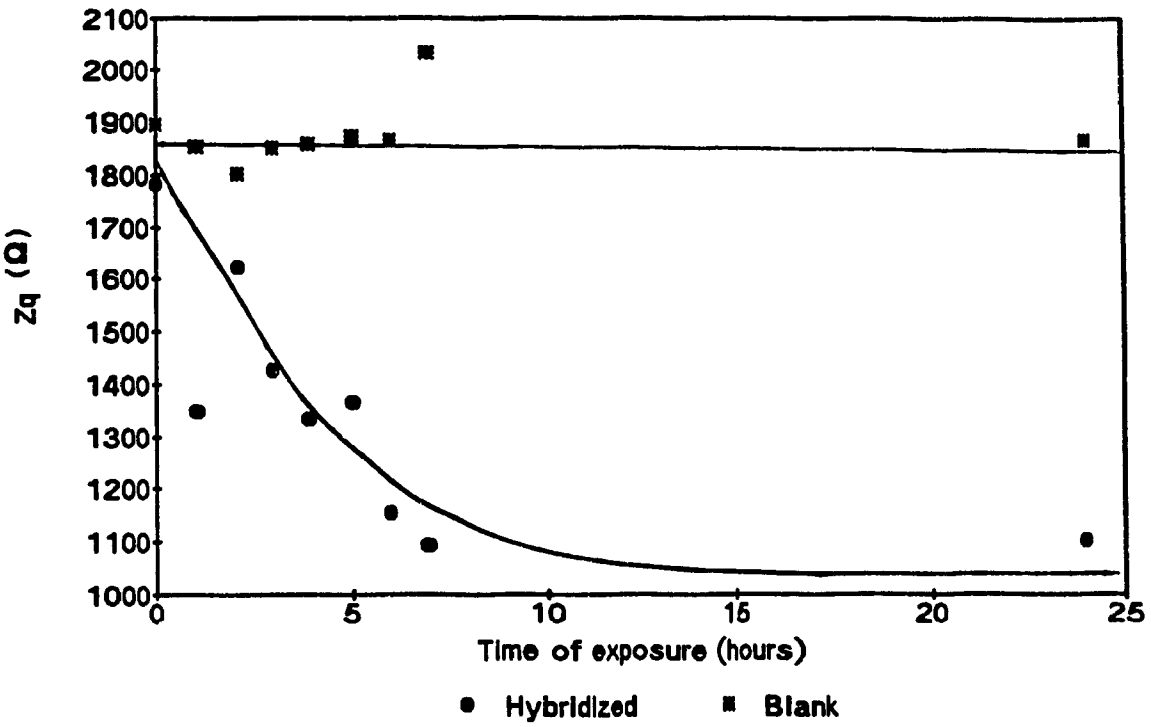

Figure 4.7 Out-of-phase impedance measurements of a Poly (dT) modified sensor, *in situ* hybridized with 20 µl of 1 mg/ml oligo$(dA)_{18}$. Values were taken at a fixed dc potential of -0.25 V.

poly(dT)-poly(dA), oligo$(dT)_{20}$-oligo$(dA)_{18}$, and oligo$(dT)_{20}$-poly(dA) (Figures II.34, II.35, and II.36). The results in Figure 4.7, show that the time required for half of the hybridization to take place is of about 2 to 4 hours. The results observed in this work are very similar to those published in a recent article by Su *et al*[64], where an acoustic network analysis was used to determine the kinetics of cDNA hybridization at the surface of piezoelectric electrodes modified with ss p PT-2DNA (4000 bases). As

proposed by Su *et al*, the very similar kinetics displayed during hybridization of our sensor devices suggest that the rapid decrease in Z_q during the first 3 hours correspond to sequence specific hybridization. Hybridization in bulk solution is considered to occur in 2 separate steps. The first is nucleation followed by a more rapid joining of remaining base residues to form the double stranded structure. Nucleation is the rate limiting step and therefore it determines the time course of hybrid formation.

In mixed phase hybridization where the concentration of probe DNA sequences in solution is much greater than that of the surface immobilized target sequences, hybrid formation is expected to follow first order kinetics[50a,66]. The time required for half of the probe sequences to hybridize with the immobilized strands is

$$t_{\frac{1}{2}} = \frac{\ln 2}{K\, c} \qquad (11)$$

where K is the first order rate constant for formation of one hybrid molecule and c is the probe concentration. The hybridization rate constant is related to the nucleation rate constant, K_n, by the following expression

$$K = \frac{K_n\, L^{\frac{1}{2}}}{N} \qquad (12)$$

where L is the probe strand length in terms of the number of base pairs and N is the molecular complexity (number of base pairs in a nonrepeating sequence). K_n is a function of ionic strength, viscosity, temperature and pH[50].

At ionic strengths between 0.4 and 1.0 M (0.4 to 1.0 M of NaCl), and at a pH ranging from 5.0 to 9.1 maximum rates of hybridization for polynucleotides in solution have been determined to occur at a temperature of about 25°C below the melting temperature of the duplex, t_m, the temperature at which half of the hybrids are dissociated. This observation also applies to mixed phase hybridizations which involve probes longer than about 150 nucleotides and, under optimal hybridization conditions equation 12 applies to oligonucleotides as short as 14 bases and can be expressed as,

$$K = \frac{(3.5 \times 10^5)\, L^{\frac{1}{2}}}{N} \qquad (13)$$

The conditions under which the *in situ* hybridizations were performed in this study, (c = 5.1 x 10^{-6} mol nucleotide/liter, ionic strength 0.05 M, pH = 7.10 and temperature = 22°C), a $t_{\frac{1}{2}}$ value of about 3 hours is observed (Figures 4.7, II.34, II.35 and II.36), which according to equation 11 yields a rough estimate of K = 12.58 liter/nucleotide s. However, if one calculates the hybridization constant from equation 13, which applies to

hybridization occuring under optimal conditions, and using for example values of L=18 and N=1 identical to that of the probe used in Figure 4.7, the value of K is found to be 1.5 x 10^6. This is a clear indication that the conditions under which the *in situ* hybridizations are performed in this study are not optimal (K value is approximately 5 orders of magnitude lower than expected for optimal conditions) and, although they are sufficient to permit observations of hybridization through impedance measurements, further optimization is expected following more detailed studies particularly concerning the dependence of these responses on temperature and ionic strength.

4.3.5 *In situ* Hybridization Concentration Dependence

Preliminary tests to asses the sensitivity cf the single stranded modified electrode to changes of the analyte concentration in the electrolyte solution have been performed. Figures II.37(A, B) represent the in-phase and out-of-phase impedance curves due to the hybridization at an oligo$(dT)_{20}$ modified electrode in contact with 10 μl of 1 mg/ml of poly(dA) in 12 ml of 10 mM Tris HCl. In the in-phase impedance versus potential plot, it can be observed that the poly(dA) incorporation does not change Z_p significantly, it has the usual effect of shifting the V_{fb} towards a more negative potential upon hybridization. In this case, the decrease in Z_q at a potential of -0.250V versus Ag/AgCl is of about 400 ohms after 24 hours (Figure

II.37B). The out-of-phase impedance versus potential curve follows a pattern similar to that observed with a higher concentration of analyte (20 μl of 1 mg/ml of poly(dA) in 12 ml of 10 mM Tris HCl). As we decrease the concentration of analyte to 40 μl of 0.1 mg/ml of poly(dA) in 12 ml of 10 mM Tris HCl, (Figures II.38(A, B)), the results are similar to those shown in Figure II.37(A, B), however the decrease in Z_q is now only of about 200 ohms at -0.250V versus Ag/AgCl (Figure II.38B). No shift could be observed at concentrations of poly(dA) lower than those mentioned.

CHAPTER 5

CONCLUSIONS AND SUGGESTIONS FOR FUTURE RESEARCH

5.1 Conclusions

The goal of this thesis was to configure an impedance-based silicon electrode capable of detecting particular DNA sequences, an aproach by which the use of labeled probes is not required. The following points, in our opinion, have been established by the work described in this thesis.

Silicon is a promising sensor material. Silicon/silicon dioxide wafers were used for detecting particular DNA sequences, and this was achieved by modifying the silicon dioxide surface with a chemically active material such as 3-aminopropyltriethoxy silane. Once this modification was obtained, a thymidylic acid oligomer or polymer was covalently bound to the previously modified electrode.

With the single stranded modified silicon electrode it is possible to detect, through batch or *in situ* methods, hybridization of DNA sequences taking place at the electrode surface. These hybridizations are clearly detected in particular by the out-of-phase impedance measurements in the depletion range and the corresponding shifts in V_{fb}. In the depletion region changes of out-of-phase impedances ranging between 800 to 1200 ohms have been observed upon direct hybridization and changes ranging from 300 to 500 ohms for *in situ* hybridization. When a hybridization takes place, the flatband potential is always shifted to a more negative

potential due to the changes in charge distribution taking place at the Si/SiO_2/electrolyte interface.

In situ hybridization gives some insight as to the kinetics of the hybridization process. We can conclude that the shifts of the silicon flatband potential observed, are attributed to the hybridization of the complementary strand in solution. Our results are very similar to those observed by Su *et al*[59] with the acoustic network analysis. Although our observations at this point are of a qualitative nature, ac impedance measurements with the Si/SiO_2/APTS/Thymidylic acid modified electrode have proven to be sensitive, selective and reasonably reproducible under the experimental conditions described in this study.

5.2 Suggestions for Future Research

A number of the conclusions reached during this investigation suggest possibilities for further research.

A direct attempt to determine the amount of single stranded DNA bonded to the APTS modified silicon surface as well as the amount of the complementary strand which hybridizes should be tried.

An in depth study of the layer thickness and the dielectric constant of the modified sensor is needed to determine the cause of the capacitance change obtained upon hybridization.

A similar study with impedance measurements done in this work with thymidylic acid - adenylic acid, should be

performed with the cytidylic acid - guanylic system following the same steps of modification as those that have used in this work.

There is a great potential for the application of nucleic acid probes to the detection of specific genes in the diagnosis of human genetic disorders. A closer study of the detection of the deletions and point mutations responsible for genetic diseases should be done with impedance measurements.

The electrochemical impedance measurement system can also be used to study other biological systems, such as antigen - antibody interactions. This would result in a new class of immunoassay methods, again where detectable labels are not required.

References

1 Yolken, R. *Molecular and Cellular Probes*. 1988, 2, 87.

2 Jeffreys, A.J., Wilson, V. and Thein, S.L.. *Nature*. 1985, 316, 76.

3 McElfresh, K.C., Vining-Forde, D. and Balazs, I.. *BioScience*. 1993, 43, 149.

4 Bonting, S.. "Needs for Biosensors in Space-Biology Research". *Biosensor Design and Application*. ed. P.R. Mathewson and J.W. Finley. Washington D.C., American Chemical Society, 1992, 175-183.

5 Eitel, G.. "Sampling". *Sensors in Bioprocess Control*. New York, Marcel Dekker, Inc., 1990, 17-38.

6 Bartlet, P.N.. "The Use of Electrochemical Methods in the Study of Modified Electrodes". *Biosensors, Fundamentals and Applications*. ed. A. Turner, I. Karube and G. Wilson. New York, Oxford University Press, 1987, 211-246.

7 Green, M.. "New Approaches to Electrochemical Immunoassays". *Biosensors, Fundamentals and Applications*. ed. A. Turner, I. Karube and G. Wilson. New York, Oxford University Press, 1987, 60-69.

8 Wachsmuth, K.. *Infection Control*. 1985, 6, 100.

9 Caskey, T.. *Science*. 1987, 236, 1223.

10 Hillel, J., Schaap, T., Haberfeld, A., Jeffreys, A.J., Plotzky, Y., Cahaner, A. and Lavi, U.. *Genetics*. 1990, 124, 783.

11 Sutherland, G. and Mulley, J.. "The Study and Diagnosis of Human Genetic Disorders Using Nucleic Acid Probes", ed. R.H. Symons *Nucleic Acid Probes*. Florida, CRC Press 1989, 159-201.

12 Kricka, L. *Nonisotopic DNA Probe Techniques*. Toronto, Academic Press, 1992, 3-19.

13 Sibbald, A. *IEE Proceedings*. 1983, (1), 130, 233.

14 Janata, J. *Principles of Chemical Sensors*. New York, Plenum Press, 1989, 81-237.

15 Bergveld, P. *Sensors and Actuators*. 1981, 1, 17.

16 Covington, A. and Whalley, P.D.. *J. Chem. Society, Faraday Trans. I*. 1986, 82, 1209.

17 Janata, Jiri. *Chem. Rev.* 1990, 90, 691.

18 Van den Berg, V., Bergveld, P., Reinhoudt, D.N. and Sudholter, E.J.R.. *Sensors and Actuators*. 1985, 8, 129., and references therein.

19 de Rooij, N.F. and Bergveld, P.. ed. S.T. Pantelides *The Physics of SiO_2 and its Interfaces*. New York, Pergamon Press, 1978, 433.

20 McBride, P.T., Janata, J., Comte, P.A., Moss, S.D., and Johnson, C.. *Anal. Chim. Acta*. 1978, 101, 239.

21 Esashi, M. and Matsuo, T.. *IEEE Trans. Biomed. Eng.* 1978, 25, 184.

22 Moss, S., Johnson, G. and Janata, J. *IEEE Trans. Biomed. Eng.* 1978, 25, 49.

23 Caras, S. and Janata, J. *Anal. Chem.* 1980, 52, 1935.

24 Nakajima, H., Esashi, M. and Matsuo, T.. *J. Electrochem* 1982, 129, 141.

25 Bergveld, P.. *IEEE Trans. Biomed. Eng.* 1972, 19, 342.

26 Clark, L.C.. "The Enzyme Electrode", *Biosensors, Fundamentals and Applications*, ed. A. Turner, I. Karube and G. Wilson. New York, Oxford University Press, 1987, 3-12.

27 Kuan, S.S. and Guibault, G.G.. "Ion Selective Electrodes and Biosensors based on ISEs", *Biosensors, Fundamentals and Applications*, ed. A. Turner, I. Karube and G. Wilson. New York, Oxford University Press, 1987, 135-152.

28 Gardies, F., Martelet, C., Colin, B. and Mandrand, B.. *Sensors and Actuators*. 1989, 17, 461.

29 Diot, J.L., Joseph, J., Martin, J.R. and Clechet, P.. *J Electroanal. Chem. and Interfacial Electrochem.* 1985, 193, 75.

30 Janata, J. and Bezegh, A.. *Anal. Chem.* 1988, 60, 62R.

31 Bergveld, P., van den Berg, A., van der Wal, P.D. , Skowronski-Plasinska, M., Sudholter, E.J.R. and Reinhoudt, D.N.. *Sensors and Actuators*. 1989, 18, 309.

32 Van den Blekkert, H., Francis, C., Grisel, A. and de Rooij, N.. *Analyst*. 1988, 113, 1029.

33 Bataillard, P., Clechet, P., Jaffrezeic-Renault, N., Kong, X.G. and Martelet, C.. *Sensors and Actuators*. 1987, 12, 245.

34 Jaffrezic-Renault, N. and Martelet, C.. *Sensors and Actuators A*. 1992, 32, 307.

35 Clechet, P., Jaffrezic-Renault, N. and Martelet, C.. "Sensitization of Dielectric Surfaces by Chemical Grafting Application to ISFET and ENFET", *Chemical Sensor Technology.*, Vol. 4, ed. S. Yamauchi, New York, Elsevier 1992, 205-224.

36 Carajaval, S., Leyden, D., Quinting, G. and Marciel, G.. *Anal. Chem.* 1988, 60, 1776.

37 Mathews, J. and Kricka, L.. *Anal. Biochem.* 1988, 169, 1-25.

38 Malcolm, A., Fallon, R., Langdale, J., Figueiredo, H., Nicholls, P., Voss, U., Wickenden, C. and Woodhead, L.. *Biochemistry Society Symposium*. 1987, 53, 131.

39 Wolfe, H.J.. *J Clin. Pathology*. 1988, 90, 340.

40 Gill, P., Jeffreys, A. and Werrett, D.. *Nature*. 1985, 318, 577.

41 Gill, P., Lygo, J., Fowler, S. and Werrett, D.. *Electrophoresis*. 1987, 8, 38.

42 Kerem, B., Rommens, J.M et al. *Science*. 1989, 245, 1066.

43 Riordan, J.R., Rommens, J.M. et al. *Science*. 1989, 245, 1073.

44 Woo, S., Lidsky, A., Guttler, F., Chandra,T. and Robson, K.. *Nature*. 1983, 306, 151.

45 DiLella, A., Marvit, J., Lidsky, A., Guttler, F. and Woo, S.L.. *Nature*. 1986, 322, 799.

46 Saiki, R., Scharf, S., Faloona, F., Mullis, K., Horn, G., Erlich, H. and Arnheim, N.. *Science*. 1985, 230, 1350.

47 Thornton, J.. *Chemical and Engineering News*. 1989, Nov 20, 18.

48 Watson, J.D. and Crick, F.H.C.. *Nature*. 1953, 171, 738.

49 Millan, K. and Mikkelsen, S.. *Anal. Chem.* 1993, 65, 2317.

50 Keller, G. and Manak, M.. *DNA Probes*. New York, Macmillan Publishers, 1989, a 1-27 and b 149-210.

51 Keller, G., Cummina, C., Haung, D., Monak, M. and Ting, R. *Anal. Biochem.* 1988, 170, 441.

52 Sze, S.M.. *Physics of Semiconductor Devices*. Toronto, Wiley-InterScience, 1981, 485.

53 Vanmaelkelbergh, D. and Cardon, F.. *Electrochimica Acta*. 1992, 37, 837.

54 Daniels, F., Alberty, R., Williams, J.W., Cornwell, D., Bender, P. and Harriman, J. *Experimental Physical Chemistry* Toronto, McGraw-Hill Book, 1970, 13-46.

55 Nagasubramanian, G., Wheeler, B.L., Fan, F. and Bard, A.J. *J. Electrochem.* 1982, 129, 1742.

56 Wolfe, C., Holonyak, N. and Stillman, G.. *Physical Properties of Semiconductors*. New Jersey, Prentice Hall, 1989, 37-54.

57 Harris, D.C., *Quantitative Chemical Analysis*. W.H Freeman and Company, 2nd ed. New York, 1987, 726.

58 Technical Service, Sigma Chemical Company, United States, personal communication, February 1994.

59 Keith, F. *DNA Cloning/Sequencing Workshop*. New York, Ellis Horwood, 1991, 27-48.

60 *Digest of Literature on Dielectrics*. Vol 37, ed. W. Vaughan, Washington, National Academy of Science, 1975. 602-653.

61 Takashima, S.. *J Phys. Chem.* 1970, 74, 4446.

62 Cole, R.. *Annals of the New York Academy of Science (USA)*. 1977, 303, 59.

63 Pethig, R.. *Dielectric and Electronic Properties of Biological Materials*. New York, Wiley, 1979, 52-83.

64 Su, H., Kallury, K. and Thompson, M. *Anal.Chem.* 1994, 66, 769.

65 Koryta, J.. *Ions, Electrodes and Membranes*. Toronto, John Wiley & Sons, 1982, 1-44.

66 Meinkoth, J. and Wahl, G. *Anal. Biochem.* 1984, 138, 267.

APPENDIX I

Program for Electrochemical Impedance Measurements

```
/*                    Impedance Measurements                    */
/*                              by                              */
/*          Caroline Wilson and Marcus Lawrence                 */
/*                    Concordia University                      */


/* Library Declarations                                         */
#include <dos.h>
#include <stdio.h>
#include <stdlib.h>
#include <string.h>
#include <ctype.h>
#include <math.h>
#include <conio.h>
#include <io.h>
#include <dir.h>
#include <graphics.h>
#include "c:\at-gpib\c\decl.h"

FILE *outfile;
FILE *ptrfile;

#define ABORT 0
#define IGNORED 0


/* Function Declarations                                        */
int configuration;
int cover();
int instruction;
char namefile();
int set_constant();
char set_up_pot();
int set_up_amp();
int read_amp();
float resistance();
float capacitance();
int print_table();
int sensor();
int sensation();
int c_break();
int hardcopy();
char strdel();


/* Variable Declarations                                        */
char date[10];
char electrode[20];
char electrolyte[20];
char lpot[9]="\0";
char hpot[9]="\0";
char temp[25];
```

```
char potential[9];
char voltage[15];
char rd[25];
char pos[]="+";
char stand[]="PS IT1 E11 EST";
char outs [30];
char end[]=" \r\n";
char num[4];
char freq[25];
char sensitivity[6];
char acfreq[]="X 5, ";
char sensit[]="G ";
char acouts[15];
char sensout[12];
char tempfile[80];
char buffer[81];
char slash[4]="\\";
char point[3]=".";
char pathname[MAXPATH],
     drive[MAXDRIVE],
     dir[MAXDIR],
     filename[MAXFILE],
     ext[MAXEXT];
char slow[30],
     sresist[30],
     scapacit[30],
     spotin[15],
     spotout[15];
char frac[15],
     sacc[10],
     sdcc[10],
     pot[15],
     spotinf[15],
     spotoutf[15];

float amplitude,
     accurrent,
     dccurrent,
     rdfrf,
     irdp,
     tirdp,
     step;
long frequence;
int  points,
     t,
     load,
     sense,
     times;
int  dev1,
     dev2,
     brd0,
     dev3;
float volt,
     voltout,
```

```
      low,
      lowest_pot,
      highest_pot;
double aver,
      avec;
float frequency,
      acur,
      pcurrent,
      potin,
      potout;
double apotin,
      apotout,
      tempa,
      tempb,
      incur,
      outcur;
double resist,
      x,
      imped,
      capacit;
float voltf,
      voltoutf,
      potinf,
      potoutf;

double pi = 3.141592654;


/* Main Program                                                    */
main(void)   {
      double volta, voltouta;
      int p, t;
      char ans;
      cover();
      clrscr();

      namefile();
      clrscr();
      printf("       *** Impedance Measurements ***       \n");
      ptintf("\n"); printf("\n"); printf("\n");

      configuration();
      set_constant();
      set_up_pot();
      set_up_amp();

      if((outfile = fopen(filename,"w+"))==NULL) {
        printf("Error opening file.\n");
        exit(0);  }

      if((ptrfile = fopen(filename,"w+"))==NULL) {
        printf("Error opening printer file.\n");
        exit(0);  }
```

```
      clrscr();
      textattr(WHITE + (BLACK<<4));
      for(t=0; t<12; t++) { printf("\n"); }
      printf("  MAKE SURE THE LOAD CELL IS CONNECTED AND
              WIRED PROPERLY\n");
      printf(t=0; t<6; t++)  {printf("\n");}
      printf("        HIT SPACE BAR WHEN READY\n");
      while(!kbhit()) {
         for (t=0; t<30000; t++);  }

      clrscr();
      for(t=0; t<4; t++)    {printf("\n"); }
      printf("THE SYSTEM IS NOW BEING CONFIGURLD WITH \n\n");
      printf("THE PARAMETERS THAT YOU HAVE SPECIFIED.\n\n");
      printf("THE SYSTEM WILL SET UP FIRST THE
              POTENTIOSTAT,\n\n");
      printf("THEN THE LOCKIN SR530 AND FINALLY THE
              SRR10.\n");
      printf("\n\n\n\n\n");
      printf("THE SYSTEM WILL START READING THE VALUES
              IN A FEW SECONDS...\n");

      ibcmd(brd0, "?_@!", 4L);
      ibsic(brd0);
      ibsic(dev1);
      ibwrt(dev1, "ZA \r\n", 6L);

      if (lowest_pot > 0) {
        strcpy(potential, pos);
        sprintf(temp, "%.3f\n", lowest_pot);
        strncat(potential, temp, 9);
      else {
        sprintf(potential, "%.3f\n", lowest_pot);  }

      strcpy(outs, stand);
      strncat(outs, potential, 9);
      strncat(outs, end, 5);
      ibcmd(brd0, "?_@!", 4L);
      ibsic(brd0);
      ibsic(dev1);
      ibtmo(dev1, 16);
      ibtmo(dev1, 15);
      ibtmo(dev1, 9);
      ibwrt(dev1, outs, 30);
      delay(5000);

/* Set up SR530 Lockin Amplifier to standard settings      */
      ibsic(brd0);
      ibsic(dev2);
      ibwrt(dev2, "\r\n", 4L);
      ibwrt(dev2, "\r\n", 4L);
      ibwrt(dev2, "B 1 \r\n", 4L);
      ibwrt(dev2, "C 1 \r\n", 4L);
      ibwrt(dev2, "D 1 \r\n", 4L);
```

```
        ibwrt(dev2, "E 1, 0 \r\n", 4L);
        ibwrt(dev2, "L 1, 1 \r\n", 6L);
        ibwrt(dev2, "S 0 \r\n", 4L);
        ibwrt(dev2, "M 0 \r\n", 4L);
        ibwrt(dev2, "R 1 \r\n", 4L);
        ibwrt(dev2, acouts, 8L);
        delay (1000);
        ibwrt(dev2, "P 0 \r\n", 6L);
        ibwrt(dev2, "G 24 \r\n, 4L);
        delay(500);
        ibwrt(dev2, "F \r\n", 4L);
        ibcmd(brd0, "?_c ", 4L);
        delay (2000);
        ibrd(dev2, frac, 15);
        rdfrf = atof(frac);
             ibcmd(brd0, "?_@C", 4L);
             ibwrt(dev2, "F \r\n", 4L);
             ibcmd(brd0, "?_c ", 4L);
             delay (2000);
             ibrd(dev2, frac, 15);
             rdfrf = atof(frac);


/* Set up SR510 Lockin Amplifier for standard settings     */
        ibcmd(brd0, "?_@B", 4L);
        ibsic(brd0);
        ibsic(dev3);
        ibwrt(dev3, "\r\n", 4L);
        ibwrt(dev3, "\r\n", 4L);
        ibwrt(dev3, "B 1 \r\n", 4L);
        ibwrt(dev3, "C 1 \r\n", 4L);
        ibwrt(dev3, "D 1 \r\n", 4L);
        ibwrt(dev3, "E 0 \r\n", 4L);
        ibwrt(dev3, "L 1, 1 \r\n", 6L);
        ibwrt(dev3, "R 1 \r\n", 4L);
        ibwrt(dev3, "S 0 \r\n", 4L);
        ibwrt(dev3, "M 0 \r\n", 4L);
        ibwrt(dev3, acouts, 8L);
        delay (1000);
        ibwrt(dev3, "P 90 \r\n", 6L);
        ibwrt(dev3, "G 18 \r\n", 6L);
        delay (300);

        ibcmd(brd0, "?_@C", 4L);
        ibsic(brd0);
        ibsic(dev2);
        ibwrt(dev2, "G 23 \r\n", 4L);
        ibwrt(dev2, "P 0 \r\n", 4L);
        delay (200);

        ibcmd(brd0, "?_c ", 4L);
        delay (2000);
        ibrd(dev2, frac, 15);
        rdfrf = atof(frac);
```

```
      ibcmd(brd0, "?_@C", 4L);
      ibwrt(dev2, "F \r\n", 4L);
      ibcmd(brd0, "?_c ", 4L);
      delay (2000);
      ibrd (dev2, frac, 15);
      rdfrf = atof (frac);

delay (20000);

for(low=lowest_pot;low< highest_pot + step; low +=step){
  aver = 0.0;
  avec = 0.0;
  incur = 0.0;
  outcur = 0.0;
  apotin = 0.0;
  apotout = 0.0;

  clrscr();
  for(t=0;t<12;t++);  { printf("\n");}
  printf("  The Potential Applied is: %.3f V\n", low);
  if (low > 0) {
    strcpy(potential, pos);
    sprintf(temp, "%.3f\n", low);
    strncat(potential, temp, 9);   }
  else  {
    sprintf(potential, "%.3f\n", low);  }

  strcpy(outs, stand);
  strncat(outs, potential, 9);
  strncat(outs, end, 5);

  ibcmd(brd0, "?_@!", 4L);
  ibsic(brdo);
  ibsic(dev1);
  ibwrt(dev1, outs, 40);
  delay (4000);

  ibcmd(brd0, "?_@C", 4L);
  ibsic(brd0);
  ibsic(dev2);
  ibwrt(dev2, "G 24 \r\n", 4L);
  ibwrt(dev2, "P 0 \r\n", 4L);
  delay (200);
  ibwrt(dev2, "Q 1 \r\n", 4L);
  ibcmd(brd0, "?_c ", 4L);
  ibrd(dev2, voltage, 15);
  volt = atof(voltage);
  sensor (volt);

  ibcmd(brd0, "?_@B", 4L);

  ibsic(brd0);
  ibsic(dev3);
  ibwrt(dev3, "G 18 \r\n", 4L);
```

```
ibwrt(dev3, "P 90 \r\n", 6L);
delay(400);
ibwrt(dev3, "Q \r\n", 4L);
ibcmd(brd0, "?_b ", 4L);
ibrd(dev3, pot, 12);
potin = atof(pot);
sensation(potin);

delay (6000);

for (times=0; times<points; times++)  {
   volt =0.0;          delay(200);
   ibcmd(brd0, "?_@C", 4L);
   ibwrt(dev2, "Q 1 \r\n", 4L);
   ibcmd(brd0, "?_c ", 4L);
   ibsic(brd0);
   ibsic(dev2);
   ibrd(dev2, voltage, 12);  delay (400);
   volta = atof(voltage);
   volt = (volta/1000000);
   incur = incur + volt;
   voltf = incur/points;    }

for(times = 0; times<points; times++)  {
   potin = 0.0;
   ibcmd(brd0, "?_@B", 4L);
   ibwrt(dev3, "Q \r\n");
   ibcmd(brd0, "?_b ", 4L);
   ibsic(brd0);
   ibsic(dev3);
   ibrd(dev3, pot, 12);  delay(500);
   potin = atof(pot);
   apotin = apotin + potin;
   potinf = apotin/points;  }

ibcmd(brd0, "?_@C", 4L);
ibsic(brd0);
ibsic(dev2);
ibwrt(dev2, "G 24 \r\n", 4L);
ibwrt(dev2, "P 90 \r\n", 6L);
delay (200);
ibwrt(dev2, "Q 1 \r\n", 4L);
ibcmd(brd0, "?_c ", 4L);
ibrd(dev2, voltage, 12);
voltout = atof(voltage);
sensor(voltout);

ibcmd(brd0, "?_@B", 4L);
ibsic(brd0);
ibsic(dev3);
ibwrt(dev3, "G 24 \r\n", 4L);
ibwrt(dev3, "P -180 \r\n", 6L);
delay(300);
ibwrt(dev3, "Q \r\n", 4L);
```

```
ibrd(dev3, pot, 12);
potout = atof(pot);
sensation(potout);

delay(6000);

for(times=0; times<points; times++)  {
   voltout = 0.0;
   ibcmd(brd0, "?_@C", 4L);
   ibwrt(dev2, "Q 1 \r\n", 4L);
   ibcmd(brd0, "?_c ", 4L);
   ibsic(brd0);
   ibsic(dev2);
   ibrd(dev2, voltage, 12);
   voltouta = atof(voltage);
   voltout = (voltouta/1000000);
   outcur = outcur + voltout;
   voltoutf = outcur/poits;  }

for (times=0; times < points; times++) {
   potout = 0.0;   delay(200);
   ibcmd(brd0, "?_@B", 4L);
   ibwrt(dev3, "Q \r\n", 4L);
   ibcmd(brd0, "?_b ", 4L);
   ibsic(brd0);
   ibsic(dev3);
   ibrd(dev3, pot, 12);     delay(500);
   potout = atof(pot);
   apotout = apotout + potout;
   potoutf = apotout/points;   }

resistance();
capacitance();

tempa = incur/points;
tempb = outcur/points;

printf("The in phase impedance is: %.0f\n", resist);
printf("The out of phase impedance is:
        %.0f\n",capacit);
printf("The in phase current is: %.3E A\n", tempa);
printf("The out of phase current is: %.3E A\n",
       tempb);
delay(1500);
sprintf(slow, "%6.3f", low);
fputs(slow, outfile);
sprintf(sresist, "%8.0f", resist);
fputs(sresist, outfile);
sprintf(scapacit, "%8.0f", capacit);
fputs(scapacit, outfile);
sprintf(sacc, "%15.3E", voltf);
fputs(sacc, outfile);
sprintf(sdcc, "%12.3E", voltout);
fputs(sdcc, outfile);
```

```
   sprintf(spotinf, "%12.3E", potinf);
   fputs(spotinf, outfile);
   sprintf(spotoutf, "%12.3E\n", potout);
   fputs(spotoutf, outfile);

   ibcmd(brd0, "?_@C", 4L);
   ibsic(brd0);
   ibsic(dev2);
   ibwrt(dev2, "G 24 \r\n", 4L);
   ibwrt(dev2, "P 0 \r\n", 4L);
   ibcmd(brd0, "?_@B", 4L);
   ibsic(brd0);
   ibsic(dev3);
   ibwrt(dev3, "G 24 \r\n", 4L);
   ibwrt(dev3, "P 90 \r\n", 6L);

  clrscr();    }

ibcmd(brd0, "?_@C", 4L);
ibsic(brd0);
ibsic(dev2);
ibwrt(dev2, "Z \r\n", 4L);
ibcmd(brd0, "?_@B", 4L);
ibsic(brd0);
ibsic(dev3);
ibwrt(dev3, "Z \r\n", 4L);

rewind(outfile);
printf("Measurements Impedance In Phase and Out of
       Phase\n");
printf("\n");      printf("\n");
printf("Date:  %s\n", date);
printf("Electrode: %s\n", electrode);
printf("Electrolyte: %s\n", electrolyte);
printf("Frequency: %ld Hz\n", frequence);
printf("Reference Frequency: %.1f Hz\n");
printf("AC modulation: %.3f V\n", amplitude);
printf("Filename: %s\n", filename);
printf("\n"); printf("\n");
printf("Potential   Zp   Zq        Ip   Iq        Vp
       Vq\n");
printf("\n");
while(fgets(buffer, 80, outfile) != NULL) {
  printf(buffer);  }

ibcmd(brd0, "?_@!", 4L);
ibsic(brd0);
ibsic(dev1);
ibtmo(dev1, 15);
ibwrt(dev1, "ZA \r\n", 6L);

sound(540);
sleep(1);
nosound();
```

```
     hardcopy();
     rewind(ptrfile);
     fclose(outfile);
     fclose(ptrfile);

}     /*  END OF MAIN   */


int cover()          /*  Welcome  Screen   */
{
int t;
clrscr();
for (t=0; t<15; t++)  {
     printf("\n");  }
printf("          IMPEDANCE  MEASUREMENTS  \n");
printf("\n");
printf("                        by  \n");
printf("\n");
printf("             Caroline Wilson  \n");
for(t=0; t<12; t++) {
     printf("\n");  }
printf("          TO ABORT PROGRAM HIT CTRL-BREAK\n");
printf("\n");
printf("          PLEASE PRESS SPACE BAR TO CONTINUE");
while(!kbhit()) {
     for(t=0; t<30000; t++);  }
}


char namefile()      /*  Create a new file for results */
{
clrscr();
printf("           Create a new file\n");
printf("\n");  printf("\n");   printf("\n");
printf("Enter drive letter:  ");
gets(drive);  printf("\n");
printf("Enter directory path, optional (%d characters max):
       ", MAXDIR-1);
gets(dir);     printf("\n");
printf("Enter filename (%d characters max): ", MAXFILE-1);
gets(filename);   printf("\n");
printf("Enter extension (up to 4 letters): ");
gets(ext);    printf("\n");
fnmerge(pathname, drive, dir, filename, ext);
}


int set_constant()   /* Information required to identify
                        substrates analyzed */
{
char numstr[80];
printf("Enter Date 'MM-DD-YY':  ");
```

```
gets(date);  printf("\n");
printf("Enter type of electrode:");
gets(electrode);
printf("Enter electrolyte:");
gets(electrolyte);
}


char set_up_pot()    /* Obtain potential settings */
{
char numstr[80];
system("cls");
points = 0;
printf("\n");    printf("\n");
printf("   Information Required For Potentiostat Set Up\n");
printf("\n");  printf("\n");   printf("\n");
printf("Enter lowest potential (+/-n.nnn):");
gets(lpot);
lowest_pot = atof(lpot);
if (lowest_pot < -2.0)  {
     printf("Error, potential out of range.\n");
     printf("Please enter lowest potential: ");
     gets(lpot);
     lowest_pot = atof(lpot);  }
printf("Enter highest potential (+/-n.nnn):");
gets(hpot);
highest_pot = atof(hpot);
if (highest_pot > 2.0) {
     printf("Error, potential out of range.\n");
     printf("Please enter highest potential: ");
     gets(hpot);
     highest_pot = atof(hpot);  }
printf("Enter step increment (mV):");
gets(numstr);
step = atoi(numstr) * .001;
printf("Enter measurements per point:");
gets(numstr);
points = atoi(numstr);
}


int set_up_amp()
{
char numstr[80];  printf("\n");  printf("\n");
printf("          Information Required for Lockin Amplifier
          Set  Up\n");
printf("\n");    printf("\n");
delay(500);
printf("The lockin amplifier generates an AC potential with
        an amplitude of 10mV, 100mV or 1V controlled in the
        rear panel, it must be adjusted manually.\n");
printf("\n");
printf("Enter the amplitude (mV):");
gets(numstr);
```

```
amplitude = atoi(numstr) * .001;
printf("\n");
printf("The lockin amplifier frequency range must be adjusted
       in the rear panel.\n");
printf("\n");
printf("Enter AC Frequency (Hz): ");
gets(numstr);
frequence = atol(numstr);
if (frequence >= 1 && frequence < 100)
    frequency = frequence/10;
if (frequence >= 100 && frequence < 10000)
    frequency = frequence/100;
if (frequence >= 10000);
    frequency = frequence/10000;
sprintf(freq, "%.2f\n", frequency);
strcpy(acouts, acfreq);
strncat(acouts, freq, 4);
strncat(acouts, end, 5);
}


int configuration()   /*  Configure board and devices  */
{
brd0 = ibfind("BRD0");
dev1 = ibfind("DEVA");
dev2 = ibfind("LOCKIN");
dev3 = ibfind("AMPLI");

ibsic(brd0);
ibconfig(brd0, 8, 1);
ibconfig(brd0, IbcDMA, 1);
ibconfig(brd0, 7, 1);
ibconfig(brd0, IbcIRQ, 1);

ibconfig(dev1, 6, 0);
ibconfig(dev1, 15, 10);
ibconfig(dev1, 12, 1);

ibconfig(dev2, 6, 0);
ibconfig(dev2, 12, 1);

ibconfig(dev3, 6, 0);
ibconfig(dev3, 12, 1);
}


int sensor(get)    /* Set up first amplifier */
float get;
{
float set;
char spr;
set = fabs(get);
```

```
if (set >= 0.500)  {sense = 24;}
     else if (set < 0.500 && set >= 0.200)  { sense = 23;  }
     else if (set < 0.200 && set >= 0.100)  { sense = 22;  }
     else if (set < 0.100 && set >= 0.050)  { sense = 21;  }
     else if (set < 0.050 && set >= 0.020)  { sense = 20;  }
     else if (set < 0.020 && set >= 0.010)  { sense = 19;  }
     else if (set < 0.010 && set >= 0.005)  { sense = 18;  }
     else if (set < 0.005 && set >= 0.002)  { sense = 17;  }
     else if (set < 0.002 && set >= 0.001)  { sense = 16;  }
     else if (set < 0.001 && set >= 500E-6) { sense = 15;  }
     else if (set < 500E-6 && set >= 200E-6){ sense = 14;  }
     else if (set < 200E-6 && set >= 100E-6){ sense = 13;  }
     else if (set < 100E-6 && set >= 50E-6) { sense = 12;  }
     else if (set < 50E-6 && set >= 20E-6)  { sense = 11;  }
     else if (set < 20E-6 && set >= 10E-6)  { sense = 10;  }
     else if (set < 10E-6 && set >= 5E-6)   { sense = 9;   }
     else if (set < 5E-6 && set >= 2E-6)    { sense = 8;   }
     else if (set < 2E-6 && set >= 1E-6)    { sense = 7;   }
     else if (set < 1E-6 && set >= 500E-9)  { sense = 6;   }
     else if (set < 500E-9 && set >= 200E-9){ sense = 5;   }
     else if (set < 200E-9 && set >= 100E-9){ sense = 4;   }
     else if (set < 100E-9 && set >= 50E-9) { sense = 3;   }
     else if (set < 50E-9 && set >= 20E-9)  { sense = 2;   }
     else if (set < 20E-9 && set >= 10E-9)  { sense = 1;   }

sprintf(sensitivity, "%i\n", sense);
strcpy(sensout, sensit);
strncat(sensout, sensitivity, 2);
strncat(sensout, end, 5);
ibwrt(dev2, sensout, 10L);
ibrsp(dev2, &spr);
delay(100);
ibrsp(dev2, &spr);
sense++;
sense++;

while (spr==0)  {
     sense--;
     sprintf(sensitivity, "%i\n", sense);
     strncpy(sensout, sensit);
     strncat(sensout, sensitivity, 2);
     strncat(sensout, end, 5);
     ibwrt(dev2, sensout, 10);
     delay(300);
     ibrsp(dev2, &spr);  }
sense++;
sense++;
sprintf(sensitivity, "%i\n", sense);
strcpy(sensout, sensit);
strncat(sensout, sensitivity, 2);
strncat(sensout, end, 5);
ibwrt(dev2, sensout, 10);

ibrsp(dev2, &spr);
```

```
ibrsp(dev2, &spr);
while(spr != 0)  {
     sense++;
     sprintf(sensitivity, "%i \n", sense);
     strcpy(sensout, sensit);
     strncat(sensout, sensitivity, 2);
     strncat(sensout, end, 5);
     ibwrt(dev2, sensout, 10);
     ibrsp(dev2, &spr);   }
delay(1500);
}


int sensation(get)     /*  Set up second amplifier  */
float get;
{
float set;
char spr;
set = fabs(get);
if (set >= 0.500)  {sense = 24;}
     else if (set < 0.500 && set >= 0.200)  { sense = 23;   }
     else if (set < 0.200 && set >= 0.100)  { sense = 22;   }
     else if (set < 0.100 && set >= 0.050)  { sense = 21;   }
     else if (set < 0.050 && set >= 0.020)  { sense = 20;   }
     else if (set < 0.020 && set >= 0.010)  { sense = 19;   }
     else if (set < 0.010 && set >= 0.005)  { sense = 18;   }
     else if (set < 0.005 && set >= 0.002)  { sense = 17;   }
     else if (set < 0.002 && set >= 0.001)  { sense = 16;   }
     else if (set < 0.001 && set >= 500E-6) { sense = 15;   }
     else if (set < 500E-6 && set >= 200E-6){ sense = 14;   }
     else if (set < 200E-6 && set >= 100E-6){ sense = 13;   }
     else if (set < 100E-6 && set >= 50E-6) { sense = 12;   }
     else if (set < 50E-6 && set >= 20E-6)  { sense = 11;   }
     else if (set < 20E-6 && set >= 10E-6)  { sense = 10;   }
     else if (set < 10E-6 && set >= 5E-6)   { sense = 9;    }
     else if (set < 5E-6 && set >= 2E-6)    { sense = 8;    }
     else if (set < 2E-6 && set >= 1E-6)    { sense = 7;    }
     else if (set < 1E-6 && set >= 500E-9)  { sense = 6;    }
     else if (set < 500E-9 && set >= 200E-9){ sense = 5;    }
     else if (set < 200E-9 && set >= 100E-9){ sense = 4;    }
     else if (set < 100E-9 && set >= 50E-9) { sense = 3;    }
     else if (set < 50E-9 && set >= 20E-9)  { sense = 2;    }
     else if (set < 20E-9 && set >= 10E-9)  { sense = 1;    }

sprintf(sensitivity, "%i\n", sense);
strcpy(sensout, sensit);
strncat(sensout, sensitivity, 2);
strncat(sensout, end, 5);
ibwrt(dev3, sensout, 10L);
ibrsp(dev3, &spr);
delay(100);
ibrsp(dev3, &spr);
sense++;
```

```
sense++;

while(spr==0)    {
     sense--;
     sprintf(sensitivity, "%i\n", sense);
     strcpy(sensout, sensit);
     strncat(sensout, sensitivity, 2);
     strncat(sensout, end, 5);
     ibwrt(dev3, sensout, 10);
     delay(300);
     ibrsp(dev3, &spr);  }
sense++;
sense++;
sprintf(sensitivity, "%i\n", sense);
strcpy(sensout, sensit);
strncat(sensout, sensitivity, 2);
strncat(sensout, end, 5);
ibwrt(dev3, sensout, 10);

ibrsp(dev3, &spr);
ibrsp(dev3, &spr);
while(spr != 0)  {
     sense++;
     sprintf(sensitivity, "%i \n", sense);
     strcpy(sensout, sensit);
     strncat(sensout, sensitivity, 2);
     strncat(sensout, end, 5);
     ibwrt(dev3, sensout, 10L);
     ibrsp(dev3, &spr);
     delay(200);
     ibrsp(dev3, &spr);    }
delay(1500);
}


char strdel(str, n)     /* Delete character from string  */
char str[];
int n;
{
strcpy(&str[n], &str[n+1]);
}



float resistance()    /* Impedance in phase calculation */
{
double Vp, Vq, Ip, Iq, Zp;
Zp = 0.0;
Vp = potinf;
Vq = potoutf;
Ip = voltf*voltf;
Iq = voltoutf*voltoutf;
Zp = (Vp*voltf + Vq*voltoutf)/(Ip + Iq);
resist = Zp;
```

```
return(0);
}


float capaciatance()   /*Impedance out of phase calculation*/
{
double Vp, Vq, Ip, Iq, Zq;
Vp = potinf;
Vq = potoutf;
Ip = voltf*voltf;
Iq = voltoutf*voltoutf;
Zq = 0.0;
Zq = (-Vp*voltoutf + Vq*voltf)/(Ip + Iq);
capacit = Zq;
return(0);
}


int c_break(void)  {
printf("Control-break hit.  Program aborting......\n");
return(ABORT);
}


int hardcopy ()  {     /* Hardcopy function */
char stdfile[81];
int ch;
for(t=0; t<2; t++)   {
     printf("\n");   }
printf("PRESS 'ENTER TO GET A PRINTOUT OUT OF %s,filename);
ch = getchar();
if (ch=='n') goto quit;
sprintf(stdfile, "\n\n\n");
fputs(stdfile, ptrfile);
sprintf(stdfile, "Measurements of Impedance in Phase and out
        of Phase\n");
fputs(stdfile, ptrfile);
sprintf(stdfile, "\n\n");
fputs(stdfile, ptrfile);
sprintf(stdfile, "Date: %s\n", date);
fputs(stdfile, ptrfile);
sprintf(stdfile, "Electrode: %s\n", electrode);
fputs(stdfile, ptrfile);
sprintf(stdfile, "Electrolyte: %s\n", electrolyte);
fputs(stdfile, ptrfile);
sprintf(stdfile, "Frequency: %ld Hz\n", frequence);
fputs(stdfile, ptrfile);
sprintf(stdfile, "Reference Frequency: %.0f Hz \n", rdfrf);
fputs(stdfile, ptrfile);
sprintf(stdfile, "AC Modulation: %.3f V\n", amplitude);
fputs(stdfile, ptrfile);
```

```
sprintf(stdfile, "Filename: %s\n", filename");
fputs(stdfile, ptrfile);
sprintf(stdfile, "\n\n");
fputs(stdfile, ptrfile);
sprintf(stdfile,"Potential    Zp    Zq        Ip    Iq
     Vp    Vq\n\n");
fputs(stdfile, ptrfile);

rewind(ptrfile);
while(fgets(tempfile, 80, ptrfile) != NULL)
     { fputs(tempfile, stdprn);  }

rewind(outfile);
while(fgets(buffer, 80, outfile) != NULL)
     { fputs(buffer, stdprn);  }

quit:  return(0);
}
```

A second program, identical to the first one, was written with the purpose of calculating the capacitance of the working electrode. The function called impedance in the first program was removed and another function was introduced in order to calculate $1/C^2$. Small changes were made in function hardcopy in order to obtain the correct printout.

```
float schottky()   /* Function to calculate 1/C² */
{
double Vp, Vq, Ip, Iq, C;

C= (capacit*capacit)*(2*3.1416*rdfrf)*(2*3.1416*rdfrf);
resist = C;
return(0);
}
```

APPENDIX II

Additional Impedance Curves

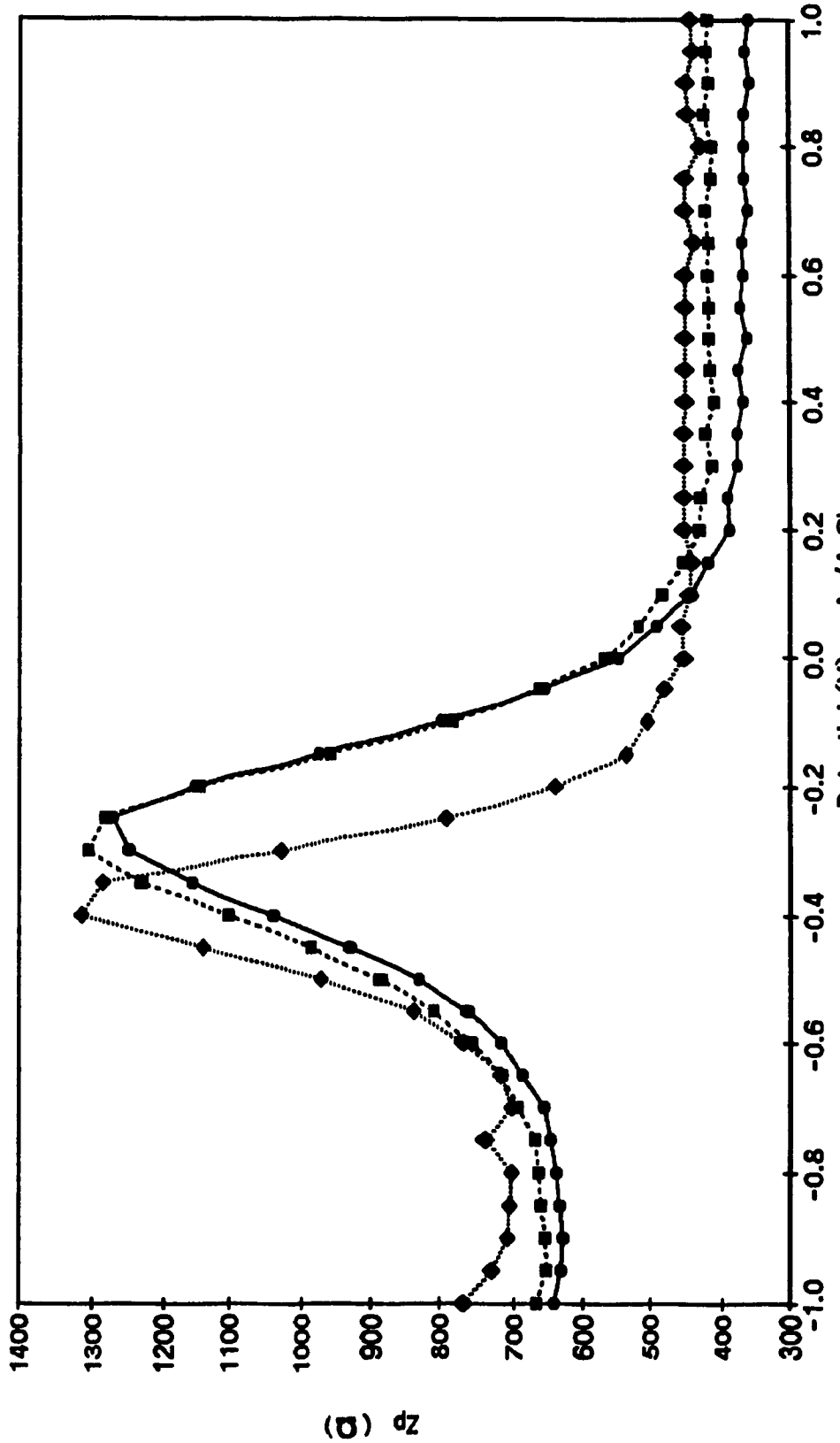

Figure II.1A Comparison of in-phase impedance measurements of a sulfochromic treated, APTS modified and poly(dT) modified electrode.

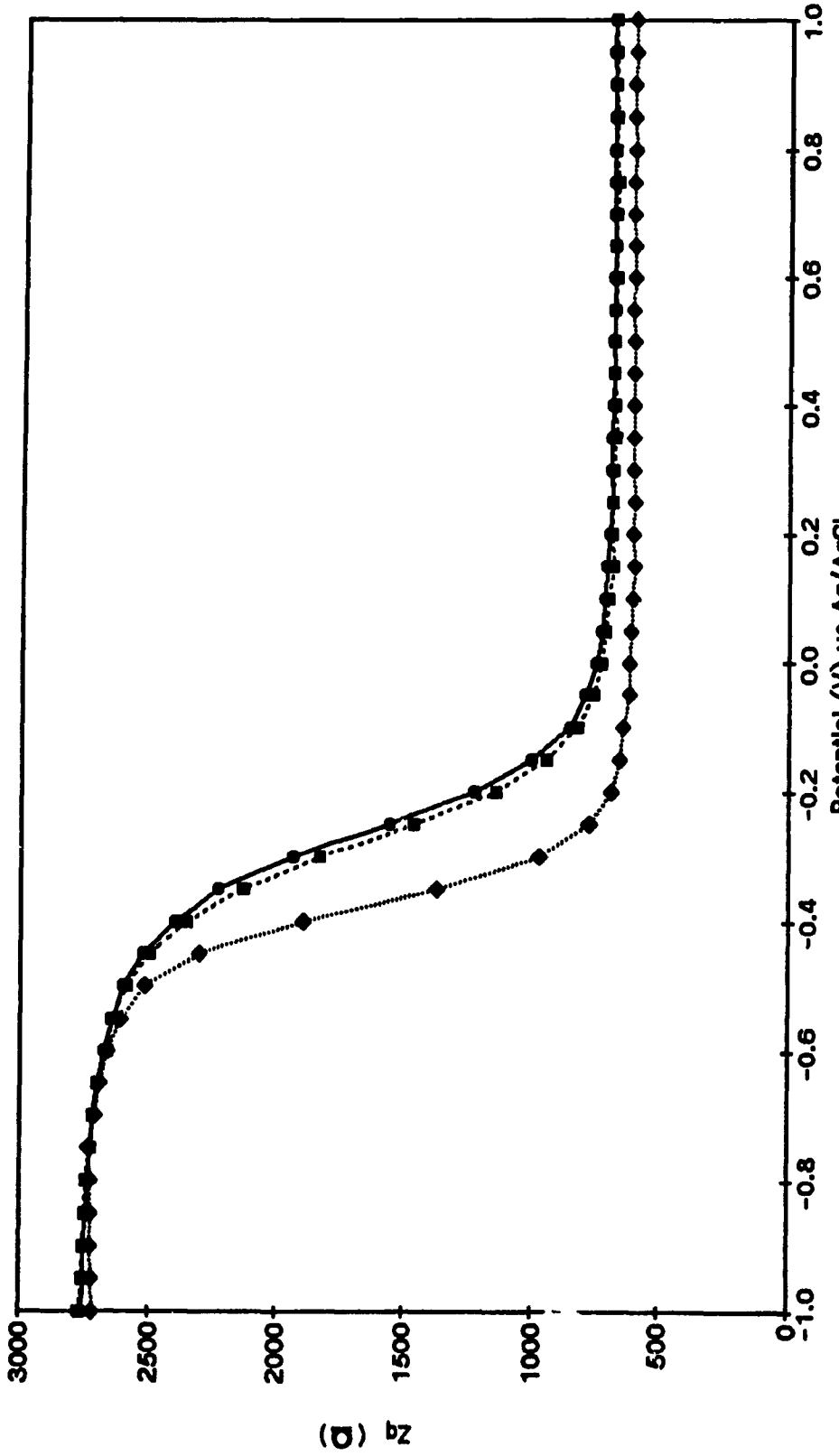

Figure II.1B Comparison of out-of-phase impedance measurements of a sulfochromic treated, APTS modified and poly(dT) modified electrode.

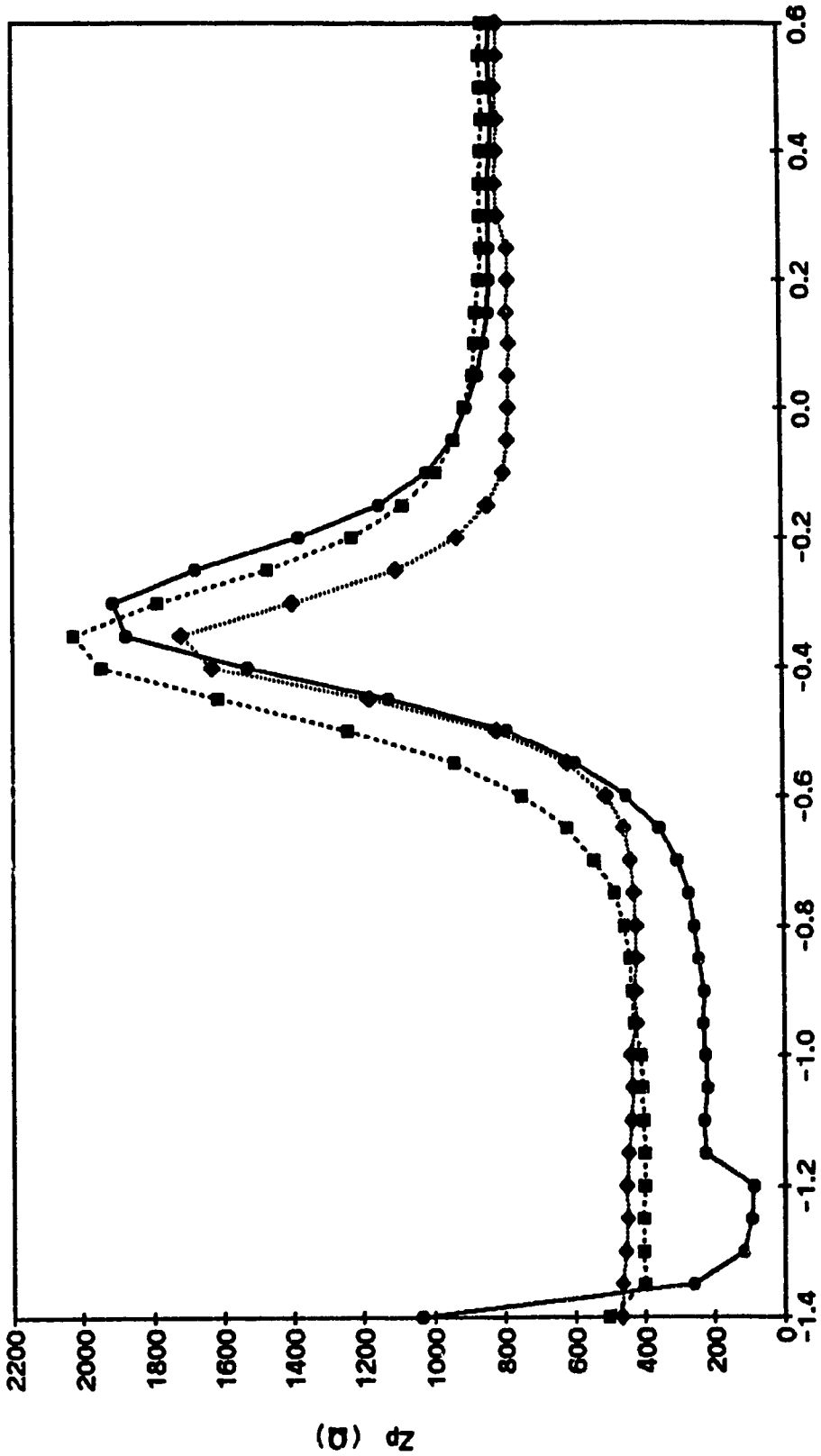

Figure II.2A In-phase impedance measurements of an APTS modified electrode before and after boiling in deionized water.

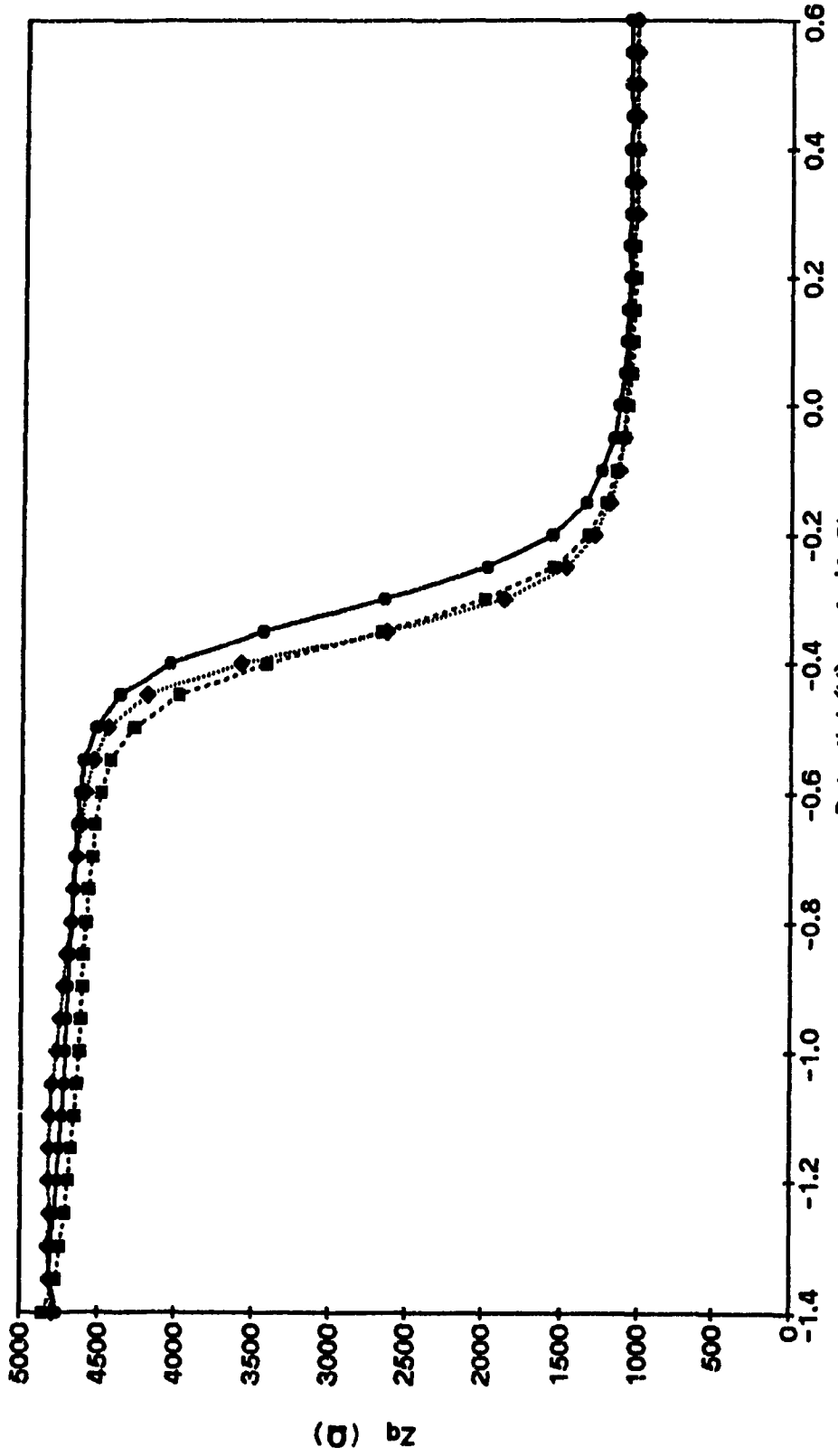

Figure II.2B Out-of-phase impedance measurements of an APTS modified electrode before and after boiling in deionized water.

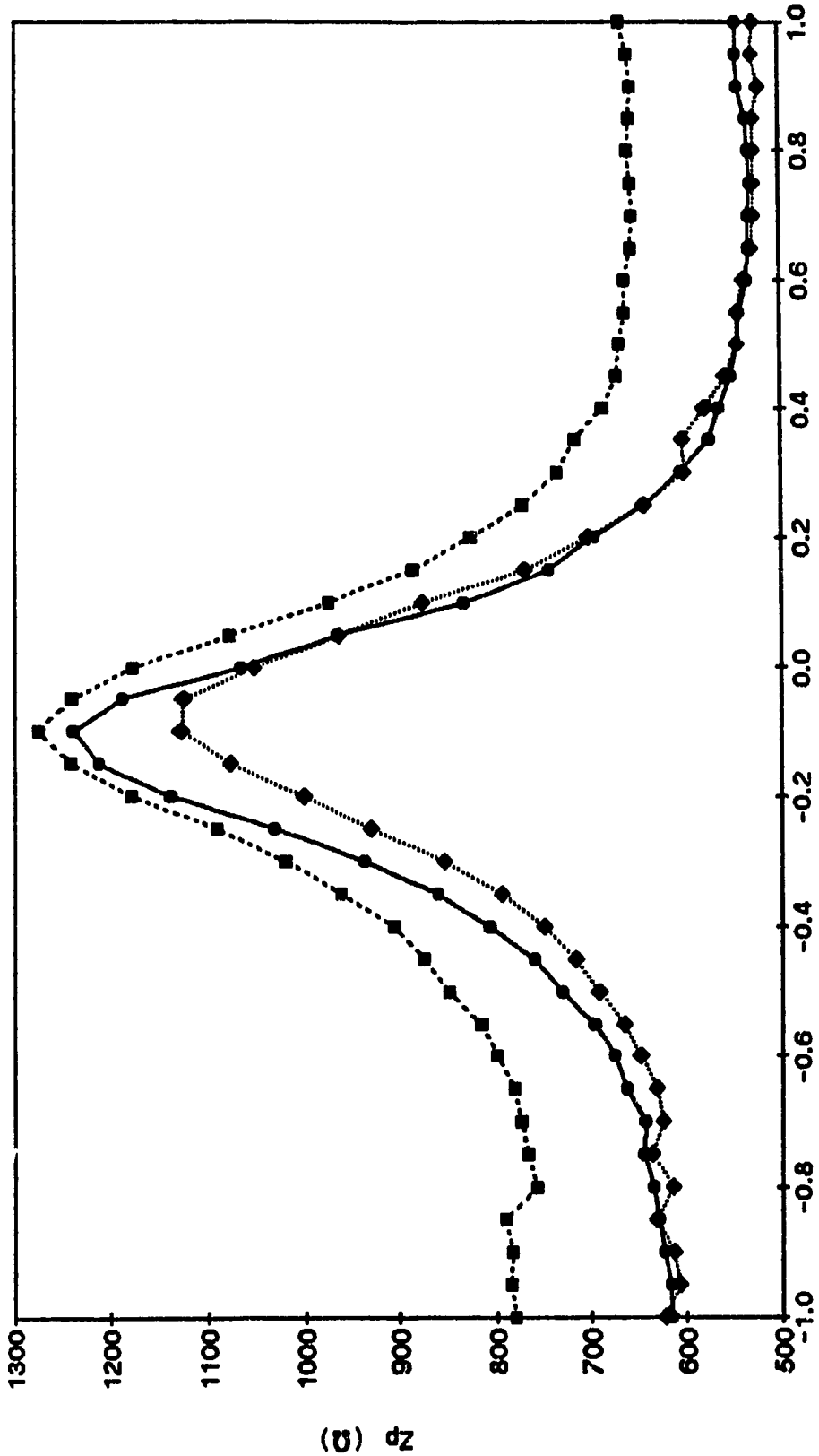

Figure II.3A In-phase impedance measurements of an oligo(dT)$_{20}$ modified electrode before and after the boiling steps. The curves corresponding to the third and fourth boiling steps are omitted for clarity.

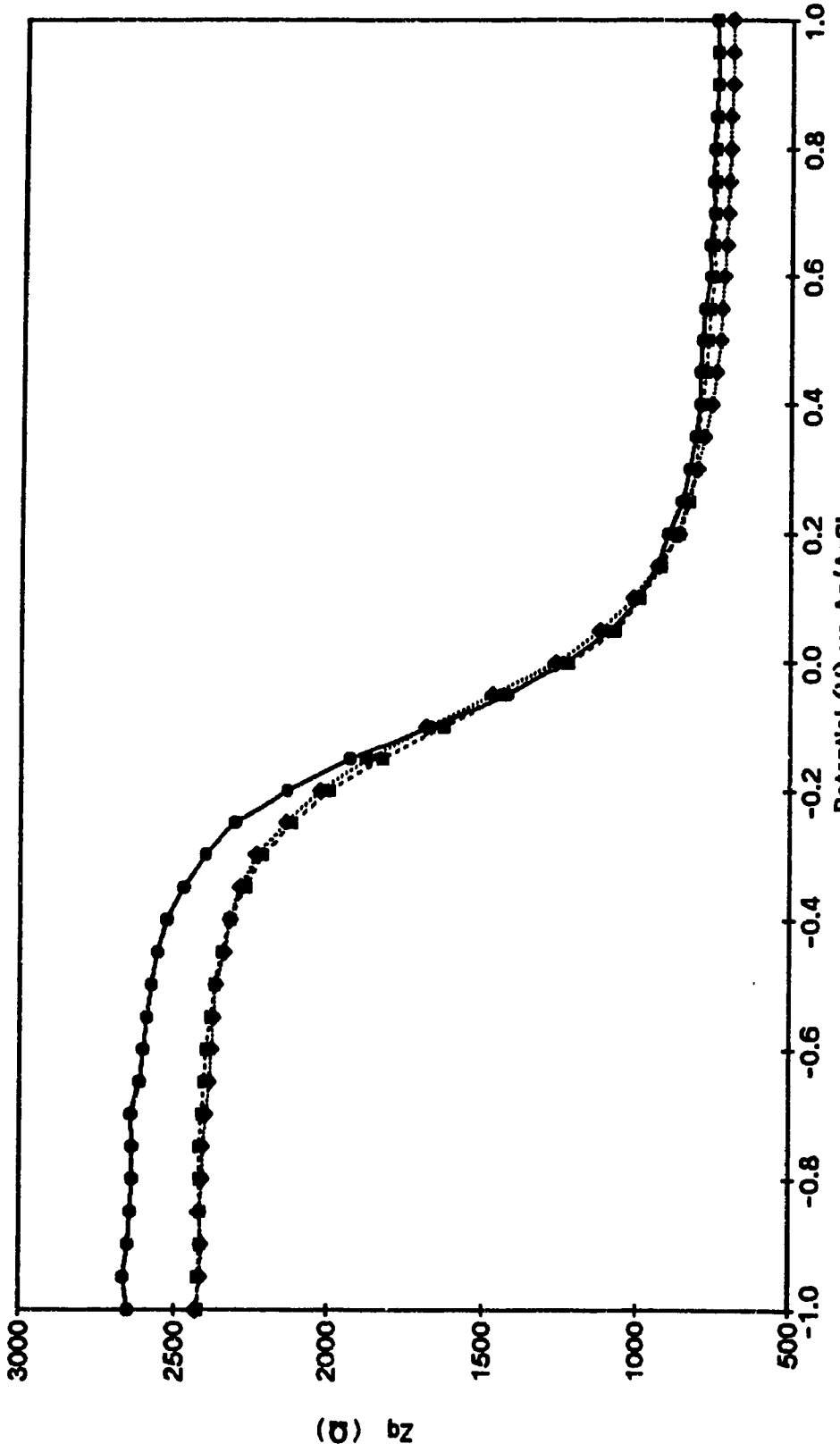

Figure II.3B Out-of-phase impedance measurements of an oligo(dT)$_{20}$ modified electrode before and after the boiling steps. The curves corresponding to the third and fourth boiling steps are omitted for clarity.

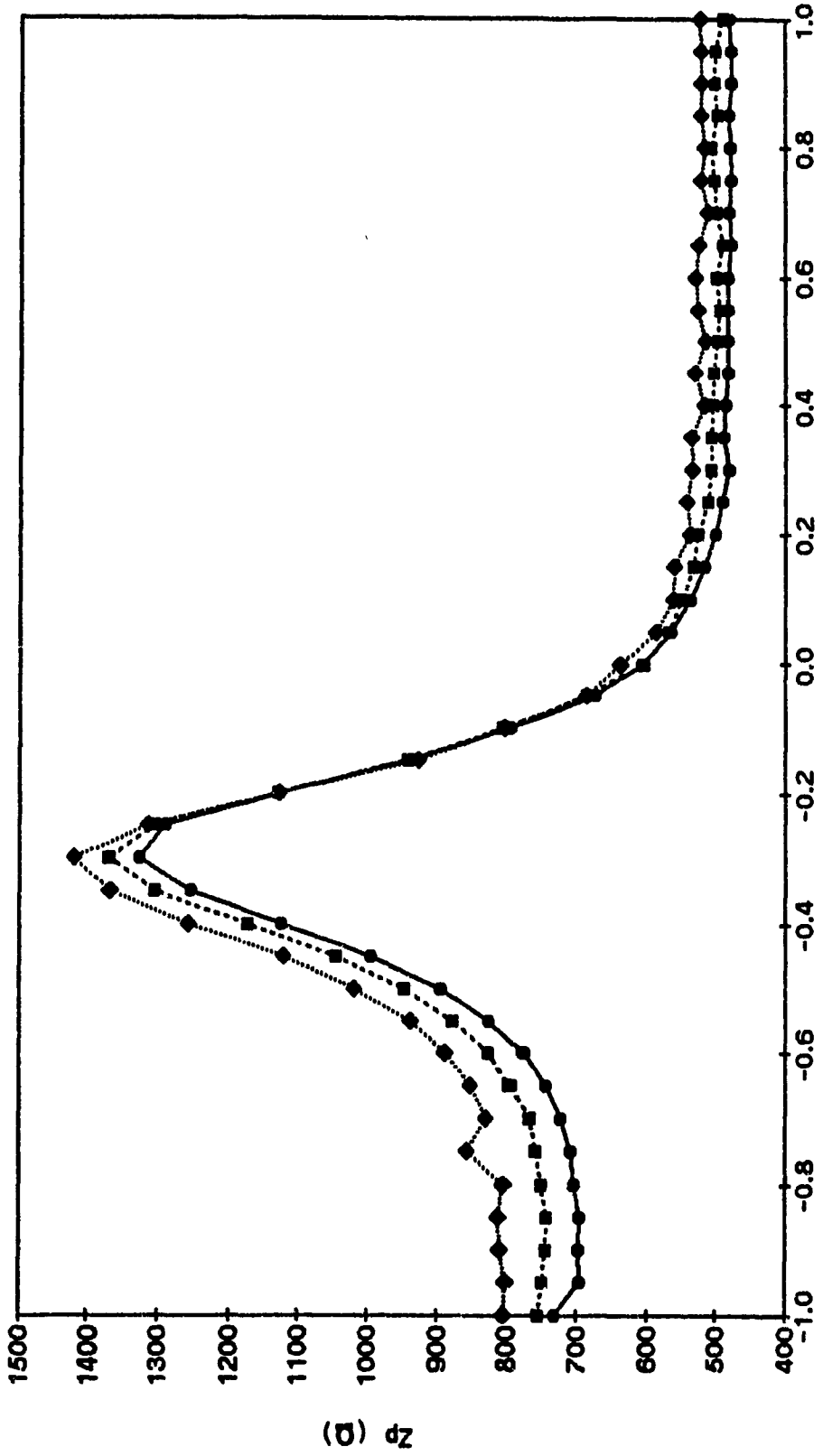

Figure II.4A In-phase impedance measurements of a poly(dT) modified electrode before and after the boiling steps. The curves corresponding to the third and fourth boiling steps are omitted for clarity.

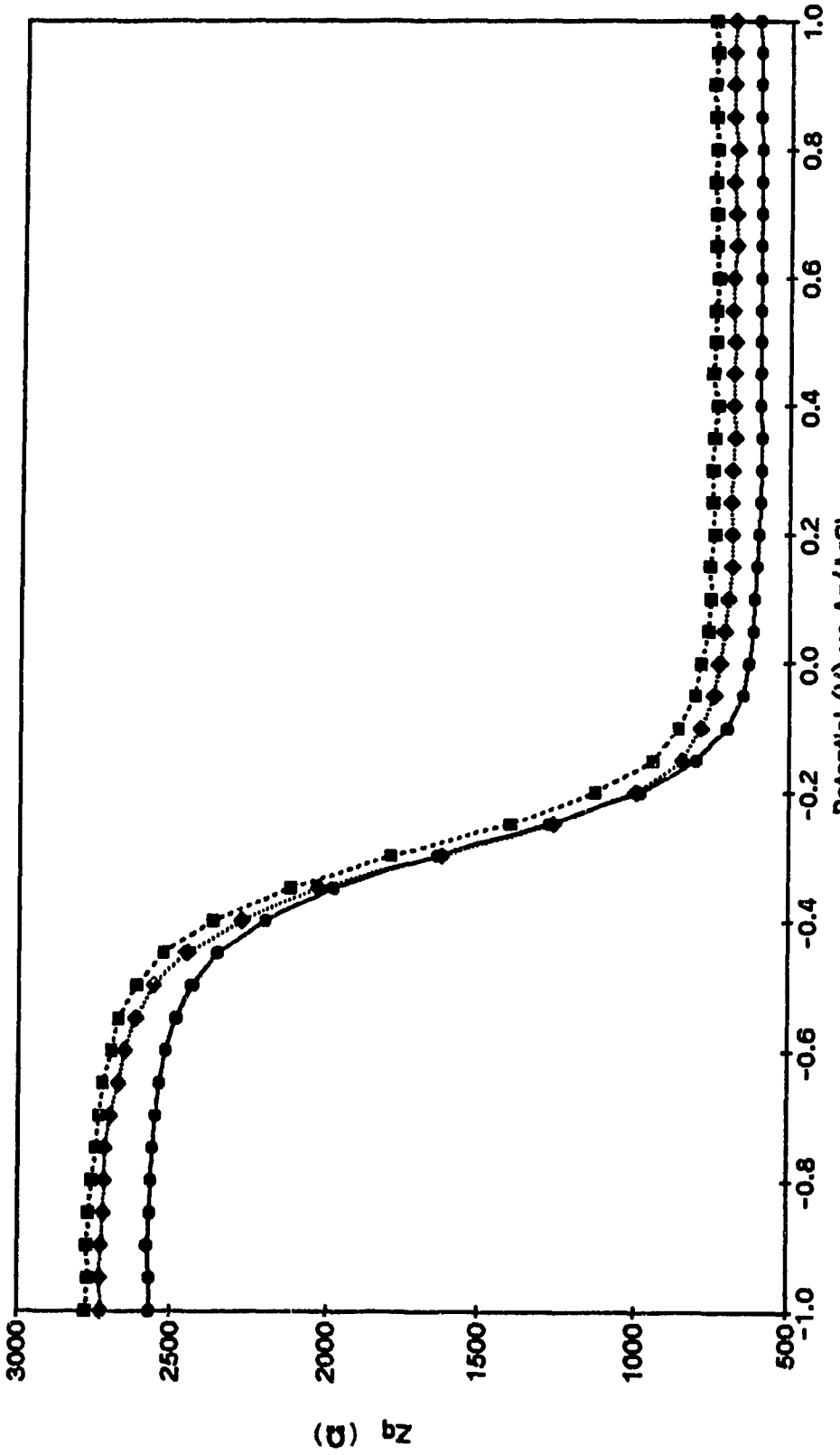

Figure II.4B Out-of-phase impedance measurements of a poly(dT) modified electrode before and after the boiling steps. The curves corresponding to the third and fourth boiling steps are omitted for clarity.

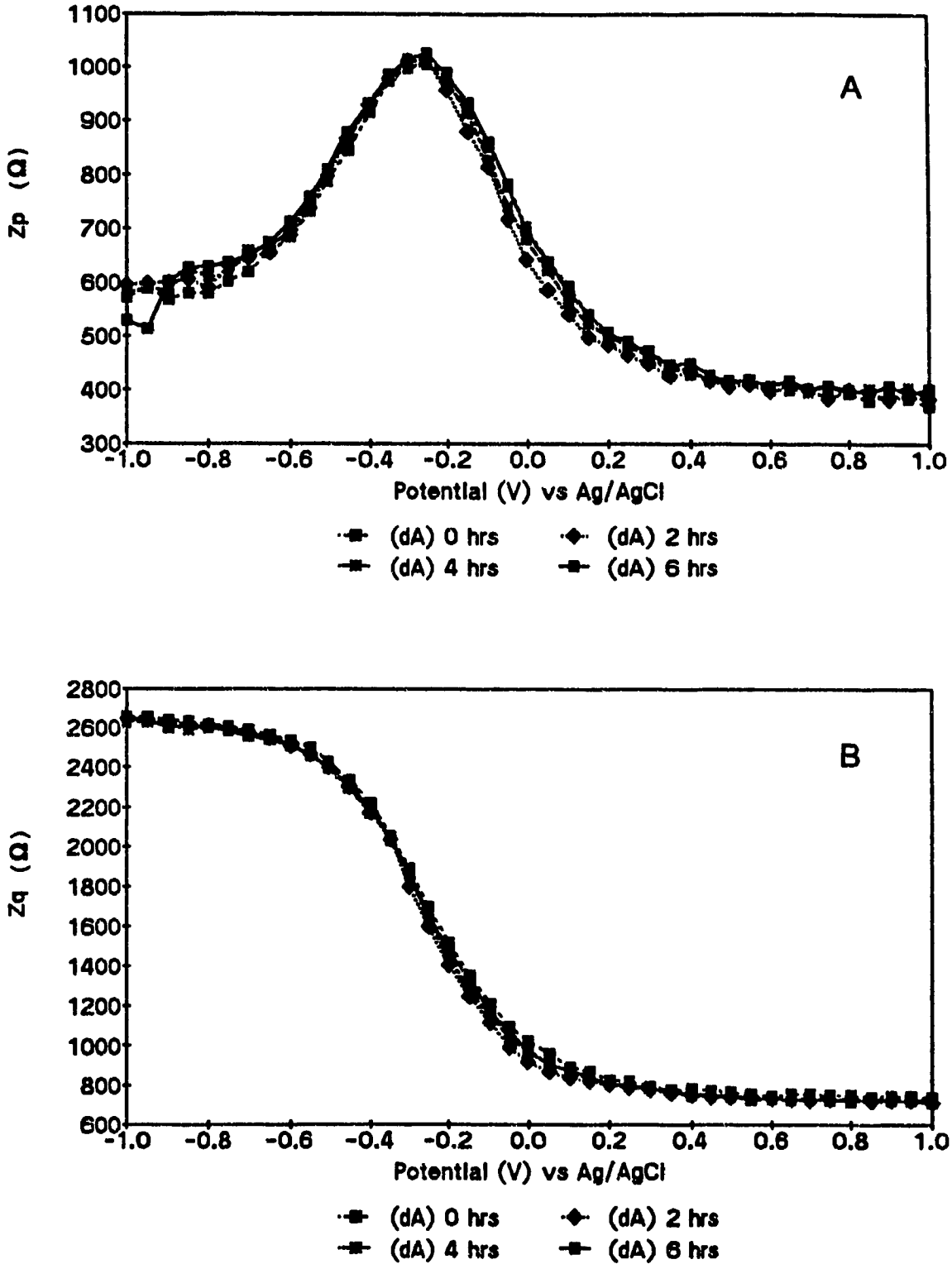

Figure II.5 (A) In-phase and (B) Out-of-phase impedance measurements to study storage stability of a poly(dT) modified electrode in Tris HCl.

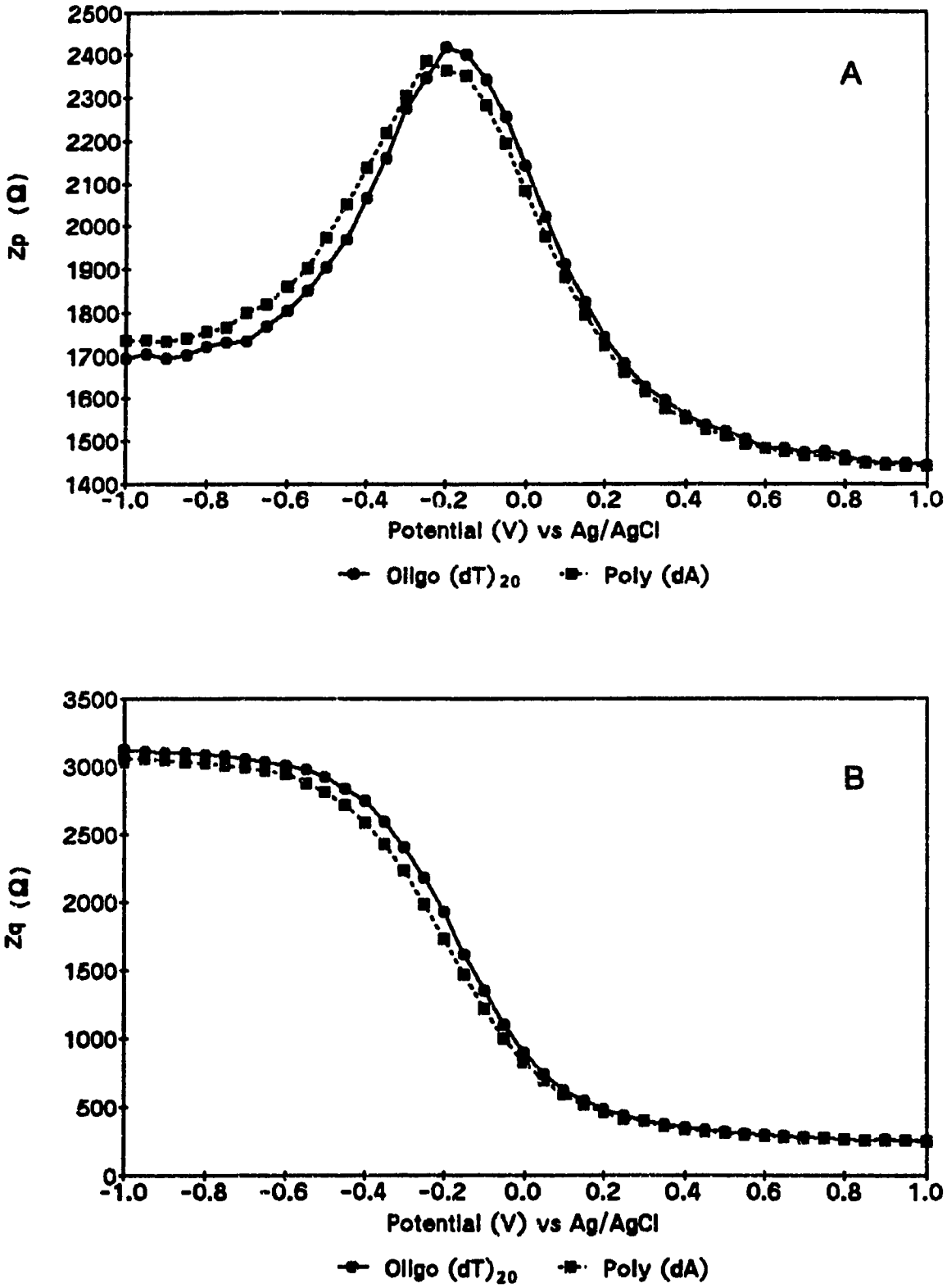

Figure II.6 (A) In-phase and (B) Out-of-phase impedance measurements of an oligo$(dT)_{20}$ - poly(dA) modified electrode.

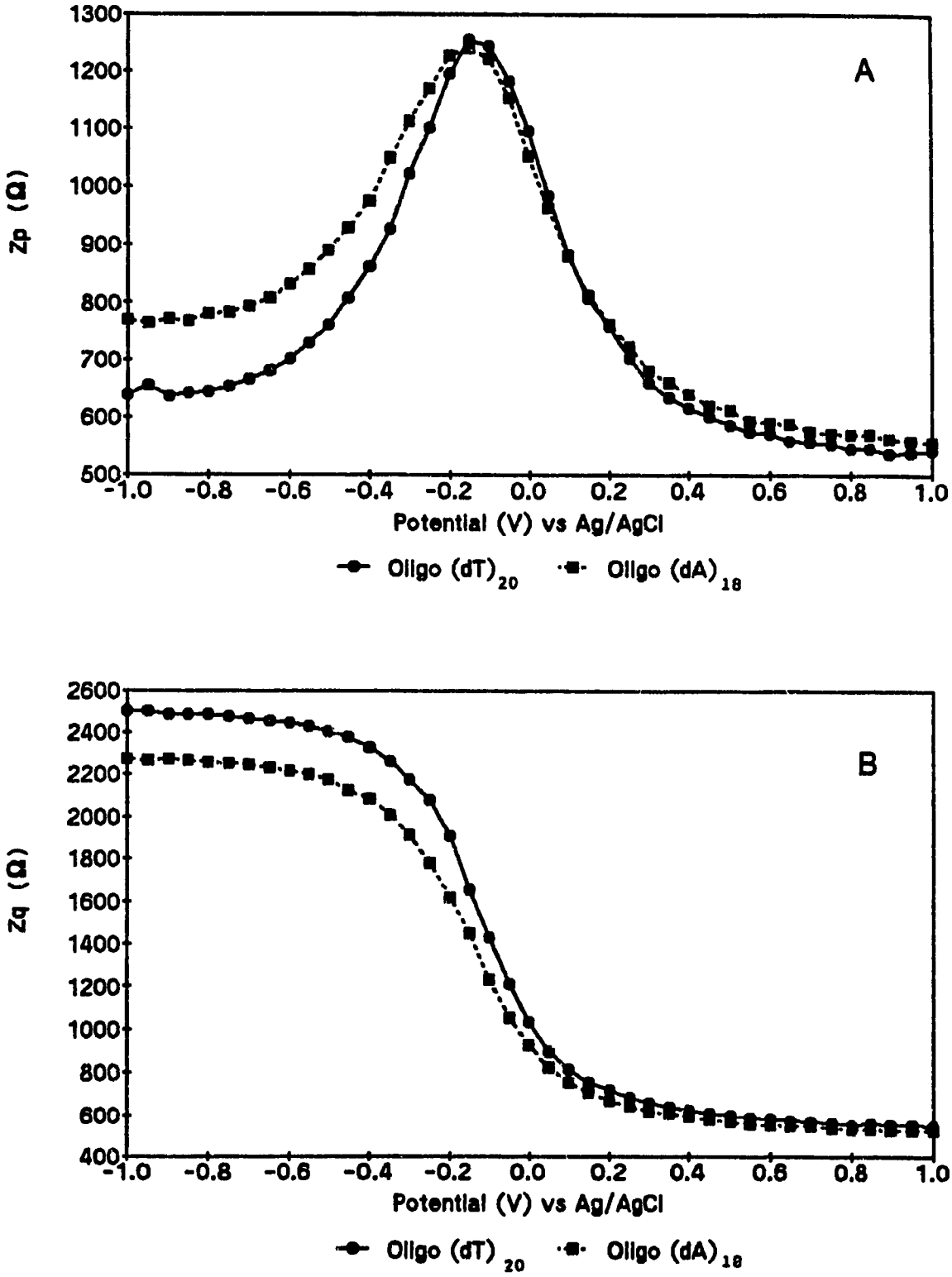

Figure II.7 (A) In-phase and (B) Out-of-phase impedance measurements of an oligo$(dT)_{20}$ - oligo$(dA)_{18}$ modified electrode.

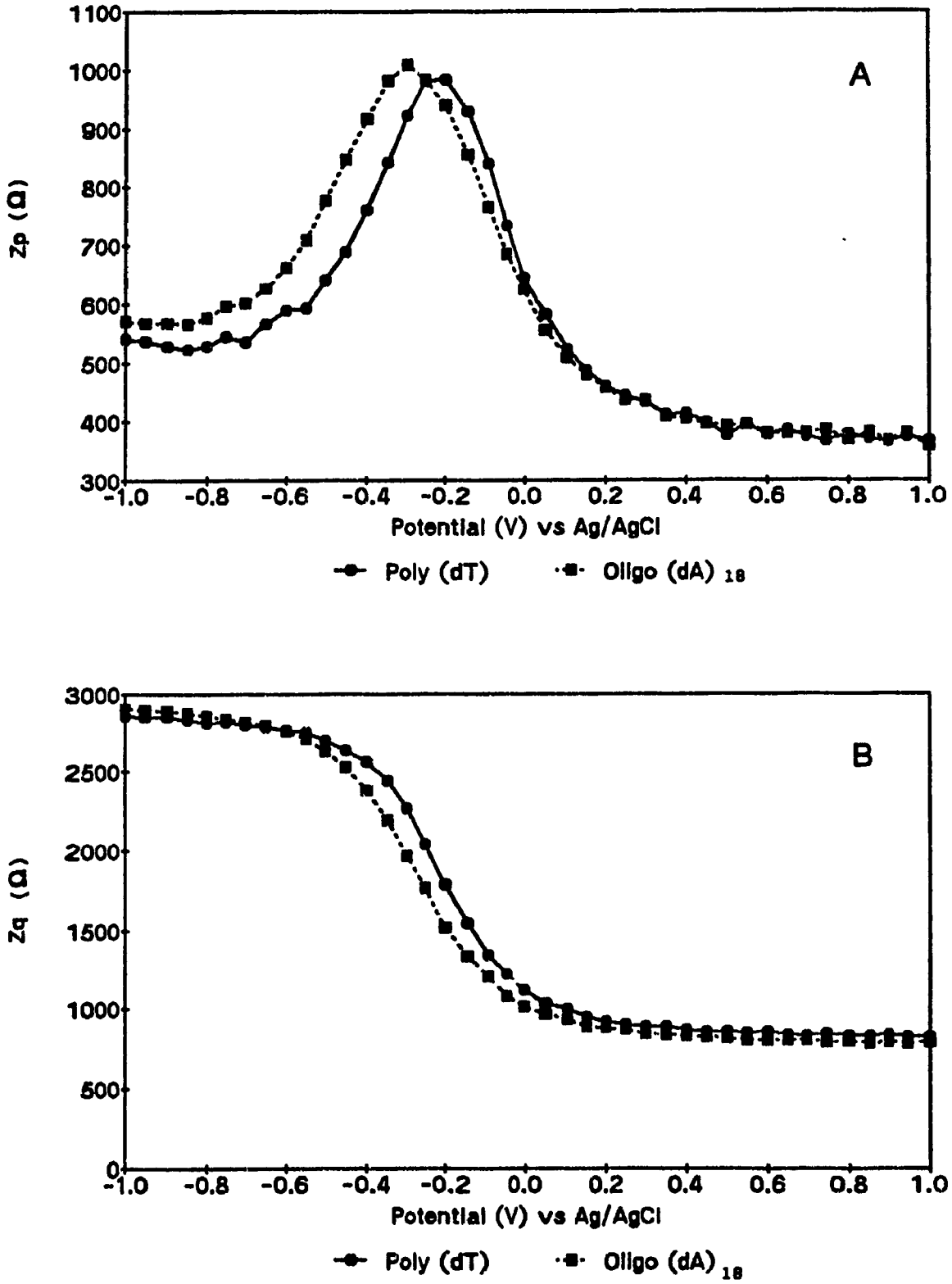

Figure II.8 (A) In-phase and (B) Out-of-phase impedance measurements of a poly(dT) - oligo$(dA)_{18}$ modified electrode.

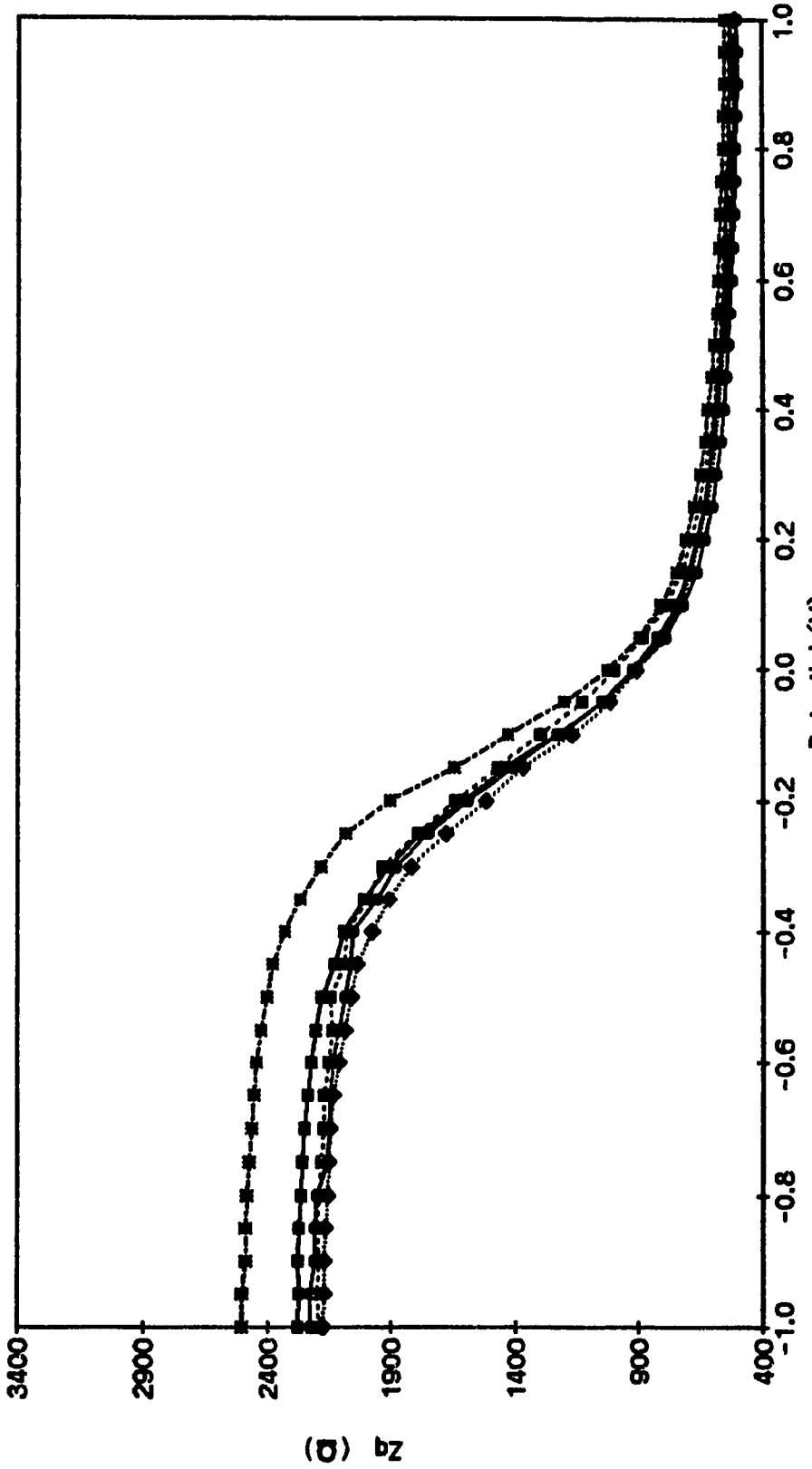

Figure II.9 Out-of-phase impedance measurements of an oligo(dT)$_{20}$ modified electrode, hybridized with oligo (dA)$_{18}$. Values used to calculate the capacitance values of Figure 4.3.

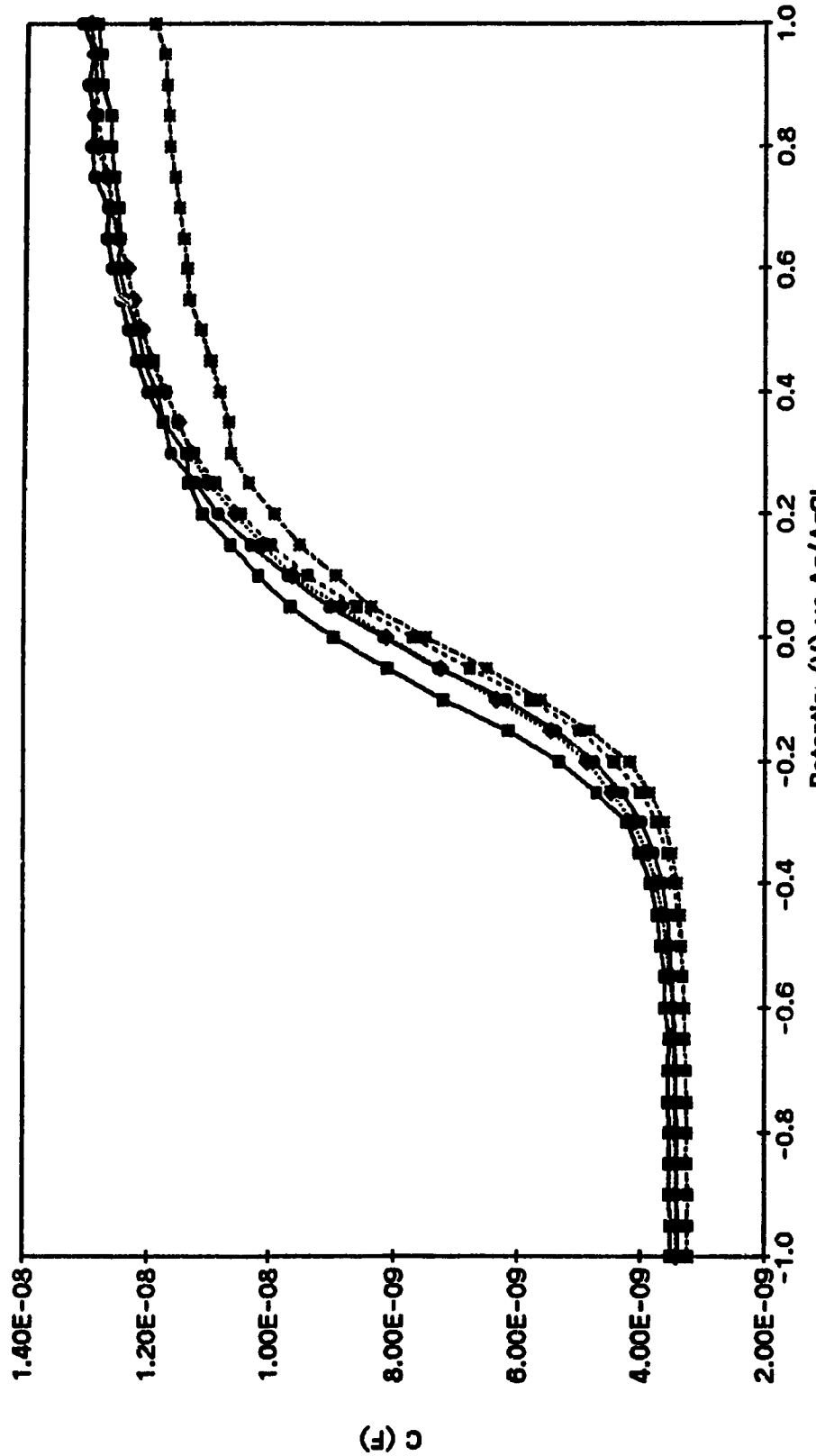

Figure II.10A Capacitance measurements of an oligo(dT)$_{20}$ modified electrode hybridized with poly(dA).

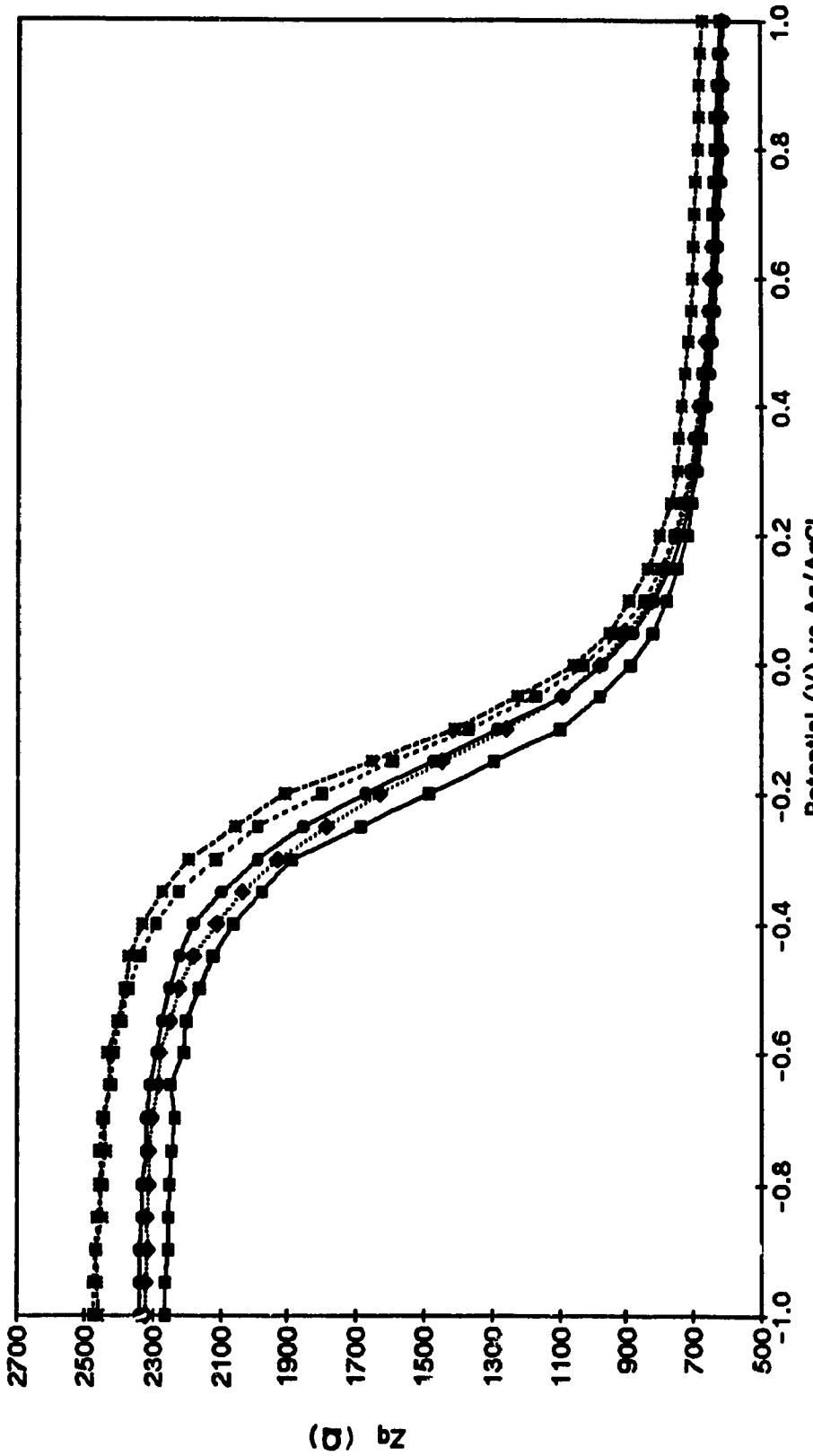

Figure II.10B Out-of-phase impedance measurements of an oligo(dT)$_{20}$ modified electrode, hybridized with poly(dA).

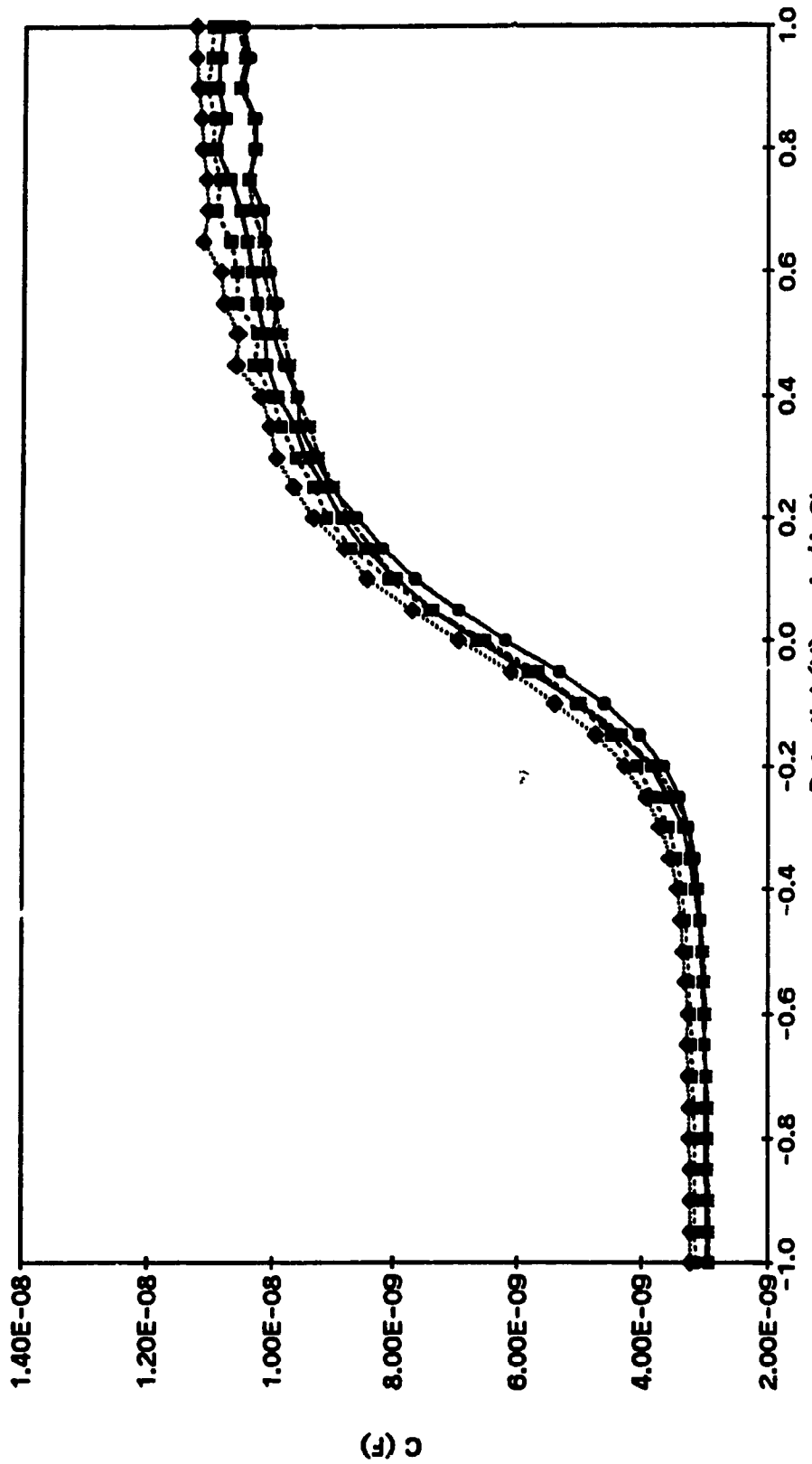

Figure II.11A Capacitance measurements of a poly(dT) modified electrode hybridized with poly(dA).

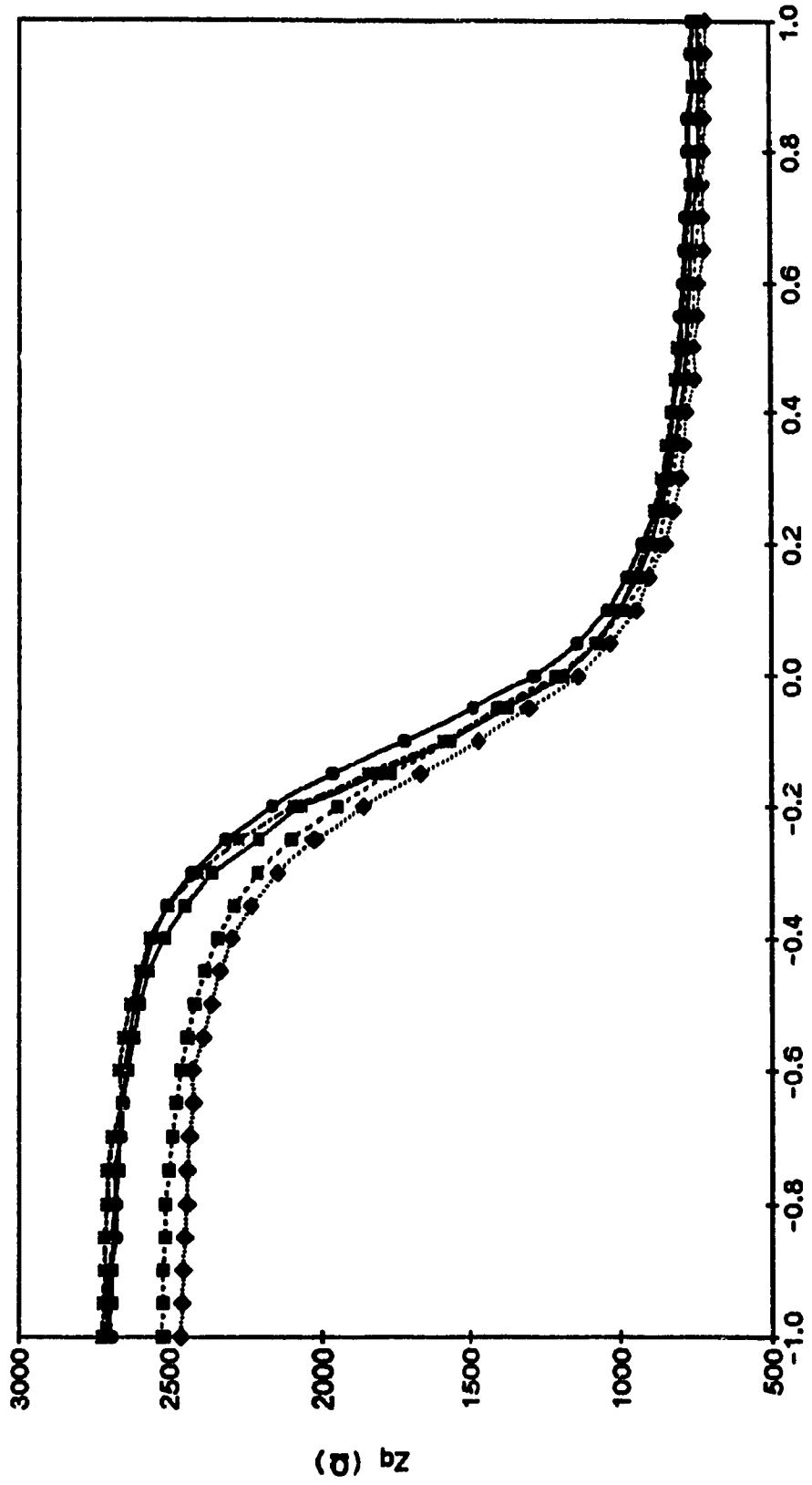

Figure II.11B Out-of-phase impedance measurements of a poly(dT) modified electrode, hybridized with poly(dA).

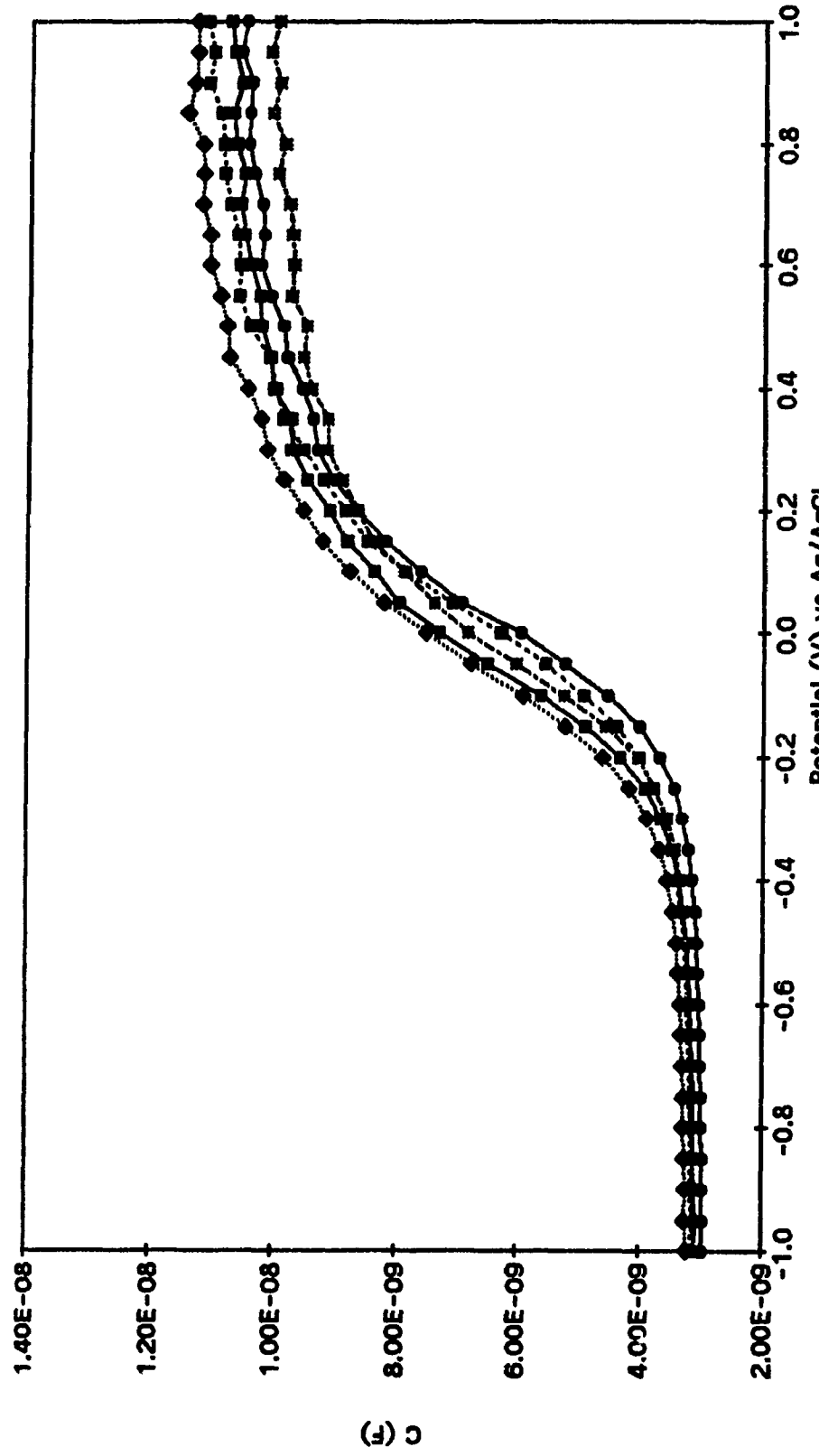

Figure II.12A Capacitance measurements of a poly(dT) modified electrode hybridized with oligo(dA)$_{18}$.

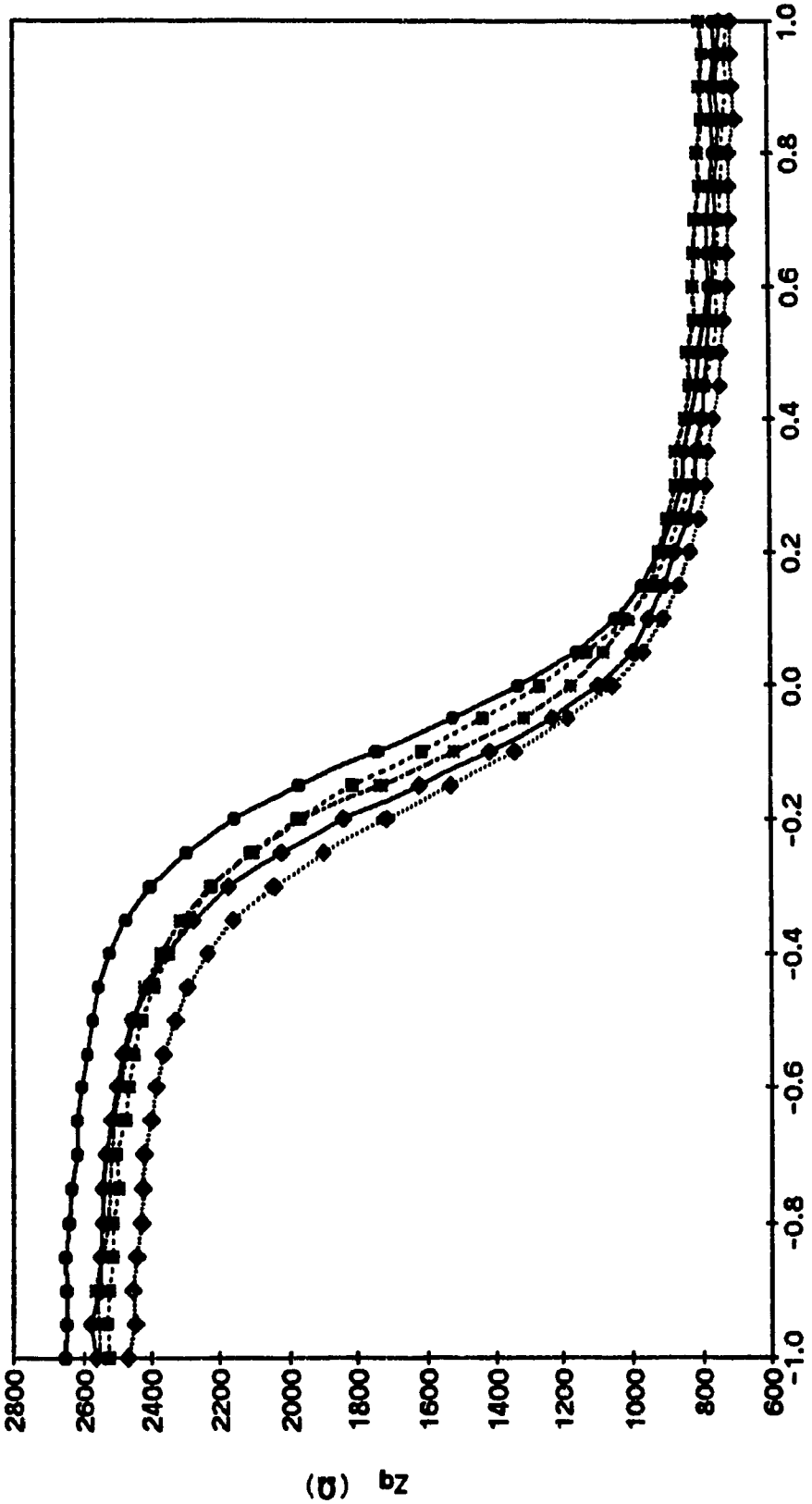

Figure II.12B Out-of-phase impedance measurements of a poly(dT) modified electrode, hybridized with oligo$(dA)_{18}$.

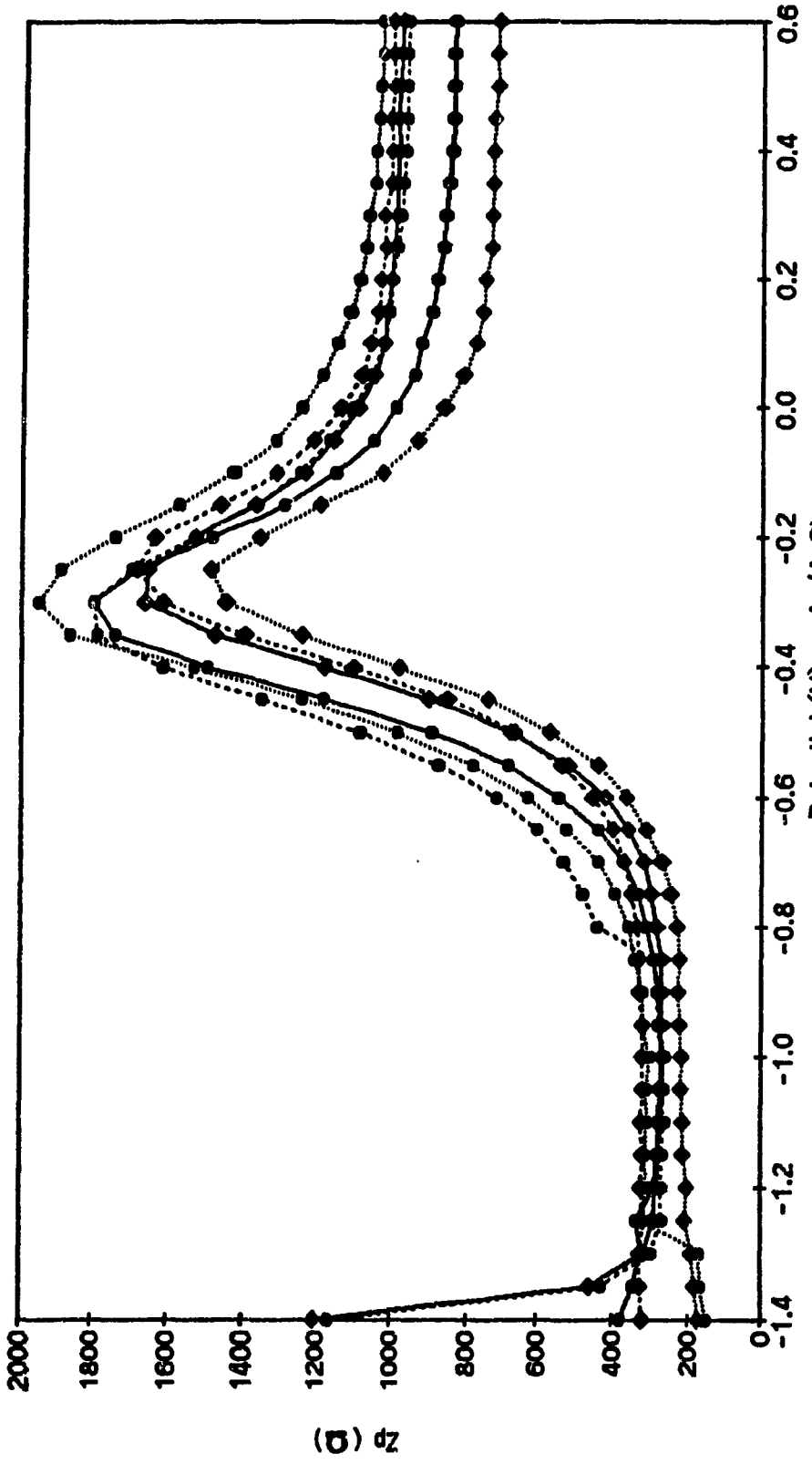

Figure II.13A In-phase impedance measurements of an oligo(dT)$_{20}$ modified electrode rehybridized twice with poly(dA).

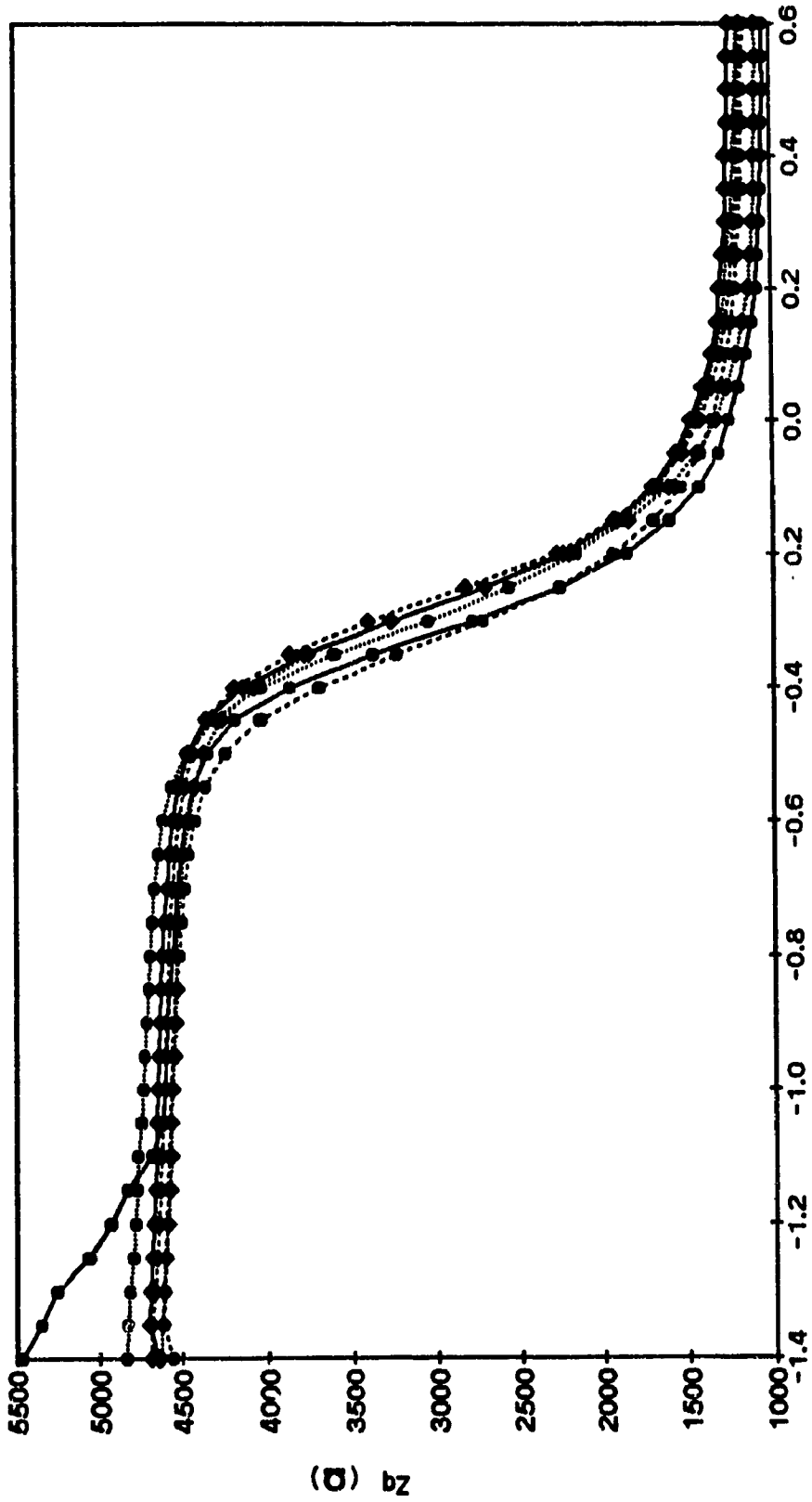

Figure II.13B Out-of-phase impedance measurements of an oligo(dT)$_{20}$ modified electrode rehybridized twice with poly(dA).

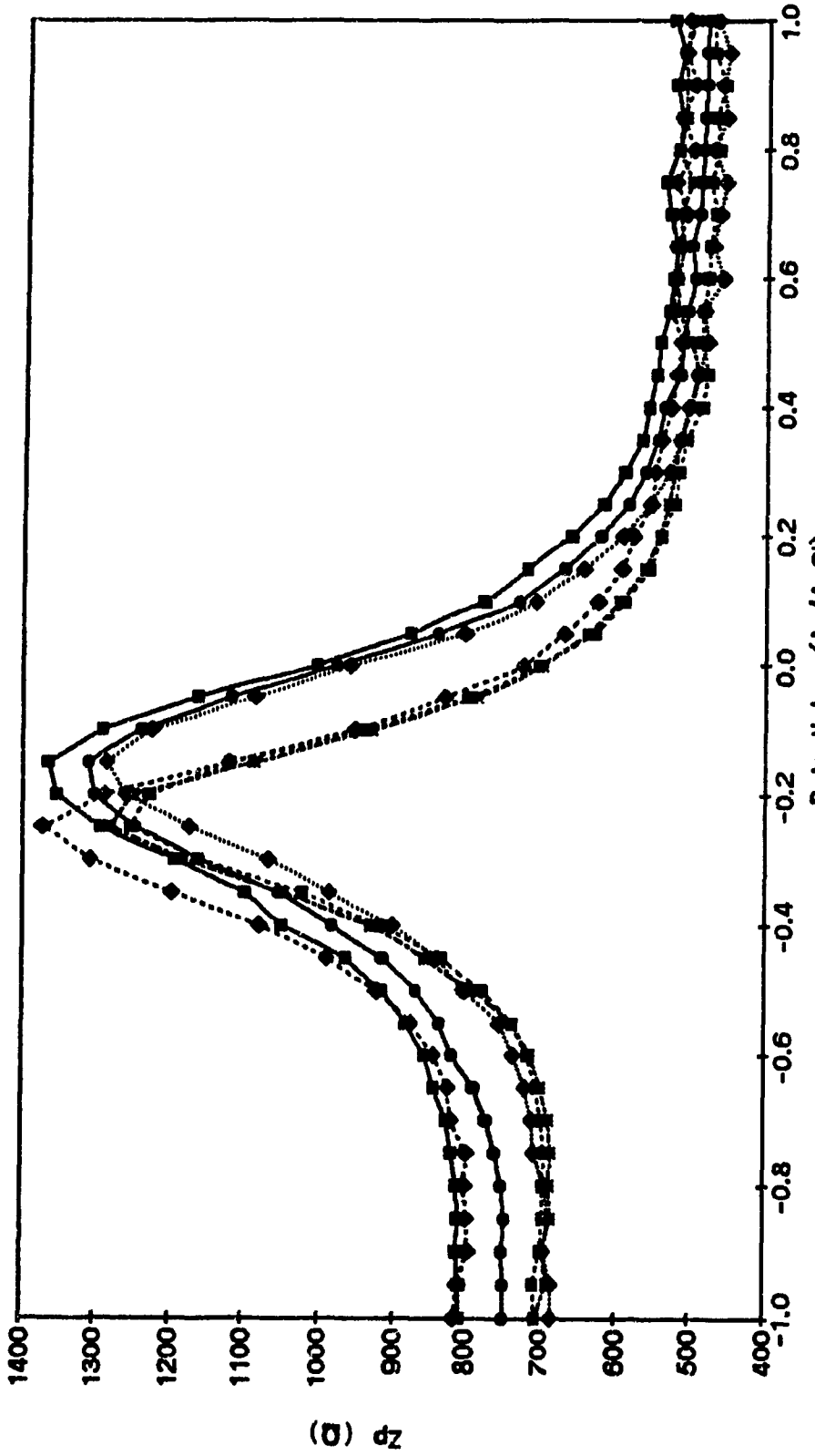

Figure II.14A In-phase impedance measurements of a poly(dT) modified electrode rehybridized twice with oligo(dA)$_{18}$.

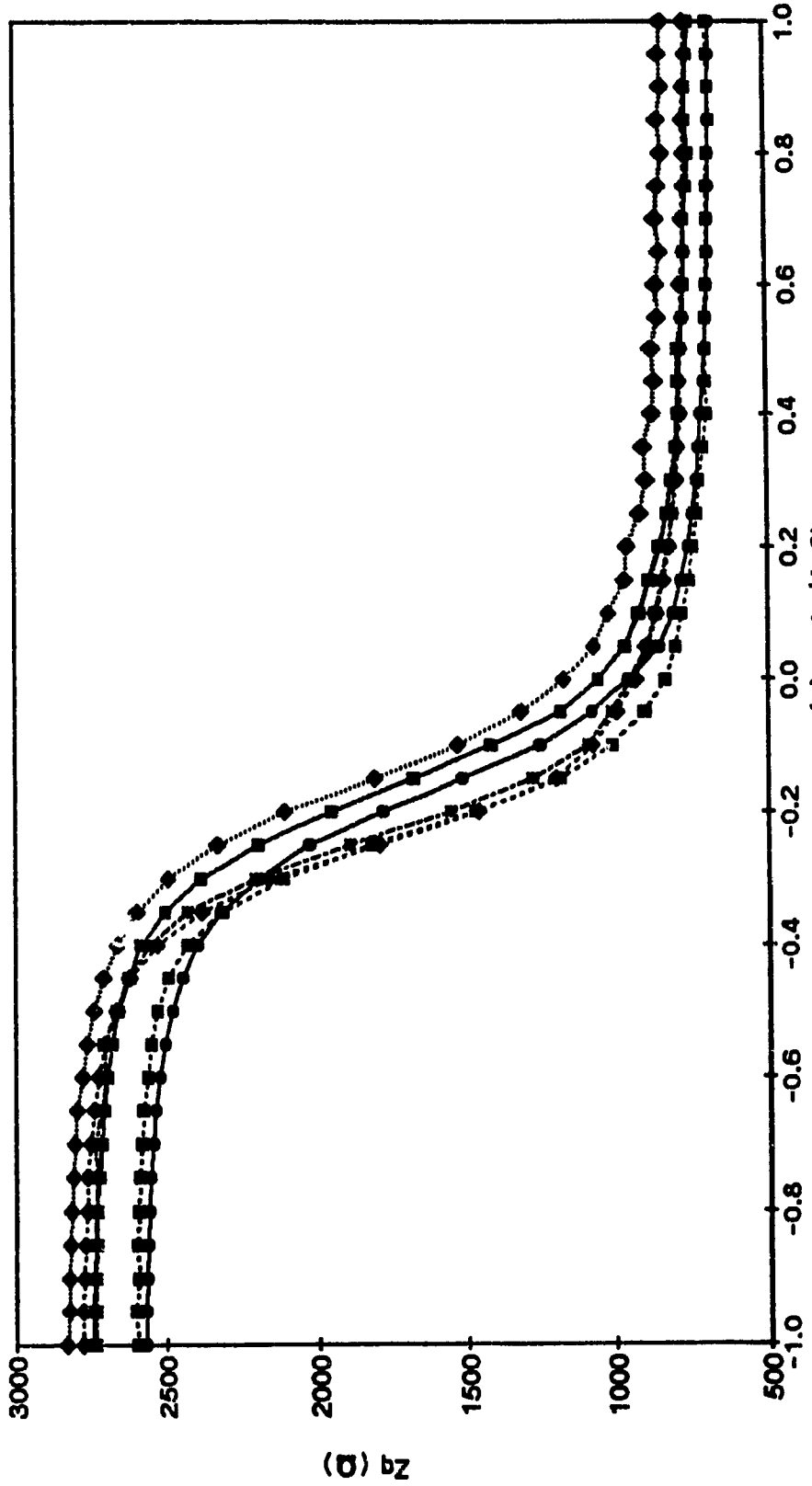

Figure II.14B Out-of-phase impedance measurements of a poly(dT) modified electrode rehybridized twice with oligo$(dA)_{18}$.

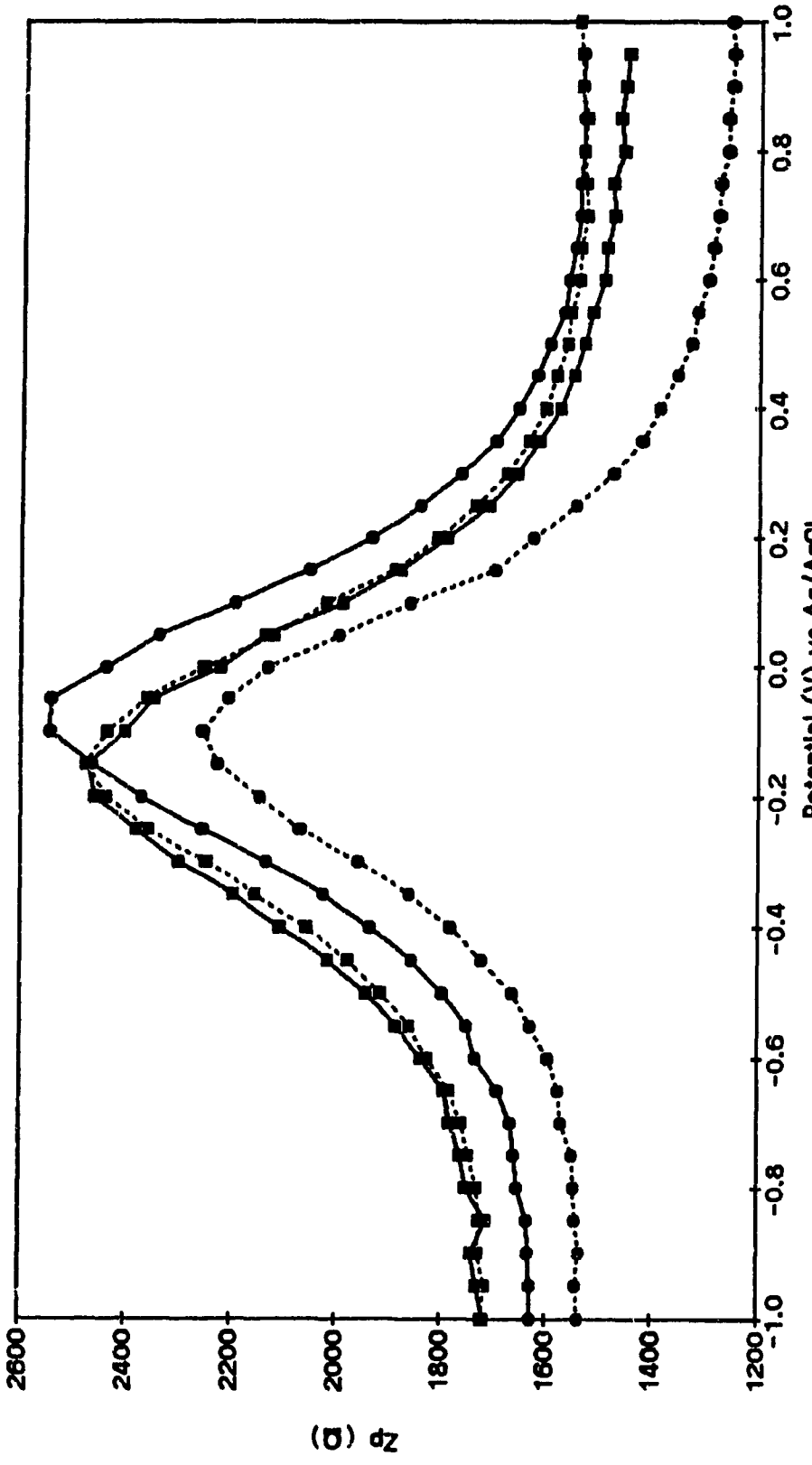

Figure II.15A In-phase impedance measurements of an oligo(dT)$_{20}$ modified electrode hybridized twice with poly(dA).

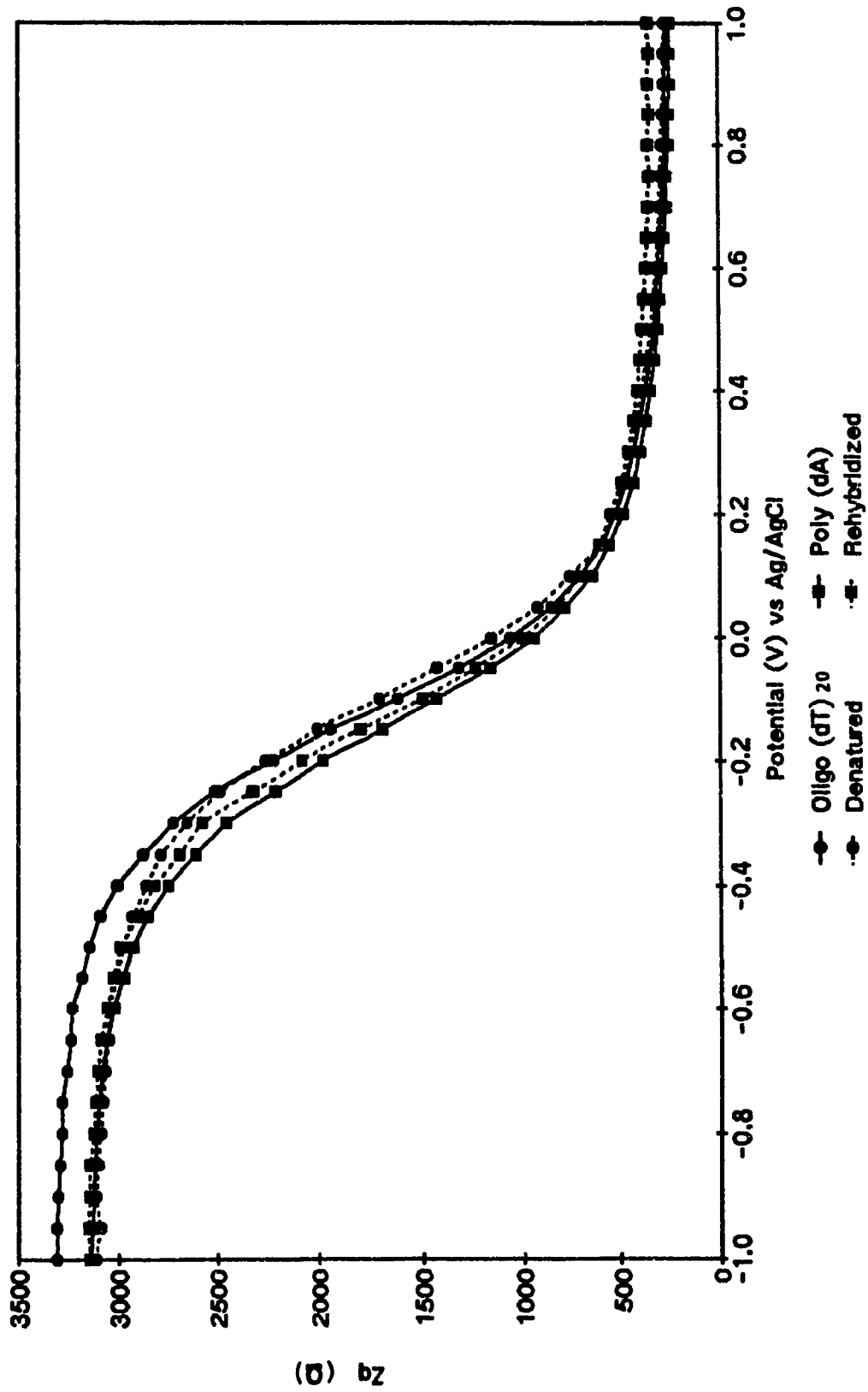

Figure II.15B Out-of-phase impedance measurements of an oligo(dT)$_{20}$ modified electrode hybridized twice with poly(dA).

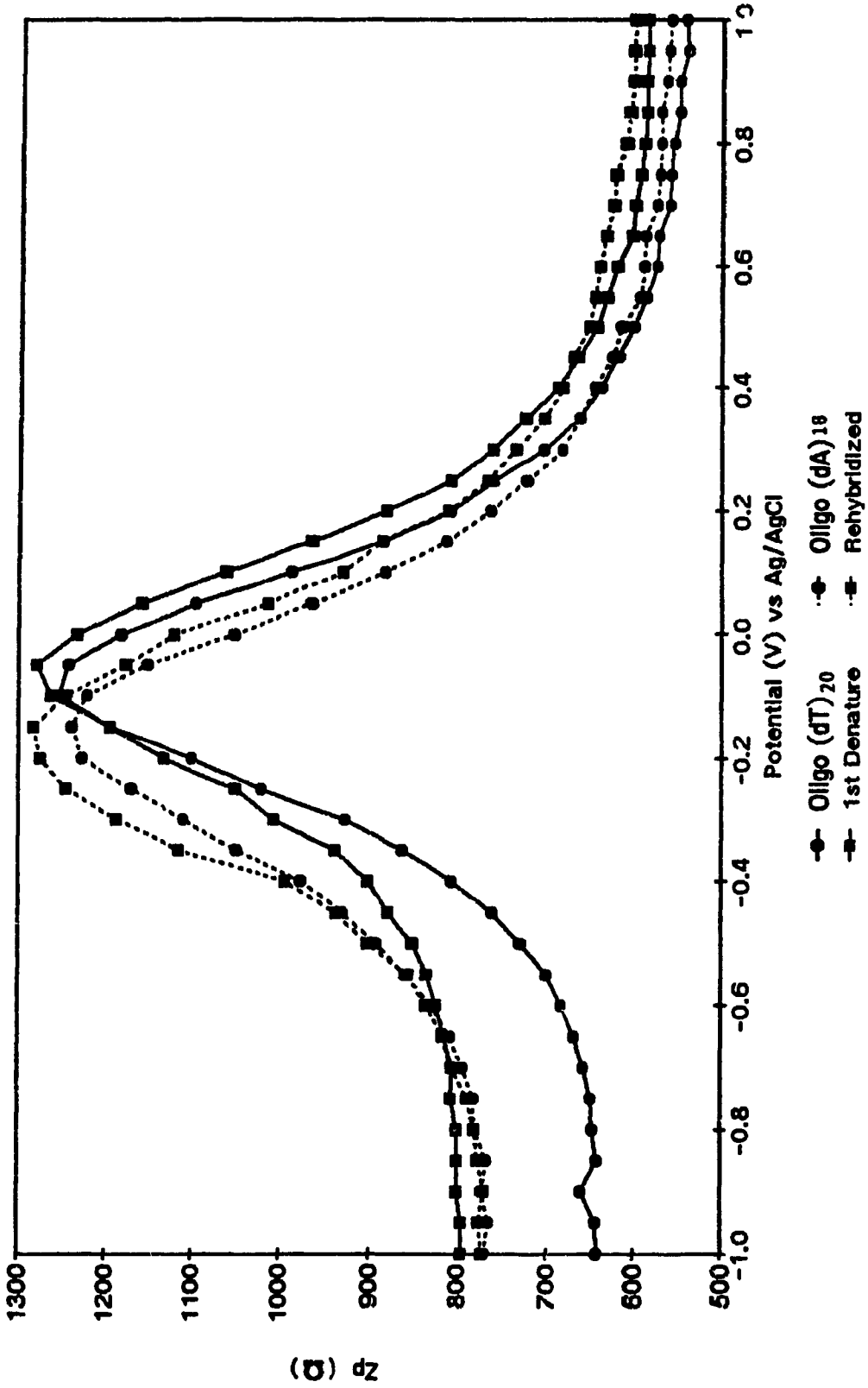

Figure II.16A In-phase impedance measurements of an oligo(dT)$_{20}$ modified electrode rehybridized with oligo(dA)$_{18}$.

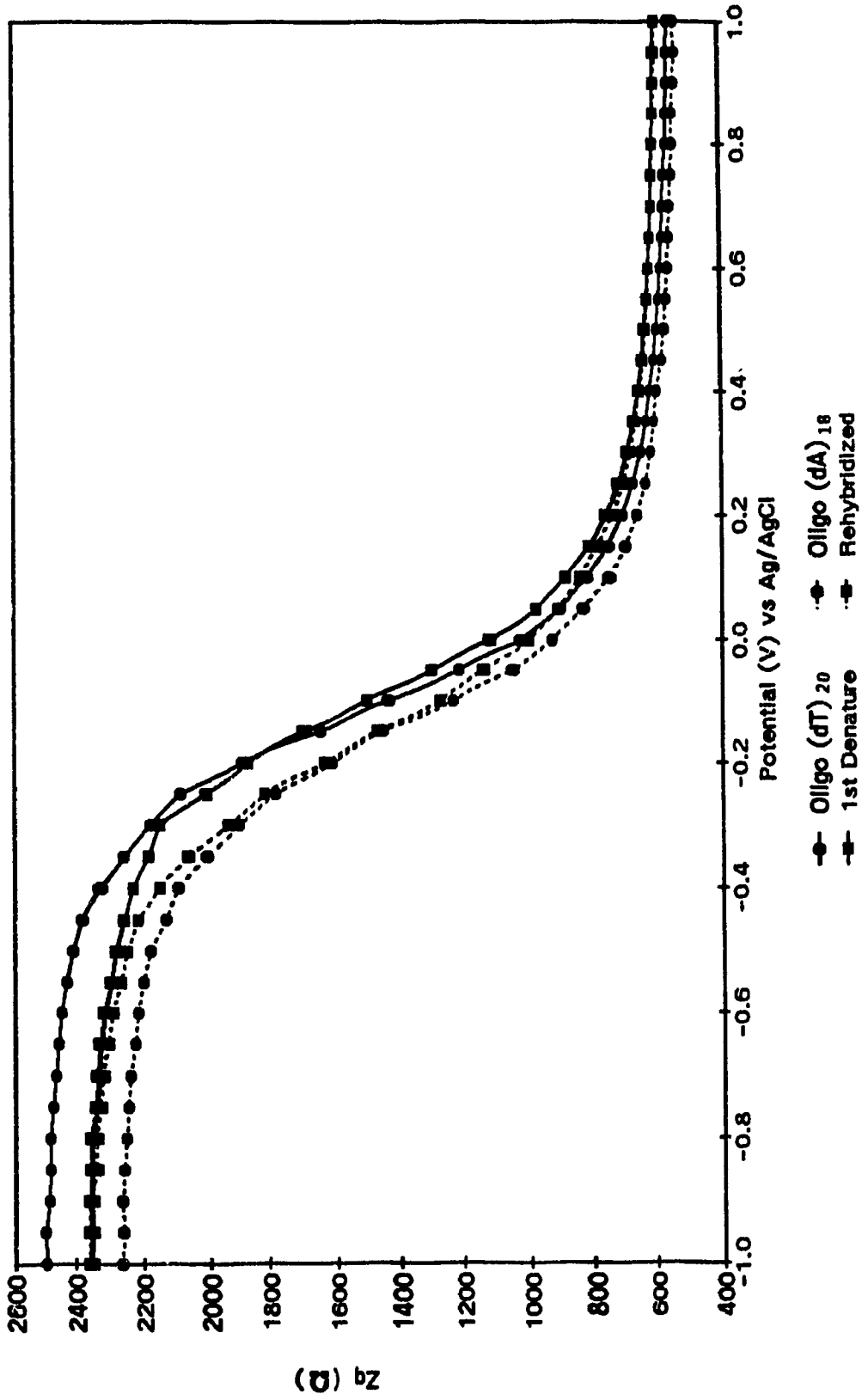

Figure II.16B Out-of-phase impedance measurements of an oligo(dT)$_{20}$ modified electrode rehybridized with oligo (dA)$_{18}$.

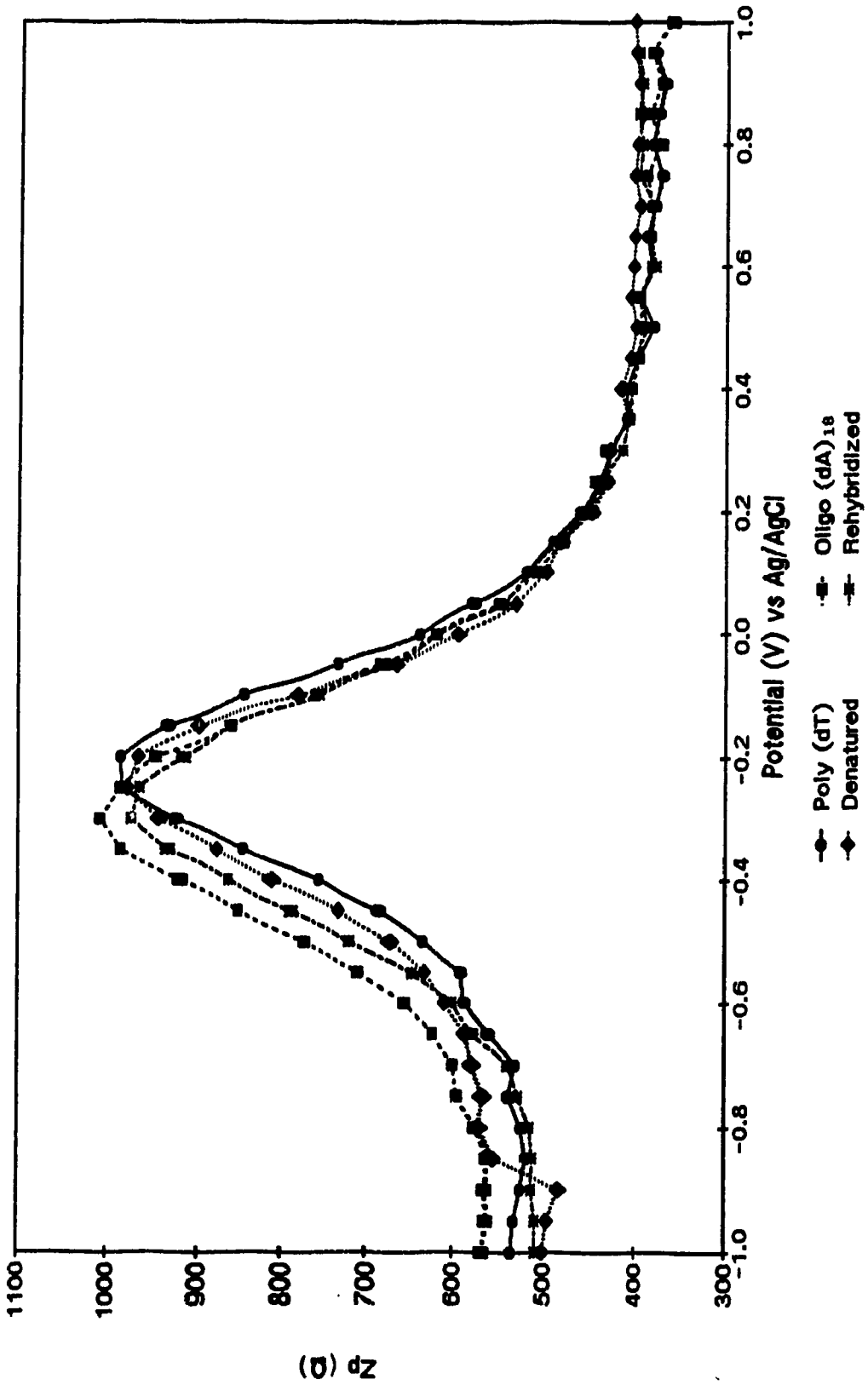

Figure II.17A In-phase impedance measurements of a poly(dT) modified electrode rehybridized with oligo(dA)$_{18}$.

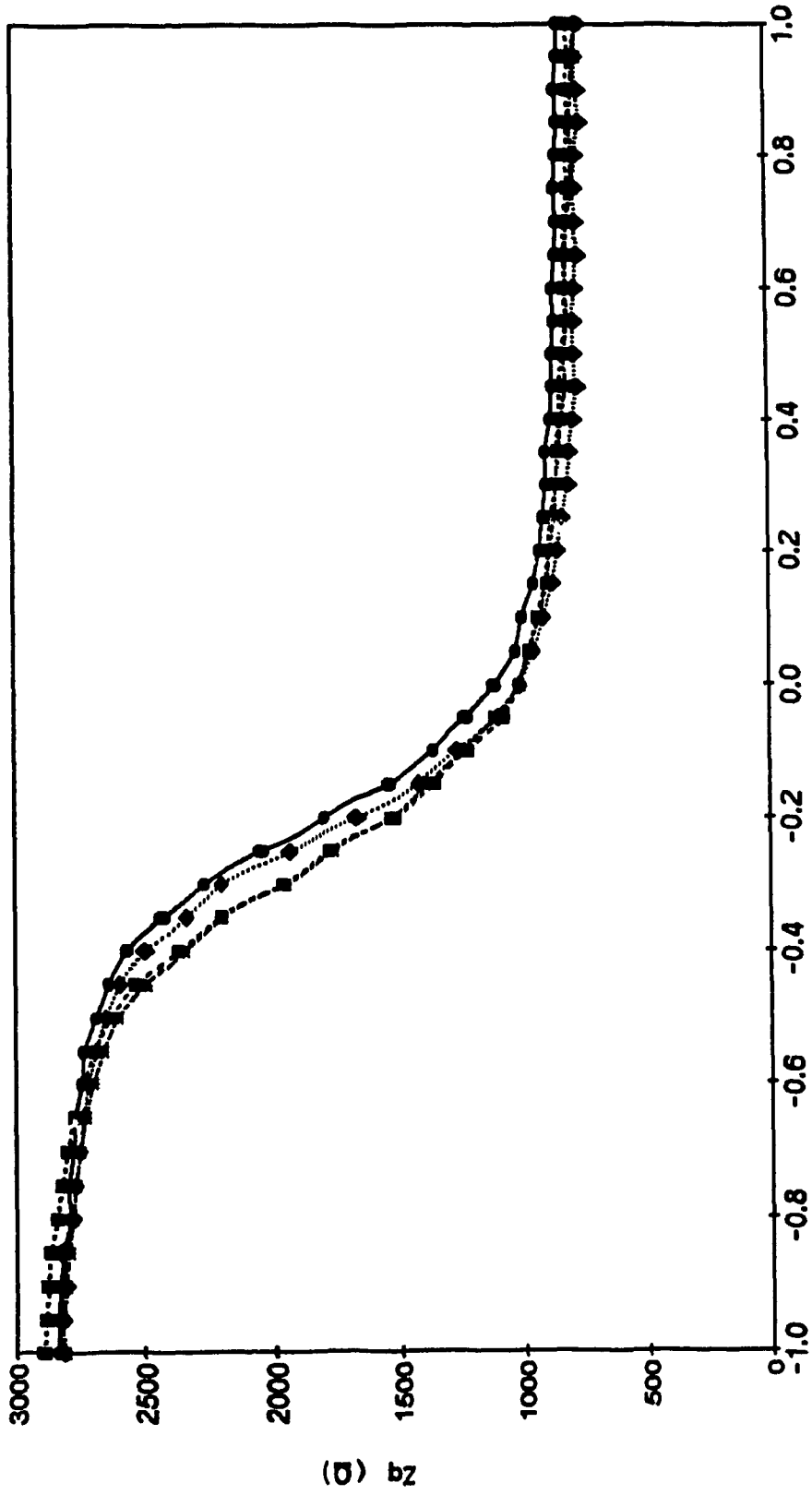

Figure II.17B Out-of-phase impedance measurements of a poly(dT) modified electrode rehybridized with oligo(dA)$_{18}$.

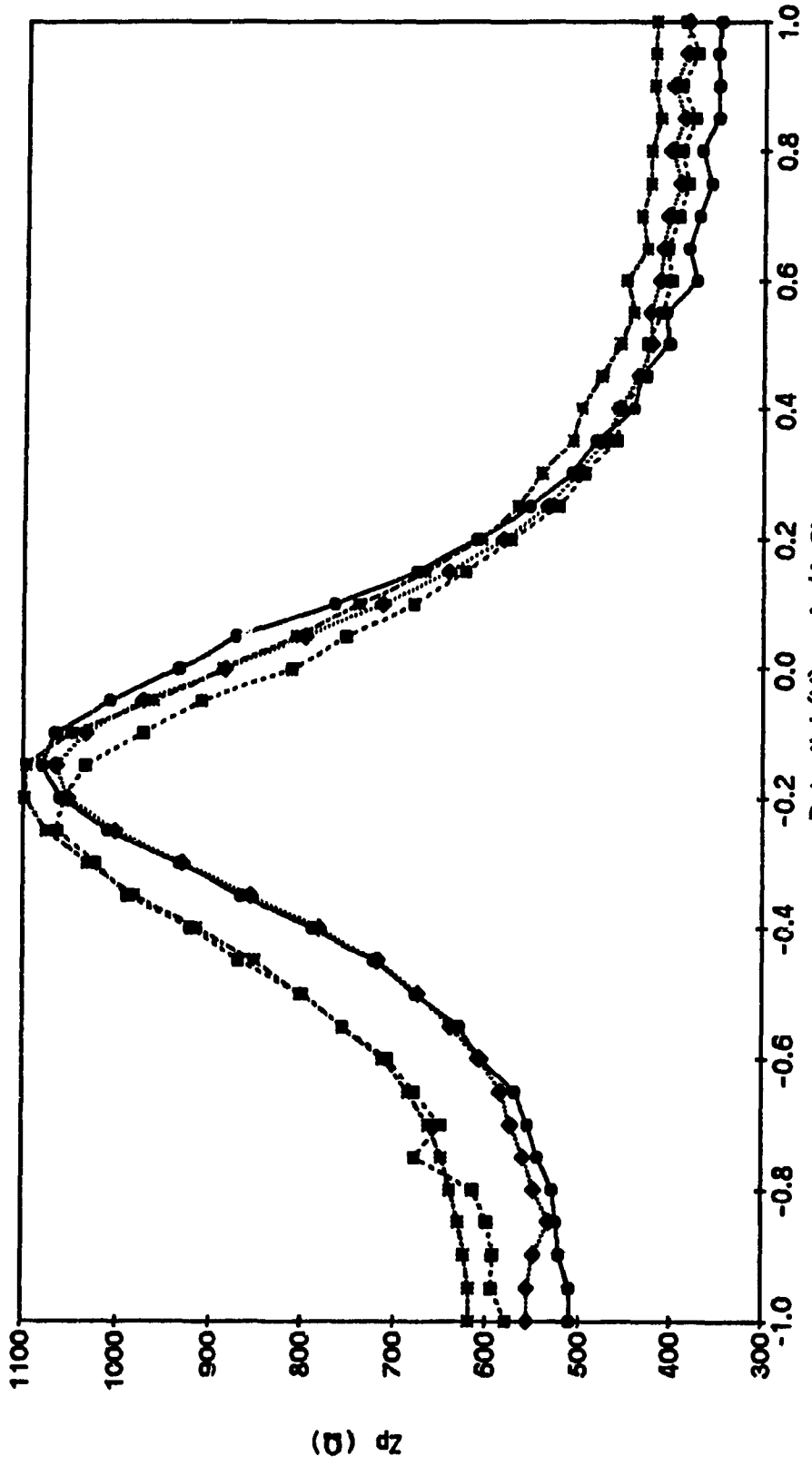

Figure II.18A In-phase impedance measurements of an oligo(dT)$_{20}$ modified electrode hybridized with single stranded calf thymus DNA at room temperature.

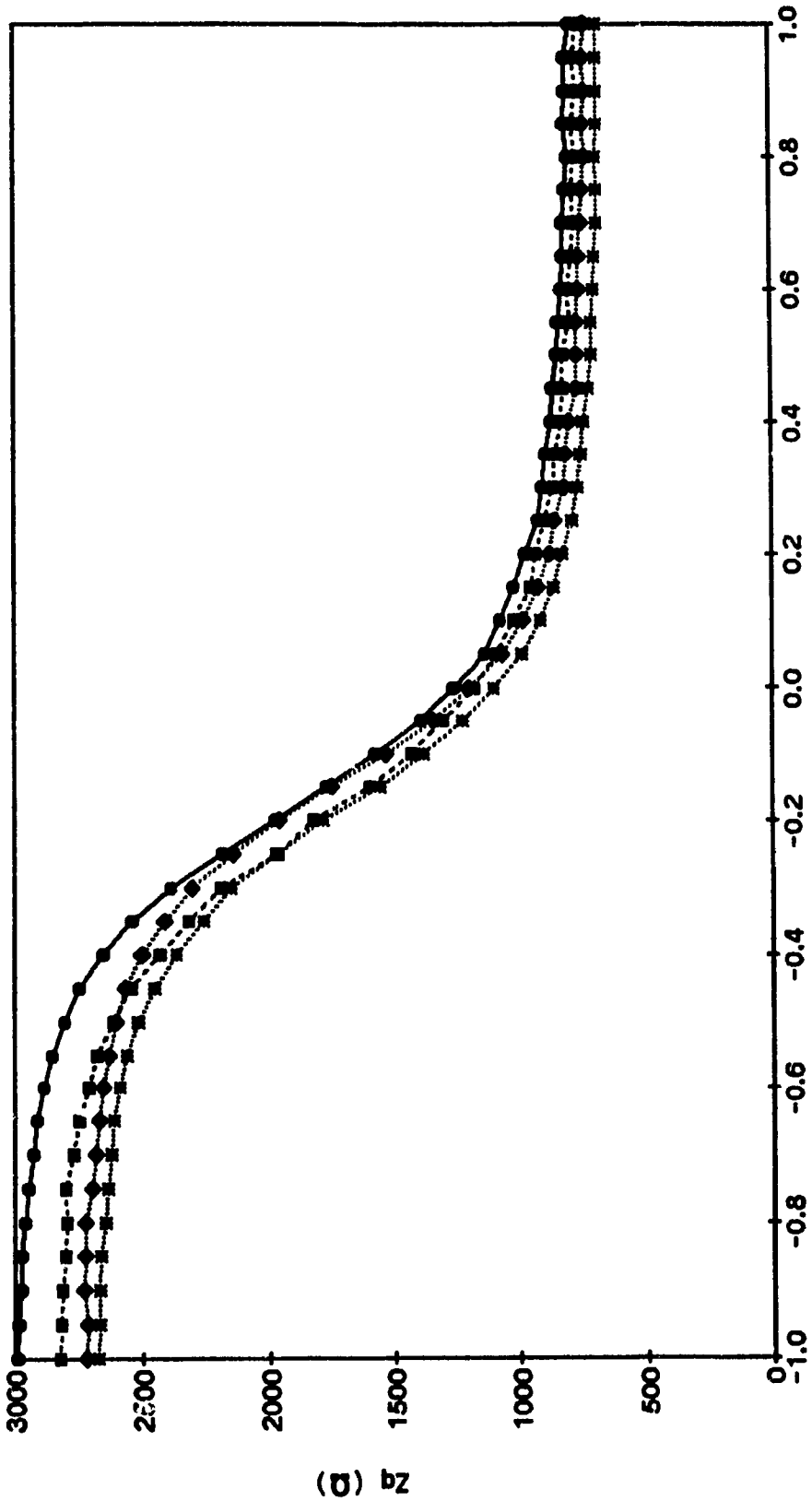

Figure II.18B Out-of-phase impedance measurements of an oligo(dT)$_{20}$ modified electrode hybridized with single stranded calf thymus DNA at room temperature.

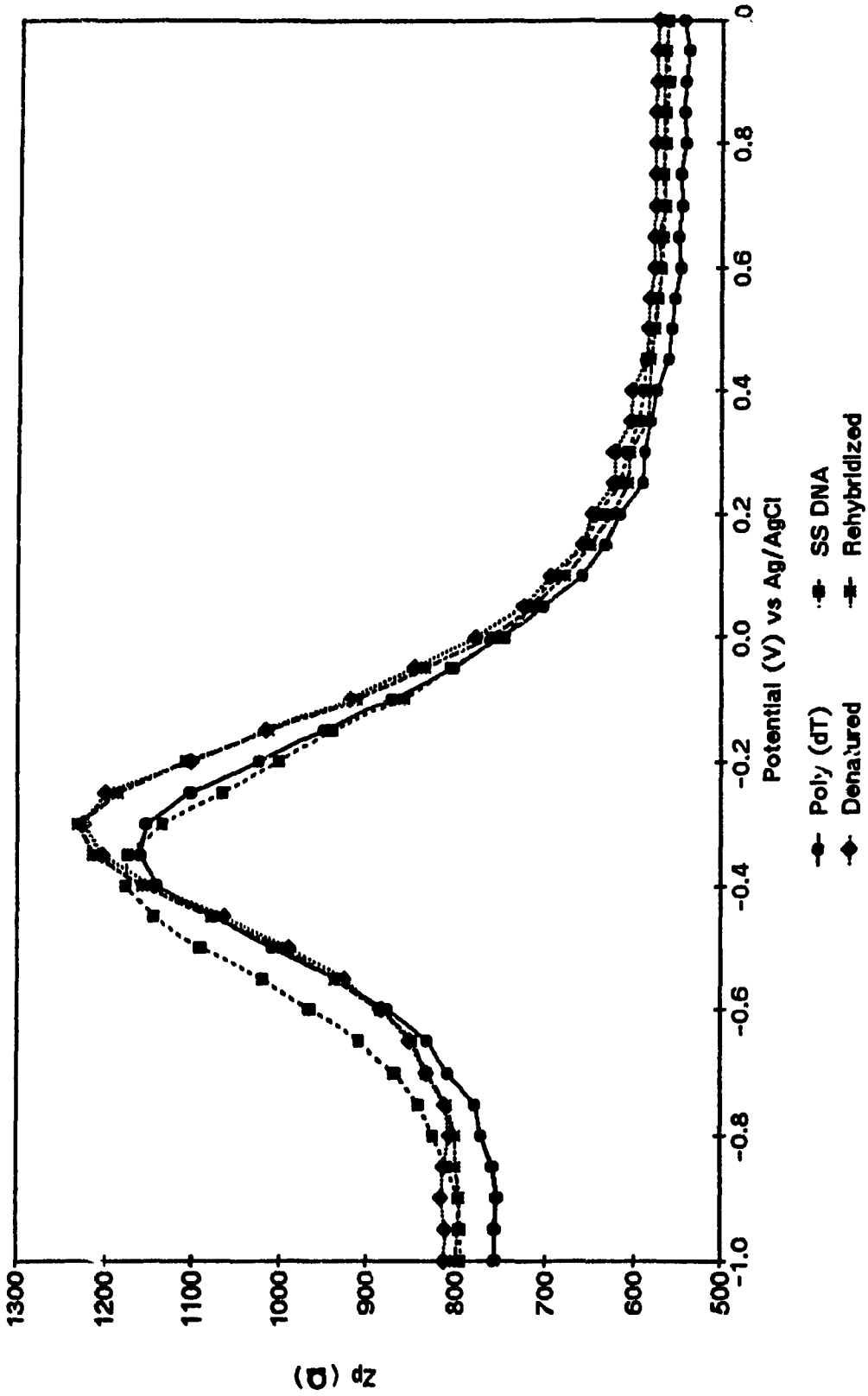

Figure II.19A In-phase impedance measurements of a poly(dT) modified electrode hybridized with single stranded calf thymus DNA at room temperature.

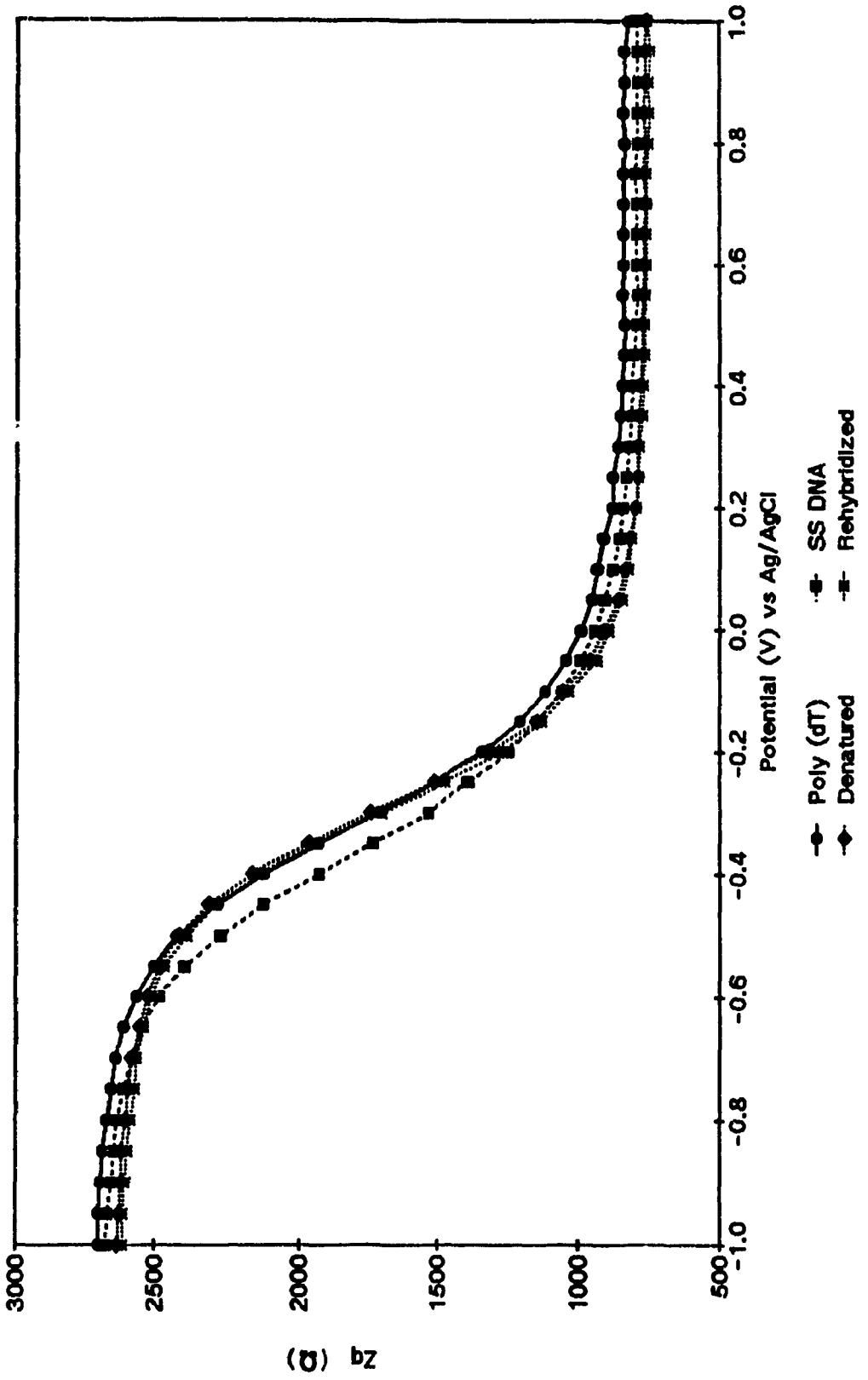

Figure II.19B Out-of-phase impedance measurements of a poly(dT) modified electrode hybridized with single stranded calf thymus DNA at room temperature.

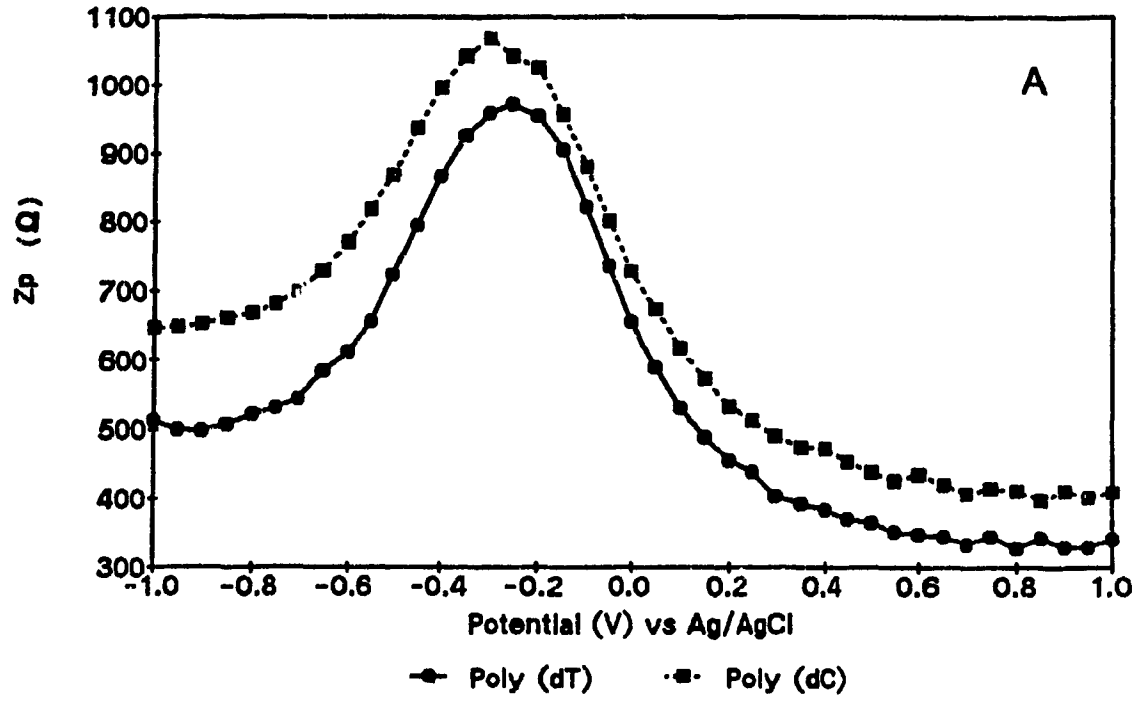

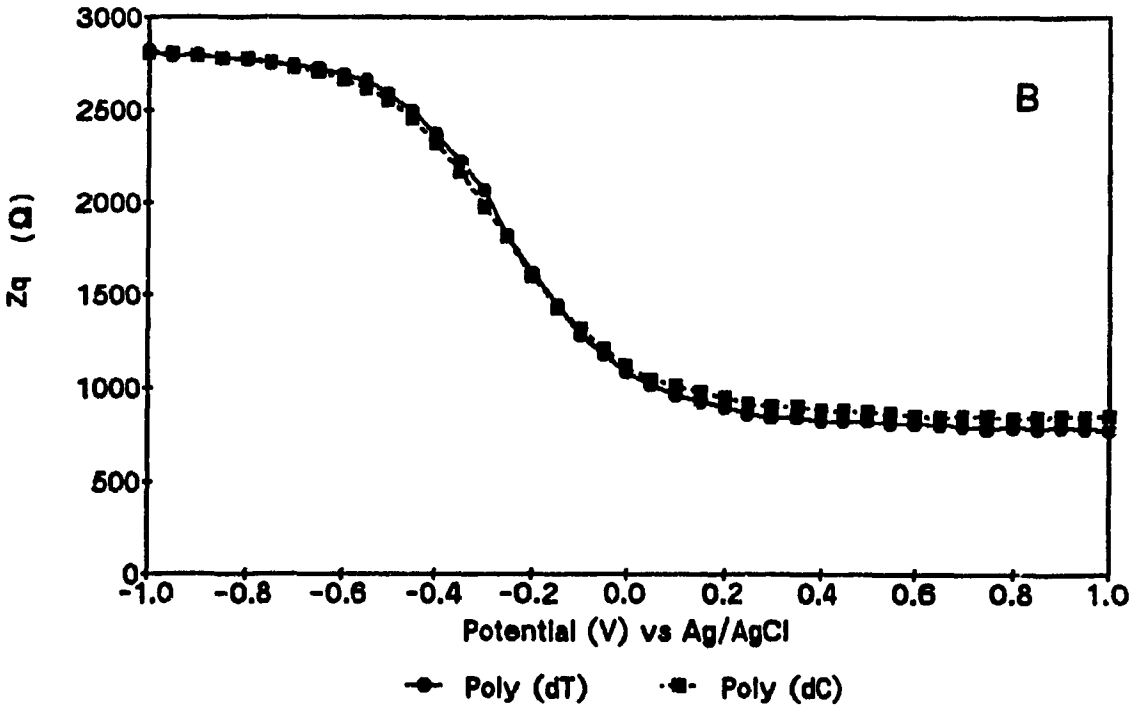

Figure II.20 (A) In-phase and (B) Out-of-phase impedance measurements of a poly(dT) modified electrode hybridized with poly(dC).

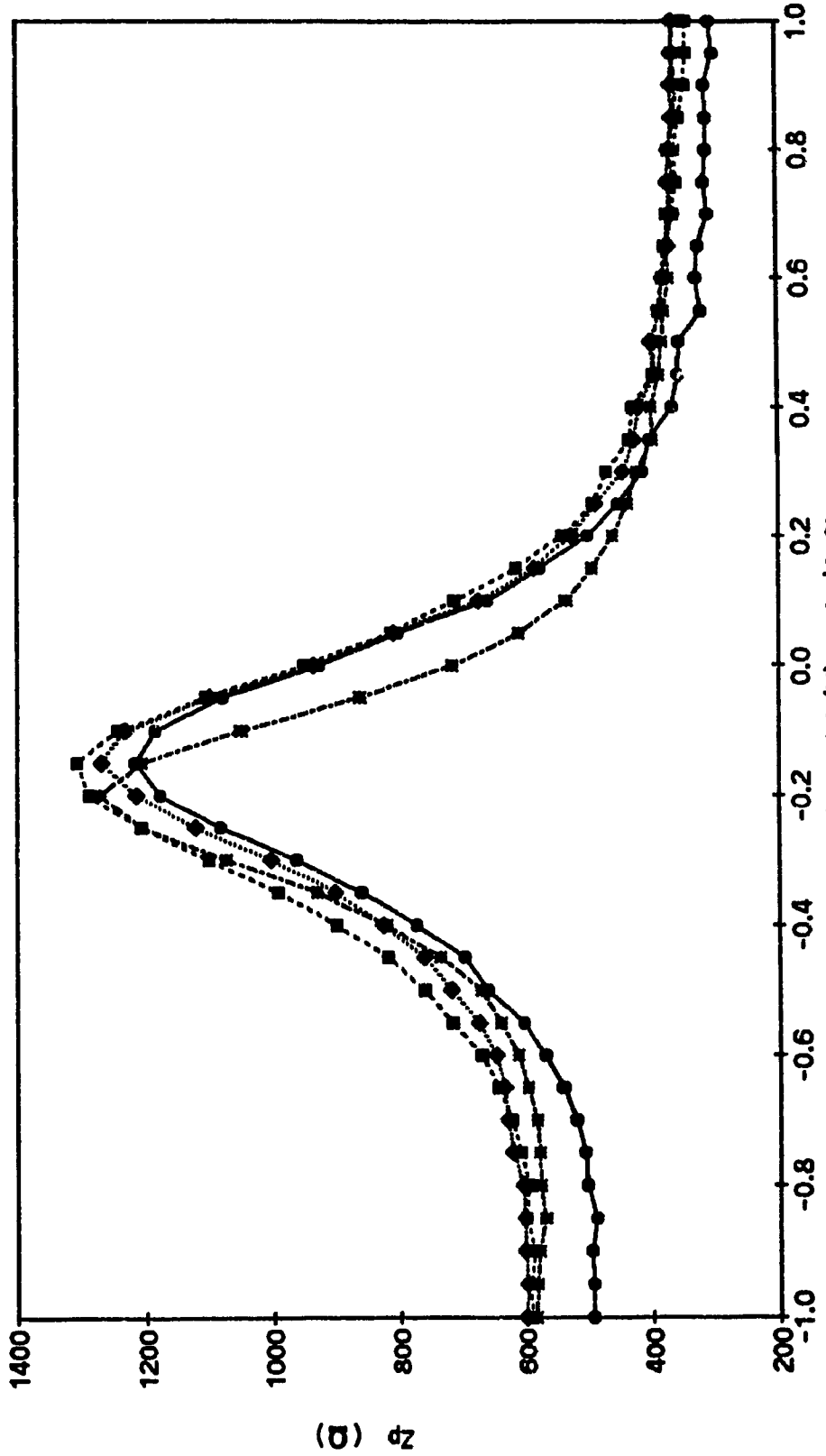

Figure II.21A In-phase impedance measurements of an oligo(dT)$_{20}$ modified electrode with a blank hybridization.

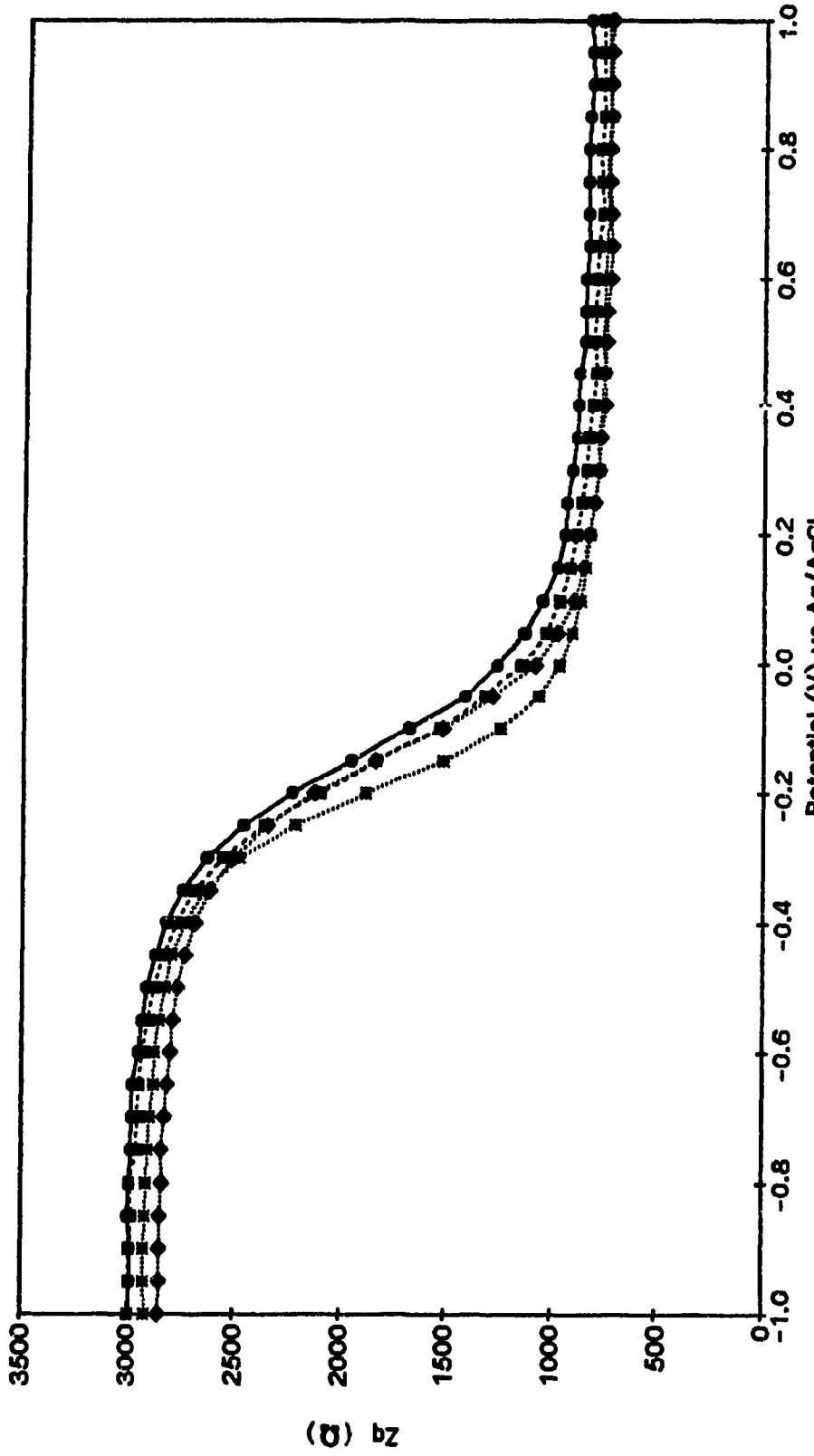

Figure II.21B Out-of-phase impedance measurements of an oligo(dT)$_{20}$ modified electrode with a blank hybridization.

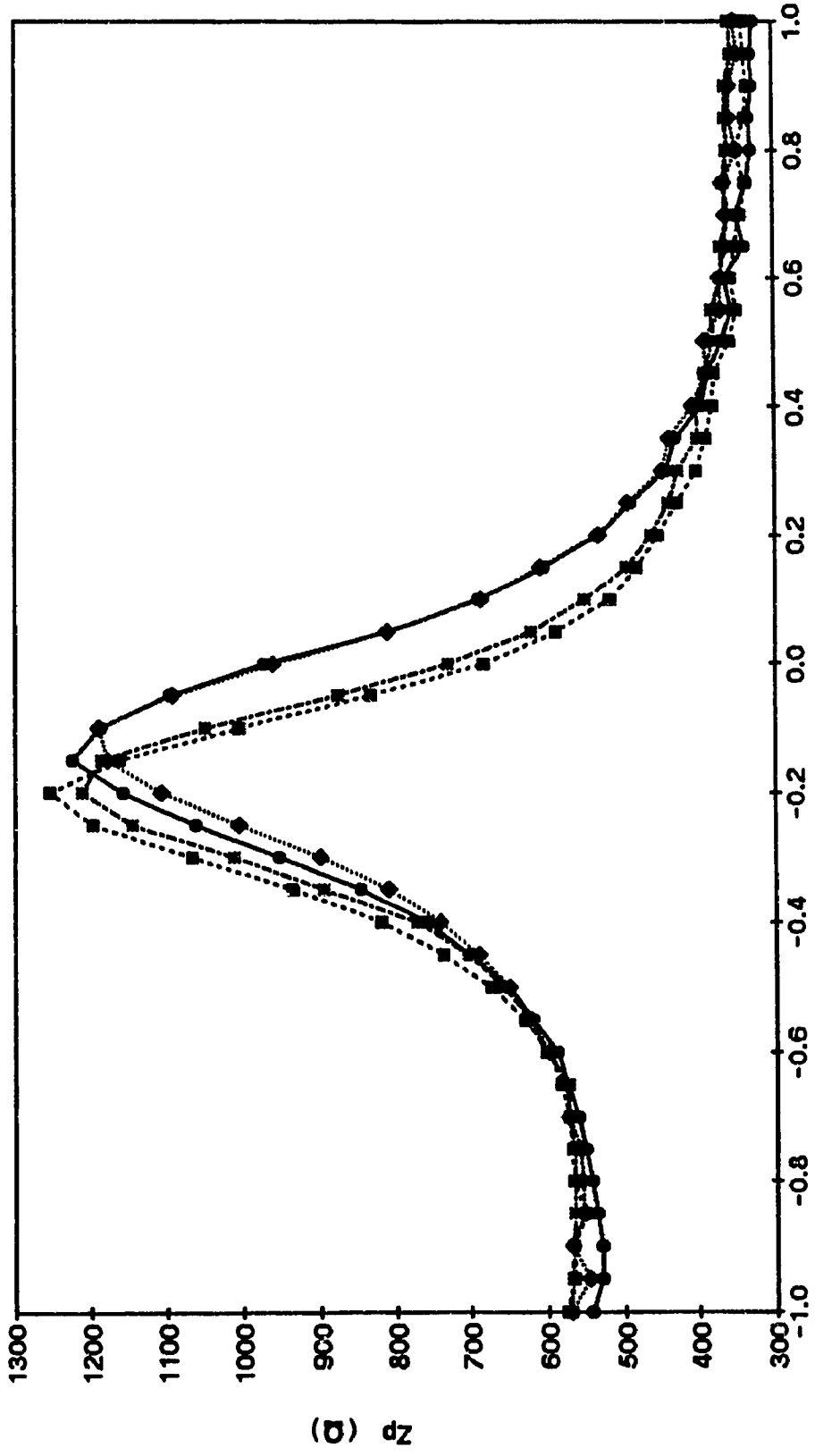

Figure II.22A In-phase impedance measurements of an oligo(dT)$_{20}$ modified electrode hybridized with a mixture of oligo(dA)$_{18}$ and single stranded calf thymus DNA.

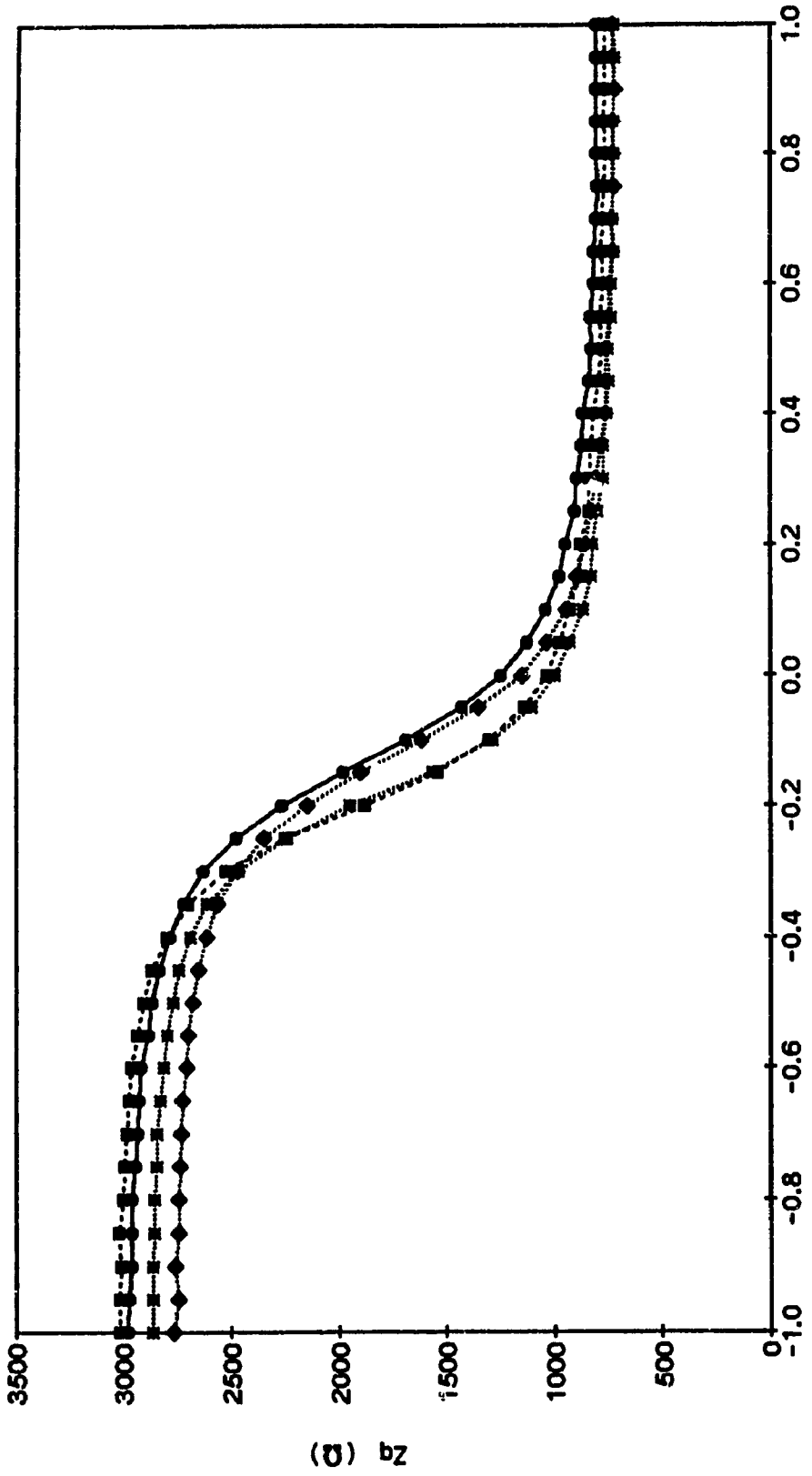

Figure II.22B Out-of-phase impedance measurements of an oligo$(dT)_{20}$ modified electrode hybridized with a mixture of oligo$(dA)_{18}$ and single stranded calf thymus DNA.

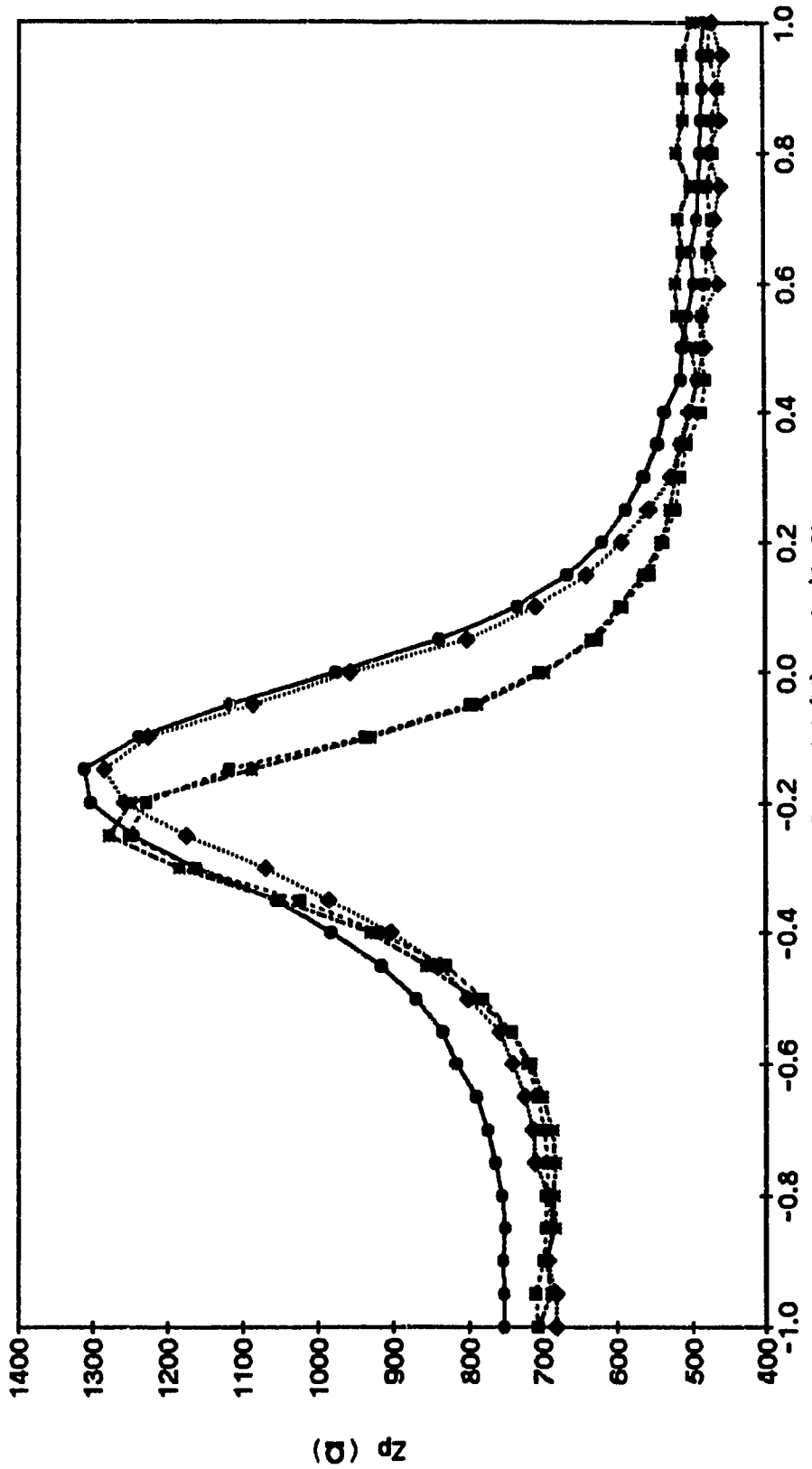

Figure II.23A In-phase impedance measurements of a poly(dT) modified electrode hybridized with a mixture of oligo(dA)$_{18}$ and single stranded calf thymus DNA.

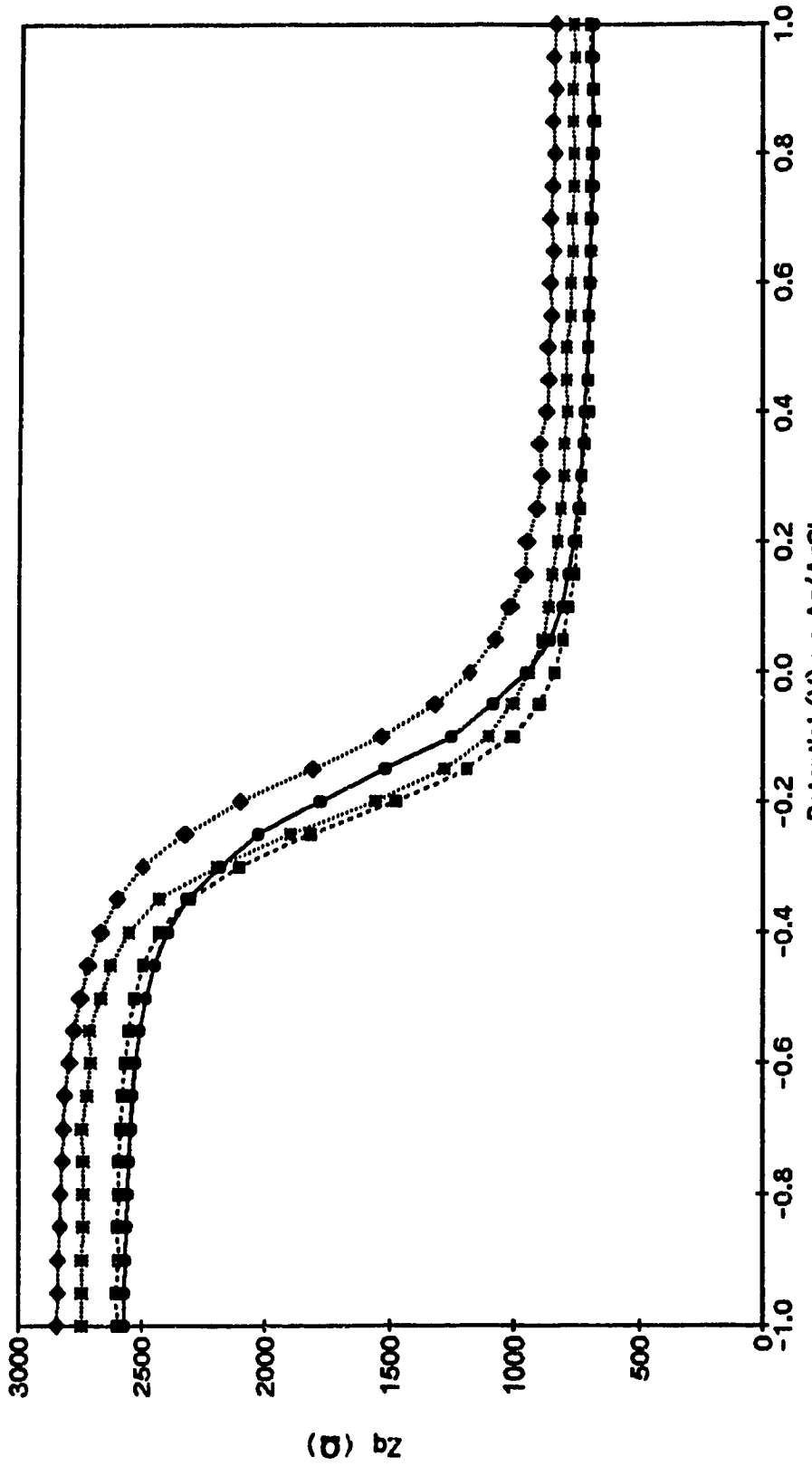

Figure II.23B Out-of-phase impedance measurements of a poly(dT) modified electrode hybridized with a mixture of oligo$(dA)_{18}$ and single stranded calf thymus DNA.

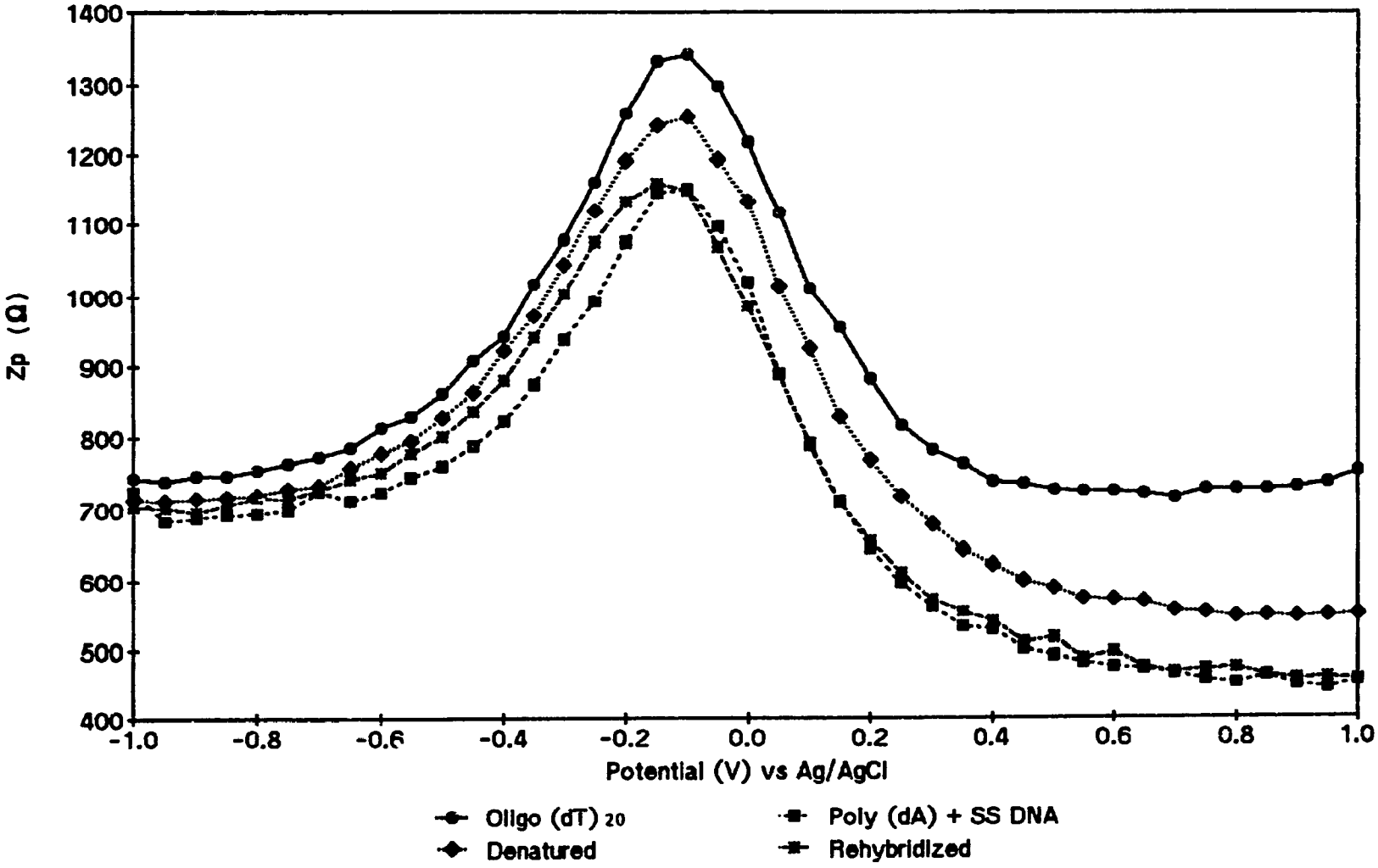

Figure II.24A In-phase impedance measurements of an oligo $(dT)_{20}$ modified electrode hybridized with a mixture of poly(dA) and single stranded calf thymus DNA.

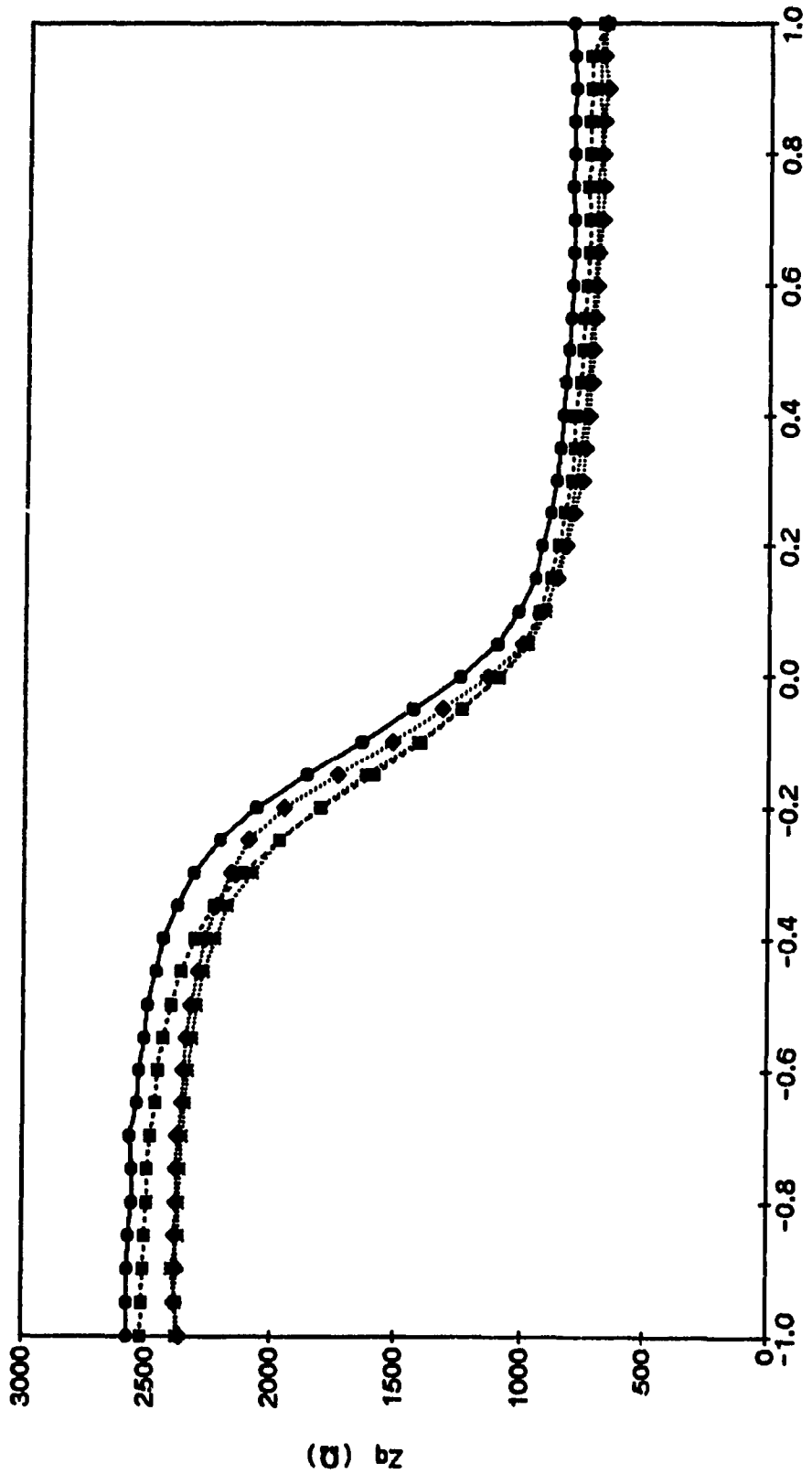

Figure II.24B Out-of-phase impedance measurements of an oligo$(dT)_{20}$ modified electrode hybridized with a mixture of poly(dA) and single stranded calf thymus DNA.

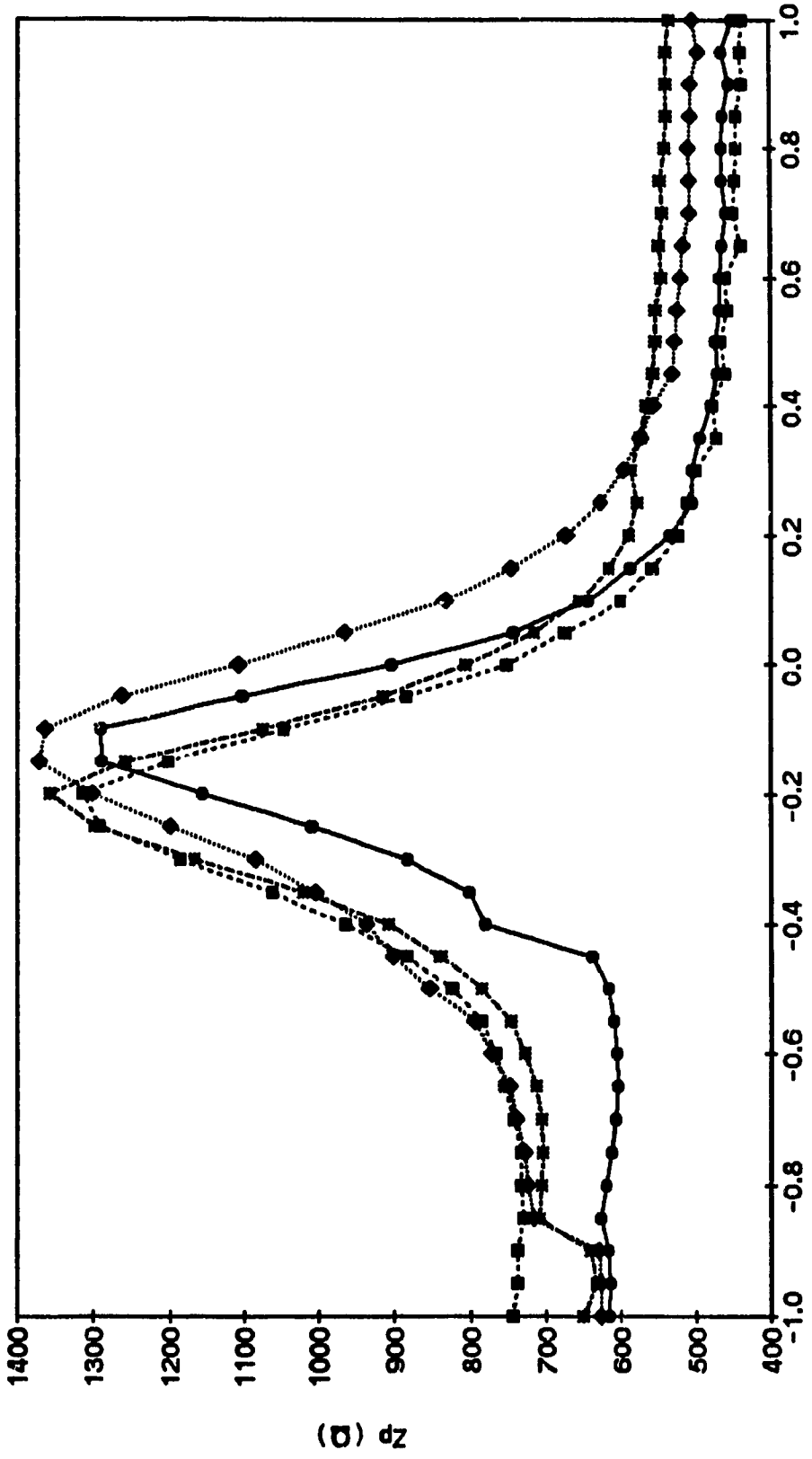

Figure II.25A In-phase impedance measurements of a poly(dT) modified electrode hybridized with a mixture of poly(dA) and single stranded calf thymus DNA.

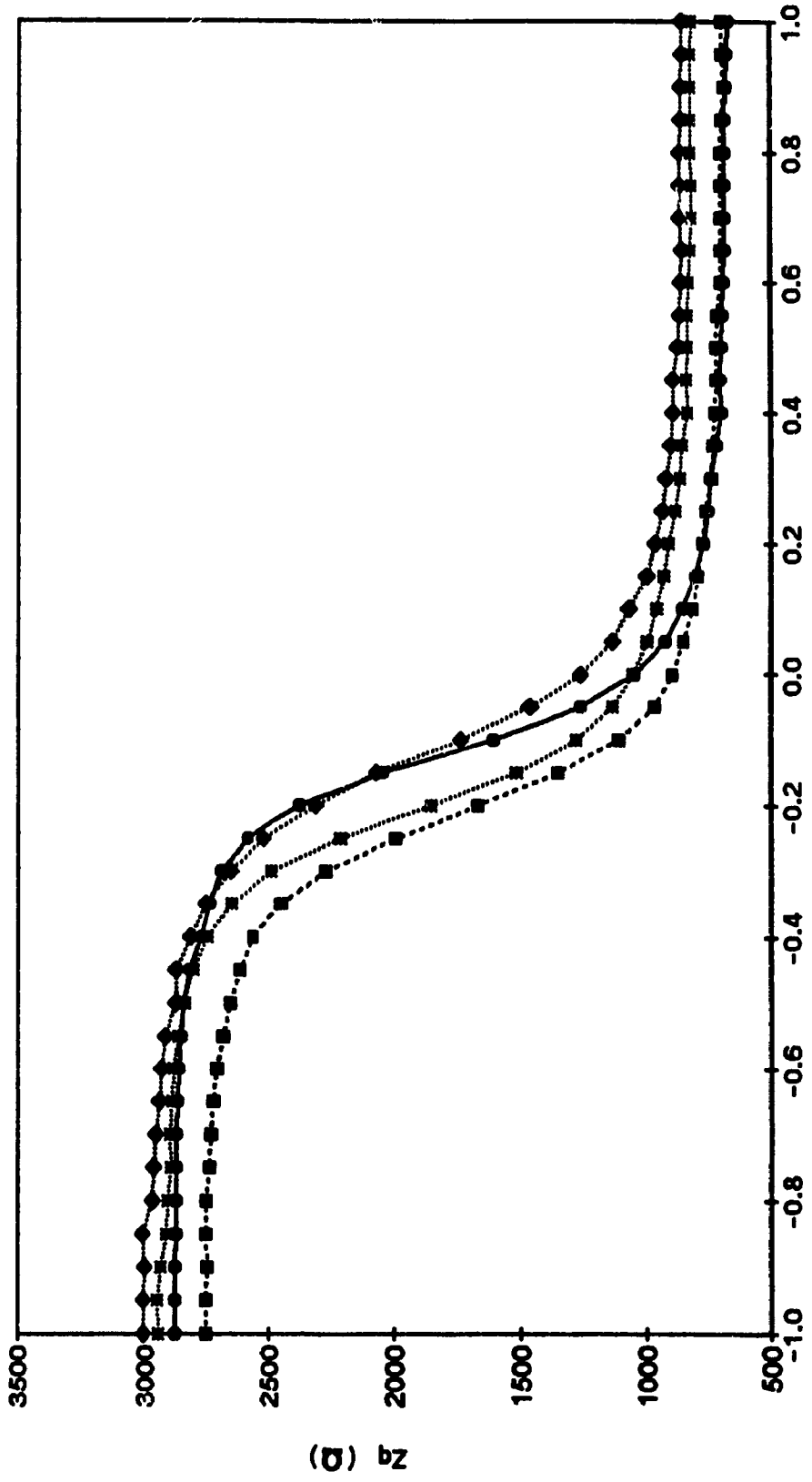

Figure II.25B Out-of-phase impedance measurements of a poly(dT) modified electrode hybridized with a mixture of poly(dA) and single stranded calf thymus DNA.

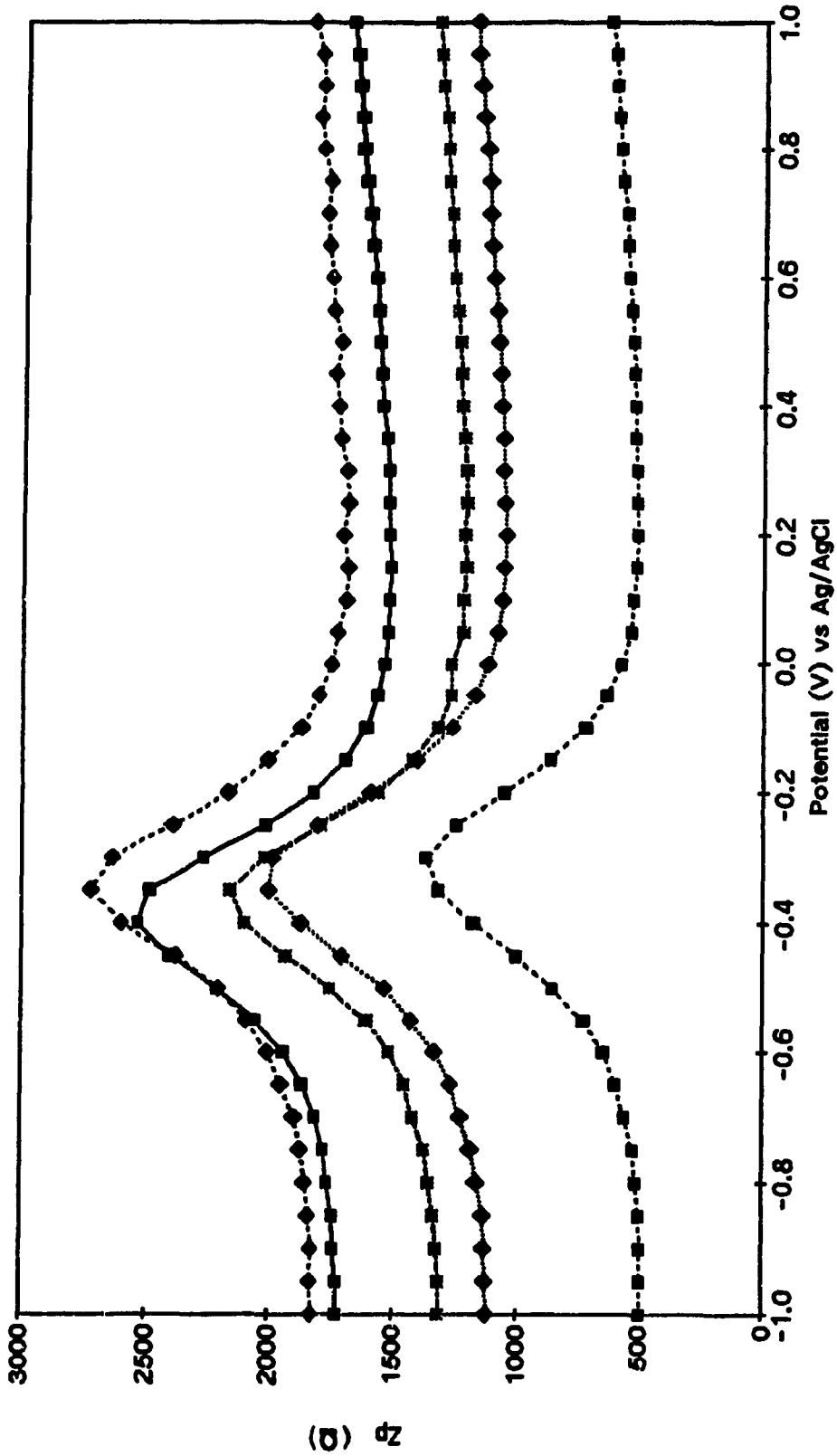

Figure II.26A In-phase impedance measurements of a poly(dT) modified electrode, *in situ* hybridized with oligo$(dA)_{18}$.

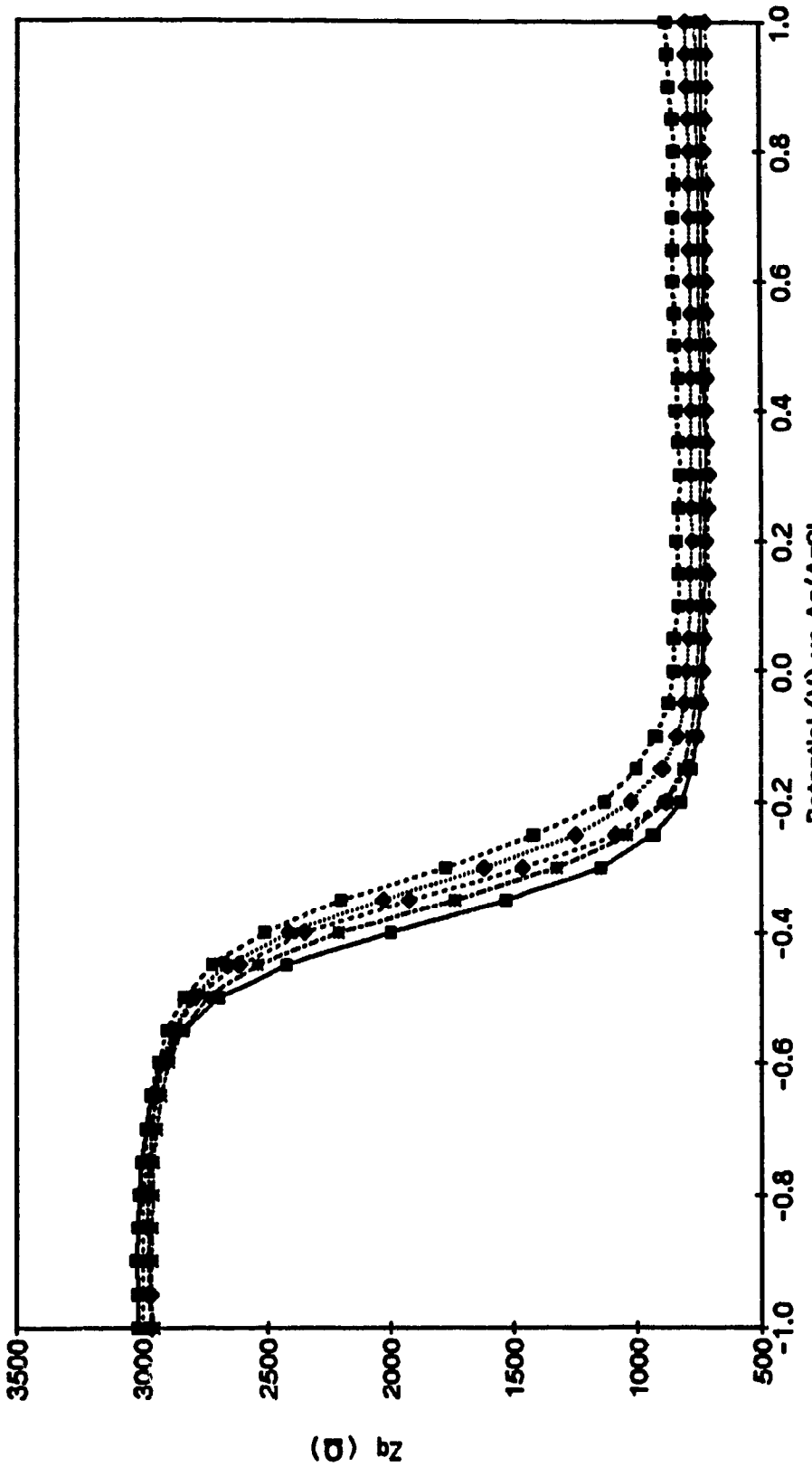

Figure II.26B Out-of-phase impedance measurements of a poly (dT) modified electrode, *in situ* hybridized with oligo$(dA)_{18}$.

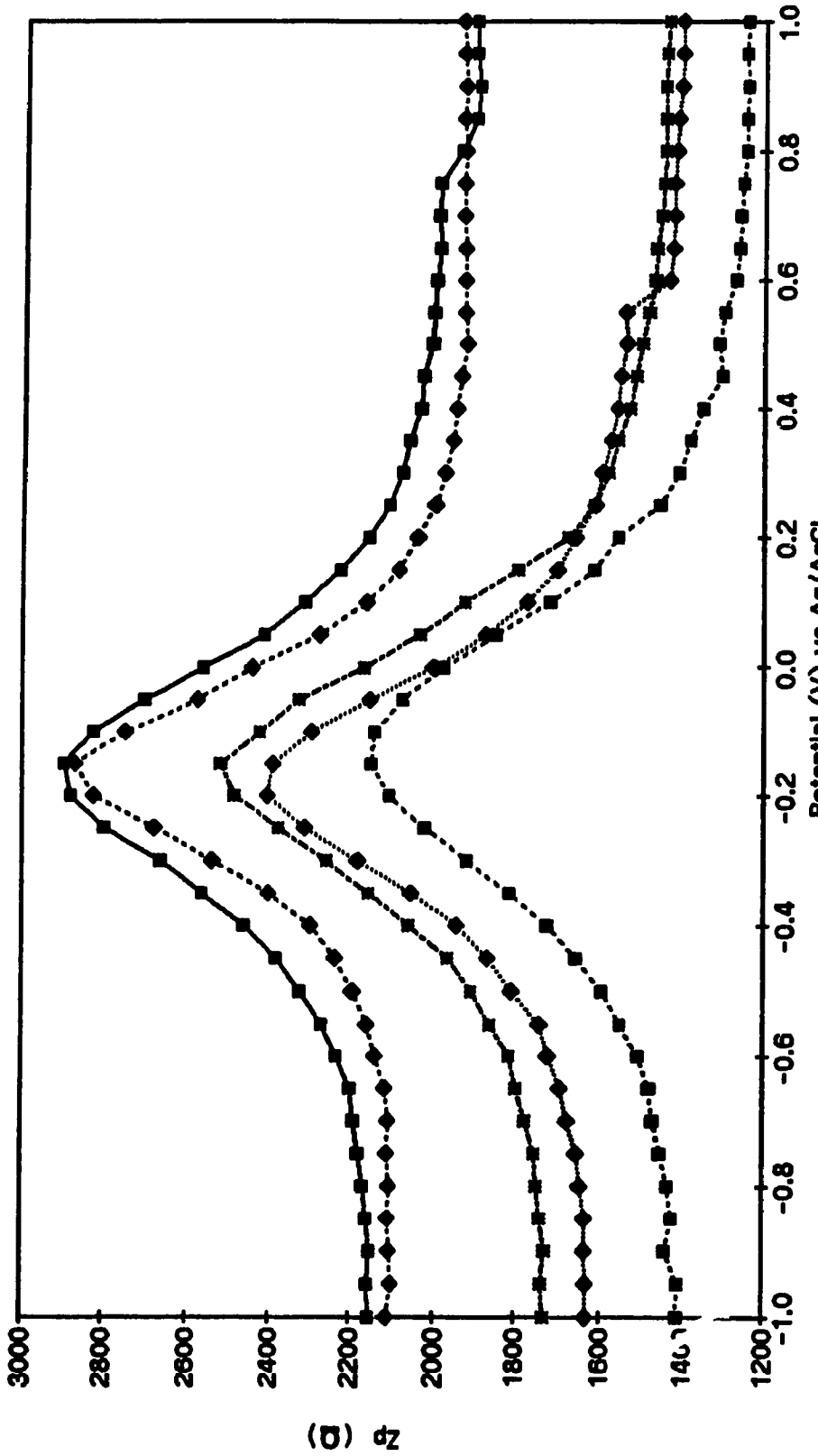

Figure II.27A In-phase impedance measurements of an oligo(dT)$_{20}$ modified electrode, *in situ* hybridized with poly(dA).

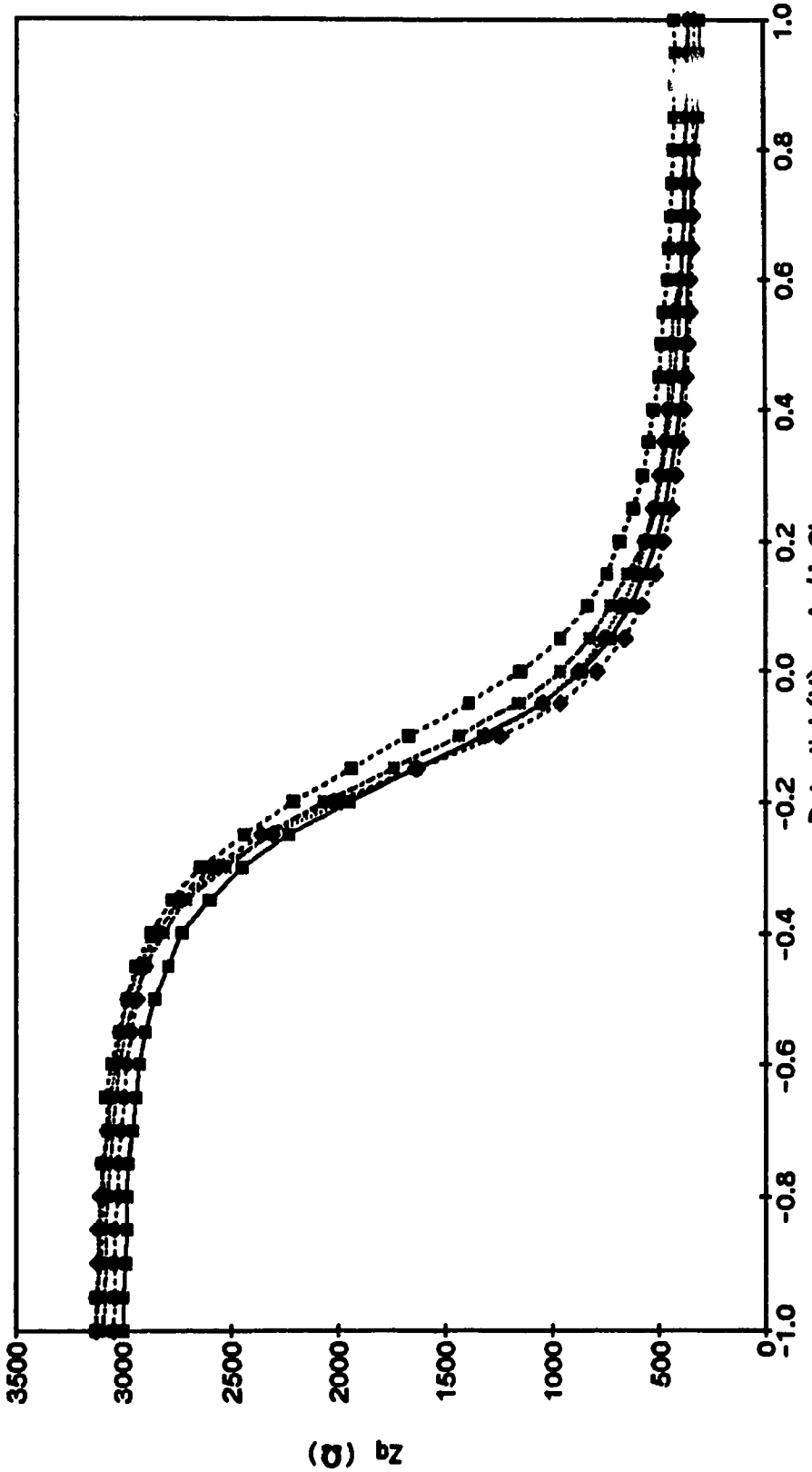

Figure II.27B Out-of-phase impedance measurements of an oligo(dT)$_{20}$ modified electrode, *in situ* hybridized with poly(dA).

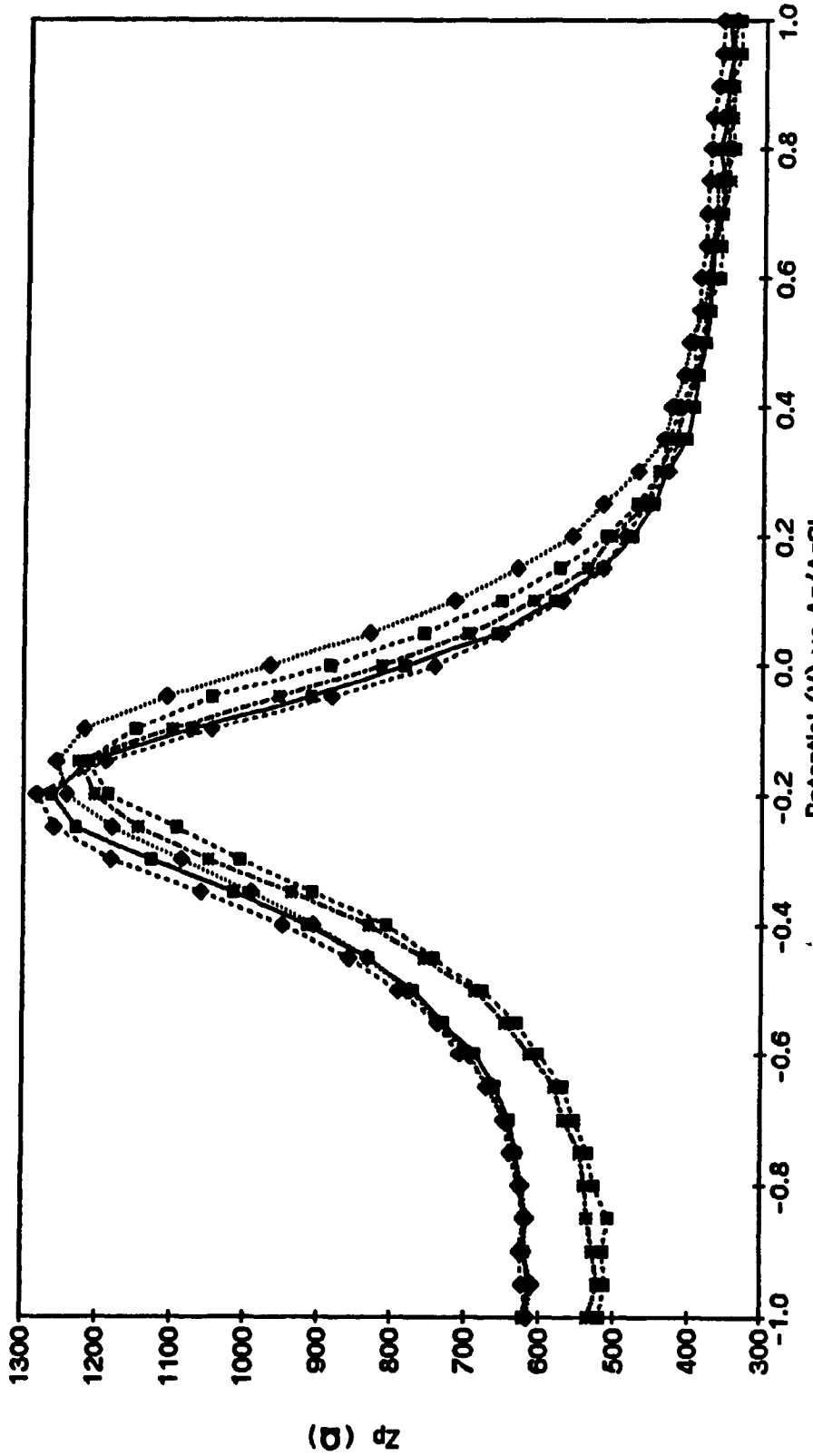

Figure II.28A In-phase impedance measurements of a poly(dT) modified electrode, *in situ* hybridized with poly(dA).

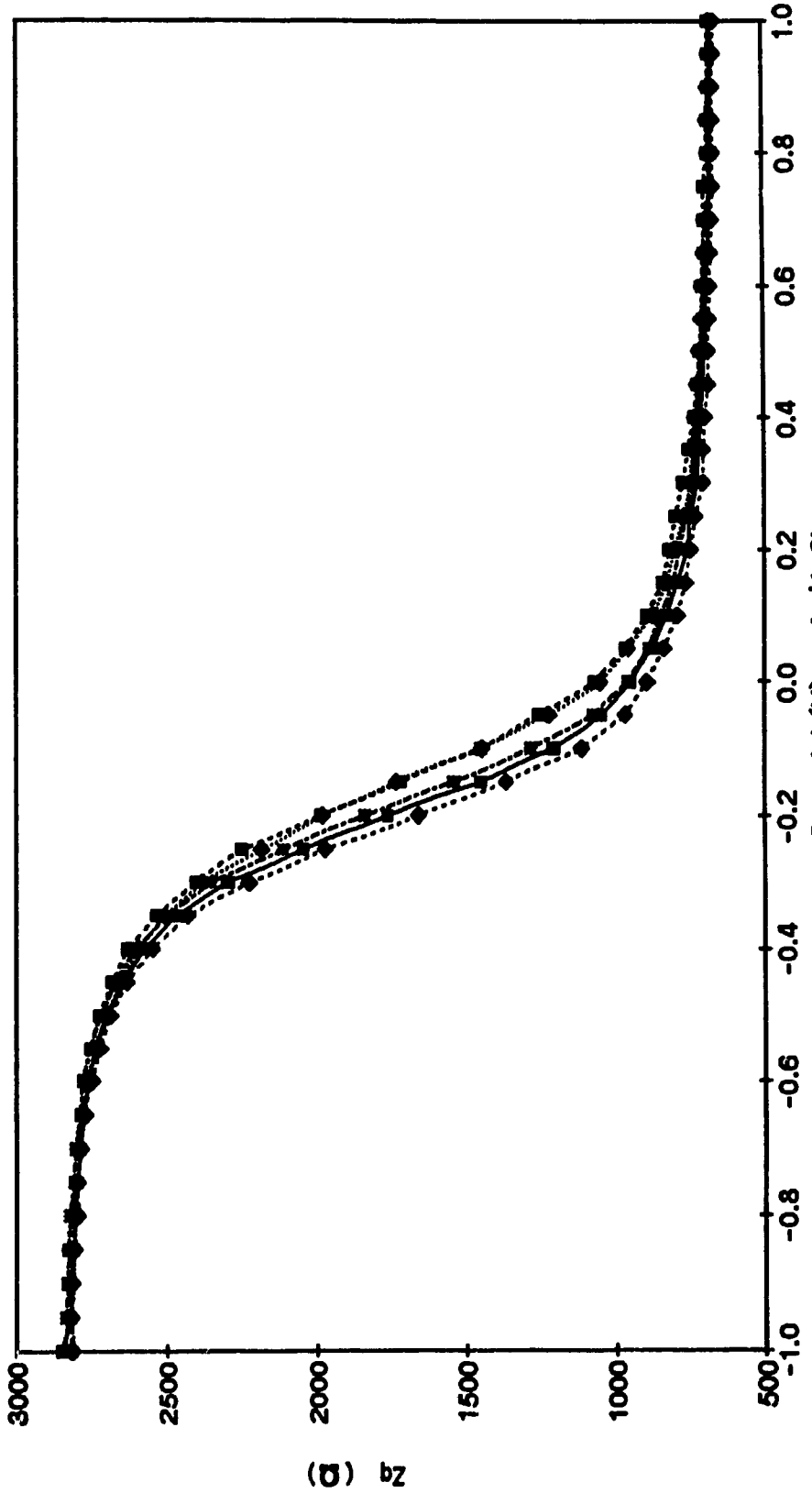

Figure II.28B Out-of-phase impedance measurements of a poly(dT) modified electrode, *in situ* hybridized with poly(dA).

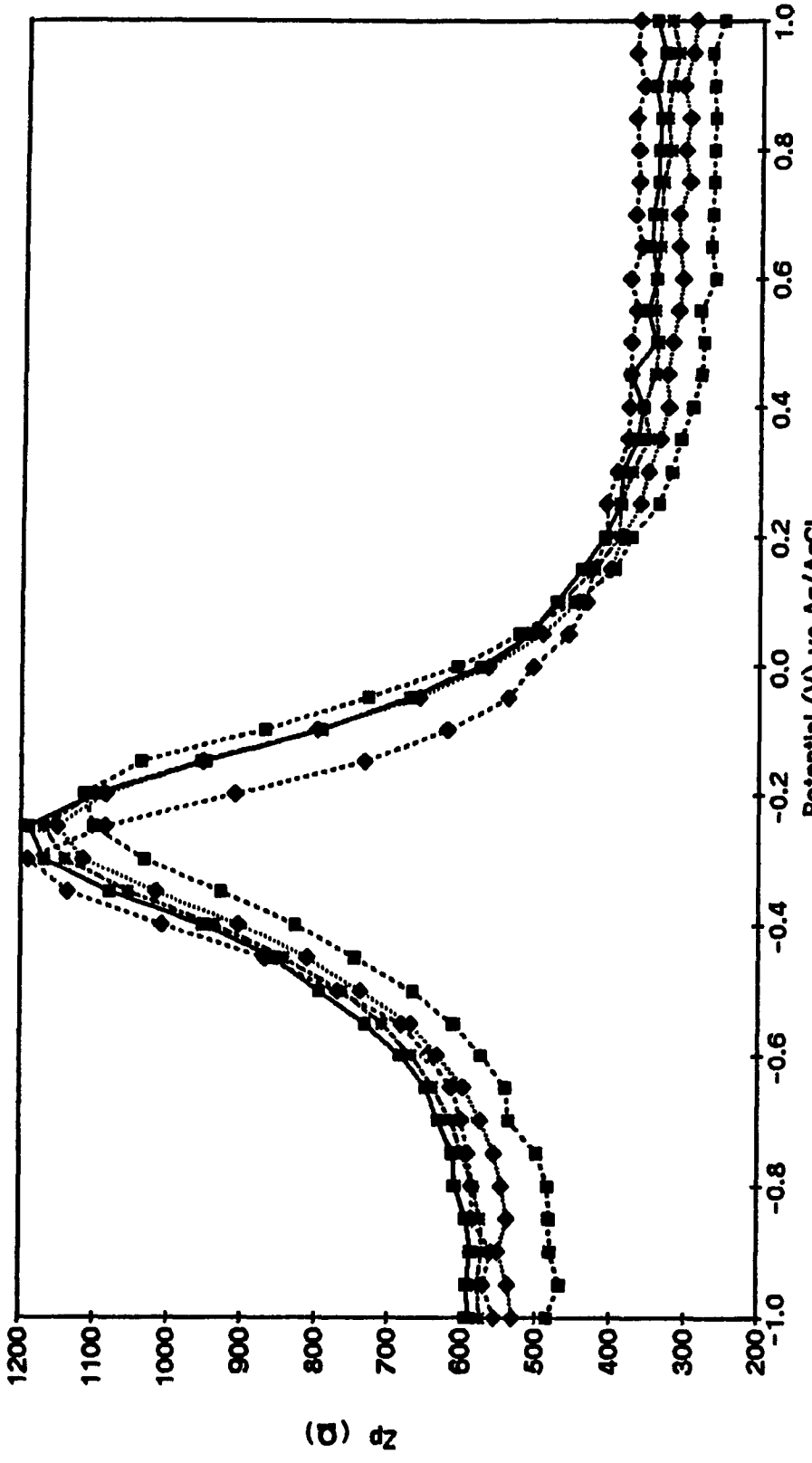

Figure II.29A In-phase impedance measurements of a poly(dT) modified electrode, *in situ* hybridized with a solution of poly(dA) and single stranded calf thymus DNA (1:1).

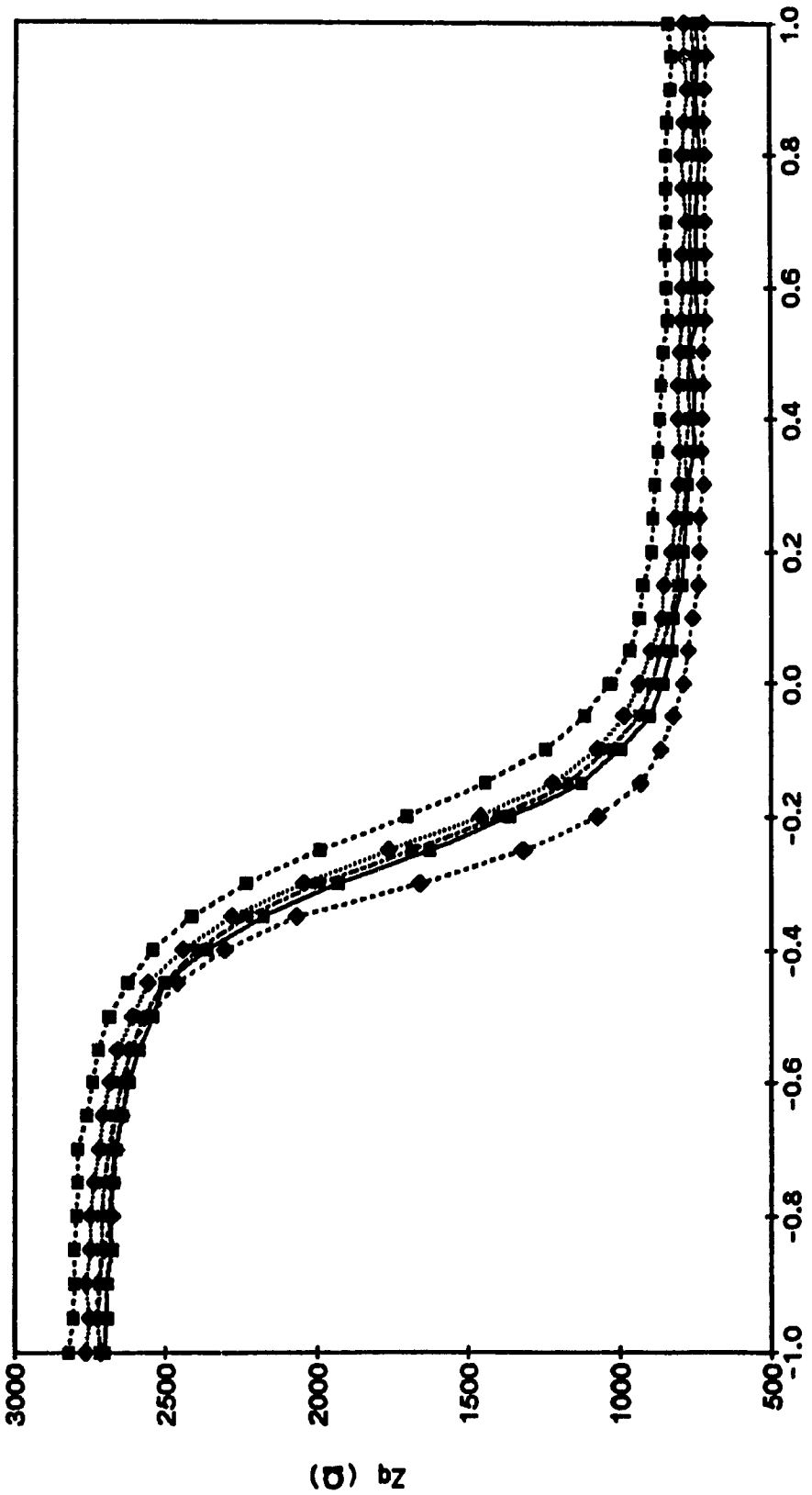

Figure II.29B Out-of-phase impedance measurements of a poly(dT) modified electrode, *in situ* hybridized with a solution of poly(dA) and single stranded calf thymus DNA (1:1).

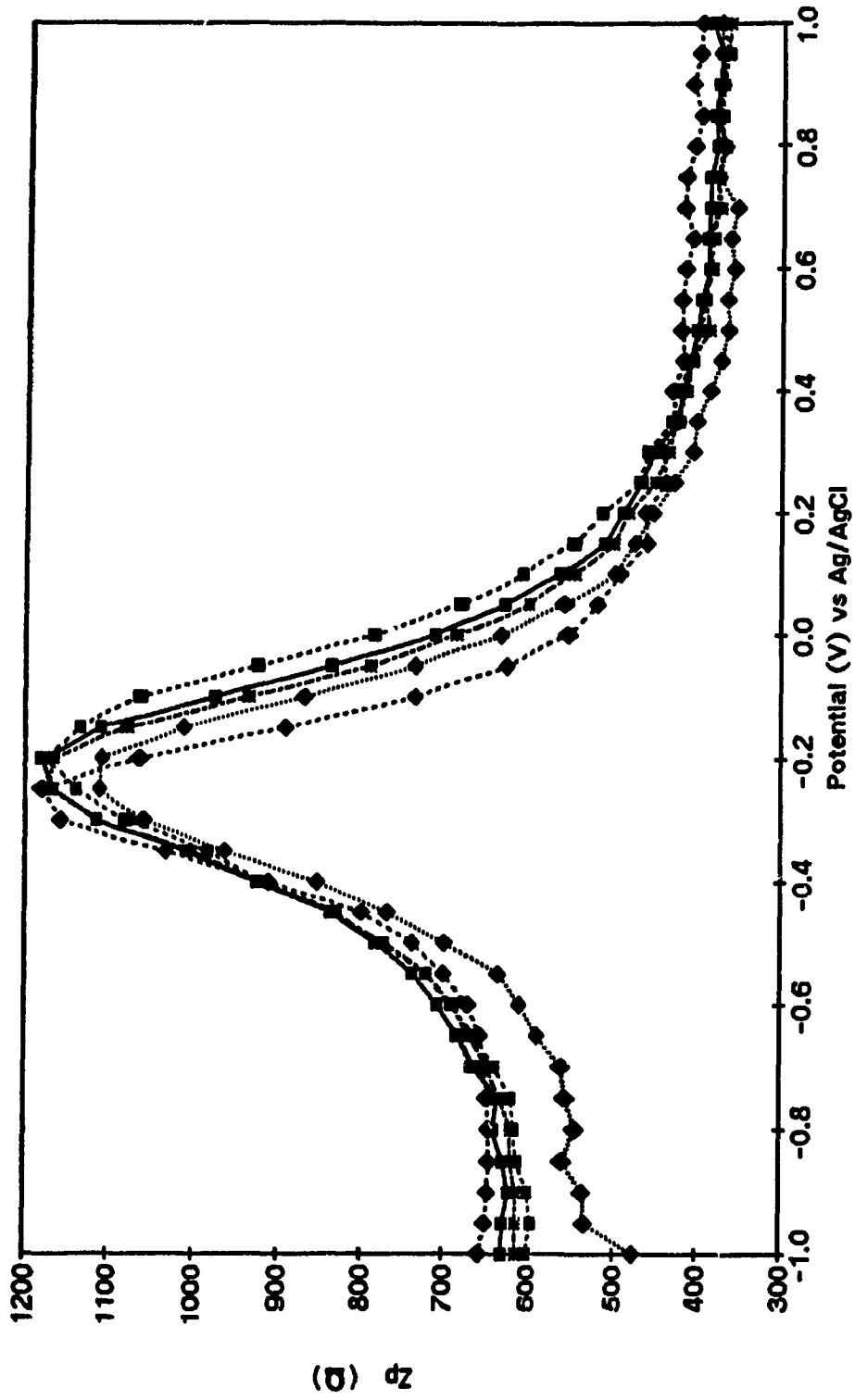

Figure II.30A In-phase impedance measurements of a poly(dT) modified electrode, *in situ* hybridized with a solution of oligo$(dA)_{18}$ and single stranded calf thymus DNA (1:1).

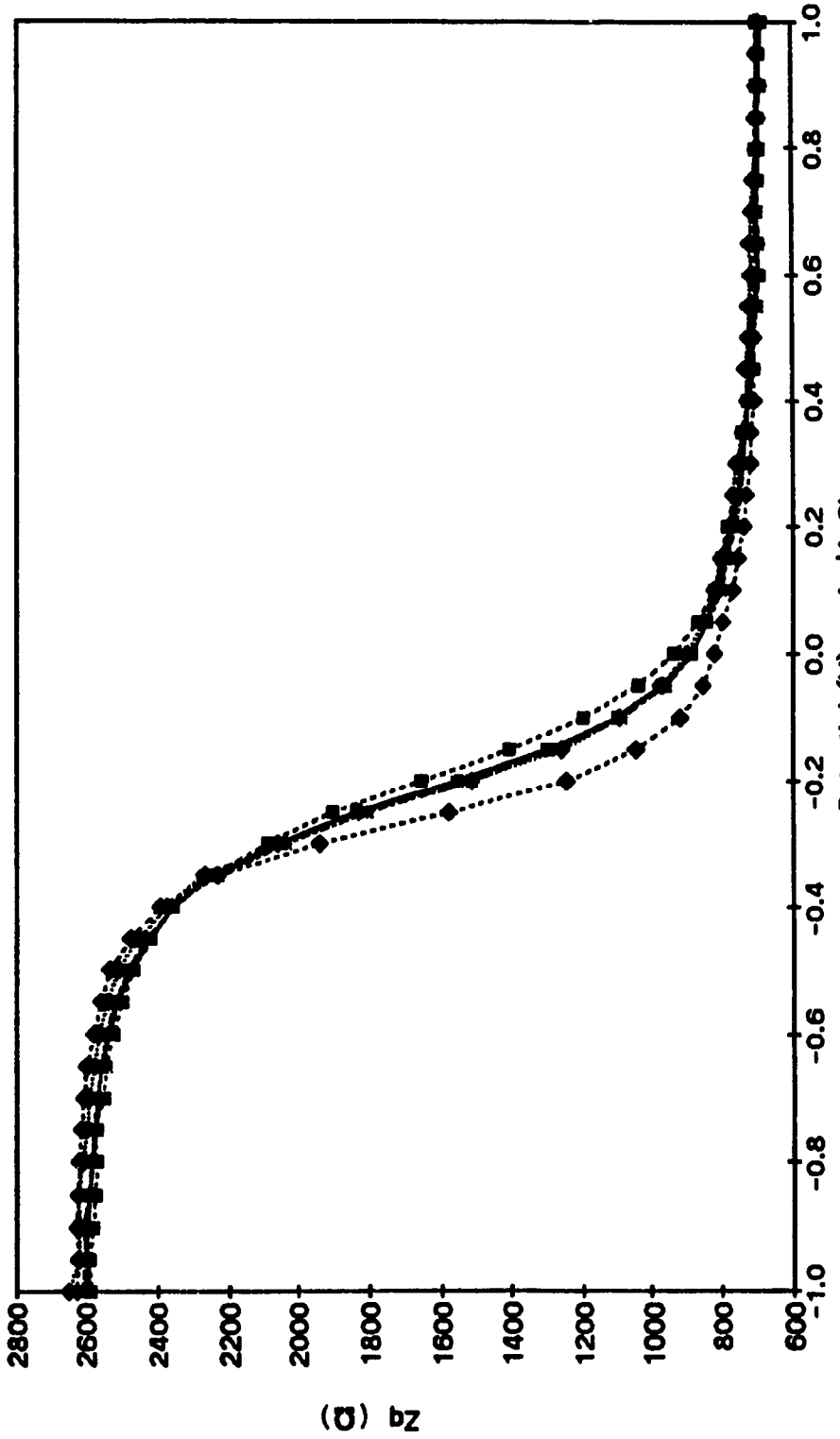

Figure II.30B Out-of-phase impedance measurements of a poly(dT) modified electrode, *in situ* hybridized with a solution of oligo$(dA)_{18}$ and single stranded calf thymus DNA (1:1).

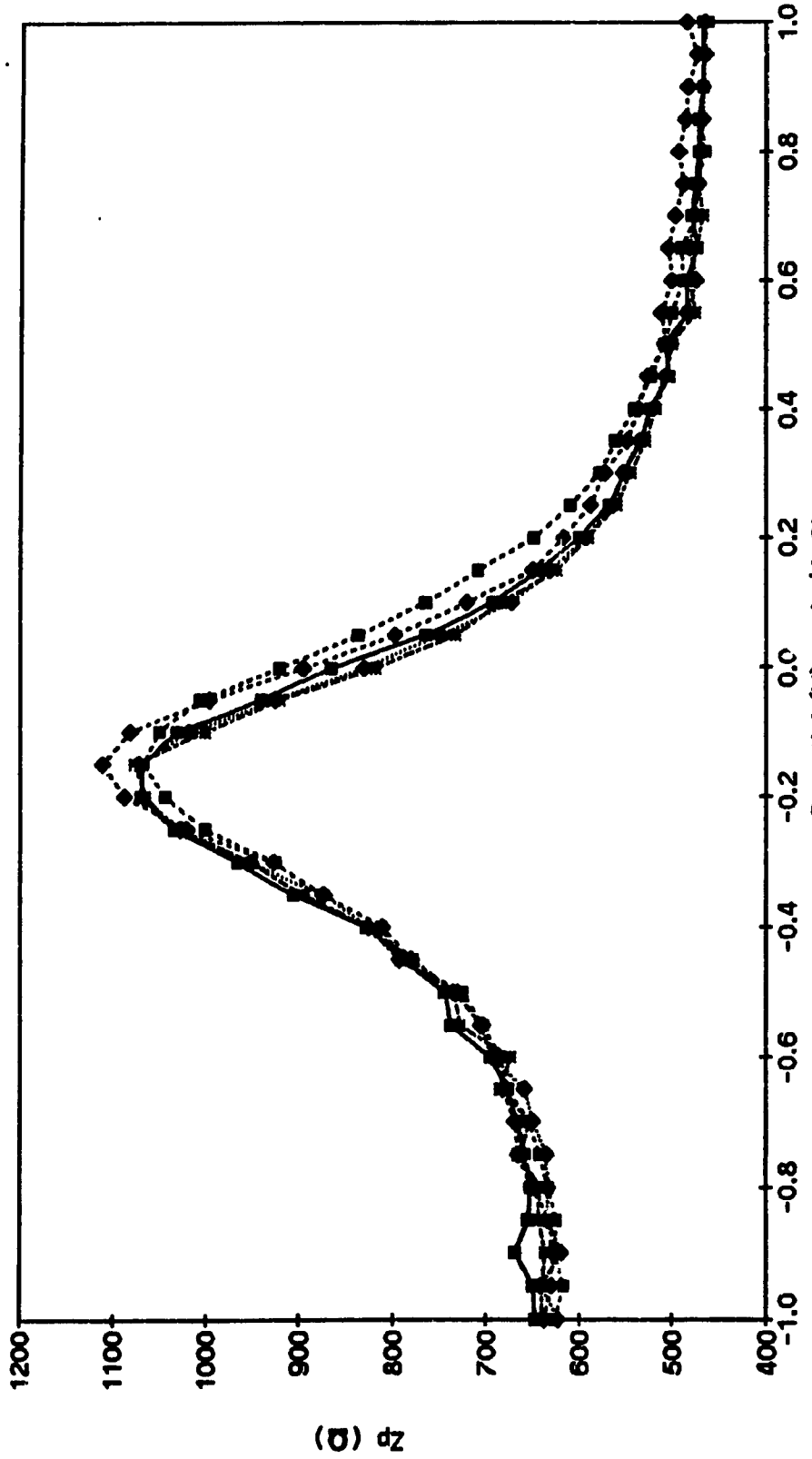

Figure II.31A In-phase impedance measurements of an oligo(dT)$_{20}$ modified electrode, *in situ* hybridized with a solution of poly(dA) and single stranded calf thymus DNA (1:1).

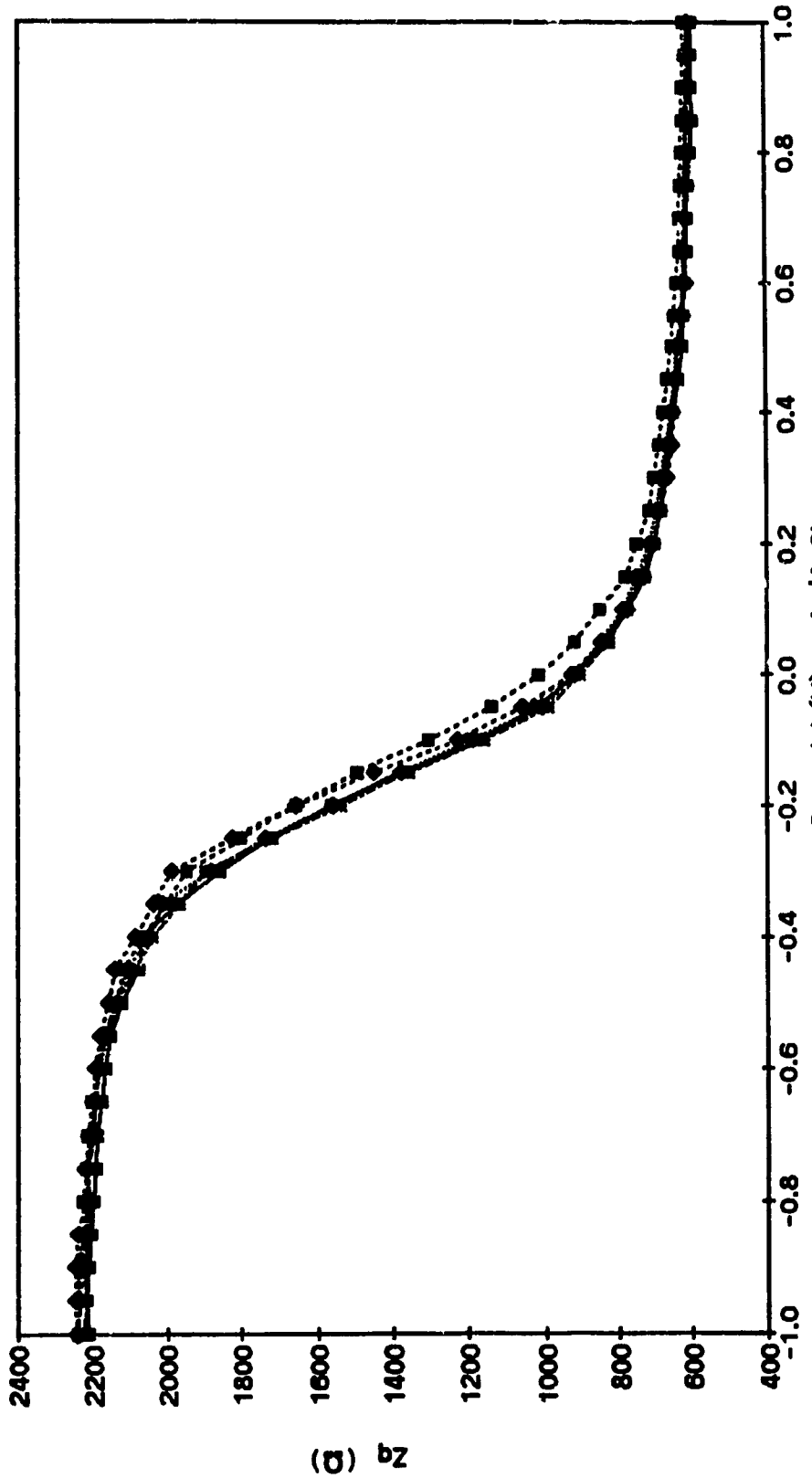

Figure II.31B Out-of-phase impedance measurements of an oligo(dT)$_{20}$ modified electrode, *in situ* hybridized with a solution of poly(dA) and single stranded calf thymus DNA (1:1).

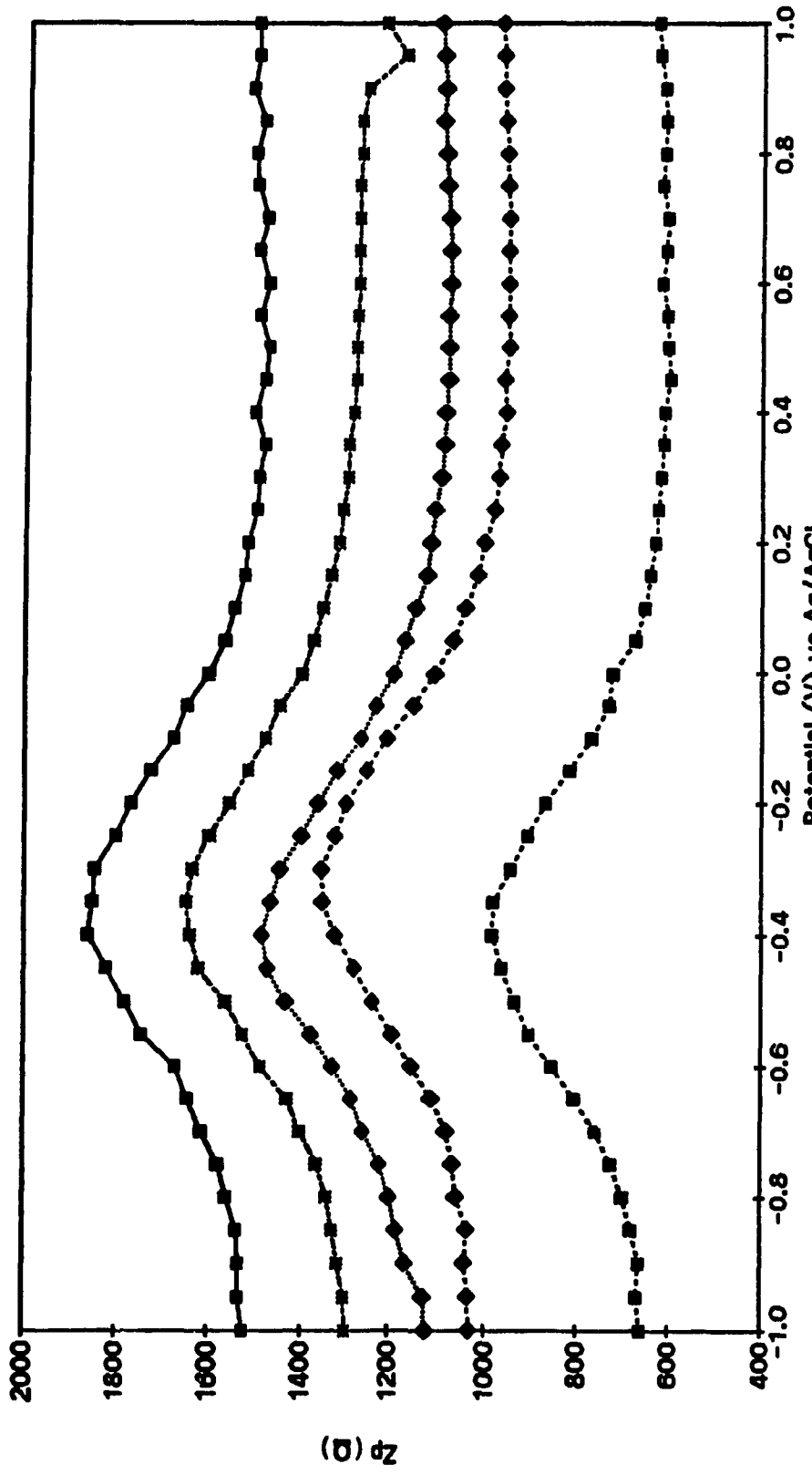

Figure II.32A In-phase impedance measurements of an oligo(dT)$_{20}$ modified electrode, *in situ* hybridized with a solution of oligo(dA)$_{18}$ and single stranded calf thymus DNA (1:1).

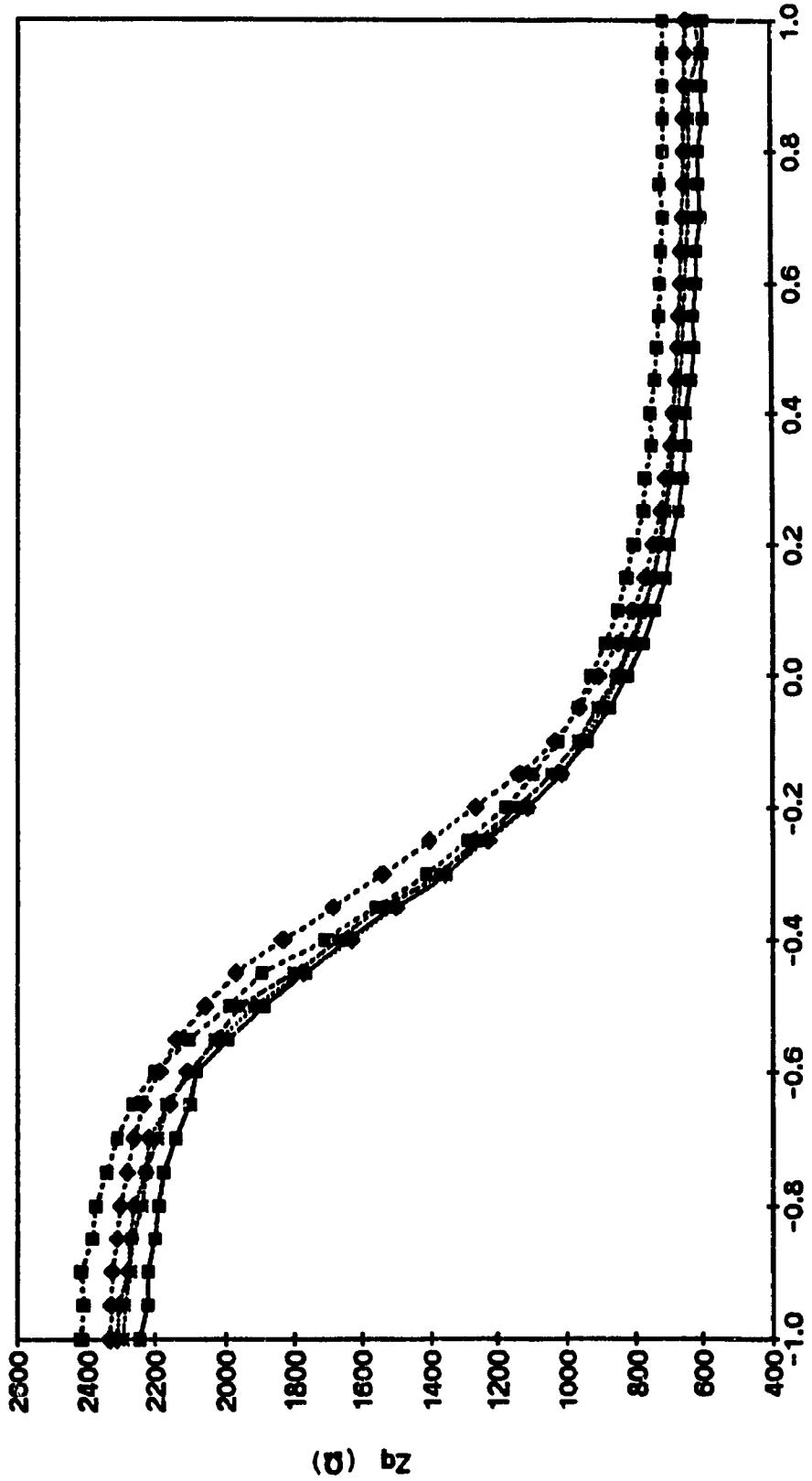

Figure II.32B Out-of-phase impedance measurements of an oligo(dT)$_{20}$ modified electrode, *in situ* hybridized with a solution of oligo(dA)$_{18}$ and single stranded calf thymus DNA (1:1).

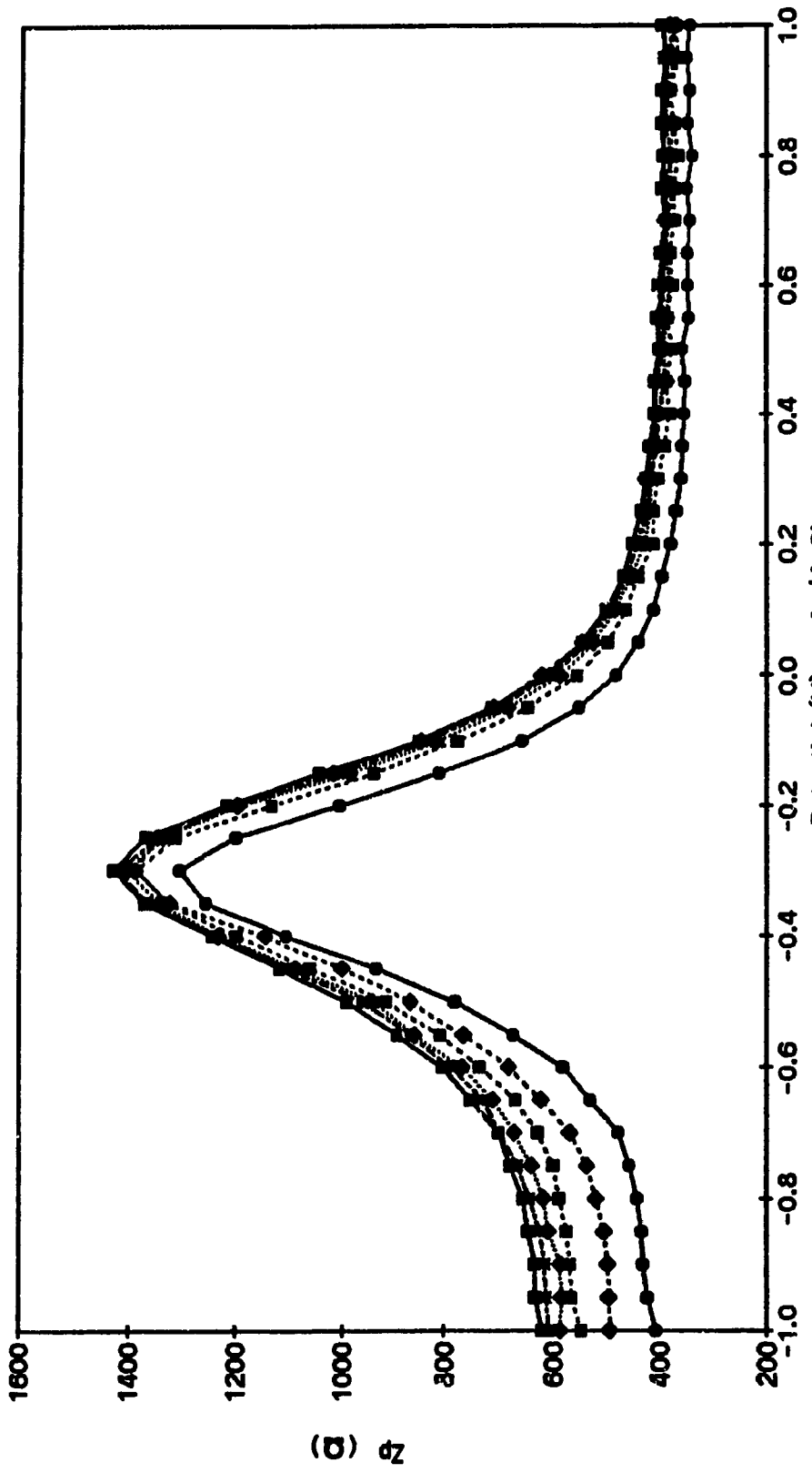

Figure II.33A In-phase impedance measurements of a poly(dT) modified electrode, *in situ* hybridized with single stranded calf thymus DNA.

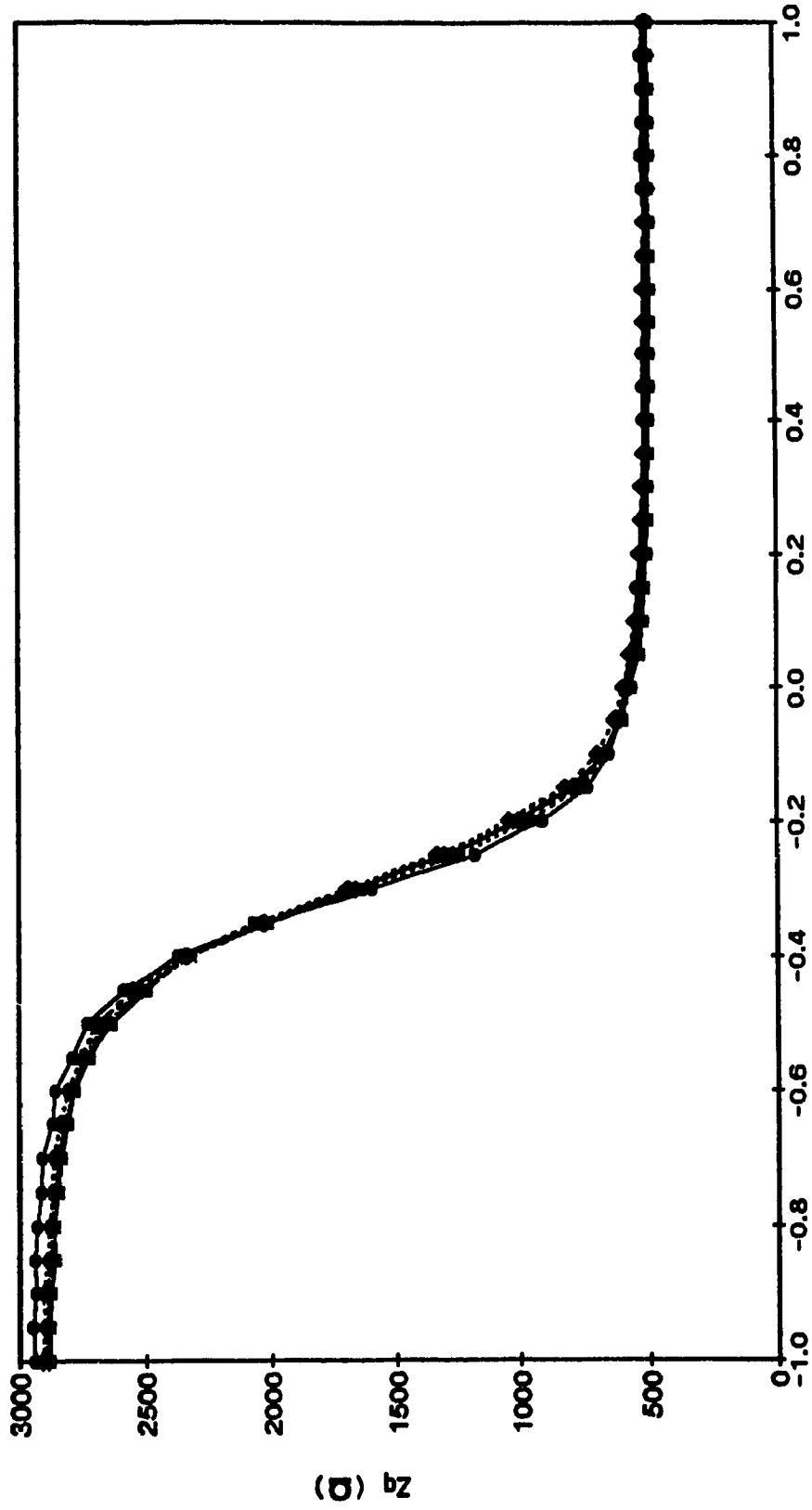

Figure II.33B Out-of-phase impedance measurements of a poly(dT) modified electrode, *in situ* hybridized with single stranded calf thymus DNA.

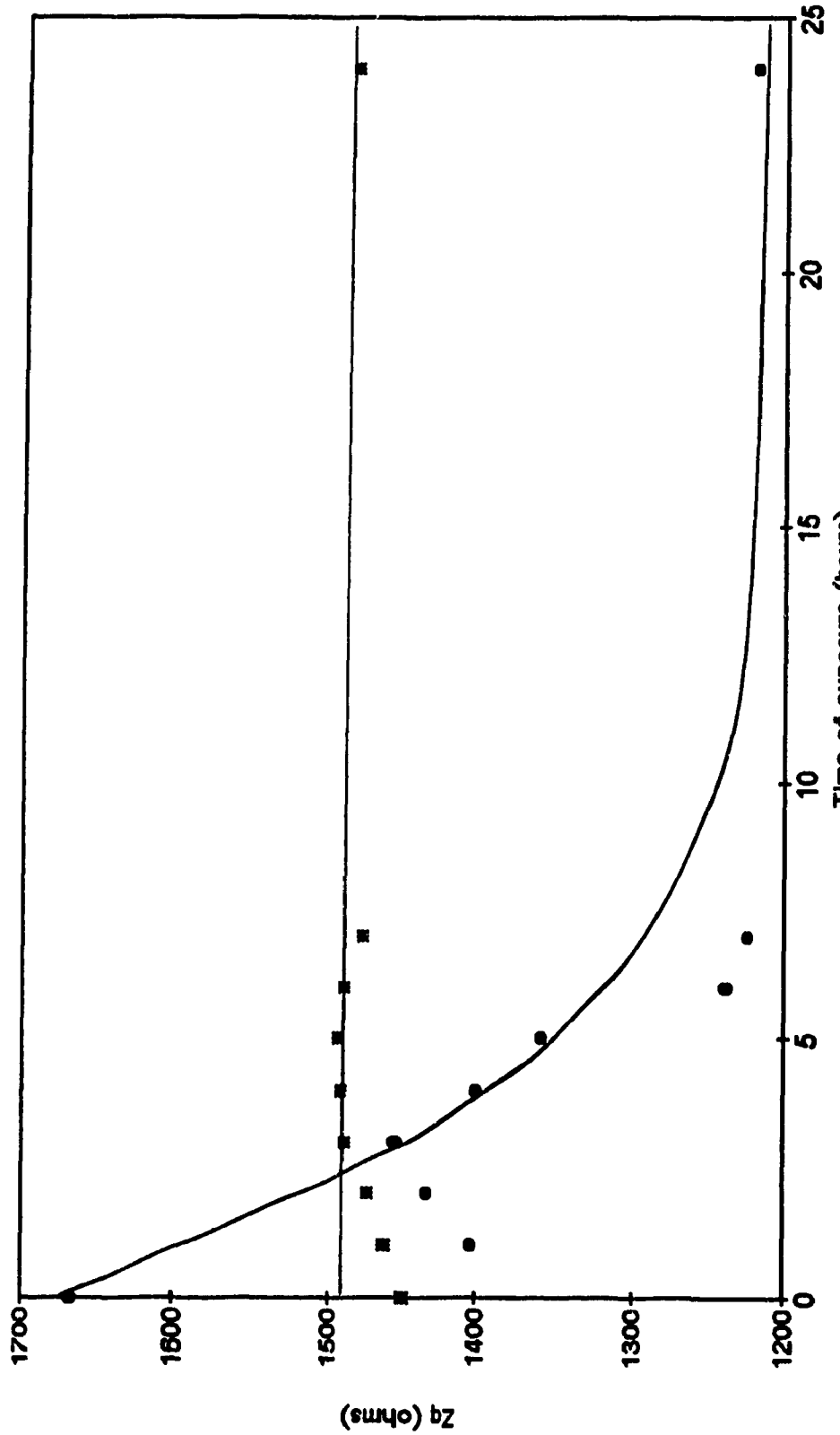

Figure II.34 Out-of-phase impedance measurements of an oligo(dT)$_{20}$ modified electrode, *in situ* hybridized with poly(dA), at a dc potential of -0.250V.

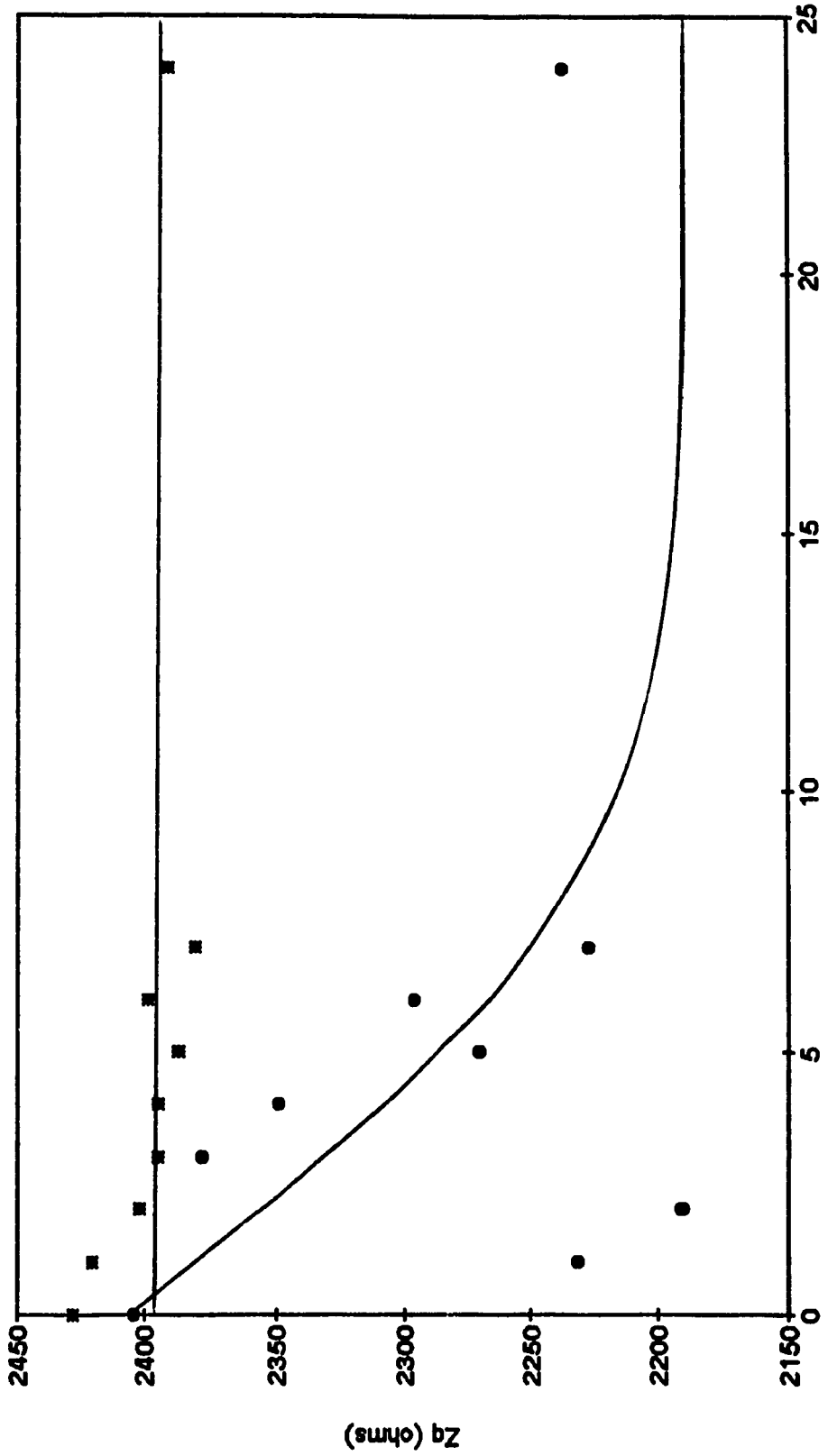

Figure II.35 Out-of-phase impedance measurements of a poly(dT) modified electrode, *in situ* hybridized with poly(dA), at a dc potential of -0.250V.

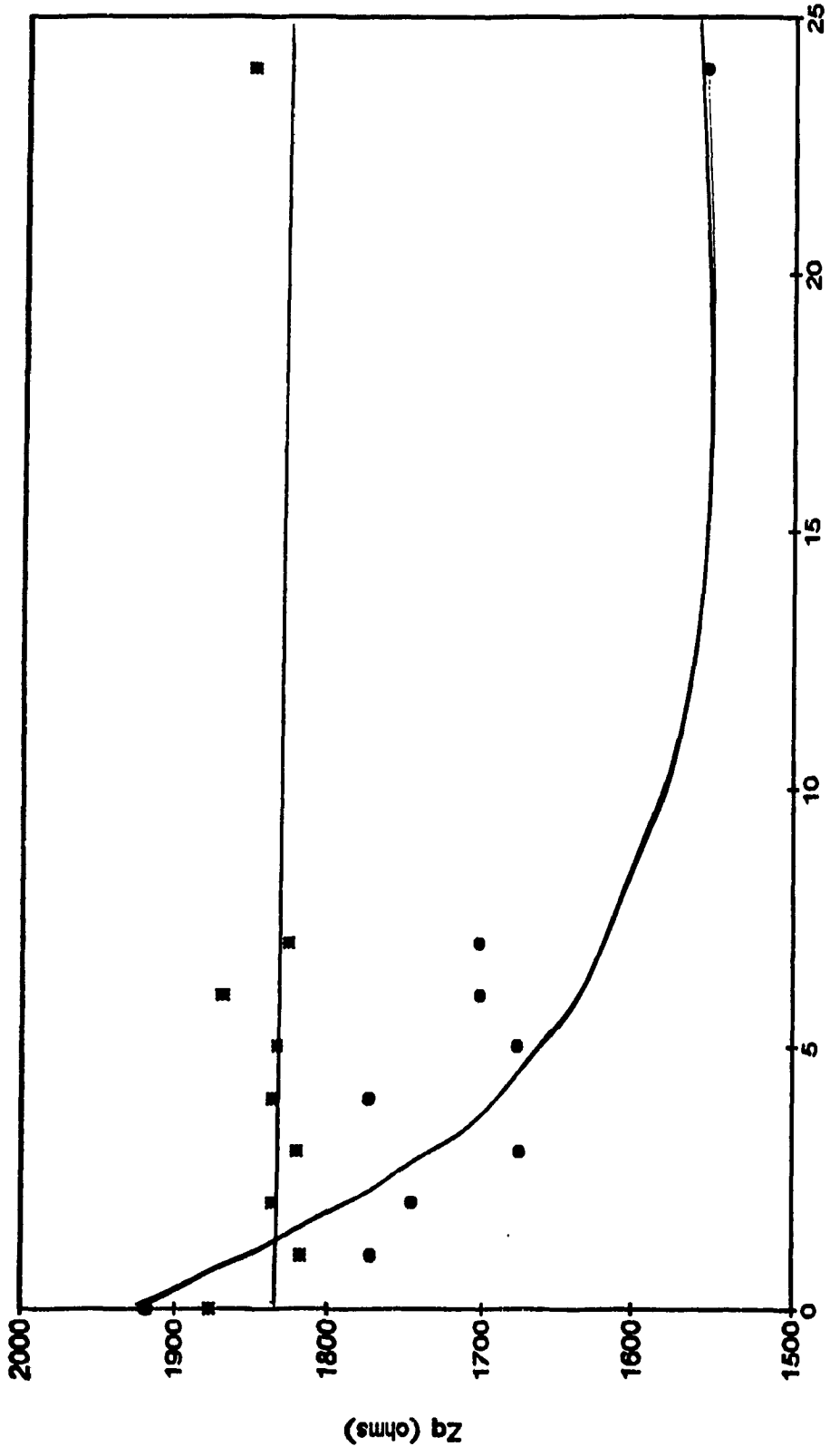

Figure II.36 Out-of-phase impedance measurements of an oligo(dT)$_{20}$ modified electrode, *in situ* hybridized with oligo(dA), at a dc potential of -0.250V.

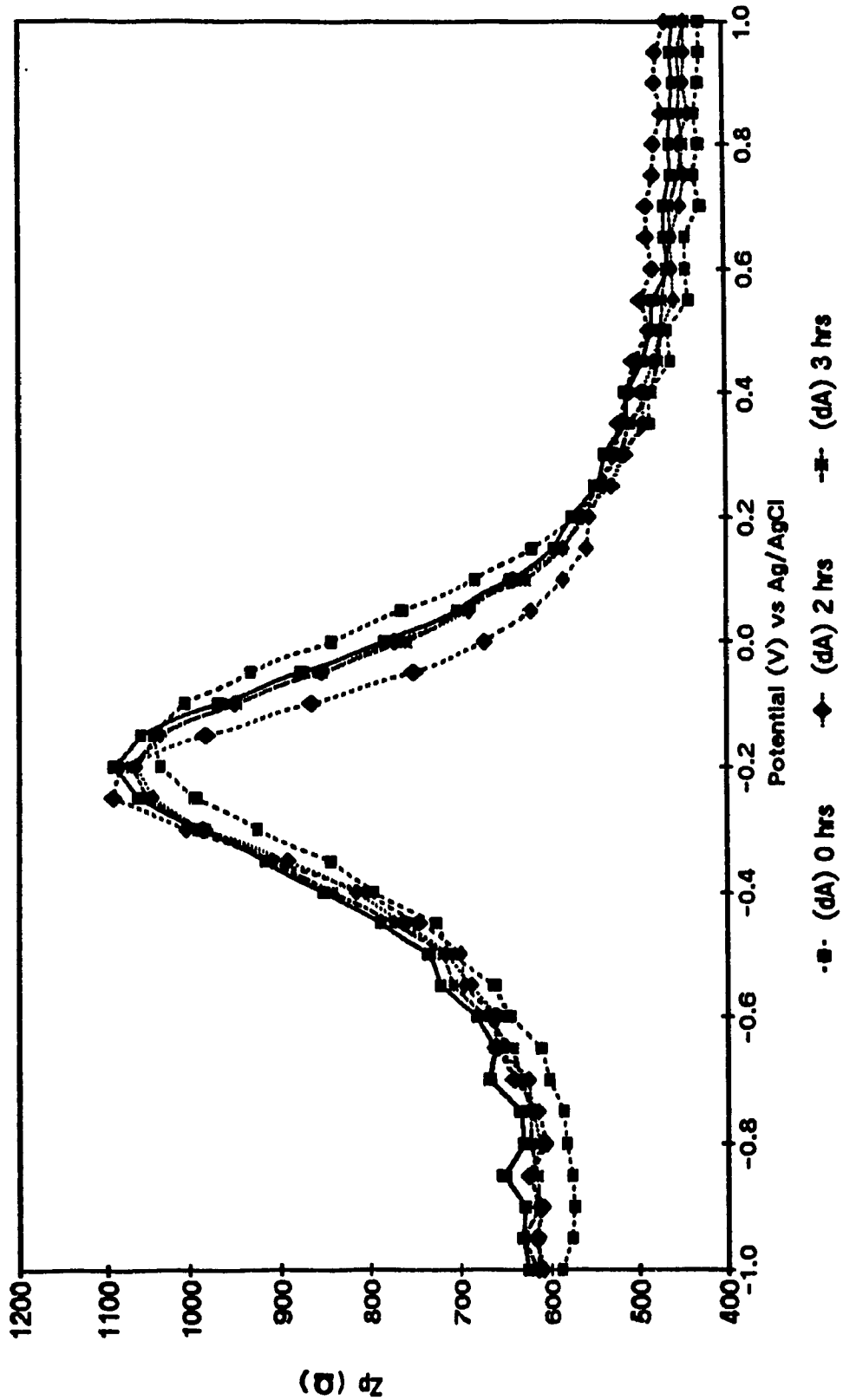

Figure II.37A In-phase impedance measurements of an oligo$(dT)_{20}$ modified electrode, *in situ* hybridized with 10 μl of 1 mg/ml poly(dA).

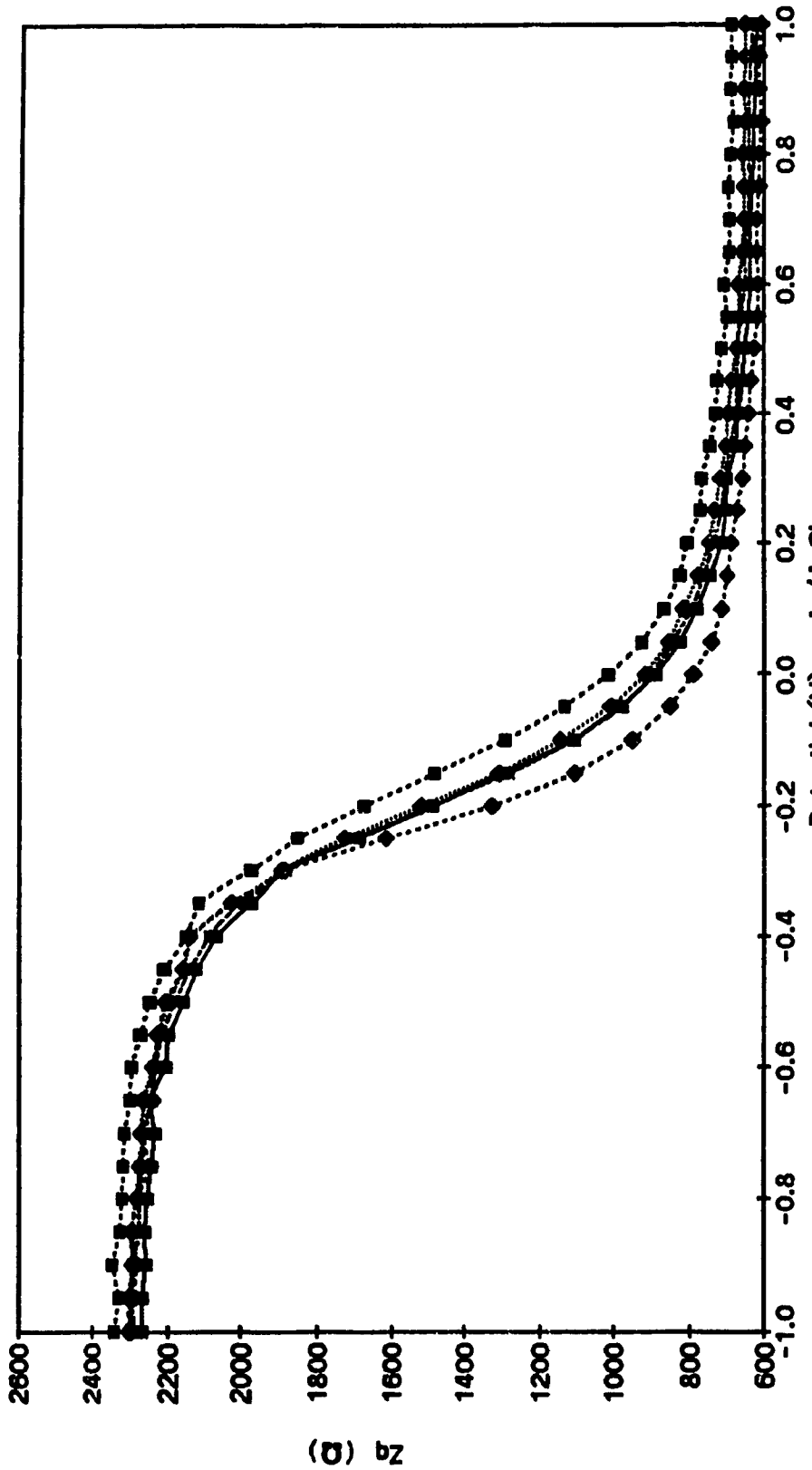

Figure II.37B Out-of-phase impedance measurements of an oligo(dT)$_{20}$ modified electrode, *in situ* hybridized with 10 µl of 1 mg/ml poly(dA).

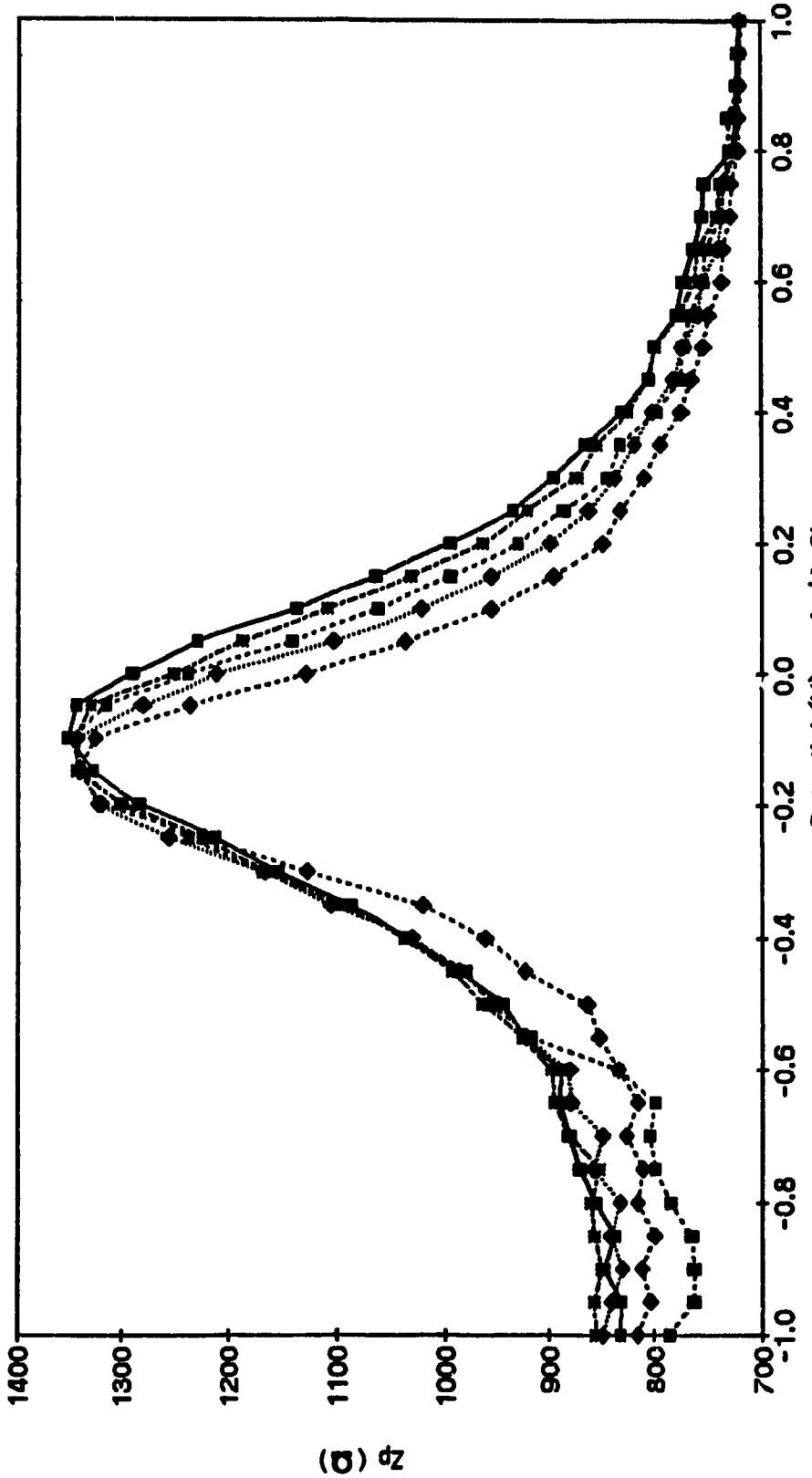

Figure II.38A In-phase impedance measurements of an oligo(dT)$_{20}$ modified electrode, *in situ* hybridized with 40 µl of 0.1 mg/ml of poly(dA).

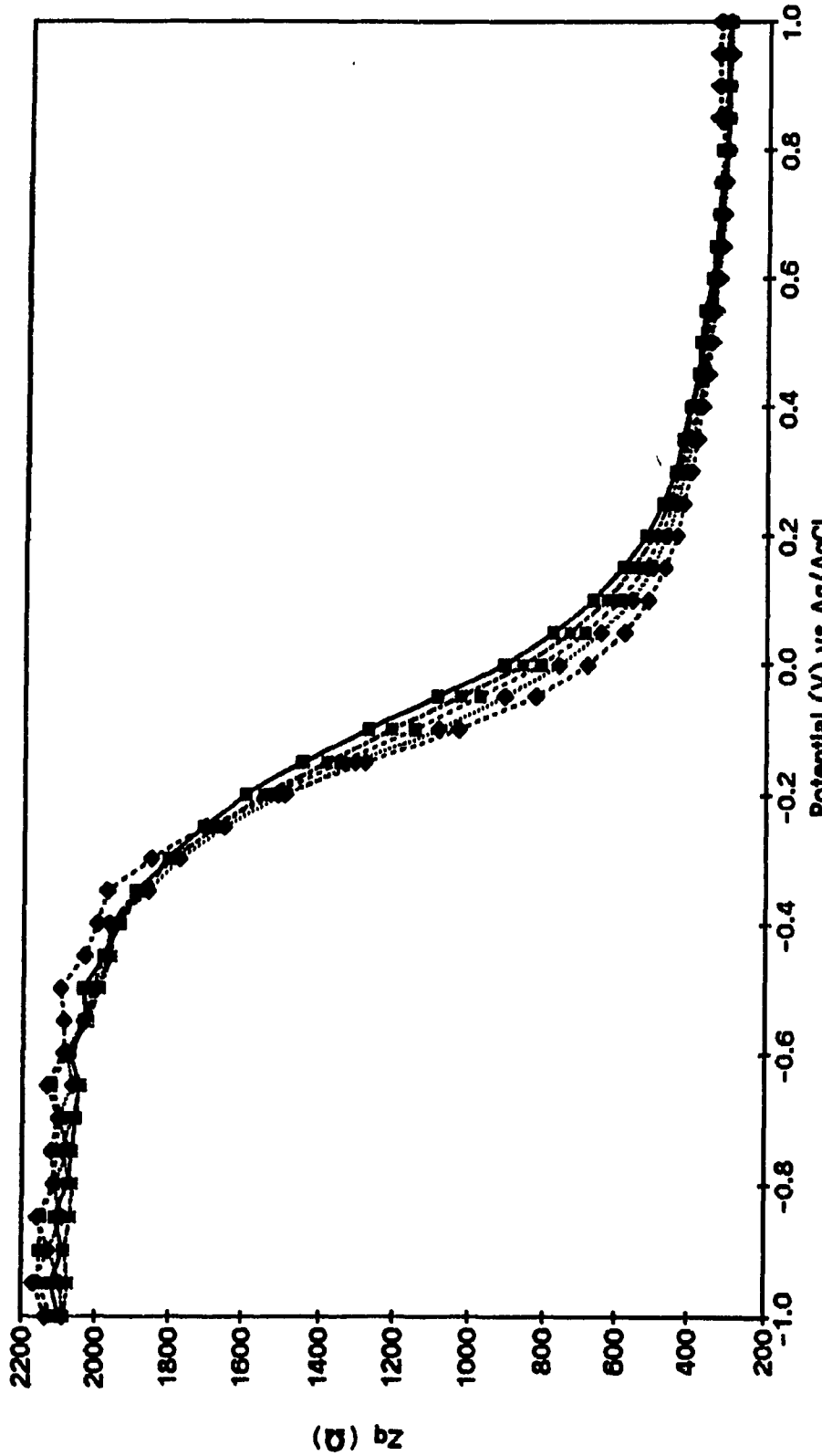

Figure II.38B Out-of-phase impedance measurements of an oligo(dT)$_{20}$ modified electrode, *in situ* hybridized with 40 µl of 0.1 mg/ml of poly(dA).

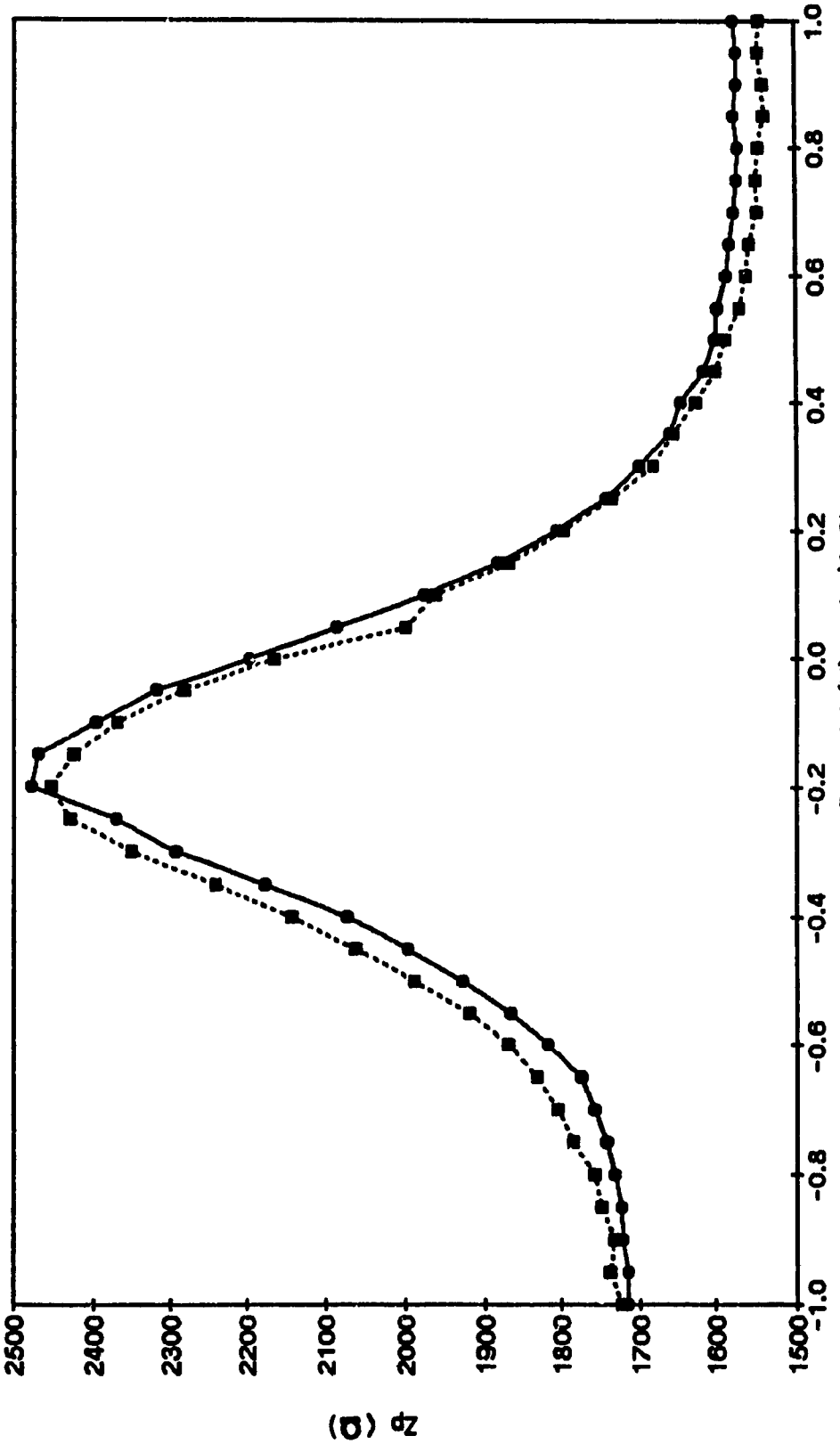

Figure II.39A In-phase impedance measurements of an oligo(dT)$_{20}$ modified electrode hybridized with 10 µl of 0.1 mg/ml poly(dA).

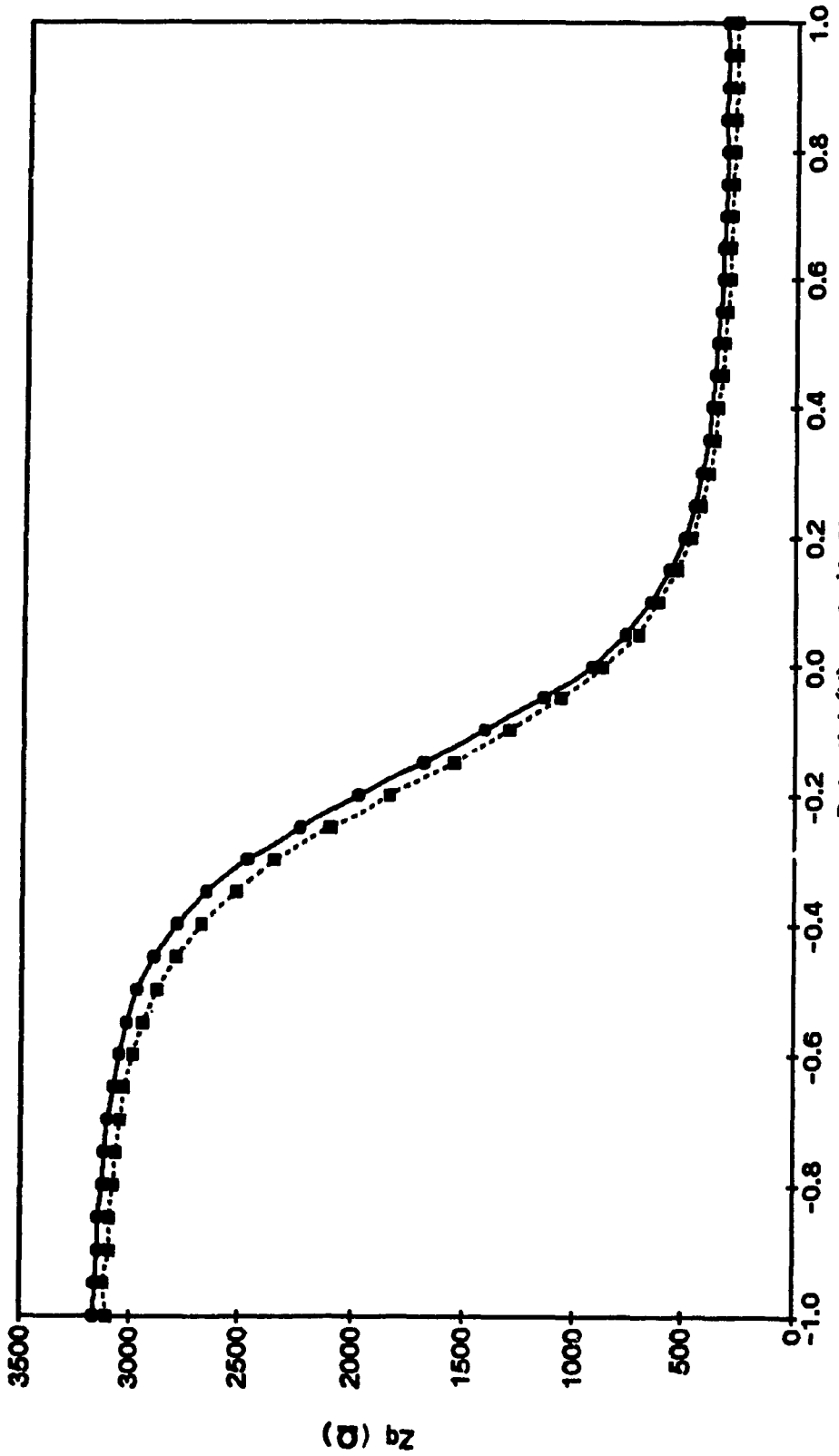

Figure II.39B Out-of-phase impedance measurements of an oligo(dT)$_{20}$ modified electrode hybridized with 10 μl of 0.1 mg/ml poly(dA).